International Earth Rotation and Reference Systems Service (IERS)
Service International de la Rotation Terrestre et des Systèmes de Référence

IERS Technical Note No. 32

IERS Conventions (2003)

Dennis D. McCarthy[1] and Gérard Petit[2] (eds.)

IERS Conventions Centre

[1] US Naval Observatory (USNO)
[2] Bureau International des Poids et Mesures (BIPM)

Report Documentation Page	*Form Approved* *OMB No. 0704-0188*

Public reporting burden for the collection of information is estimated to average 1 hour per response, including the time for reviewing instructions, searching existing data sources, gathering and maintaining the data needed, and completing and reviewing the collection of information. Send comments regarding this burden estimate or any other aspect of this collection of information, including suggestions for reducing this burden, to Washington Headquarters Services, Directorate for Information Operations and Reports, 1215 Jefferson Davis Highway, Suite 1204, Arlington VA 22202-4302. Respondents should be aware that notwithstanding any other provision of law, no person shall be subject to a penalty for failing to comply with a collection of information if it does not display a currently valid OMB control number.

1. REPORT DATE **2004**	2. REPORT TYPE **N/A**	3. DATES COVERED **-**	
4. TITLE AND SUBTITLE **IERS Convetions (2003)**		5a. CONTRACT NUMBER	
		5b. GRANT NUMBER	
		5c. PROGRAM ELEMENT NUMBER	
6. AUTHOR(S)		5d. PROJECT NUMBER	
		5e. TASK NUMBER	
		5f. WORK UNIT NUMBER	
7. PERFORMING ORGANIZATION NAME(S) AND ADDRESS(ES) **U.S. Naval Observatory Library 3450 Massachusetts Avenue, N.W. Washington, DC 20392-5420**		8. PERFORMING ORGANIZATION REPORT NUMBER	
9. SPONSORING/MONITORING AGENCY NAME(S) AND ADDRESS(ES)		10. SPONSOR/MONITOR'S ACRONYM(S)	
		11. SPONSOR/MONITOR'S REPORT NUMBER(S)	
12. DISTRIBUTION/AVAILABILITY STATEMENT **Approved for public release, distribution unlimited**			
13. SUPPLEMENTARY NOTES			
14. ABSTRACT			
15. SUBJECT TERMS			

16. SECURITY CLASSIFICATION OF:			17. LIMITATION OF ABSTRACT **UU**	18. NUMBER OF PAGES **127**	19a. NAME OF RESPONSIBLE PERSON
a. REPORT **unclassified**	b. ABSTRACT **unclassified**	c. THIS PAGE **unclassified**			

Standard Form 298 (Rev. 8-98)
Prescribed by ANSI Std Z39-18

IERS Conventions (2003)

Dennis D. McCarthy and Gérard Petit (eds.)

(IERS Technical Note ; No. 32)

Table of Contents

Introduction

This document is intended to define the standard reference systems realized by the International Earth Rotation Service (IERS) and the models and procedures used for this purpose. It is a continuation of the series of documents begun with the Project MERIT Standards (Melbourne *et al.*, 1983) and continued with the IERS Standards (McCarthy, 1989; McCarthy, 1992) and IERS Conventions (McCarthy, 1996). The current issue of the IERS Conventions is called the IERS Conventions (2003). When referenced in recommendations and articles published in past years, this document may have been referred to as the IERS Conventions (2000).

All of the products of the IERS may be considered to be consistent with the description in this document. If contributors to the IERS do not fully comply with these guidelines, they will carefully identify the exceptions. In these cases, the contributor provides an assessment of the effects of the departures from the conventions so that its results can be referred to the IERS Reference Systems. Contributors may use models equivalent to those specified herein. Products obtained with different observing methods have varying sensitivity to the adopted standards and reference systems, but no attempt has been made in this document to assess this sensitivity.

The reference systems and procedures of the IERS are based on the resolutions of international scientific unions. The celestial system is based on IAU (International Astronomical Union) Resolution A4 (1991). It was officially initiated and named by IAU Resolution B2 (1997) and its definition was further refined by IAU Resolution B1 (2000). The terrestrial system is based on IUGG Resolution 2 (1991). The transformation between celestial and terrestrial systems is based on IAU Resolution B1 (2000). The definition of time coordinates and time transformations, the models for light propagation and the motion of massive bodies are based on IAU Resolution A4 (1991), further defined by IAU Resolution B1 (2000). In some cases, the procedures used by the IERS, and the resulting conventional frames produced by the IERS, do not completely follow these resolutions. These cases are identified in this document and procedures to obtain results consistent with the resolutions are indicated.

The units of length, mass, and time are in the International System of Units (Le Système International d'Unités (SI), 1998) as expressed by the meter (m), kilogram (kg) and second (s). The astronomical unit of time is the day containing 86400 SI seconds. The Julian century contains 36525 days and is represented by the symbol c. When possible, the notations in this document have been made consistent with ISO Standard 31 on quantities and units.

While the recommended models, procedures and constants used by the IERS follow the research developments and the recommendations of international scientific unions, continuity with the previous IERS Standards and Conventions is essential. In this respect, the principal changes are listed below.

Differences between this Document and IERS Technical Note 21

The most significant changes from previous IERS standards and conventions are due to the incorporation of the recommendations of the 24th IAU General Assembly held in 2000. These are shown in Appendix 1 of this document. These recommendations clarify and extend the concepts of the reference systems in use by the IERS and introduce a major revision of the procedures used to transform between them. A new theory of precession-nutation has been adopted by the IAU and this is introduced in this document. The IAU 2000 recommendations also extend

the procedures for the application of relativity. Other major changes are due to the adoption by the IERS of a new Terrestrial Reference Frame (ITRF2000) (Altamimi *et al.*, 2002), the recommendation of a new geopotential model and the modification of the solid Earth tide model to be consistent with the model of nutation.

The authors and major contributors are outlined below along with the significant changes made for each chapter.

Chapter 1: General Definitions and Numerical Standards

This chapter was prepared principally by D. McCarthy and G. Petit with major contributions from M. Burša, N. Capitaine, T. Fukushima, E. Groten, P. M. Mathews, P. K. Seidelmann, E. M. Standish, and P. Wolf. It provides general definitions for topics that belong to different chapters of the document and also the values of numerical standards that are used in the document. It incorporates the previous Chapter 4, which has been updated to provide consistent notation throughout the IERS Conventions and to comply with the recommendations of the most recent reports of the appropriate working groups of the International Association of Geodesy (IAG) and the IAU.

Chapter 2: Conventional Celestial Reference System and Frame

This chapter (previously Chapter 1) has been updated by E. F. Arias with contributions from J. Kovalevsky, C. Ma, F. Mignard, and A. Steppe to comply with the recommendations of the IAU 2000 24th General Assembly.

Chapter 3: Conventional Dynamical Realization of the ICRS

In this chapter (previously Chapter 2), the conventional solar system ephemeris has been changed to the Jet Propulsion Laboratory (JPL) DE405. It was prepared by E. M. Standish with contributions from F. Mignard and P. Willis.

Chapter 4: Conventional Terrestrial Reference System and Frame

This chapter (previously Chapter 3) has been rewritten by Z. Altamimi, C. Boucher, and P. Sillard with contributions from J. Kouba, G. Petit, and J. Ray. It incorporates the new Terrestrial Reference Frame of the IERS (ITRF2000), which was introduced in 2001.

Chapter 5: Transformation Between the Celestial and Terrestrial Systems

This chapter has been updated principally by N. Capitaine, with major contributions from P. M. Mathews and P. Wallace to comply with the recommendations of the IAU 2000 24th General Assembly. Significant contributions from P. Bretagnon, R. Gross, T. Herring, G. Kaplan, D. McCarthy, Burghard Richter and P. Simon were also incorporated.

Chapter 6: Geopotential

This chapter was prepared principally by V. Dehant, P. M. Mathews, and E. Pavlis. Major contributions were also made by P. Defraigne, S. Desai, F. Lemoine, R. Noomen, R. Ray, F. Roosbeek, and H. Schuh. A new geopotential model is recommended.

Chapter 7: Displacement of Reference Points

Chapter 7 has been updated to be consistent with the geopotential model recommended in Chapter 6. It was prepared principally by V. Dehant, P. M. Mathews, and H.-G. Scherneck. Major contributions were also made by Z. Altamimi, S. Desai, S. Dickman, R. Haas, R. Langley, R. Ray, M. Rothacher, H. Schuh, and T. van Dam. A model for post-glacial rebound is no longer recommended and a new ocean-loading model is suggested. The VLBI antenna deformation has been enhanced.

Chapter 8: Tidal Variations in the Earth's Rotation

Changes have been introduced to be consistent with the nutation model adopted at the 24th IAU General Assembly. The model of the diurnal/semidiurnal variations has been enhanced to include more tidal constituents. The principal authors of Chapter 8 were Ch. Bizouard, R. Eanes, and R. Ray. P. Brosche, P. Defraigne, S. Dickman, D. Gambis, and R. Gross also made significant contributions.

Chapter 9: Tropospheric Model

This chapter has been changed to recommend an updated model. It is based on the work of C. Ma, E. Pavlis, M. Rothacher, and O. Sovers, with contributions from C. Jacobs, R. Langley, V. Mendes, A. Niell, T. Otsubo, and A. Steppe.

Chapter 10: General Relativistic Models for Space-time Coordinates and Equations of Motion

This chapter (previously Chapter 11), has been updated to be in compliance with the IAU resolutions and the notation they imply. It was prepared principally by T. Fukushima and G. Petit with major contributions from P. Bretagnon, A. Irwin, G. Kaplan, S. Klioner, T. Otsubo, J. Ries, M. Soffel, and P. Wolf.

Chapter 11: General Relativistic Models for Propagation

This chapter (previously Chapter 12), has been updated to be in compliance with the IAU resolutions and the notation they imply. It is based on the work of T. M. Eubanks and J. Ries. Significant contributions from S. Kopeikin, G. Petit, L. Petrov, A. Steppe, O. Sovers, and P. Wolf were incorporated.

The IERS Conventions are the product of the IERS Conventions Product Center. However, this volume would not be possible without the contributions acknowledged above. In addition, we would also like to acknowledge the comments and contributions of S. Allen, Y. Bar-Sever, A. Brzeziński, M. S. Carter, P. Cook, H. Fliegel, M. Folgueira, J. Gipson, S. Howard, T. Johnson, M. King, S. Kudryavtsev, Z. Malkin, S. Pagiatakis, S. Pogorelc, J. Ray, S. Riepl, C. Ron, and T. Springer.

Conventions Product Center

E. F. Arias   B. J. Luzum   D. D. McCarthy   G. Petit   P. Wolf

References

Arias E. F., Charlot P., Feissel M., Lestrade J.-F., 1995, "The Extragalactic Reference System of the International Earth Rotation Service, ICRS," *Astron. Astrophys.*, **303**, pp. 604–608.

Altamimi, Z., Sillard, P., and Boucher, C., 2002, "ITRF2000: A New Release of the International Terrestrial Reference Frame for Earth Science Applications," *J. Geophys. Res.*, **107, B10**, 10.1029/2001JB000561.

Le Système International d'Unités (SI), 1998, Bureau International des Poids et Mesures, Sèvres, France.

McCarthy, D. D. (ed.), 1989, IERS Standards, IERS Technical Note 3, Observatoire de Paris, Paris.

McCarthy, D. D. (ed.), 1992, IERS Standards, IERS Technical Note 13, Observatoire de Paris, Paris.

McCarthy, D. D. (ed.), 1996, IERS Conventions, IERS Technical Note 21, Observatoire de Paris, Paris.

Melbourne, W., Anderle, R., Feissel, M., King, R., McCarthy, D., Smith, D., Tapley, B., Vicente, R., 1983, Project MERIT Standards, U.S. Naval Observatory Circular No. 167.

1 General Definitions and Numerical Standards

This chapter provides general definitions for some topics and the values of numerical standards that are used in the document. Those are based on the most recent reports of the appropriate working groups of the International Association of Geodesy (IAG) and the International Astronomical Union (IAU).

1.1 Permanent Tide

Some geodetic parameters are affected by tidal variations. The gravitational potential in the vicinity of the Earth, which is directly accessible to observation, is a combination of the tidal gravitational potential of external bodies (the Moon, the Sun, and the planets) and the Earth's own potential which is perturbed by the action of the tidal potential. The (external) tidal potential contains both time independent (permanent) and time dependent (periodic) parts, and so does the tide-induced part of the Earth's own potential. Similarly, the observed site positions are affected by displacements associated with solid Earth deformations produced by the tidal potential; these displacements also include permanent and time dependent parts. On removing from the observed site positions/potential the time dependent part of the tidal contributions, the resulting station positions are on the "mean tide" (or simply "mean") crust; and the potential which results is the "mean tide" potential. The permanent part of the deformation produced by the tidal potential is present in the mean crust; the associated permanent change in the geopotential, and also the permanent part of the tidal potential, are included in the mean tide geopotential. These correspond to the actual mean values, free of periodic variations due to tidal forces. The "mean tide" geoid, for example, would correspond to the mean ocean surface in the absence of non-gravitational disturbances (currents, winds). In general, quantities referred to as "mean tide" (*e.g.* flattening, dynamical form factor, equatorial radius, *etc.*) are defined in relation to the mean tide crust or the mean tide geoid.

If the deformation due to the permanent part of the tidal potential is removed from the mean tide crust, the result is the "tide free" crust. As regards the potential, removal of the permanent part of the *external* potential from the mean tide potential results in the "zero tide" potential which is strictly a geopotential. The permanent part of the deformation-related contribution is still present; if that is also removed, the result is the "tide free" geopotential. It is important to note that unlike the case of the potential, the term "zero tide" as applied to the *crust* is synonymous with "mean tide."

In a "tide free" quantity, the total tidal effects have been removed with a model. Because the perturbing bodies are always present, a truly "tide free" quantity is unobservable. In this document, the tidal models used for the geopotential (Chapter 6) and for the displacement of points on the crust (Chapter 7) are based on nominal Love numbers; the reference geopotential model and terrestrial reference frame, which are obtained by removal of tidal contributions using such models, are termed "conventional tide free." Because the deformational response to the permanent part of the tide generating potential is characterized actually by the secular (or fluid limit) Love numbers, which differ substantially from the nominal ones, "conventional tide free" values of quantities do *not* correspond to truly tide free values that would be observed if tidal perturbations were absent. The true effect of the permanent tide could be estimated using the fluid limit Love numbers for this purpose, but this calculation is not included in this document because it is not needed for the tidal correction procedure.

Resolution 16 of the 18th General Assembly of the IAG (1983), "recognizing the need for the uniform treatment of tidal corrections to various geodetic quantities such as gravity and station positions," recommended that "the indirect effect due to the permanent yielding of the Earth be not removed," *i.e.* the use of "zero-tide" values for quantities associated with the geopotential and "mean-tide" values for quantities associated with station displacements. This recommendation, however, has not been implemented in the algorithms used for tide modeling by the geodesy community in the analysis of space geodetic data in general. As a consequence, the station coordinates that go with such analyses (see Chapter 4) are "conventional tide free" values.

The geopotential can be realized in the three different cases (*i.e.*, mean tide, zero tide or tide free). For those parameters for which the difference is relevant, the values given in Table 1.1 are "zero-tide" values, according to the IAG Resolution.

The different notions related to the treatment of the permanent tide are shown pictorially in Figures 1.1 and 1.2.
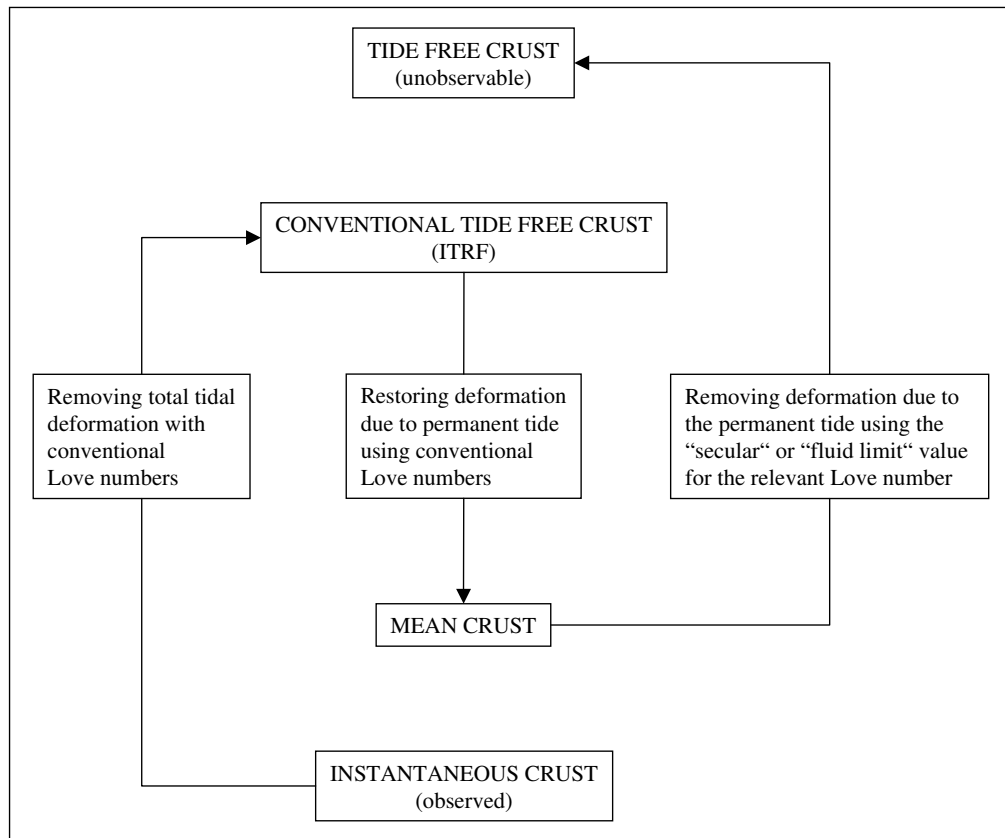
Fig. 1.1   Treatment of observations to account for tidal deformations in terrestrial reference systems (see Chapters 4 and 7).
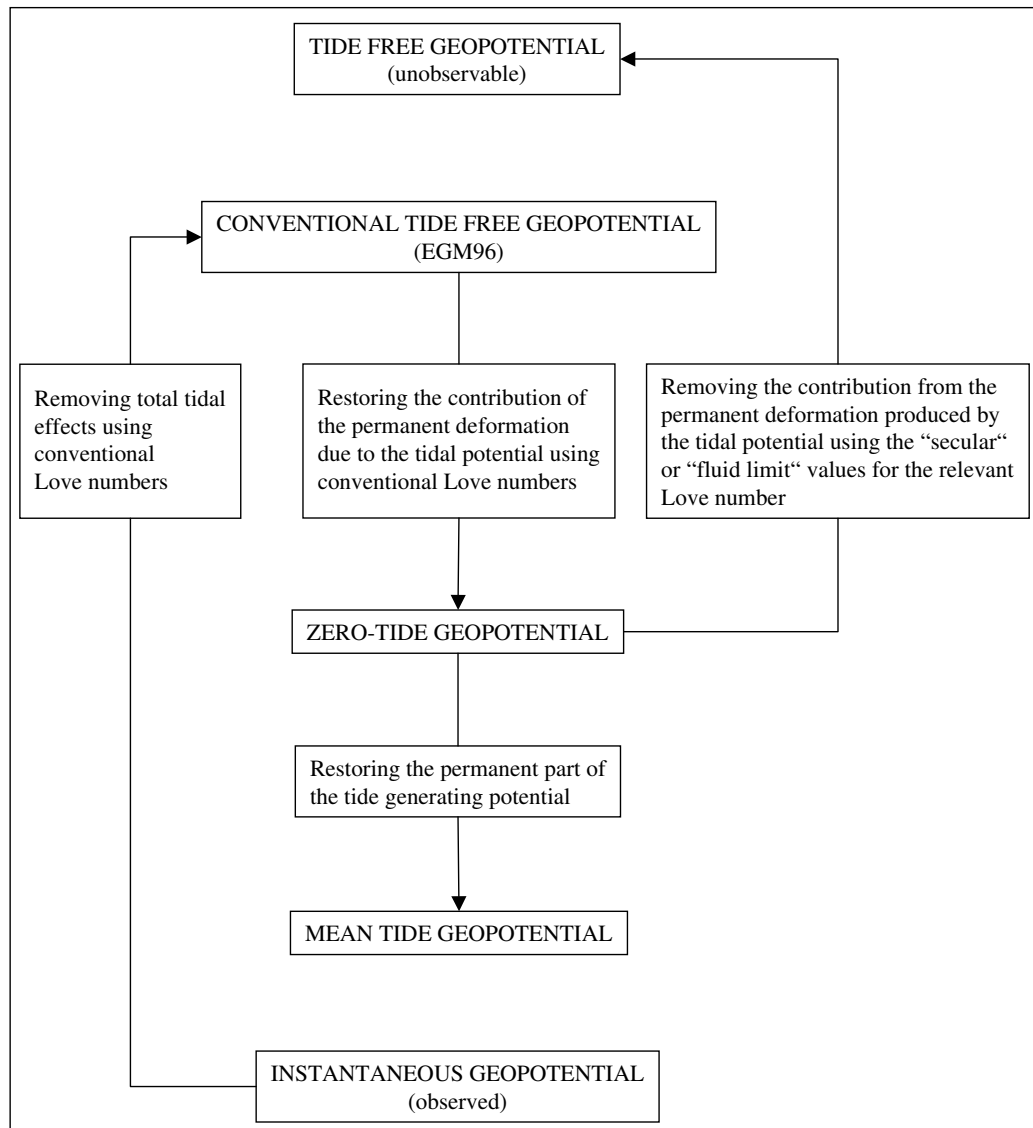
Fig. 1.2   Treatment of observations for tidal effects in the geopotential (see Chapter 6).

1.2   Numerical Standards

Table 1.1 listing numerical standards is organized into 5 columns: item, value, uncertainty, reference, comment. Most of the values are given in terms of SI units (*Le Système International d'Unités (SI)*, 1998), *i.e.* they are consistent with the use of Geocentric Coordinate Time TCG as a time coordinate for the geocentric system, and of Barycentric Coordinate Time TCB for the barycentric system. The values of τ_A, $c\tau_A$, and ψ_1, however, are given in so-called "TDB" units, having been determined previously using Barycentric Dynamical Time TDB as a time coordinate for the barycentric system. In this book some quantities are also given in so-called "TT" units, having been determined using Terrestrial Time TT as a time coordinate for the geocentric system. See Chapter 10 for further details on the transformations between time scales and Chapter 3 for a discussion of the time scale used in the ephemerides.

TDB and TCB units of time, t, and length, ℓ, may be easily related by the expressions (Seidelmann and Fukushima, 1992)

$$t_{TDB} = t_{TCB}/(1 - L_B), \quad \ell_{TDB} = \ell_{TCB}/(1 - L_B),$$

where L_B is given in Table 1.1. Therefore a quantity X with the dimension of time or length has a numerical value x_{TCB} when using "TCB" (SI) units which differs from its value x_{TDB} when using "TDB" units by

$$x_{TDB} = x_{TCB} \times (1 - L_B).$$

Similarly, the numerical value x_{TCG} when using "TCG" (SI) units differs from the numerical value x_{TT} when using "TT" units by

$$x_{TT} = x_{TCG} \times (1 - L_G)$$

where L_G is given in Table 1.1.

The IAU 1976 System of Astronomical Constants (*Astronomical Almanac for the Year 1984*) is adopted for all astronomical constants which do not appear in Table 1.1.

Table 1.1   IERS Numerical Standards.

ITEM	VALUE	UNCERTAINTY	REF.	COMMENTS
c	$299792458 ms^{-1}$	Defining	[2]	Speed of light
L_B	$1.55051976772 \times 10^{-8}$	2×10^{-17}	[4]	Average value of 1-d(TT)/d(TCB)
L_C	$1.48082686741 \times 10^{-8}$	2×10^{-17}	[4]	Average value of 1-d(TCG)/d(TCB)
L_G	$6.969290134 \times 10^{-10}$	Defining	[4]	1-d(TT)/d(TCG)
G	$6.673 \times 10^{-11} m^3 kg^{-1} s^{-2}$	$1 \times 10^{-13} m^3 kg^{-1} s^{-2}$	[2]	Constant of gravitation
$GM_\odot$	$1.32712442076 \times 10^{20} m^3 s^{-2}$	$5 \times 10^{10} m^3 s^{-2}$	[from 3]	Heliocentric gravitational constant
τ_A[†]	$499.0047838061 s$	$0.00000002 s$	[3]	Astronomical unit in seconds
$c\tau_A$[†]	$149597870691 m$	$6 m$	[3]	Astronomical unit in meters
ψ_1[†]	$5038.47875''/c$	$0.00040''/c$	[6]	IAU(1976) value of precession of the equator at J2000.0 corrected by $-0.29965''$. See Chapter 5.
ϵ_0	$84381.4059''$	$0.0003''$	[5]	Obliquity of the ecliptic at J2000.0. See Chapter 5 for value used in IAU precession-nutation model.
$J_{2\odot}$	2×10^{-7}	(adopted for DE405)		Dynamical form-factor of the Sun
μ	0.0123000383	5×10^{-10}	[3]	Moon-Earth mass ratio
$GM_\oplus$	$3.986004418 \times 10^{14} m^3 s^{-2}$	$8 \times 10^5 m^3 s^{-2}$	[1]	Geocentric gravitational constant (EGM96 value)
a_E[‡]	$6378136.6 m$	$0.10 m$	[1]	Equatorial radius of the Earth
$1/f$[‡]	298.25642	0.00001	[1]	Flattening factor of the Earth
$J_{2\oplus}$[‡]	1.0826359×10^{-3}	1.0×10^{-10}	[1]	Dynamical form-factor
ω	$7.292115 \times 10^{-5} rad s^{-1}$	variable	[1]	Nominal mean angular velocity of the Earth
g_e[‡]	$9.7803278 ms^{-2}$	$1 \times 10^{-6} ms^{-2}$	[1]	Mean equatorial gravity
W_0	$62636856.0 m^2 s^{-2}$	$0.5 m^2 s^{-2}$	[1]	Potential of the geoid
R_0[††]	$6363672.6 m$	$0.1 m$	[1]	Geopotential scale factor

[†]   The values for τ_A, $c\tau_A$, and ψ_1 are given in "TDB" units (see discussion above).

[‡]   The values for a_E, $1/f$, $J_{2\oplus}$ and g_E are "zero tide" values (see the discussion in section 1.1 above). Values according to other conventions may be found from reference [1].

[††] $R_0 = GM_\oplus/W_0$

[1]   Groten, E., 1999, Report of the IAG. Special Commission SC3, Fundamental Constants, XXII IAG General Assembly.

[2]   Mohr, P. J. and Taylor, B. N., 1999, *J. Phys. Chem. Ref. Data*, **28, 6**, p. 1713.

[3]   Standish, E. M., 1998, JPL IOM 312-F.

[4]   IAU XXIV General Assembly. See Appendix 1.

[5]   Fukushima, T., 2003, Report on astronomical constants, *Highlights of Astronomy*, in press.

[6]   Mathews, P. M., Herring, T. A., and Buffett, B. A., 2002, Modeling of nutation-precession: New nutation series for nonrigid Earth, and insights into the Earth's interior, *J. Geophys. Res.* **107, B4**, 10.1029/2001JB00390.

References

Astronomical Almanac for the Year 1984, U.S. Government Printing Office, Washington, DC.

Le Système International d'Unités (SI), 1998, Bureau International des Poids et Mesures, Sèvres, France.

Seidelmann, P. K. and Fukushima, T., 1992, "Why New Time Scales?" *Astron. Astrophys.*, **265**, pp. 833–838.

2 Conventional Celestial Reference System and Frame

The celestial reference system is based on a kinematical definition, making the axis directions fixed with respect to the distant matter of the universe. The system is materialized by a celestial reference frame defined by the precise coordinates of extragalactic objects, mostly quasars, BL Lac sources and few active galactic nuclei (AGNs), on the grounds that these sources are so far away that their expected proper motions should be negligibly small. The current positions are known to better that a milliarcsecond, the ultimate accuracy being primarily limited by the structure instability of the sources in radio wavelengths. The USNO Special Analysis Center for Source Structure has a web site at <[1]>.

The related IAU recommendations (see McCarthy, 1992) specify that the origin is to be at the barycenter of the solar system and the directions of the axes should be fixed with respect to the quasars. These recommendations further stipulate that the celestial reference system should have its principal plane as close as possible to the mean equator at J2000.0 and that the origin of this principal plane should be as close as possible to the dynamical equinox of J2000.0. This system was prepared by the IERS and has been adopted by the IAU General Assembly of 1997 under the name of the International Celestial Reference System (ICRS). It officially replaced the FK5 system on January 1, 1998, considering that all the conditions set up by the 1991 resolutions were fulfilled, including the availability of an optical reference frame realizing the ICRS with an accuracy significantly better than the FK5.

2.1 The ICRS

The necessity of maintaining the reference directions fixed and the continuing improvement in the source coordinates requires regular maintenance of the frame. Realizations of the IERS celestial reference frame have been computed every year between 1989 and 1995 (see the IERS annual reports) keeping the same IERS extragalactic celestial reference system. The number of defining sources has progressively grown from 23 in 1988 to 212 in 1995. Comparisons between successive realizations have shown that there were small shifts from year to year until the process converged to better than 0.1 mas and to 0.02 mas for the relative orientation between successive realizations. The IERS proposed that the 1995 version of the IERS system be taken as the International Celestial Reference System (ICRS). This was formally accepted by the IAU in 1997 and is described in Arias *et al.* (1995).

2.1.1 Equator

The IAU recommendations call for the principal plane of the conventional reference system to be close to the mean equator at J2000.0. The VLBI observations used to establish the extragalactic reference frame are also used to monitor the motion of the celestial pole in the sky (precession and nutation). In this way, the VLBI analyses provide corrections to the conventional IAU models for precession and nutation (Lieske *et al.*, 1977; Seidelmann, 1982) and accurate estimation of the shift of the mean pole at J2000.0 relative to the Conventional Reference Pole of the ICRS. Based on the VLBI solutions submitted to the IERS in 2001, the shift of the pole at J2000.0 relative to the ICRS celestial pole has been estimated by using (a) the updated nutation model IERS(1996) and (b) the new MBH2000 nutation model (Mathews *et al.*, 2002). The direction of the mean pole at J2000.0 in the ICRS is +17.1mas in the direction 12[h] and +5.0mas in the direction 18[h] when the IERS(1996) model is used, and

---

[1]http://rorf.usno.navy.mil/ivs_saac

+16.6mas in the direction 12$^\text{h}$ and +6.8mas in the direction 18$^\text{h}$ when the MBH2000 model is adopted (IERS, 2001).

The IAU recommendations stipulate that the direction of the Conventional Reference Pole should be consistent with that of the FK5. The uncertainty in the direction of the FK5 pole can be estimated by considering (1) that the systematic part is dominated by a correction of about $-0.30''$/c to the precession constant used in the construction of the FK5 System, and (2) by adopting Fricke's (1982) estimation of the accuracy of the FK5 equator ($\pm 0.02''$), and Schwan's (1988) estimation of the limit of the residual rotation ($\pm 0.07''$/c), taking the epochs of observations from Fricke *et al.* (1988). Assuming that the error in the precession rate is absorbed by the proper motions of stars, the uncertainty in the FK5 pole position relative to the mean pole at J2000.0 estimated in this way is ± 50 mas. The ICRS celestial pole is therefore consistent with that of the FK5 within the uncertainty of the latter.

2.1.2 Origin of Right Ascension

The IAU recommends that the origin of right ascensions of the ICRS be close to the dynamical equinox at J2000.0. The x axis of the IERS celestial system was implicitly defined in its initial realization (Arias *et al.*, 1988) by adopting the mean right ascension of 23 radio sources in a group of catalogs that were compiled by fixing the right ascension of the quasar 3C 273B to the usual (Hazard *et al.*, 1971) conventional FK5 value (12$^\text{h}$29$^\text{m}$6.6997$^\text{s}$ at J2000.0) (Kaplan *et al.*, 1982).

The uncertainty of the determination of the FK5 origin of right ascensions can be derived from the quadratic sum of the accuracies given by Fricke (1982) and Schwan (1988), considering a mean epoch of 1955 for the proper motions in right ascension (see last paragraph of the previous section for further details). The uncertainty thus obtained is ± 80 mas. This was confirmed by Lindegren *et al.* (1995) who found that the comparison of FK5 positions with those of the Hipparcos preliminary catalogue shows a systematic position error in FK5 of the order of 100 mas. This was confirmed by Mignard and Froeschlé (2000) when linking the final Hipparcos catalog to the ICRS.

Analyses of LLR observations (Chapront *et al.*, 2002; IERS, 2000) indicate that the origin of right ascensions in the ICRS is shifted from the inertial mean equinox at J2000.0 on the ICRS reference plane by -55.4 ± 0.1 mas (direct rotation around the polar axis). Note that this shift of -55.4 mas on the ICRS equator corresponds to a shift of -14.6 mas on the mean equator of J2000.0, that is used in Chapter 5. The equinox of the FK5 was found by Mignard and Froeschlé (2000) to be at -22.9 ± 2.3 mas from the origin of the right ascensions of the IERS. These results indicate that the ICRS origin of right ascension complies with the IAU recommendations.

2.2 The ICRF

The ICRS is materialized by the International Celestial Reference Frame (ICRF). A realization of the ICRF consists of a set of precise coordinates of extragalactic radio sources. The objects in the frame are divided in three subsets: "defining," "candidate" and "other" sources. Defining sources should have a large number of observations over a sufficiently long data span to assess position stability; they maintain the axes of the ICRS. Sources with an insufficient number of observations or an observing time span too short to be considered as defining sources are designated as candidate; they could be potential defining sources in future realizations of the ICRF. The category of "other" sources includes those objects with poorly determined positions which are useful in deriving various frame links.

A first realization of the ICRF was constructed in 1995 by a reanalysis of the available VLBI observations. The set of positions obtained by this analysis was rotated to the ICRS; the position formal uncertainties were calibrated to render their values more realistic (IERS, 1997; Ma *et al.*, 1998). Following the maintenance process which characterizes the ICRS, an extension of the frame, ICRF-Ext.1 was constructed by using VLBI data available until April 1999 (IERS, 1999). For defining sources, the positions and errors are unchanged from the first realization of the ICRF. The 212 defining extragalactic radio sources are distributed over the sky with a median uncertainty of ±0.35 mas in right ascension and of ±0.40 mas in declination. The uncertainty from the representation of the ICRS is then established to be smaller than 0.01 mas. The scattering of rotation parameters of different comparisons performed, shows that these axes are stable to ±0.02 mas. Note that this frame stability is based upon the assumption that the sources have no proper motion and that there is no global rotation of the universe. The assumption concerning proper motion was checked regularly on the successive IERS frames (Ma and Shaffer, 1991; Eubanks *et al.*, 1994) as well as the different subsets of the final data (IERS, 1997). For candidate and other sources, new positions and errors have been calculated. All of them are listed in the catalog in order to have a larger, usable, consistent catalog. The total number of objects in ICRF-Ext.1 is 667.

The most precise direct access to the quasars is done through VLBI observations, a technique which is not widely available to users. Therefore, while VLBI is used for the maintenance of the primary frame, the tie of the ICRF to the major practical reference frames may be obtained through the use of the IERS Terrestrial Reference Frame (ITRF, see Chapter 4), the HIPPARCOS Galactic Reference Frame, and the JPL ephemerides of the solar system (see Chapter 3).

2.2.1 HIPPARCOS Catalogue

The 1991 IAU recommendation stipulates that as long as the relationship between the optical and extragalactic radio frame is not sufficiently accurately determined, the FK5 catalog will be considered as a provisional realization of the celestial reference system. In 1997, the IAU decided that this condition was fulfilled by the Hipparcos Catalogue (ESA, 1997).

The Hipparcos Catalogue provides the equatorial coordinates of about 118000 stars in the ICRS at epoch 1991.25 along with their proper motions, their parallaxes and their magnitudes in the wide band Hipparcos system. Actually, the astrometric data concerns only 117,955 stars. The median uncertainty for bright stars (Hipparcos wide band magnitude <9) are ±0.77 and ±0.64 mas in right ascension and declination respectively. Similarly, the median uncertainties in annual proper motion are ±0.88 and ±0.74 mas/yr respectively.

The alignment of the Hipparcos Catalogue to the ICRF was realized with a standard error of of ±0.6 mas for the orientation at epoch (1991.25) and ±0.25 mas/year for the spin (Kovalevsky *et al.*, 1997). This was obtained by comparing positions and proper motions of Hipparcos stars with the same subset determined with respect to the ICRF and, for the spin, to optical galaxies.

2.2.2 Availability of the Frame

The catalogue of source coordinates published in IERS (1999) (see also Ma *et al.*, 1998) provides access to the ICRS. It includes a total of 667 objects. Maintenance of the ICRS requires the monotoring of the source coordinate stability based on new observations and new analyses; the appropriate warnings and updates appear in IERS publications.

The principles on which the ITRF is established and maintained are described in Chapter 4. The IERS Earth Orientation Parameters provide the permanent tie of the ICRF to the ITRF. They describe the orientation of the Celestial Ephemeris Pole in the terrestrial system and in the celestial system (polar coordinates x, y; celestial pole offsets $d\psi$, $d\epsilon$) and the orientation of the Earth around this axis (UT1−UTC), as a function of time. This tie is available daily with an accuracy of ± 0.3 mas in the IERS publications.

The other ties to major celestial frames are established by differential VLBI observations of solar system probes, galactic stars relative to quasars and other ground- or space-based astrometry projects. The tie of the solar system ephemerides of the Jet Propulsion Laboratory (JPL) is described by Standish *et al.* (1995). Its estimated precision is ± 3 mas, according to Folkner *et al.* (1994). Other links to the dynamical system are obtained using laser ranging to the Moon, with the ITRF as an intermediate frame (Chapront *et al.*, 2002; IERS, 2000; IERS, 2001).

Ties to the frames related to catalogs at other wavelengths will be available from the IERS as observational analyses permit.

References

Arias E. F., Charlot P., Feissel M., Lestrade J.-F., 1995, "The Extragalactic Reference System of the International Earth Rotation Service, ICRS," *Astron. Astrophys.*, **303**, pp. 604–608.

Arias, E. F., Feissel, M., and Lestrade, J.-F., 1988, "An Extragalactic Celestial Reference Frame Consistent with the BIH Terrestrial System (1987)," *BIH Annual Rep. for 1987*, pp. D-113–D-121.

Chapront, J., Chapront-Touzé M., and Francou, G., 2002, "A new determination of lunar orbital parameters, precession constant and tidal acceleration from LLR measurements," *Astron. Astrophys.*, **387**, pp. 700–709.

ESA, 1997, "The Hipparcos and Tycho catalogues," *European Space Agency Publication*, Novdrijk, SP–1200, June 1997, 19 volumes.

Eubanks, T. M., Matsakis, D. N., Josties, F. J., Archinal, B. A., Kingham, K. A., Martin, J. O., McCarthy, D. D., Klioner, S. A., Herring, T. A., 1994, "Secular motions of extragalactic radio sources and the stability of the radio reference frame," *Proc. IAU Symposium 166*, J. Kovalevsky (ed.).

Folkner, W. M., Charlot, P., Finger, M. H., Williams, J. G., Sovers, O. J., Newhall, X X, and Standish, E. M., 1994, "Determination of the extragalactic-planetary frame tie from joint analysis of radio interferometric and lunar laser ranging measurements," *Astron. Astrophys.*, **287**, pp. 279–289.

Fricke, W., 1982, "Determination of the Equinox and Equator of the FK5," *Astron. Astrophys.*, **107**, pp. L13–L16.

Fricke, W., Schwan, H., and Lederle, T., 1988, *Fifth Fundamental Catalogue, Part I. Veroff. Astron. Rechen Inst.*, Heidelberg.

Hazard, C., Sutton, J., Argue, A. N., Kenworthy, C. N., Morrison, L. V., and Murray, C. A., 1971, "Accurate radio and optical positions of 3C273B," *Nature Phys. Sci.*, **233**, p. 89.

IERS, 1995, 1994 International Earth Rotation Service Annual Report, Observatoire de Paris, Paris.

IERS, 1997, *IERS Technical Note 23*, "Definition and realization of the International Celestial Reference System by VLBI Astrometry of Extragalactic Objects," Ma, C. and Feissel, M. (eds.),Observatoire de Paris, Paris.

IERS, 1999, 1998 International Earth Rotation Service Annual Report, Observatoire de Paris, Paris.

IERS, 2001, 2000 International Earth Rotation Service Annual Report, Observatoire de Paris, Paris.

Kaplan, G. H., Josties, F. J., Angerhofer, P. E., Johnston, K. J., and Spencer, J. H., 1982, "Precise Radio Source Positions from Interferometric Observations," *Astron. J.*, **87**, pp. 570–576.

Kovalevsky, J., Lindegren, L., Perryman, M. A. C., Hemenway, P. D., Johnston, K. J., Kislyuk, V. S., Lestrade, J.-F., Morrison, L. V., Platais, I., Röser, S., Schilbach, E., Tucholke, H.-J., de Vegt, C., Vondrák, J., Arias, F., Gontier, A.-M., Arenou, F., Brosche, P., Florkowski, D. R., Garrington, S. T., Preston, R. A., Ron, C., Rybka, S. P., Scholz, R.-D., and Zacharias, N., 1997, "The Hipparcos Catalogue as a realization of the extragalactic reference system," *Astron. Astrophys.*, **323**, pp. 620–633.

Lieske, J. H., Lederle, T., Fricke, W., and Morando, B., 1977, "Expression for the Precession Quantities Based upon the IAU (1976) System of Astronomical Constants," *Astron. Astrophys.*, **58**, pp. 1–16.

Lindegren, L., Röser, S., Schrijver, H., Lattanzi, M. G., van Leeuwen, F., Perryman, M. A. C., Bernacca, P. L., Falin, J. L., Froeschlé, M., Kovalevsky, J., Lenhardt, H., and Mignard, F., 1995, "A comparison of ground-based stellar positions and proper motions with provisional Hipparcos results," *Astron. Astrophys.*, **304**, pp. 44–51.

Ma, C. and Shaffer, D. B., 1991, "Stability of the extragalactic reference frame realized by VLBI," in *Reference Systems*, Hughes, J. A., Smith, C. A., and Kaplan, G. H. (eds), U. S. Naval Observatory, Washington, pp. 135–144.

Ma, C., Arias, E. F., Eubanks, T. M., Fey, A. L., Gontier, A.-M., Jacobs, C. S., Sovers, O. J., Archinal, B. A. and Charlot, P., 1998, "The International Celestial Reference Frame as Realized by Very Long Baseline Interferometry," *Astron. J.*, **116**, pp. 516–546.

Mathews, P. M., Herring T. A., and Buffet, B. A., 2002, "Modeling of nutation-precession: New nutation series for nonrigid Earth, and insights into the Earth's interior", *J. Geophys. Res.*, **107, B4**, 10.1029/2001JB000390.

Mignard, F. and Froeschlé, M., 2000, "Global and local bias in the FK5 from the Hipparcos data," *Astron. Astrophys.*, **354**, pp. 732–739.

McCarthy D.D. (ed.), 1992, "IERS Standards," *IERS Technical Note 13*, Observatoire de Paris, Paris.

Schwan, H., 1988, "Precession and galactic rotation in the system of FK5," *Astron. Astrophys.*, **198**, pp. 116–124.

Seidelmann, P. K., 1982, "1980 IAU Nutation: The Final Report of the IAU Working Group on Nutation," *Celest. Mech.*, **27**, pp. 79–106.

Standish, E. M., Newhall, X. X., Williams, J. G., and Folkner, W. F., 1995, "JPL Planetary and Lunar Ephemerides, DE403/LE403," JPL IOM 314.10–127.

3 Conventional Dynamical Realization of the ICRS

The planetary and lunar ephemerides recommended for the IERS standards are the JPL Development Ephemeris DE405 and the Lunar Ephemeris LE405, available on a CD from the publisher, Willmann-Bell. See also the website $<^2>$; click on the button, "Where to Obtain Ephemerides."

Note that the time scale for DE405/LE405 is not Barycentric Coordinate Time (TCB) but rather, a coordinate time, T_{eph}, which is related to TCB by an offset and a scale. The ephemerides based upon the coordinate time T_{eph} are automatically adjusted in the creation process so that the rate of T_{eph} has no overall difference from the rate of Terrestrial Time (TT) (see Standish, 1998), therefore also no overall difference from the rate of Barycentric Dynamical Time (TDB). For this reason space coordinates obtained from the ephemerides are consistent with TDB.

The reference frame of DE405 is that of the International Celestial Reference Frame (ICRF). DE405 was adjusted to all relevant observational data, including, especially, VLBI observations of spacecraft in orbit around Venus and Mars, taken with respect to the ICRF. These highly accurate observations serve to orient the ephemerides; observations with respect to other frames (*e.g.*, FK5) were referenced to the ICRF using the most recent transformations then available.

It is expected that DE405/LE405 will eventually replace DE200/LE200 (Standish, 1990) as the basis for the international almanacs. Table 3.1 shows the IAU 1976 values of the planetary masses and the values used in the creations of both DE200/LE200 and of DE405/LE405. Also shown in the table are references for the DE405 set, the current best estimates.

Table 3.1   1976 IAU, DE200 and DE405 planetary mass values, expressed in reciprocal solar masses.

Planet	1976 IAU	DE200	DE405	Reference for DE405 value
Mercury	6023600.	6023600.	6023600.	Anderson *et al.*, 1987
Venus	408523.5	408523.5	408523.71	Sjogren *et al.*, 1990
Earth & Moon	328900.5	328900.55	328900.561400	Standish, 1997
Mars	3098710.	3098710.	3098708.	Null, 1969
Jupiter	1047.355	1047.350	1047.3486	Campbell and Synott, 1985
Saturn	3498.5	3498.0	3497.898	Campbell and Anderson, 1989
Uranus	22869.	22960.	22902.98	Jacobson *et al.*, 1992
Neptune	19314.	19314.	19412.24	Jacobson *et al.*, 1991
Pluto	3000000.	130000000.	135200000.	Tholen and Buie, 1997

Also associated with the ephemerides is the set of astronomical constants used in the ephemeris creation; these are listed in Table 3.2. They are provided directly with the ephemerides and should be considered to be an integral part of them; they will sometimes differ from a more standard set, but the differences are necessary for the optimal fitting of the data.

Table 3.2   Auxiliary constants from the JPL Planetary and Lunar Ephemerides DE405/LE405.

Scale (km/au)	149597870.691	GM_{Ceres}	$4.7 \times 10^{-10} GM_{Sun}$
Scale (s/au)	499.0047838061	GM_{Pallas}	$1.0 \times 10^{-10} GM_{Sun}$
Speed of light (km/s)	299792.458	GM_{Vesta}	$1.3 \times 10^{-10} GM_{Sun}$
Obliquity of the ecliptic	$23°26'21.409''$	density$_{classC}$	1.8
Earth-Moon mass ratio	81.30056	density$_{classS}$	2.4
		density$_{classM}$	5.0

---

[2]http://ssd.jpl.nasa.gov/iau-comm4

References

Astronomical Almanac for the Year 1984, U.S. Government Printing Office, Washington, DC.

Anderson, J. D., Colombo, G., Esposito, P. B., Lau, E. L., and Trager, G. B., 1987, "The Mass Gravity Field and Ephemeris of Mercury," *Icarus*, **71**, pp. 337–349.

Campbell, J. K. and Anderson, J. D., 1989, "Gravity Field of the Saturnian System from Pioneer and Voyager Tracking Data," *Astron. J.*, **97**, pp. 1485–1495.

Campbell, J. K. and Synott, S. P., 1985, "Gravity Field of the Jovian System from Pioneer and Voyager Tracking Data," *Astron. J.*, **90**, pp. 364–372.

Jacobson, R. A., Riedel, J. E. and Taylor, A. H., 1991, "The Orbits of Triton and Nereid from Spacecraft and Earth-based Observations," *Astron. Astrophys.*, **247**, pp. 565–575.

Jacobson, R. A., Campbell, J. K., Taylor, A. H. and Synott, S. P., 1992, "The Masses of Uranus and its Major Satellites from Voyager Tracking Data and Earth-based Uranian Satellite Data," *Astron J.*, **103**(6), pp. 2068–2078.

Null, G. W., 1969, "A Solution for the Mass and Dynamical Oblateness of Mars Using Mariner-IV Doppler Data," *Bull. Amer. Astron. Soc.*, **1**, p. 356.

Sjogren, W. L., Trager, G. B., and Roldan G. R., 1990, "Venus: A Total Mass Estimate," *Geophys. Res. Lett.*, **17**, pp. 1485–1488.

Standish, E. M., 1990, "The Observational Basis for JPL's DE200, the Planetary Ephemerides of the Astronomical Almanac," *Astron. Astrophys.*, **233**, pp. 252–271.

Standish, E. M., 1997, (result from least squares adjustment of DE405/ LE405).

Standish, E. M., 1998, "Time Scales in the JPL and CfA Ephemerides," *Astron. Astrophys.*, **336**, pp. 381–384.

Tholen, D. J. and Buie, M. W., 1997, "The Orbit of Charon. I. New Hubble Space Telescope Observations," *Icarus*, **125**, pp. 245–260.

4   Conventional Terrestrial Reference System and Frame

4.1   Concepts and Terminology

4.1.1   Basic Concepts

A Terrestrial Reference System (TRS) is a spatial reference system co-rotating with the Earth in its diurnal motion in space. In such a system, positions of points attached to the solid surface of the Earth have coordinates which undergo only small variations with time, due to geophysical effects (tectonic or tidal deformations). A Terrestrial Reference Frame (TRF) is a set of physical points with precisely determined coordinates in a specific coordinate system (Cartesian, geographic, mapping...) attached to a Terrestrial Reference System. Such a TRF is said to be a realization of the TRS. These concepts have been defined extensively by the astronomical and geodetic communities (Kovalevsky *et al.*, 1989, Boucher, 2001).

Ideal Terrestrial Reference Systems. An ideal Terrestrial Reference System (TRS) is defined as a reference trihedron close to the Earth and co-rotating with it. In the Newtonian framework, the physical space is considered as an Euclidian affine space of dimension 3. In this case, such a reference trihedron is an Euclidian affine frame (O,E). O is a point of the space named **origin**. E is a basis of the associated vector space. The currently adopted restrictions on E are to be right-handed, orthogonal with the same length for the basis vectors. The triplet of unit vectors collinear to the basis vectors will express the **orientation** of the TRS and the common length of these vectors its **scale**,

$$\lambda = \|\vec{E}_i\|_{i=1,2,3}. \tag{1}$$

We consider here systems for which the origin is close to the Earth's center of mass (geocenter), the orientation is equatorial (the Z axis is the direction of the pole) and the scale is close to an SI meter. In addition to Cartesian coordinates (naturally associated with such a TRS), other coordinate systems, *e.g.* geographical coordinates, could be used. For a general reference on coordinate systems, see Boucher (2001).

Under these hypotheses, the general transformation of the Cartesian coordinates of any point close to the Earth from TRS (1) to TRS (2) will be given by a three-dimensional similarity ($\vec{T}_{1,2}$ is a translation vector, $\lambda_{1,2}$ a scale factor and $R_{1,2}$ a rotation matrix)

$$\vec{X}^{(2)} = \vec{T}_{1,2} + \lambda_{1,2} \cdot R_{1,2} \cdot \vec{X}^{(1)}. \tag{2}$$

This concept can be generalized in the frame of a relativistic background model such as Einstein's General Relativity, using the spatial part of a local Cartesian frame (Boucher, 1986). For more details concerning general relativistic models, see Chapters 10 and 11.

In the application of (2), the IERS uses the linearized formulas and notation. The standard transformation between two reference systems is a Euclidian similarity of seven parameters: three translation components, one scale factor, and three rotation angles, designated respectively, $T1$, $T2$, $T3$, D, $R1$, $R2$, $R3$, and their first time derivatives: $\dot{T}1$, $\dot{T}2$, $\dot{T}3$, $\dot{D}$, $\dot{R}1$, $\dot{R}2$, $\dot{R}3$. The transformation of a coordinate vector $\vec{X}_1$, expressed in reference system (1), into a coordinate vector $\vec{X}_2$, expressed in reference system (2), is given by

$$\vec{X}_2 = \vec{X}_1 + \vec{\mathcal{T}} + D\vec{X}_1 + \mathcal{R}\vec{X}_1, \tag{3}$$

$\lambda_{1,2} = 1 + D$, $R_{1,2} = (I + \mathcal{R})$, and I is the identity matrix with

$$\mathcal{T} = \begin{pmatrix} T1 \\ T2 \\ T3 \end{pmatrix}, \quad \mathcal{R} = \begin{pmatrix} 0 & -R3 & R2 \\ R3 & 0 & -R1 \\ -R2 & R1 & 0 \end{pmatrix}.$$

It is assumed that equation (3) is linear for sets of station coordinates provided by space geodesy techniques. Origin differences are about a few hundred meters, and differences in scale and orientation are at the level of 10^{-5}. Generally, $\vec{X}_1, \vec{X}_2, \mathcal{T}, D, \mathcal{R}$ are functions of time. Differentiating equation (3) with respect to time gives

$$\dot{\vec{X}}_2 = \dot{\vec{X}}_1 + \dot{\mathcal{T}} + \dot{D}\vec{X}_1 + D\dot{\vec{X}}_1 + \dot{\mathcal{R}}\vec{X}_1 + \mathcal{R}\dot{\vec{X}}_1. \tag{4}$$

D and $\mathcal{R}$ are at the 10^{-5} level and $\dot{X}$ is about 10 cm per year, the terms $D\dot{\vec{X}}_1$ and $\mathcal{R}\dot{\vec{X}}_1$ which represent about 0.1 mm over 100 years are negligible. Therefore, equation (4) could be written as

$$\dot{\vec{X}}_2 = \dot{\vec{X}}_1 + \dot{\mathcal{T}} + \dot{D}\vec{X}_1 + \dot{\mathcal{R}}\vec{X}_1. \tag{5}$$

Conventional Terrestrial Reference System (CTRS). A CTRS is defined by the set of all conventions, algorithms and constants which provide the origin, scale and orientation of that system and their time evolution.

Conventional Terrestrial Reference Frame (CTRF). A Conventional Terrestrial Reference Frame is defined as a set of physical points with precisely determined coordinates in a specific coordinate system as a realization of an ideal Terrestrial Reference System. Two types of frames are currently distinguished, namely dynamical and kinematical, depending on whether or not a dynamical model is applied in the process of determining these coordinates.

4.1.2 TRF in Space Geodesy

Seven parameters are needed to fix a TRF at a given epoch, to which are added their time-derivatives to define the TRF time evolution. The selection of the 14 parameters, called "datum definition," establishes the TRF origin, scale, orientation and their time evolution.

Space geodesy techniques are not sensitive to all the parameters of the TRF datum definition. The origin is theoretically accessible through dynamical techniques (LLR, SLR, GPS, DORIS), being the center of mass (point around which the satellite orbits). The scale depends on some physical parameters (*e.g.* geo-gravitational constant GM and speed of light c) and relativistic modelling. The orientation, unobservable by any technique, is arbitrary or conventionally defined. Meanwhile it is recommended to define the orientation time evolution using a no-net-rotation condition with respect to horizontal motions over the Earth's surface.

Since space geodesy observations do not contain all the necessary information to completely establish a TRF, some additional information is then needed to complete the datum definition. In terms of normal equations, usually constructed upon space geodesy observations, this situation is reflected by the fact that the normal matrix, N, is singular, since it has a rank deficiency corresponding to the number of datum parameters which are not reduced by the observations.

In order to cope with this rank deficiency, the analysis centers currently add one of the following constraints upon all or a sub-set of stations:

1. Removable constraints: solutions for which the estimated station positions and/or velocities are constrained to external values within

an uncertainty $\sigma \approx 10^{-5}$ m for positions and m/y for velocities. This type of constraint is easily removable, see for instance Altamimi *et al.* (2002a; 2002b).

2. Loose constraints: solutions where the uncertainty applied to the constraints is $\sigma \geq 1$ m for positions and ≥ 10 cm/y for velocities.

3. Minimum constraints used solely to define the TRF using a minimum amount of required information. For more details on the concepts and practical use of minimum constraints, see for instance Sillard and Boucher (2001) and Altamimi *et al.* (2002a).

Note that the old method where very tight constraints ($\sigma \leq 10^{-10}$ m) are applied (which are numerically not easy to remove), is no longer suitable and may alter the real quality of the estimated parameters.

In case of removable or loose constraints, this amounts to adding the following observation equation

$$\vec{X} - \vec{X}_0 = 0, \tag{6}$$

where $\vec{X}$ is the vector of estimated parameters (positions and/or velocities) and $\vec{X}_0$ is that of the *a priori* parameters.

Meanwhile, in case of minimum constraints, the added equation is of the form

$$B(\vec{X} - \vec{X}_0) = 0, \tag{7}$$

where $B = (A^T A)^{-1} A^T$ and A is the design matrix of partial derivatives, constructed upon *a priori* values ($\vec{X}_0$) given by either

$$A = \begin{pmatrix} \vdots & \vdots & \vdots & \vdots & \vdots & \vdots & \vdots \\ 1 & 0 & 0 & x_0^i & 0 & z_0^i & -y_0^i \\ 0 & 1 & 0 & y_0^i & -z_0^i & 0 & x_0^i \\ 0 & 0 & 1 & z_0^i & y_0^i & -x_0^i & 0 \\ \vdots & \vdots & \vdots & \vdots & \vdots & \vdots & \vdots \end{pmatrix} \tag{8}$$

when solving for only station positions, or

$$A = \begin{pmatrix} \vdots & \vdots & \vdots & \vdots & \vdots & \vdots & \vdots & \vdots & \vdots & \vdots & \vdots & \vdots & \vdots & \vdots \\ 1 & 0 & 0 & x_i^0 & 0 & z_i^0 & -y_i^0 \\ 0 & 1 & 0 & y_i^0 & -z_i^0 & 0 & x_i^0 & & & \approx 0 \\ 0 & 0 & 1 & z_i^0 & y_i^0 & -x_i^0 & 0 \\ & & & & & & & 1 & 0 & 0 & x_i^0 & 0 & z_i^0 & -y_i^0 \\ & & \approx 0 & & & & & 0 & 1 & 0 & y_i^0 & -z_i^0 & 0 & x_i^0 \\ & & & & & & & 0 & 0 & 1 & z_i^0 & y_i^0 & -x_i^0 & 0 \\ \vdots & \vdots & \vdots & \vdots & \vdots & \vdots & \vdots & \vdots & \vdots & \vdots & \vdots & \vdots & \vdots & \vdots \end{pmatrix} \tag{9}$$

when solving for station positions and velocities.

The fundamental distinction between the two approaches is that in equation (6), we force $\vec{X}$ to be equal to $\vec{X}_0$ (to a given σ), while in equation (7) we express $\vec{X}$ in the same TRF as $\vec{X}_0$ using the projector B containing all the necessary information defining the underlying TRF. Note that the two approaches are sensitive to the configuration and quality of the subset of stations ($\vec{X}_0$) used in these constraints.

In terms of normal equations, equation (7) could be written as

$$(B^T \Sigma_\theta^{-1} B)\vec{X} = (B^T \Sigma_\theta^{-1} B)\vec{X}_0, \tag{10}$$

where Σ_θ is a diagonal matrix containing small variances for each of the transformation parameters. Adding equation (10) to the singular normal matrix N allows it to be inverted and simultaneously to express the estimated solution in the same TRF as the *a priori* solution $\vec{X}_0$. Note that the 7 columns of the design matrix A correspond to the 7 datum parameters (3 translations, 1 scale factor and 3 rotations). Therefore this matrix should be reduced to those parameters which need to be defined (*e.g.* 3 rotations in almost all techniques and 3 translations in case of VLBI). For more practical details, see, for instance, Altamimi *et al.* (2002a).

4.1.3 Crust-based TRF

In general, various types of TRF can be considered. In practice two major categories are used:

- positions of satellites orbiting around the Earth, expressed in a TRS. This is the case for navigation satellite systems or satellite radar altimetry, see section 4.3;

- positions of points fixed on solid Earth crust, mainly tracking instruments or geodetic markers (see sub-section 4.2.1).

Such crust-based TRF are those currently determined in IERS activities, either by analysis centers or by combination centers, and ultimately as IERS products (see sub-section 4.1.5).

The general model connecting the instantaneous actual position of a point anchored on the Earth's crust at epoch t, $\vec{X}(t)$, and a regularized position $\vec{X}_R(t)$ is

$$\vec{X}(t) = \vec{X}_R(t) + \sum_i \Delta \vec{X}_i(t). \tag{11}$$

The purpose of the introduction of a regularized position is to remove high-frequency time variations (mainly geophysical ones) using conventional corrections $\Delta \vec{X}_i(t)$, in order to obtain a position with regular time variation. In this case, $\vec{X}_R$ can be estimated by using models and numerical values. The current model is linear (position at a reference epoch t_0 and velocity):

$$\vec{X}_R(t) = \vec{X}_0 + \dot{\vec{X}} \cdot (t - t_0). \tag{12}$$

The numerical values are $(\vec{X}_0, \dot{\vec{X}})$. In the past (ITRF88 and ITRF89), constant values were used as models ($\vec{X}_0$), the linear motion being incorporated as conventional corrections derived from a tectonic plate motion model (see sub-section 4.2.2).

Conventional models are presented in Chapter 7 for solid Earth tides, ocean loading, pole tide, atmospheric loading, and geocenter motion.

4.1.4 The International Terrestrial Reference System

The IERS is in charge of defining, realizing and promoting the International Terrestrial Reference System (ITRS) as defined by the IUGG Resolution No. 2 adopted in Vienna, 1991 (*Geodesist's Handbook*, 1992). The resolution recommends the following definitions of the TRS: "1) CTRS to be defined from a geocentric non-rotating system by a spatial rotation leading to a quasi-Cartesian system, 2) the geocentric non-rotating system to be identical to the Geocentric Reference System (GRS) as defined in the IAU resolutions, 3) the coordinate-time of the

CTRS as well as the GRS to be the Geocentric Coordinate Time (TCG), 4) the origin of the system to be the geocenter of the Earth's masses including oceans and atmosphere, and 5) the system to have no global residual rotation with respect to horizontal motions at the Earth's surface."

The ITRS definition fulfills the following conditions.

1. It is geocentric, the center of mass being defined for the whole Earth, including oceans and atmosphere;

2. The unit of length is the meter (SI). This scale is consistent with the TCG time coordinate for a geocentric local frame, in agreement with IAU and IUGG (1991) resolutions. This is obtained by appropriate relativistic modelling;

3. Its orientation was initially given by the Bureau International de l'Heure (BIH) orientation at 1984.0;

4. The time evolution of the orientation is ensured by using a no-net-rotation condition with regards to horizontal tectonic motions over the whole Earth.

4.1.5 Realizations of the ITRS

Realizations of the ITRS are produced by the IERS ITRS Product Center (ITRS-PC) under the name International Terrestrial Reference Frame (ITRF). The current procedure is to combine individual TRF solutions computed by IERS analysis centers using observations of space geodesy techniques: VLBI, LLR, SLR, GPS and DORIS. These individual TRF solutions currently contain station positions and velocities together with full variance matrices provided in the SINEX format. The combination model used to generate ITRF solutions is essentially based on the transformation formulas of equations (3) and (5). The combination method makes use of local ties in collocation sites where two or more geodetic systems are operated. The local ties are used as additional observations with proper variances. They are usually derived from local surveys using either classical geodesy or the Global Positioning System (GPS). As they represent a key element of the ITRF combination, they should be better or at least as accurate as the individual space geodesy solutions incorporated in the ITRF combination.

Currently, ITRF solutions are published nearly annually by the ITRS-PC in the *Technical Notes* (*cf.* Boucher *et al.*, 1999). The numbers (yy) following the designation "ITRF" specify the last year whose data were used in the formation of the frame. Hence ITRF97 designates the frame of station positions and velocities constructed in 1999 using all of the IERS data available until 1998.

The reader may also refer to the report of the ITRF Working Group on the ITRF Datum (Ray *et al.*, 1999), which contains useful information related to the history of the ITRF datum definition. It also details technique-specific effects on some parameters of the datum definition, in particular the origin and the scale.

4.2 ITRF Products

4.2.1 The IERS Network

The initial definition of the IERS network

The IERS network was initially defined through all tracking instruments used by the various individual analysis centers contributing to the IERS. All SLR, LLR and VLBI systems were included. Eventually, GPS stations from the IGS were added as well as the DORIS tracking network. The network also included, from its beginning, a selection of ground

markers, specifically those used for mobile equipment and those currently included in local surveys performed to monitor local eccentricities between instruments for collocation sites or for site stability checks.

Each point is currently identified by the attribution of a DOMES number. The explanations of the DOMES numbering system is given below. Close points are clustered into a site. The current rule is that all points which could be linked by a collocation survey (up to 30 km) should be included as a unique site of the IERS network having a unique DOMES site number.

Collocations

In the frame of the IERS, the concept of collocation can be defined as the fact that two instruments are occupying simultaneously or subsequently very close locations that are very precisely surveyed in three dimensions. These include situations such as simultaneous or non-simultaneous measurements and instruments of the same or different techniques.

As typical illustrations of the potential use of such data, we can mention:

1. calibration of mobile systems, for instance SLR or GPS antennas, using simultaneous measurements of instruments of the same technique;

2. repeated measurements on a marker with mobile systems (for instance mobile SLR or VLBI), using non-simultaneous measurements of instruments of the same technique;

3. changes in antenna location for GPS or DORIS;

4. collocations between instruments of different techniques, which implies eccentricities, except in the case of successive occupancies of a given marker by various mobile systems.

Usually, collocated points should belong to a unique IERS site.

Extensions of the IERS network

Recently, following the requirements of various user communities, the initial IERS network was expanded to include new types of systems which are of potential interest. Consequently, the current types of points allowed in the IERS and for which a DOMES number can be assigned are (IERS uses a one character code for each type):

- satellite laser ranging (SLR) (L),
- lunar laser ranging (LLR) (M),
- VLBI (R),
- GPS (P),
- DORIS (D) also Doppler NNSS in the past,
- optical astrometry (A) –formerly used by the BIH–,
- PRARE (X),
- tide gauge (T),
- meteorological sensor (W).

For instance, the cataloging of tide gauges collocated with IERS instruments, in particular GPS or DORIS, is of interest for the Global Sea Level Observing System (GLOSS) program under the auspices of UNESCO.

Another application is to collect accurate meteorological surface measurements, in particular atmospheric pressure, in order to derive raw tropospheric parameters from tropospheric propagation delays that can be estimated during the processing of radio measurements, *e.g.* made

by the GPS, VLBI, or DORIS space techniques. Other systems could also be considered if it was considered as useful (for instance systems for time transfer, super-conducting or absolute gravimeters...) These developments were undertaken to support the conclusions of the CSTG Working Group on Fundamental Reference and Calibration Network.

Another important extension is the wish of some continental or national organizations to see their fiducial networks included into the IERS network, either to be computed by IERS (for instance the European Reference Frame (EUREF) permanent GPS network) or at least to get DOMES numbers (for instance the Continuously Operating Reference Stations (CORS) network in USA). Such extensions are supported by the IAG Commission X on Global and Regional Geodetic Networks (GRGN) in order to promulgate the use of the ITRS.

4.2.2   History of ITRF Products

The history of the ITRF goes back to 1984, when for the first time a combined TRF (called BTS84), was established using station coordinates derived from VLBI, LLR, SLR and Doppler/ TRANSIT (the predecessor of GPS) observations (Boucher and Altamimi, 1985). BTS84 was realized in the framework of the activities of BIH, being a coordinating center for the international MERIT project (Monitoring of Earth Rotation and Inter-comparison of Techniques) (Wilkins, 2000). Three other successive BTS realizations were then achieved, ending with BTS87, when in 1988, the IERS was created by the IUGG and the International Astronomical Union (IAU).

Until the time of writing, 10 versions of the ITRF were published, starting with ITRF88 and ending with ITRF2000, each of which superseded its predecessor.

From ITRF88 till ITRF93, the ITRF Datum Definition is summarized as follows:

- Origin and Scale: defined by an average of selected SLR solutions;

- Orientation: defined by successive alignment since BTS87 whose orientation was aligned to the BIH EOP series. Note that the ITRF93 orientation and its rate were again realigned to the IERS EOP series;

- Orientation Time Evolution: No global velocity field was estimated for ITRF88 and ITRF89 and so the AM0-2 model of (Minster and Jordan, 1978) was recommended. Starting with ITRF91 and till ITRF93, combined velocity fields were estimated. The ITRF91 orientation rate was aligned to that of the NNR-NUVEL-1 model, and ITRF92 to NNR-NUVEL-1A (Argus and Gordon, 1991), while ITRF93 was aligned to the IERS EOP series.

Since the ITRF94, full variance matrices of the individual solutions incorporated in the ITRF combination were used. At that time, the ITRF94 datum was achieved as follows (Boucher *et al.*, 1996):

- Origin: defined by a weighted mean of some SLR and GPS solutions;

- Scale: defined by a weighted mean of VLBI, SLR and GPS solutions, corrected by 0.7 ppb to meet the IUGG and IAU requirement to be in the TCG (Geocentric Coordinate Time) time-frame instead of TT (Terrestrial Time) used by the analysis centers;

- Orientation: aligned to the ITRF92;

- Orientation time evolution: aligned the velocity field to the model NNR-NUVEL-1A, over the 7 rates of the transformation parameters.

The ITRF96 was then aligned to the ITRF94, and the ITRF97 to the ITRF96 using the 14 transformation parameters (Boucher *et al.*, 1998; 1999).

The ITRF network has improved with time in terms of the number of sites and collocations as well as their distribution over the globe. Figure 4.1 shows the ITRF88 network having about 100 sites and 22 collocations (VLBI/SLR/LLR), and the ITRF2000 network containing about 500 sites and 101 collocations. The ITRF position and velocity precisions have also improved with time, thanks to analysis strategy improvements both by the IERS Analysis Centers and the ITRF combination as well as their mutual interaction. Figure 4.2 displays the formal errors in positions and velocities, comparing ITRF94, 96, 97, and ITRF2000.
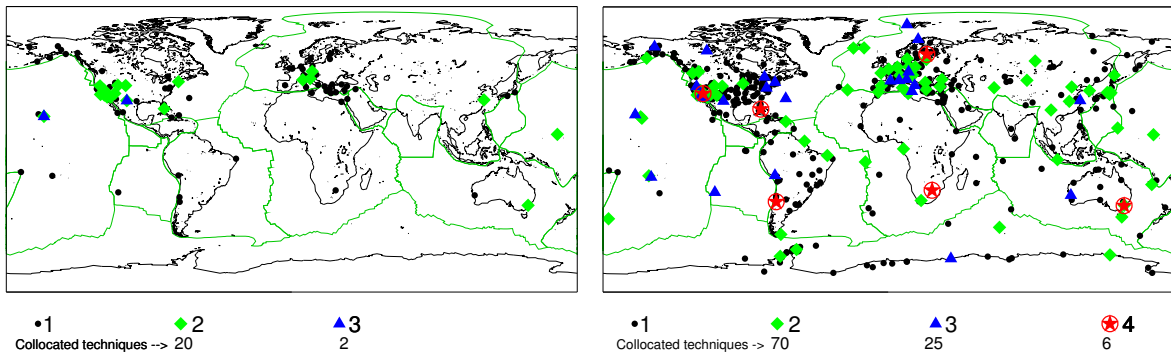
Fig. 4.1   ITRF88 (left) and ITRF2000 (right) sites and collocated techniques.
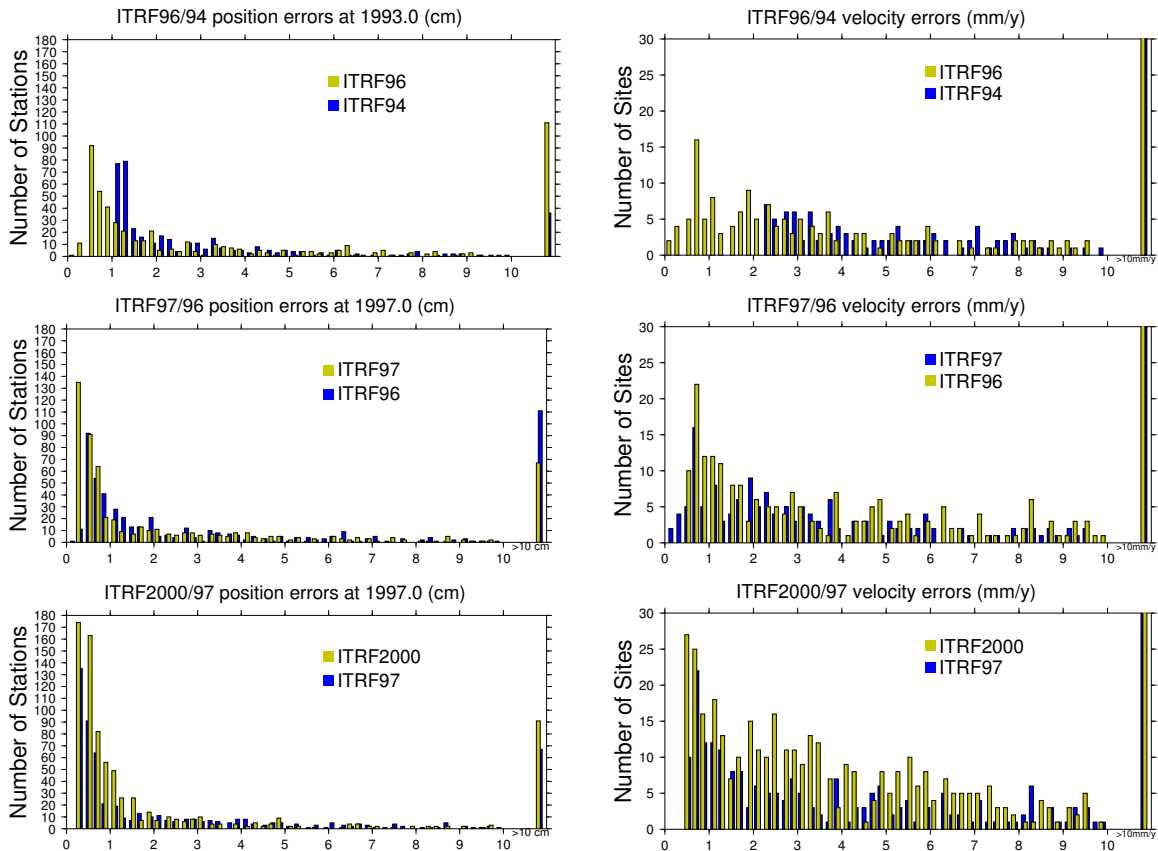
Fig. 4.2   Formal errors evolution between different ITRF versions in position (left) and velocity (right).

4.2.3 ITRF2000, the Current Reference Realization of the ITRS

The ITRF2000 is intended to be a standard solution for geo-referencing and all Earth science applications. In addition to primary core stations observed by VLBI, LLR, SLR, GPS and DORIS, the ITRF2000 is densified by regional GPS networks in Alaska, Antarctica, Asia, Europe, North and South America and the Pacific.

The individual solutions used in the ITRF2000 combination are generated by the IERS analysis centers using removable, loose or minimum constraints.

In terms of datum definition, the ITRF2000 is characterized by the following properties:

- the scale is realized by setting to zero the scale and scale rate parameters between ITRF2000 and a weighted average of VLBI and most consistent SLR solutions. Unlike the ITRF97 scale expressed in the TCG-frame, that of the ITRF2000 is expressed in the TT-frame;

- the origin is realized by setting to zero the translation components and their rates between ITRF2000 and a weighted average of most consistent SLR solutions;

- the orientation is aligned to that of the ITRF97 at 1997.0 and its rate is aligned, conventionally, to that of the geological model NNR-NUVEL-1A (Argus and Gordon, 1991; DeMets *et al.*, 1990; 1994). This is an implicit application of the no-net-rotation condition, in agreement with the ITRS definition. The ITRF2000 orientation and its rate were established using a selection of ITRF sites with high geodetic quality, satisfying the following criteria:

    1. continuous observation for at least 3 years;
    2. locations far from plate boundaries and deforming zones;
    3. velocity accuracy (as a result of the ITRF2000 combination) better than 3 mm/y;
    4. velocity residuals less than 3 mm/y for at least 3 different solutions.

The ITRF2000 results show significant disagreement with the geological model NUVEL-1A in terms of relative plate motions (Altamimi *et al.*, 2002b). Although the ITRF2000 orientation rate alignment to NNR-NUVEL-1A is ensured at the 1 mm/y level, regional site velicity differences between the two may exceed 3 mm/y. Meanwhile it should be emphasized that these differences do not at all disrupt the internal consistency of the ITRF2000, simply because the alignment defines the ITRF2000 orientation rate and nothing more. Moreover, angular velocities of tectonic plates which would be estimated using ITRF2000 velocities may significantly differ from those predicted by the NNR-NUVEL-1A model.

4.2.4 Expression in ITRS using ITRF

The procedure used in the IERS to determine ITRF products includes several steps:

1. definition of individual TRF used by contributing analysis centers. This implies knowing the particular conventional corrections adopted by each analysis center.

2. determination of the ITRF by the combination of individual TRF and datum fixing. This implies adoption for the ITRF of a set of conventional corrections and ensures the consistency of the combination by removing possible differences between corrections adopted by each contributing analysis centers;

3. definitions of corrections for users to get best estimates of positions in ITRS.

In this procedure, the current status is as follows:

A) *Solid Earth Tides*

Since the beginning, all analysis centers use a conventional tide-free correction, first published in MERIT Standards, $\Delta \vec{X}_{tidM}$. Consequently, the ITRF has adopted the same option and is therefore a "conventional tide free" frame, according to the nomenclature in the Introduction. To adopt a different model, $\Delta \vec{X}_{tid}$, a user then needs to apply the following formula to get the regularized position $\vec{X}_R$ consistent with this model:

$$\vec{X}_R = \vec{X}_{ITRF} + (\Delta \vec{X}_{tidM} - \Delta \vec{X}_{tid}). \tag{13}$$

For more details concerning tidal corrections, see Chapter 7.

B) *Relativistic scale*

All individual centers use the TT scale. In the same manner the ITRF has also adopted this option (except ITRF94, 96 and 97, see sub-section 4.2.2). It should be noted that the ITRS is specified to be consistent with the TCG scale. Consequently, the regularized positions strictly expressed in the ITRS have to be computed using

$$\vec{X}_R = (1 + L_G)\vec{X}_{ITRF} \tag{14}$$

where $L_G = 0.6969290134 \times 10^{-9}$ (IAU Resolution B1.9, 24th IAU General Assembly, Manchester 2000).

C) *Geocentric positions*

The ITRF origin is fixed in the datum definition. In any case, it should be considered as a figure origin related to the crust. In order to obtain a truly geocentric position, following the ITRS definition, one must apply the geocenter motion correction $\Delta \vec{X}_G$

$$\vec{X}_{ITRS} = \vec{X}_{ITRF} + \Delta \vec{X}_G. \tag{15}$$

Noting $O_G(t)$ the geocenter motion in ITRF, (see, Ray *et al.*, 1999), then

$$\Delta \vec{X}_G(t) = -\vec{O}_G(t). \tag{16}$$

4.2.5 Transformation Parameters between ITRF Solutions

Table 4.1 lists transformation parameters and their rates from ITRF2000 to previous ITRF versions, which should be used with equations (3) and (5) given above. The values listed in this table have been compiled from those already published in previous IERS Technical Notes as well as from the recent ITRF2000/ITRF97 comparison. Moreover, it should be noted that these parameters are adjusted values which are heavily dependent on the weighting as well as the number and distribution of the implied common sites between these frames. Therefore, using different subsets of common stations between two ITRF solutions to estimate transformation parameters would not necessarily yield values consistent with those of Table 4.1.

ITRF solutions are specified by Cartesian equatorial coordinates X, Y, and Z. If needed, they can be transformed to geographical coordinates (λ, ϕ, h) referred to an ellipsoid. In this case the GRS80 ellipsoid is recommended (semi-major axis a=6378137.0 m, eccentricity^2 =0.00669438002290). See the IERS Conventions' web page for the subroutine at $<^3>$.

---

[3]http://maia.usno.navy.mil/conv2000.html

Table 4.1 Transformation parameters from ITRF2000 to past ITRFs. "ppb" refers to parts per billion (or 10^{-9}). The units for rate are understood to be "per year."

ITRF Solution	$T1$ (cm)	$T2$ (cm)	$T3$ (cm)	D (ppb)	$R1$ (mas)	$R2$ (mas)	$R3$ (mas)	Epoch
ITRF97	0.67	0.61	-1.85	1.55	0.00	0.00	0.00	1997.0
rates	0.00	-0.06	-0.14	0.01	0.00	0.00	0.02	
ITRF96	0.67	0.61	-1.85	1.55	0.00	0.00	0.00	1997.0
rates	0.00	-0.06	-0.14	0.01	0.00	0.00	0.02	
ITRF94	0.67	0.61	-1.85	1.55	0.00	0.00	0.00	1997.0
rates	0.00	-0.06	-0.14	0.01	0.00	0.00	0.02	
ITRF93	1.27	0.65	-2.09	1.95	-0.39	0.80	-1.14	1988.0
rates	-0.29	-0.02	-0.06	0.01	-0.11	-0.19	0.07	
ITRF92	1.47	1.35	-1.39	0.75	0.0	0.0	-0.18	1988.0
rates	0.00	-0.06	-0.14	0.01	0.00	0.00	0.02	
ITRF91	2.67	2.75	-1.99	2.15	0.0	0.0	-0.18	1988.0
rates	0.00	-0.06	-0.14	0.01	0.00	0.00	0.02	
ITRF90	2.47	2.35	-3.59	2.45	0.0	0.0	-0.18	1988.0
rates	0.00	-0.06	-0.14	0.01	0.00	0.00	0.02	
ITRF89	2.97	4.75	-7.39	5.85	0.0	0.0	-0.18	1988.0
rates	0.00	-0.06	-0.14	0.01	0.00	0.00	0.02	
ITRF88	2.47	1.15	-9.79	8.95	0.1	0.0	-0.18	1988.0
rates	0.00	-0.06	-0.14	0.01	0.00	0.00	0.02	

4.3 Access to the ITRS

Several ways could be used to express point positions in the ITRS. We mention here very briefly some procedures:

- direct use of ITRF station positions;
- use of IGS products (*e.g.* orbits and clocks) which are nominally all referred to the ITRF. However, users should be aware of the ITRF version used in the generation of the IGS products. Note also that IGS/GPS orbits themselves belong to the first TRF category described in sub-section 4.1.3;
- Fixing or constraining some ITRF station coordinates in the analysis of GPS measurements of a campaign or permanent stations;
- use of transformation formulas which would be estimated between a particular TRF and an ITRF solution.

Other useful details are also available in Boucher and Altamimi (1996).

References

Altamimi, Z., Boucher, C., and Sillard, P., 2002a, "New Trends for the Realization of the International Terrestrial Reference System," *Adv. Space Res.*, **30, No. 2**, pp. 175–184.

Altamimi, Z., Sillard, P., and Boucher, C., 2002b, "ITRF2000: A New Release of the International Terrestrial Reference Frame for Earth Science Applications," *J. Geophys. Res.*, **107, B10**, 10.1029/2001JB000561.

Argus, D. F. and Gordon, R. G., 1991, "No-Net-Rotation Model of Current Plate Velocities Incorporating Plate Motion Model Nuvel-1," *Geophys. Res. Lett.*, **18**, pp. 2038–2042.

Boucher, C., 1986, "Relativistic effects in Geodynamics," in *Reference Frames in Celestial Mechanics and Astrometry*, Kovalevsky, J. and Brumberg, V. A. (eds.), Reidel, pp. 241–253.

Boucher, C., 2001, "Terrestrial coordinate systems and frames," in *Encyclopedia of Astronomy and Astrophysics*, Version 1.0, Nature Publishing Group, and Bristol: Institute of Physics Publishing, pp. 3289–3292,

Boucher, C. and Altamimi, Z., 1985, "Towards an improved realization of the BIH terrestrial frame," *The MERIT/COTES Report on Earth Rotation and Reference Frames,* Vol. 2, Mueller, I. I. (ed.), OSU/DGS, Columbus, Ohio, USA.

Boucher, C. and Altamimi, Z., 1996, "International Terrestrial Reference Frame," *GPS World*, **7**, pp. 71–74.

Boucher, C., Altamimi, Z., Feissel, M., and Sillard, P., 1996, "Results and Analysis of the ITRF94," *IERS Technical Note*, **20**, Observatoire de Paris, Paris.

Boucher, C., Altamimi, Z., and Sillard, P., 1998, "Results and and Analysis of the ITRF96," *IERS Technical Note*, **24**, Observatoire de Paris, Paris.

Boucher, C., Altamimi, Z., and Sillard, P., 1999, "The 1997 International Terrestrial Reference Frame (ITRF97)," *IERS Technical Note*, **27**, Observatoire de Paris, Paris.

DeMets , C., Gordon, R. G., Argus, D. F., and Stein S., 1990, "Current plate motions," *J. Geophys. Res.*, **101**, pp. 425–478.

DeMets, C., Gordon, R. G., Argus, D. F., and Stein, S., 1994, "Effect of recent revisions to the geomagnetic reversal time scale on estimates of current plate motions," *Geophys. Res. Lett.*, **21**, pp. 2191–2194.

*Geodesist's Handbook***,** 1992, *Bulletin Géodésique*, **66**, 128 pp.

Kovalevsky, J., Mueller, I. I., and Kolaczek, B., (Eds.), 1989, *Reference Frames in Astronomy and Geophysics,* Kluwer Academic Publisher, Dordrecht, 474 pp.

Minster, J. B., and Jordan, T. H., 1978, "Present-day plate motions," *J. Geophys. Res.*, **83**, pp. 5331–5354.

Ray, J., Blewitt, G., Boucher, C., Eanes, R., Feissel, M., Heflin, M., Herring, T., Kouba, J., Ma, C., Montag, H., Willis, P., Altamimi, Z., Eubanks, T. M., Gambis, D., Petit, G., Ries, J., Scherneck, H.-G., Sillard, P., 1999, "Report of the Working Group on ITRF Datum."

Sillard, P. and C. Boucher, 2001, "Review of Algebraic Constraints in Terrestrial Reference Frame Datum Definition," *J. Geod.*, **75**, pp. 63–73.

Wilkins, G. A. (Ed.), 2000, "Report on the Third MERIT Workshop and the MERIT-COTES Joint Meeting," Part 1, Columbus, Ohio, USA, 29-30 July and 3 August 1985, *Scientific Technical Report STR99/25,* GeoForschungsZentrum Potsdam.

5   Transformation Between the Celestial and Terrestrial Systems

The coordinate transformation to be used to transform from the terrestrial reference system (TRS) to the celestial reference system (CRS) at the epoch t of the observation can be written as:

$$[\text{CRS}] = Q(t)R(t)W(t)\ [\text{TRS}], \tag{1}$$

where $Q(t)$, $R(t)$ and $W(t)$ are the transformation matrices arising from the motion of the celestial pole in the celestial system, from the rotation of the Earth around the axis of the pole, and from polar motion respectively. The frame as realized from the [TRS] by applying the transformations $W(t)$ and then $R(t)$ will be called "the intermediate reference frame of epoch t."

5.1   The Framework of IAU 2000 Resolutions

Several resolutions were adopted by the XXIVth General Assembly of the International Astronomical Union (Manchester, August 2000) that concern the transformation between the celestial and terrestrial reference systems and are therefore to be implemented in the IERS procedures. Such a transformation being also required for computing directions of celestial objects in intermediate systems, the process to transform among these systems consistent with the IAU resolutions is also provided at the end of this chapter.

Resolution B1.3 specifies that the systems of space-time coordinates as defined by IAU Resolution A4 (1991) for the solar system and the Earth within the framework of General Relativity are now named the Barycentric Celestial Reference System (BCRS) and the Geocentric Celestial Reference System (GCRS) respectively. It also provides a general framework for expressing the metric tensor and defining coordinate transformations at the first post-Newtonian level.

Resolution B1.6 recommends that, beginning on 1 January 2003, the IAU 1976 Precession Model and IAU 1980 Theory of Nutation be replaced by the precession-nutation model IAU 2000A (MHB 2000 based on the transfer functions of Mathews *et al.*, (2002)) for those who need a model at the 0.2 mas level, or its shorter version IAU 2000B for those who need a model only at the 1 mas level, together with their associated celestial pole offsets, published in this document.

Resolution B1.7 recommends that the Celestial Intermediate Pole (CIP) be implemented in place of the Celestial Ephemeris Pole (CEP) on 1 January 2003 and specifies how to implement its definition through its direction at J2000.0 in the GCRS as well as the realization of its motion both in the GCRS and ITRS. Its definition is an extension of that of the CEP in the high frequency domain and coincides with that of the CEP in the low frequency domain (Capitaine, 2000).

Resolution B1.8 recommends the use of the "non-rotating origin" (NRO) (Guinot, 1979) both in the GCRS and the ITRS and these origins are designated as the Celestial Ephemeris Origin (CEO) and the Terrestrial Ephemeris Origin (TEO). The "Earth Rotation Angle" is defined as the angle measured along the equator of the CIP between the CEO and the TEO. This resolution recommends that UT1 be linearly proportional to the Earth Rotation Angle and that the transformation between the ITRS and GCRS be specified by the position of the CIP in the GCRS, the position of the CIP in the ITRS, and the Earth Rotation Angle. It is recommended that the IERS takes steps to implement this by 1 January 2003 and that the IERS will continue to provide users with data and algorithms for the conventional transformation.

Following the recommendations above, this chapter of the IERS Conventions provides the expressions for the implementation of the IAU resolutions using the new transformation which is described in Resolution B1.8. It also provides the expressions which are necessary to be compatible with the resolutions when using the conventional transformation. Numerical values contained in this chapter have been slightly revised from earlier provisional values to ensure continuity of the IERS products. Fortran subroutines implementing the transformations are described towards the end of the chapter. More detailed explanations about the relevant concepts, software and IERS products can be found in IERS Technical Note 29 (Capitaine *et al.*, 2002).

5.2   Implementation of IAU 2000 Resolutions

In order to follow Resolution B1.3, the celestial reference system, which is designated here CRS, must correspond to the geocentric space coordinates of the GCRS. IAU Resolution A4 (1991) specified that the relative orientation of barycentric and geocentric spatial axes in BCRS and GCRS are without any time dependent rotation. This requires that the geodesic precession and nutation be taken into account in the precession-nutation model.

Concerning the time coordinates, IAU Resolution A4 (1991) defined TCB and TCG of the BCRS and GCRS respectively, as well as another time coordinate in the GCRS, Terrestrial Time (TT), which is the theoretical counterpart of the realized time scale $TAI + 32.184$ s and has been re-defined by IAU resolution B1.9 (2000). See Chapter 10 for the relationships between these time scales.

The parameter t, used in the following expressions, is defined by

$$t = (TT - 2000 \text{ January 1d 12h TT}) \text{ in days}/36525. \qquad (2)$$

This definition is consistent with IAU Resolution C7 (1994) which recommends that the epoch J2000.0 be defined at the geocenter and at the date 2000 January 1.5 TT = Julian Date 2451545.0 TT.

In order to follow Resolution B1.6, the precession-nutation quantities to be used in the transformation matrix Q(t) must be based on the precession-nutation model IAU 2000A or IAU 2000B depending on the required precision. In order to follow Resolution B1.7, the realized celestial pole must be the CIP. This requires an offset at epoch in the conventional model for precession-nutation as well as diurnal and higher frequency variations in the Earth's orientation. According to this resolution, the direction of the CIP at J2000.0 has to be offset from the pole of the GCRS in a manner consistent with the IAU 2000A Precession-Nutation Model. The motion of the CIP in the GCRS is realized by the IAU 2000 model for precession and forced nutation for periods greater than two days plus additional time-dependent corrections provided by the IERS through appropriate astro-geodetic observations. The motion of the CIP in the ITRS is provided by the IERS through astro-geodetic observations and models including variations with frequencies outside the retrograde diurnal band.

The realization of the CIP thus requires that the IERS monitor the observed differences (reported as "celestial pole offsets") with respect to the conventional celestial position of the CIP in the GCRS based on the IAU 2000 Precession-Nutation Model together with its observed offset at epoch. It also requires that the motion of the CIP in the TRS be provided by the IERS by observations taking into account a predictable part specified by a model including the terrestrial motion of the pole corresponding to the forced nutations with periods less than two days (in the GCRS) as well as the tidal variations in polar motion. Two

equivalent procedures were given in the IERS Conventions (McCarthy, 1996) for the coordinate transformation from the TRS to the CRS. The classical procedure, which was described in detail as option 1, makes use of the equinox for realizing the intermediate reference frame of date t. It uses apparent Greenwich Sidereal Time (GST) in the transformation matrix $R(t)$ and the classical precession and nutation parameters in the transformation matrix $Q(t)$.

The second procedure, which was described in detail as option 2, makes use of the "non-rotating origin" to realize the intermediate reference frame of date t. It uses the "Earth Rotation Angle," originally referred to as "stellar angle" in the transformation matrix $R(t)$, and the two coordinates of the celestial pole in the CRS (Capitaine, 1990) in the transformation matrix $Q(t)$.

Resolutions B1.3, B1.6 and B1.7 can be implemented in any of these procedures if the requirements described above are followed for the space-time coordinates in the geocentric celestial system, for the precession and nutation model on which are based the precession and nutation quantities used in the transformation matrix $Q(t)$ and for the polar motion used in the transformation matrix $W(t)$.

On the other hand, only the second procedure can be in agreement with Resolution B1.8, which requires the use of the "non-rotating origin" both in the CRS and the TRS as well as the position of the CIP in the GCRS and in the ITRS. However, the IERS must also provide users with data and algorithms for the conventional transformation; this implies that the expression of Greenwich Sidereal Time (GST) has to be consistent with the new procedure.

The following sections give the details of this procedure and the standard expressions necessary to obtain the numerical values of the relevant parameters at the date of the observation.

5.3   Coordinate Transformation consistent with the IAU 2000 Resolutions

In the following, R_1, R_2 and R_3 denote rotation matrices with positive angle about the axes 1, 2 and 3 of the coordinate frame. The position of the CIP both in the TRS and CRS is provided by the x and y components of the CIP unit vector. These components are called "coordinates" in the following and their numerical expressions are multiplied by the factor $1296000''/2\pi$ in order to provide in arcseconds the value of the corresponding "angles" with respect to the polar axis of the reference system.

The coordinate transformation (1) from the TRS to the CRS corresponding to the procedure consistent with Resolution B1.8 is expressed in terms of the three fundamental components as given below (Capitaine, 1990)

$$W(t) = R_3(-s') \cdot R_2(x_p) \cdot R_1(y_p), \tag{3}$$

x_p and y_p being the "polar coordinates" of the Celestial Intermediate Pole (CIP) in the TRS and s' being a quantity which provides the position of the TEO on the equator of the CIP corresponding to the kinematical definition of the NRO in the ITRS when the CIP is moving with respect to the ITRS due to polar motion. The expression of s' as a function of the coordinates x_p and y_p is:

$$s'(t) = (1/2) \int_{t_0}^{t} (x_p \dot{y}_p - \dot{x}_p y_p) \, dt. \tag{4}$$

The use of the quantity s', which was neglected in the classical form prior to 1 January 2003, is necessary to provide an exact realization of the "instantaneous prime meridian."

$$R(t) = R_3(-\theta), \tag{5}$$

θ being the Earth Rotation Angle between the CEO and the TEO at date t on the equator of the CIP, which provides a rigorous definition of the sidereal rotation of the Earth.

$$Q(t) = R_3(-E) \cdot R_2(-d) \cdot R_3(E) \cdot R_3(s), \tag{6}$$

E and d being such that the coordinates of the CIP in the CRS are:

$$X = \sin d \cos E, \qquad Y = \sin d \sin E, \qquad Z = \cos d, \tag{7}$$

and s being a quantity which provides the position of the CEO on the equator of the CIP corresponding to the kinematical definition of the NRO in the GCRS when the CIP is moving with respect to the GCRS, between the reference epoch and the epoch t due to precession and nutation. Its expression as a function of the coordinates X and Y is (Capitaine *et al.*, 2000)

$$s(t) = -\int_{t_0}^{t} \frac{X(t)\dot{Y}(t) - Y(t)\dot{X}(t)}{1 + Z(t)} dt - (\sigma_0 N_0 - \Sigma_0 N_0), \tag{8}$$

where σ_0 and Σ_0 are the positions of the CEO at J2000.0 and the x-origin of the GCRS respectively and N_0 is the ascending node of the equator at J2000.0 in the equator of the GCRS. Or equivalently, within 1 microarcsecond over one century

$$s(t) = -\frac{1}{2}[X(t)Y(t) - X(t_0)Y(t_0)] + \int_{t_0}^{t} \dot{X}(t)Y(t)dt - (\sigma_0 N_0 - \Sigma_0 N_0). \tag{9}$$

The arbitrary constant $\sigma_0 N_0 - \Sigma_0 N_0$, which had been conventionally chosen to be zero in previous references (*e.g.* Capitaine *et al.*, 2000), is now chosen to ensure continuity with the classical procedure on 1 January 2003 (see expression (36)).

$Q(t)$ can be given in an equivalent form directly involving X and Y as

$$Q(t) = \begin{pmatrix} 1 - aX^2 & -aXY & X \\ -aXY & 1 - aY^2 & Y \\ -X & -Y & 1 - a(X^2 + Y^2) \end{pmatrix} \cdot R_3(s), \tag{10}$$

with $a = 1/(1 + \cos d)$, which can also be written, with an accuracy of 1 μas, as $a = 1/2 + 1/8(X^2 + Y^2)$. Such an expression of the transformation (1) leads to very simple expressions of the partial derivatives of observables with respect to the terrestrial coordinates of the CIP, UT1, and celestial coordinates of the CIP.

5.4 Parameters to be used in the Transformation

5.4.1 Schematic Representation of the Motion of the CIP

According to Resolution B1.7, the CIP is an intermediate pole separating, by convention, the motion of the pole of the TRS in the CRS into two parts:

- the celestial motion of the CIP (precession/nutation), including all the terms with periods greater than 2 days in the CRS (*i.e.* frequencies between -0.5 counts per sidereal day (cpsd) and $+0.5$ cpsd),
- the terrestrial motion of the CIP (polar motion), including all the terms outside the retrograde diurnal band in the TRS (*i.e.* frequencies lower than -1.5 cpsd or greater than -0.5 cpsd).

frequency in TRS

$\begin{array}{c}\text{----}|\text{--------}|\text{--------}|\text{--------}|\text{--------}|\text{--------}|\text{--------}|\text{ ----}\\ \text{-3.5} \quad \text{-2.5} \quad \text{-1.5} \quad \text{-0.5} \quad \text{+0.5} \quad \text{+1.5} \quad \text{+2.5 (cpsd)}\end{array}$

------ *polar motion* | | *polar motion* ------

frequency in CRS

$\begin{array}{c}\text{----}|\text{--------}|\text{--------}|\text{--------}|\text{--------}|\text{--------}|\text{--------}|\text{ ----}\\ \text{-2.5} \quad \text{-1.5} \quad \text{-0.5} \quad \text{+0.5} \quad \text{+1.5} \quad \text{+2.5} \quad \text{+3.5 (cpsd)}\end{array}$

|*nutation*|
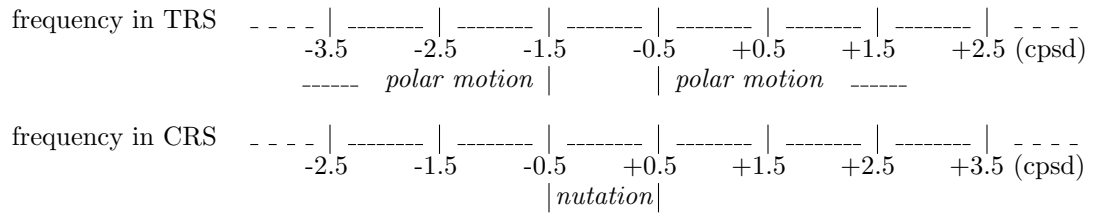
5.4.2   Motion of the CIP in the ITRS

The standard pole coordinates to be used for the parameters x_p and y_p, if not estimated from the observations, are those published by the IERS with additional components to account for the effects of ocean tides and for nutation terms with periods less than two days.

$$(x_p, y_p) = (x, y)_{IERS} + (\Delta x, \Delta y)_{tidal} + (\Delta x, \Delta y)_{nutation},$$

where $(x, y)_{IERS}$ are pole coordinates provided by the IERS, $(\Delta x, \Delta y)_{tidal}$ are the tidal components, and $(\Delta x, \Delta y)_{nutation}$ are the nutation components. The corrections for these variations are described below.

Corrections $(\Delta x, \Delta y)_{tidal}$ for the diurnal and sub-diurnal variations in polar motion caused by ocean tides can be computed using a routine available on the website of the IERS Conventions (see Chapter 8). Table 8.2 (from Ch. Bizouard), based on this routine, provides the amplitudes and arguments of these variations for the 71 tidal constituents considered in the model. These subdaily variations are not part of the polar motion values reported to and distributed by the IERS and are therefore to be added after interpolation.

Recent models for rigid Earth nutation (Souchay and Kinoshita, 1997; Bretagnon *et al.*, 1997; Folgueira *et al.*, 1998a; Folgueira *et al.*, 1998b; Souchay *et al.*, 1999; Roosbeek, 1999; Bizouard *et al.*, 2000; Bizouard *et al.*, 2001) include prograde diurnal and prograde semidiurnal terms with respect to the GCRS with amplitudes up to $\sim 15\,\mu$as in $\Delta\psi \sin\epsilon_0$ and $\Delta\epsilon$. The semidiurnal terms in nutation have also been provided both for rigid and nonrigid Earth models based on Hamiltonian formalism (Getino *et al.*, 2001, Escapa *et al.*, 2002a and b). In order to realize the CIP as recommended by Resolution B1.7, nutations with periods less than two days are to be considered using a model for the corresponding motion of the pole in the ITRS. The prograde diurnal nutations correspond to prograde and retrograde long periodic variations in polar motion, and the prograde semidiurnal nutations correspond to prograde diurnal variations in polar motion (see for example Folgueira *et al.* 2001). A table for operational use of the model for these variations $(\Delta x, \Delta y)_{nutation}$ in polar motion for a nonrigid Earth has been provided by an *ad hoc* Working Group (Brzeziński, 2002) based on nonrigid Earth models and developments of the tidal potential (Brzeziński, 2001; Brzeziński and Capitaine, 2002; Mathews and Bretagnon, 2002). The amplitudes of the diurnal terms are in very good agreement with those estimated by Getino *et al.* (2001). Components with amplitudes greater than 0.5 μas are given in Table 5.1. The contribution from the triaxiality of the core to the diurnal waves, while it can exceed the adopted cut-off level (Escapa *et al.*, 2002b; Mathews and Bretagnon, 2002), has not been taken into account in the table due to the large uncertainty in the triaxiality of the core (Dehant, 2002, private communication). The Stokes coefficients of the geopotential are from the model JGM-3.

The diurnal components of these variations should be considered similarly to the diurnal and semidiurnal variations due to ocean tides. They are not part of the polar motion values reported to the IERS and distributed by the IERS and should therefore be added after interpolation. The long-periodic terms, as well as the secular variation, are already contained in the observed polar motion and need not be added to the reported values.

Table 5.1 Coefficients of sin(argument) and cos(argument) in $(\Delta x, \Delta y)_{nutation}$ due to tidal gravitation (of degree n) for a nonrigid Earth. Units are μas; χ denotes GMST$+\pi$ and the expressions for the fundamental arguments (Delaunay arguments) are given by (40).

		argument					Doodson	Period	x_p		y_p	
n	χ	l	l'	F	D	Ω	number	(days)	sin	cos	sin	cos
4	0	0	0	0	0	−1	055.565	6798.3837	−0.03	0.63	−0.05	−0.55
3	0	−1	0	1	0	2	055.645	6159.1355	1.46	0.00	−0.18	0.11
3	0	−1	0	1	0	1	055.655	3231.4956	−28.53	−0.23	3.42	−3.86
3	0	−1	0	1	0	0	055.665	2190.3501	−4.65	−0.08	0.55	−0.92
3	0	1	1	−1	0	0	056.444	438.35990	−0.69	0.15	−0.15	−0.68
3	0	1	1	−1	0	−1	056.454	411.80661	0.99	0.26	−0.25	1.04
3	0	0	0	1	−1	1	056.555	365.24219	1.19	0.21	−0.19	1.40
3	0	1	0	1	−2	1	057.455	193.55971	1.30	0.37	−0.17	2.91
3	0	0	0	1	0	2	065.545	27.431826	−0.05	−0.21	0.01	−1.68
3	0	0	0	1	0	1	065.555	27.321582	0.89	3.97	−0.11	32.39
3	0	0	0	1	0	0	065.565	27.212221	0.14	0.62	−0.02	5.09
3	0	−1	0	1	2	1	073.655	14.698136	−0.02	0.07	0.00	0.56
3	0	1	0	1	0	1	075.455	13.718786	−0.11	0.33	0.01	2.66
3	0	0	0	3	0	3	085.555	9.1071941	−0.08	0.11	0.01	0.88
3	0	0	0	3	0	2	085.565	9.0950103	−0.05	0.07	0.01	0.55
2	1	−1	0	−2	0	−1	135.645	1.1196992	−0.44	0.25	−0.25	−0.44
2	1	−1	0	−2	0	−2	135.655	1.1195149	−2.31	1.32	−1.32	−2.31
2	1	1	0	−2	−2	−2	137.455	1.1134606	−0.44	0.25	−0.25	−0.44
2	1	0	0	−2	0	−1	145.545	1.0759762	−2.14	1.23	−1.23	−2.14
2	1	0	0	−2	0	−2	145.555	1.0758059	−11.36	6.52	−6.52	−11.36
2	1	−1	0	0	0	0	155.655	1.0347187	0.84	−0.48	0.48	0.84
2	1	0	0	−2	2	−2	163.555	1.0027454	−4.76	2.73	−2.73	−4.76
2	1	0	0	0	0	0	165.555	0.9972696	14.27	−8.19	8.19	14.27
2	1	0	0	0	0	−1	165.565	0.9971233	1.93	−1.11	1.11	1.93
2	1	1	0	0	0	0	175.455	0.9624365	0.76	−0.43	0.43	0.76
Rate of secular polar motion (μas/y) due to the zero frequency tide												
4	0	0	0	0	0	0	555.555			−3.80		−4.31

5.4.3 Position of the TEO in the ITRS

The quantity s' is only sensitive to the largest variations in polar motion. Some components of s' have to be evaluated, in principle, from the measurements and can be extrapolated using the IERS data. Its main component can be written as:

$$s' = -0.0015(a_c^2/1.2 + a_a^2)t, \tag{11}$$

a_c and a_a being the average amplitudes (in arc seconds) of the Chandlerian and annual wobbles, respectively in the period considered (Capitaine et al., 1986). The value of s' will therefore be less than 0.4 mas through the next century, even if the amplitudes for the Chandlerian and annual wobbles reach values of the order of $0.5''$ and $0.1''$ respectively. Using the current mean amplitudes for the Chandlerian and annual wobbles gives (Lambert and Bizouard, 2002):

$$s' = -47 \ \mu\text{as} \ t. \tag{12}$$

5.4.4 Earth Rotation Angle

The Earth Rotation Angle, θ, is obtained by the use of its conventional relationship with UT1 as given by Capitaine et al. (2000),

$$\theta(T_u) = 2\pi(0.7790572732640 + 1.00273781191135448T_u), \tag{13}$$

where T_u=(Julian UT1 date$-$2451545.0), and UT1=UTC+(UT1$-$UTC), or equivalently

$$\theta(T_u) \quad = \quad \begin{aligned} &2\pi(\text{UT1 Julian day number elapsed since 2451545.0} \\ &+0.7790572732640 + 0.00273781191135448T_u), \end{aligned} \quad (14)$$

the quantity UT1$-$UTC to be used (if not estimated from the observations) being the IERS value.

This definition of UT1 based on the CEO is insensitive at the microarcsecond level to the precession-nutation model and to the observed celestial pole offsets. Therefore, in the processing of observational data, the quantity s provided by Table 5.2c must be considered as independent of observations.

5.4.5   Motion of the CIP in the GCRS

Developments of the coordinates X and Y of the CIP in the GCRS, valid at the microarcsecond level, based on the IERS 1996 model for precession, nutation and pole offset at J2000.0 with respect to the pole of the GCRS, have been provided by Capitaine *et al.* (2000). New developments of X and Y based on the IAU 2000A or IAU 2000B model (see the following section for more details) for precession-nutation and on their corresponding pole offset at J2000.0 with respect to the pole of the GCRS have been computed at the same accuracy (Capitaine *et al.*, 2003a). These developments have the following form:

$$\begin{aligned} X = \quad &-0.01661699'' + 2004.19174288''t - 0.42721905''t^2 \\ &-0.19862054''t^3 - 0.00004605''t^4 + 0.00000598''t^5 \\ &+\textstyle\sum_i[(a_{s,0})_i \sin(\text{ARGUMENT}) + (a_{c,0})_i \cos(\text{ARGUMENT})] \\ &+\textstyle\sum_i[(a_{s,1})_i t \sin(\text{ARGUMENT}) + (a_{c,1})_i t \cos(\text{ARGUMENT})] \\ &+\textstyle\sum_i[(a_{s,2})_i t^2 \sin(\text{ARGUMENT}) + (a_{c,2})_i t^2 \cos(\text{ARGUMENT})] \\ &+\cdots, \end{aligned} \quad (15)$$

$$\begin{aligned} Y = \quad &-0.00695078'' - 0.02538199''t - 22.40725099''t^2 \\ &+0.00184228''t^3 + 0.00111306''t^4 + 0.00000099''t^5 \\ &+\textstyle\sum_i[(b_{c,0})_i \cos(\text{ARGUMENT}) + (b_{s,0})_i \sin(\text{ARGUMENT})] \\ &+\textstyle\sum_i[(b_{c,1})_i t \cos(\text{ARGUMENT}) + (b_{s,1})_i \ t \sin(\text{ARGUMENT})] \\ &+\textstyle\sum_i[(b_{c,2})_i t^2 \cos(\text{ARGUMENT}) + (b_{s,2})_i t^2 \sin(\text{ARGUMENT})] \\ &+\cdots, \end{aligned} \quad (16)$$

the parameter t being given by expression (2) and ARGUMENT being a function of the fundamental arguments of the nutation theory whose expressions are given by (40) for the lunisolar ones and (41) for the planetary ones.

These series are available electronically on the IERS Convention Center website (Tables 5.2a and 5.2b) at $<$[4]$>$. `tab5.2a.txt` for the X coordinate and at `tab5.2b.txt` for the Y coordinate. An extract from Tables 5.2a and 5.2b for the largest non-polynomial terms in X and Y is given hereafter.

The numerical values of the coefficients of the polynomial part of X and Y are derived from the development as a function of time of the precession in longitude and obliquity and pole offset at J2000.0 and the amplitudes $(a_{s,j})_i$, $(a_{c,j})_i$, $(b_{c,j})_i$, $(b_{s,j})_i$ for $j = 0, 1, 2, ...$ are derived from the amplitudes of the precession and nutation series. The amplitudes $(a_{s,0})_i$, $(b_{c,0})_i$ of the sine and cosine terms in X and Y respectively are equal to the amplitudes $A_i \times \sin \epsilon_0$ and B_i of the series for nutation

---

[4]ftp://maia.usno.navy.mil/conv2000/chapter5/

Extract from Tables 5.2a and 5.2b (available at $<^4>$) for the largest non-polynomial terms in the development (15) for $X(t)$ (top part) and (16) for $Y(t)$ (bottom part) compatible with IAU 2000A Precession-Nutation Model (unit μas). The expressions for the fundamental arguments appearing in columns 4 to 17 are given by (40) and (41).

i	$(a_{s,0})_i$	$(a_{c,0})_i$	l	l'	F	D	Ω	L_{Me}	L_{Ve}	L_E	L_{Ma}	L_J	L_{Sa}	L_U	L_{Ne}	p_A
1	−6844318.44	1328.67	0	0	0	0	1	0	0	0	0	0	0	0	0	0
2	−523908.04	−544.76	0	0	2	−2	2	0	0	0	0	0	0	0	0	0
3	−90552.22	111.23	0	0	2	0	2	0	0	0	0	0	0	0	0	0
4	82168.76	−27.64	0	0	0	0	2	0	0	0	0	0	0	0	0	0
5	58707.02	470.05	0	1	0	0	0	0	0	0	0	0	0	0	0	0
.....																
i	$(a_{s,1})_i$	$(a_{c,1})_i$	l	l'	F	D	Ω	L_{Me}	L_{Ve}	L_E	L_{Ma}	L_J	L_{Sa}	L_U	L_{Ne}	p_A
1307	−3328.48	205833.15	0	0	0	0	1	0	0	0	0	0	0	0	0	0
1308	197.53	12814.01	0	0	2	−2	2	0	0	0	0	0	0	0	0	0
1309	41.19	2187.91	0	0	2	0	2	0	0	0	0	0	0	0	0	0
.....																
i	$(b_{s,0})_i$	$(b_{c,0})_i$	l	l'	F	D	Ω	L_{Me}	L_{Ve}	L_E	L_{Ma}	L_J	L_{Sa}	L_U	L_{Ne}	p_A
1	1538.18	9205236.26	0	0	0	0	1	0	0	0	0	0	0	0	0	0
2	−458.66	573033.42	0	0	2	−2	2	0	0	0	0	0	0	0	0	0
3	137.41	97846.69	0	0	2	0	2	0	0	0	0	0	0	0	0	0
4	−29.05	−89618.24	0	0	0	0	2	0	0	0	0	0	0	0	0	0
5	−17.40	22438.42	0	1	2	−2	2	0	0	0	0	0	0	0	0	0
.....																
i	$(b_{s,1})_i$	$(b_{c,1})_i$	l	l'	F	D	Ω	L_{Me}	L_{Ve}	L_E	L_{Ma}	L_J	L_{Sa}	L_U	L_{Ne}	p_A
963	153041.82	878.89	0	0	0	0	1	0	0	0	0	0	0	0	0	0
964	11714.49	−289.32	0	0	2	−2	2	0	0	0	0	0	0	0	0	0
965	2024.68	−50.99	0	0	2	0	2	0	0	0	0	0	0	0	0	0
.....																

in longitude $\times \sin \epsilon_0$ and obliquity, except for a few terms in each coordinate X and Y which contain a contribution from crossed-nutation effects. The coordinates X and Y contain Poisson terms in $t \sin$, $t \cos$, $t^2 \sin$, $t^2 \cos$, ... which originate from crossed terms between precession and nutation.

The contributions (in μas) to expressions (15) and (16) from the frame biases are

$$\begin{aligned} dX &= -16617.0 - 1.6\ t^2 + 0.7\ \cos \Omega, \\ dY &= -6819.2 - 141.9\ t + 0.5\ \sin \Omega, \end{aligned} \qquad (17)$$

the first term in each coordinate being the contribution from the celestial pole offset at J2000.0 and the following ones from the equinox offset at J2000.0 also called "frame bias in right ascension."

The celestial coordinates of the CIP, X and Y, can also be obtained at each time t as a function of the precession and nutation quantities provided by the IAU 2000 Precession-Nutation Model. The developments to be used for the precession quantities and for the nutation angles referred to the ecliptic of date are described in the following section and a subroutine is available for the computation.

The relationships between the coordinates X and Y and the precession-nutation quantities are (Capitaine, 1990):

$$\begin{aligned} X &= \bar{X} + \xi_0 - d\alpha_0\ \bar{Y}, \\ Y &= \bar{Y} + \eta_0 + d\alpha_0\ \bar{X}, \end{aligned} \qquad (18)$$

where ξ_0 and η_0 are the celestial pole offsets at the basic epoch J2000.0 and $d\alpha_0$ the right ascension of the mean equinox of J2000.0 in the CRS. (See the numbers provided below in (19) and (28) for these quantities.)

The mean equinox of J2000.0 to be considered is not the "rotational dynamical mean equinox of J2000.0" as used in the past, but the "inertial dynamical mean equinox of J2000.0" to which the recent numerical or analytical solutions refer. The latter is associated with the ecliptic in the inertial sense, which is the plane perpendicular to the vector angular momentum of the orbital motion of the Earth-Moon barycenter as computed from the velocity of the barycenter relative to an *inertial frame*. The rotational equinox is associated with the ecliptic in the rotational sense, which is perpendicular to the vector angular momentum computed from the velocity referred to the *rotating* orbital plane of the Earth-Moon barycenter. (The difference between the two angular momenta is the angular momentum associated with the rotation of the orbital plane.) See Standish (1981) for more details. The numerical value for $d\alpha_0$ as derived from Chapront *et al.* (2002) to be used in expression (18) is

$$d\alpha_0 = (-0.01460 \pm 0.00050)''. \qquad (19)$$

Quantities $\bar{X}$ and $\bar{Y}$ are given by:

$$
\begin{aligned}
\bar{X} &= \sin\omega\sin\psi, \\
\bar{Y} &= -\sin\epsilon_0\cos\omega + \cos\epsilon_0\sin\omega\cos\psi
\end{aligned}
\qquad (20)
$$

where ϵ_0 ($= 84381.448''$) is the obliquity of the ecliptic at J2000.0, ω is the inclination of the true equator of date on the fixed ecliptic of epoch and ψ is the longitude, on the ecliptic of epoch, of the node of the true equator of date on the fixed ecliptic of epoch; these quantities are such that

$$\omega = \omega_A + \Delta\epsilon_1; \qquad \psi = \psi_A + \Delta\psi_1, \qquad (21)$$

where ψ_A and ω_A are the precession quantities in longitude and obliquity (Lieske *et al.*, 1977) referred to the ecliptic of epoch and $\Delta\psi_1$, $\Delta\epsilon_1$ are the nutation angles in longitude and obliquity referred to the ecliptic of epoch. (See the numerical developments provided for the precession quantities in (30) and (31).) $\Delta\psi_1$, $\Delta\epsilon_1$ can be obtained from the nutation angles $\Delta\psi$, $\Delta\epsilon$ in longitude and obliquity referred to the ecliptic of date. The following formulation from Aoki and Kinoshita (1983) has been verified to provide an accuracy better than one microarcsecond after one century:

$$
\begin{aligned}
\Delta\psi_1\sin\omega_A &= \Delta\psi\sin\epsilon_A\cos\chi_A - \Delta\epsilon\sin\chi_A, \\
\Delta\epsilon_1 &= \Delta\psi\sin\epsilon_A\sin\chi_A + \Delta\epsilon\cos\chi_A,
\end{aligned}
\qquad (22)
$$

ω_A and ϵ_A being the precession quantities in obliquity referred to the ecliptic of epoch and the ecliptic of date respectively and χ_A the planetary precession along the equator (Lieske *et al.*, 1977).

As VLBI observations have shown that there are deficiencies in the IAU 2000A of the order of 0.2 mas (Mathews *et al.*, 2002), the IERS will continue to publish observed estimates of the corrections to the IAU 2000 Precession-Nutation Model. The observed differences with respect to the conventional celestial pole position defined by the models are monitored and reported by the IERS as "celestial pole offsets." Such time dependent offsets from the direction of the pole of the GCRS must be provided as corrections δX and δY to the X and Y coordinates. These corrections can be related to the current celestial pole offsets $\delta\psi$ and $\delta\epsilon$ using the relationship (20) between X and Y and the precession-nutation quantities and (22) for the transformation from ecliptic of date to ecliptic of epoch. The relationship can be written with one microarcsecond accuracy for one century:

$$
\begin{aligned}
\delta X &= \delta\psi\sin\epsilon_A + (\psi_A\cos\epsilon_0 - \chi_A)\delta\epsilon, \\
\delta Y &= \delta\epsilon - (\psi_A\cos\epsilon_0 - \chi_A)\delta\psi\sin\epsilon_A.
\end{aligned}
\qquad (23)
$$

These observed offsets include the contribution of the Free Core Nutation (FCN) described in sub-section 5.5.1 on the IAU 2000 Precession-Nutation Model. Using these offsets, the corrected celestial position of the CIP is given by

$$X = X(\text{IAU 2000}) + \delta X, \qquad Y = Y(\text{IAU 2000}) + \delta Y. \qquad (24)$$

This is practically equivalent to replacing the transformation matrix Q with the rotation

$$\tilde{Q} = \begin{pmatrix} 1 & 0 & \delta X \\ 0 & 1 & \delta Y \\ -\delta X & -\delta Y & 1 \end{pmatrix} Q_{\text{IAU}}, \qquad (25)$$

where Q_{IAU} represents the $Q(t)$ matrix based on the IAU 2000 Precession-Nutation Model.

5.4.6 Position of the CEO in the GCRS

The numerical development of s compatible with the IAU 2000A Precession-Nutation Model as well as the corresponding celestial offset at J2000.0 has been derived in a way similar to that based on the IERS Conventions 1996 (Capitaine *et al.*, 2000). It results from the expression for s (8) using the developments of X and Y as functions of time given by (15) and (16) (Capitaine *et al.*, 2003a). The numerical development is provided for the quantity $s + XY/2$, which requires fewer terms to reach the same accuracy than a direct development for s.

The constant term for s, which was previously chosen so that $s(J2000.0) = 0$, has now been fit (Capitaine *et al.*, 2003b) in order to ensure continuity of UT1 at the date of change (1 January 2003) consistent with the Earth Rotation Angle (ERA) relationship and the current VLBI procedure for estimating UT1 (see (36)).

The complete series for $s + XY/2$ with all terms larger than 0.1 μas is available electronically on the IERS Convention Center website at `tab5.2c.txt` and the terms larger than 0.5 μas over 25 years in the development of s are provided in Table 5.2c with microarcsecond accuracy.

Table 5.2c   Development of $s(t)$ compatible with IAU 2000A Precession-Nutation Model: all terms exceeding 0.5 μas during the interval 1975–2025 (unit μas).

$s(t)$ = $-XY/2 + 94 + 3808.35t - 119.94t^2 - 72574.09t^3 + \sum_k C_k \sin \alpha_k$
$+1.71t \sin \Omega + 3.57t \cos 2\Omega + 743.53t^2 \sin \Omega + 56.91t^2 \sin(2F - 2D + 2\Omega)$
$+9.84t^2 \sin(2F + 2\Omega) - 8.85t^2 \sin 2\Omega$

Argument α_k	Amplitude C_k
Ω	-2640.73
2Ω	-63.53
$2F - 2D + 3\Omega$	-11.75
$2F - 2D + \Omega$	-11.21
$2F - 2D + 2\Omega$	$+4.57$
$2F + 3\Omega$	-2.02
$2F + \Omega$	-1.98
3Ω	$+1.72$
$l' + \Omega$	$+1.41$
$l' - \Omega$	$+1.26$
$l + \Omega$	$+0.63$
$l - \Omega$	$+0.63$

5.5 IAU 2000A and IAU 2000B Precession-Nutation Model

5.5.1 Description of the Model

The IAU 2000A Precession-Nutation Model has been adopted by the IAU (Resolution B1.6) to replace the IAU 1976 Precession Model (Lieske *et al.*, 1977) and the IAU 1980 Theory of Nutation (Wahr, 1981; Seidelmann, 1982). See Dehant *et al.* (1999) for more details. This model, developed by Mathews *et al.* (2002), is based on the solution of the linearized dynamical equation of the wobble-nutation problem and makes use of estimated values of seven of the parameters appearing in the theory, obtained from a least-squares fit of the theory to an up-to-date precession-nutation VLBI data set (Herring *et al.*, 2002). The nutation series relies on the Souchay *et al.* (1999) Rigid Earth nutation series, rescaled by 1.000012249 to account for the change in the dynamical ellipticity of the Earth implied by the observed correction to the lunisolar precession of the equator. The nonrigid Earth transformation is the MHB2000 model of Mathews *et al.* (2002) which improves the IAU 1980 Theory of Nutation by taking into account the effect of mantle anelasticity, ocean tides, electromagnetic couplings produced between the fluid outer core and the mantle as well as between the solid inner core and fluid outer core (Buffett *et al.*, 2002) and the consideration of nonlinear terms which have hitherto been ignored in this type of formulation.

The resulting nutation series includes 678 lunisolar terms and 687 planetary terms which are expressed as "in-phase" and "out-of-phase" components with their time variations (see expression (29)). It provides the direction of the celestial pole in the GCRS with an accuracy of 0.2 mas. It includes the geodesic nutation contributions to the annual, semiannual and 18.6-year terms to be consistent with including the geodesic precession p_g in the precession model and so that the BCRS and GCRS are without any time-dependent rotation. The IAU 1976 Precession Model uses $p_g = 1.92''/c$ and the theoretical geodesic nutation contribution (Fukushima, 1991) used in the MHB model (Mathews *et al.*, 2002) is, in μas, for the nutations in longitude $\Delta\psi_g$ and obliquity $\Delta\epsilon_g$

$$
\begin{aligned}
\Delta\psi_g &= -153 \ \sin l' - 2 \ \sin 2l' + 3 \ \sin\Omega, \\
\Delta\epsilon_g &= 1 \ \cos\Omega,
\end{aligned}
\tag{26}
$$

where l' is the mean anomaly of the Sun and Ω the longitude of the ascending node of the Moon. On the other hand, the FCN, being a free motion which cannot be predicted rigorously, is not considered a part of the IAU 2000A model.

The IAU 2000 nutation series is associated with improved numerical values for the precession rate of the equator in longitude and obliquity, which correspond to the following correction to the IAU 1976 precession:

$$
\begin{aligned}
\delta\psi_A &= (-0.29965 \pm 0.00040)''/\text{c}, \\
\delta\omega_A &= (-0.02524 \pm 0.00010)''/\text{c},
\end{aligned}
\tag{27}
$$

as well as with the following offset (originally provided as frame bias in $\text{d}\psi_{bias}$ and $\text{d}\epsilon_{bias}$) of the direction of the CIP at J2000.0 from the direction of the pole of the GCRS:

$$
\begin{aligned}
\xi_0 &= (-0.0166170 \pm 0.0000100)'', \\
\eta_0 &= (-0.0068192 \pm 0.0000100)''.
\end{aligned}
\tag{28}
$$

The IAU 2000 Nutation Model is given by a series for nutation in longitude $\Delta\psi$ and obliquity $\Delta\epsilon$, referred to the mean ecliptic of date, with t measured in Julian centuries from epoch J2000.0:

$$
\begin{aligned}
\Delta\psi &= \sum_{i=1}^{N}(A_i + A_i't)\sin(\text{ARGUMENT}) + (A_i'' + A_i'''t)\cos(\text{ARGUMENT}), \\
\Delta\epsilon &= \sum_{i=1}^{N}(B_i + B_i't)\cos(\text{ARGUMENT}) + (B_i'' + B_i'''t)\sin(\text{ARGUMENT}).
\end{aligned}
\tag{29}
$$

More details about the coefficients and arguments of these series (see extract of the Tables 5.3a and 5.3b below) will be given in section 5.8.

These series are available electronically on the IERS Convention Center website, for the lunisolar and planetary components, respectively at `tab5.3a.txt` and `tab5.3b.txt`.

Extract from Tables 5.3a (lunisolar nutations) and 5.3b (planetary nutations) (available at $<^4>$) providing the largest components for the "in-phase" and "out-of-phase" terms in longitude and obliquity. Units are mas and mas/c for the coefficients and their time variations respectively. Periods are in days.

l l' F D Ω	Period	A_i	A'_i	B_i	B'_i	A''_i	A'''_i	B''_i	B'''_i
0 0 0 0 1	-6798.383	-17206.4161	-17.4666	9205.2331	0.9086	3.3386	0.0029	1.5377	0.0002
0 0 2 -2 2	182.621	-1317.0906	-0.1675	573.0336	-0.3015	-1.3696	0.0012	-0.4587	-0.0003
0 0 2 0 2	13.661	-227.6413	-0.0234	97.8459	-0.0485	0.2796	0.0002	0.1374	-0.0001
0 0 0 0 2	-3399.192	207.4554	0.0207	-89.7492	0.0470	-0.0698	0.0000	-0.0291	0.0000
0 1 0 0 0	365.260	147.5877	-0.3633	7.3871	-0.0184	1.1817	-0.0015	-0.1924	0.0005
0 1 2 -2 2	121.749	-51.6821	0.1226	22.4386	-0.0677	-0.0524	0.0002	-0.0174	0.0000
1 0 0 0 0	27.555	71.1159	0.0073	-0.6750	0.0000	-0.0872	0.0000	0.0358	0.0000
0 0 2 0 1	13.633	-38.7298	-0.0367	20.0728	0.0018	0.0380	0.0001	0.0318	0.0000
1 0 2 0 2	9.133	-30.1461	-0.0036	12.9025	-0.0063	0.0816	0.0000	0.0367	0.0000
0 -1 2 -2 2	365.225	21.5829	-0.0494	-9.5929	0.0299	0.0111	0.0000	0.0132	-0.0001

l l' F D Ω	L_{Me} L_{Ve} L_E L_{Ma} L_J L_{Sa} L_U L_{Ne} p_A	Period	Longitude		Obliquity	
			A_i	A''_i	B_i	B''_i
0 0 1 -1 1	0 0 -1 0 -2 5 0 0 0	311921.26	-0.3084	0.5123	0.2735	0.1647
0 0 0 0 0	0 0 0 0 -2 5 0 0 1	311927.52	-0.1444	0.2409	-0.1286	-0.0771
0 0 0 0 0	0 -3 5 0 0 0 0 0 2	2957.35	-0.2150	0.0000	0.0000	0.0932
0 0 1 -1 1	0 -8 12 0 0 0 0 0 0	-88082.01	0.1200	0.0598	0.0319	-0.0641
0 0 0 0 0	0 0 0 0 2 0 0 0 2	2165.30	-0.1166	0.0000	0.0000	0.0505
0 0 0 0 0	0 0 4 -8 3 0 0 0 0	-651391.30	-0.0462	0.1604	0.0000	0.0000
0 0 0 0 0	0 1 -1 0 0 0 0 0 0	583.92	0.1485	0.0000	0.0000	0.0000
0 0 0 0 0	0 0 8 -16 4 5 0 0 0	34075700.82	0.1440	0.0000	0.0000	0.0000
0 0 0 0 0	0 0 1 0 -1 0 0 0 0	398.88	-0.1223	-0.0026	0.0000	0.0000
0 0 0 0 1	0 0 -1 2 0 0 0 0 0	37883.60	-0.0460	-0.0435	-0.0232	0.0246

The IAU 2000A subroutine, provided by T. Herring, is available electronically on the IERS Convention Center website at $<^5>$.

It produces the quantities to implement the IAU 2000A Precession-Nutation Model based on the MHB 2000 model: nutation in longitude and obliquity, plus the contribution of the corrections to the IAU 1976 precession rates, plus the frame bias $d\psi_{bias}$ and $d\epsilon_{bias}$ in longitude and obliquity. The "total nutation" includes all components with the exception of the free core nutation (FCN). The software can also be used to model the expected FCN based on the most recent astronomical observations.

As recommended by Resolution B1.6, an abridged model, designated IAU 2000B, is available for those who need a model only at the 1 mas level. Such a model has been developed by McCarthy and Luzum (2003). It includes fewer than 80 lunisolar terms plus a bias to account for the effect of the planetary terms in the time period under consideration. It provides the celestial pole motion with an accuracy that does not result in a difference greater than 1 mas with respect to that of the IAU 2000A model during the period 1995–2050. The IAU 2000B subroutine is available electronically on the IERS Convention Center website at $<^6>$.

---

[5] ftp://maia.usno.navy.mil/conv2000/chapter5/IAU2000A.f
[6] ftp://maia.usno.navy.mil/conv2000/chapter5/IAU2000B.f

5.5.2   Precession Developments compatible with the IAU2000 Model

The numerical values for the precession quantities compatible with the IAU 2000 Precession-Nutation Model can be provided by using the developments (30) of Lieske *et al.* (1977) to which the estimated corrections (27) $\delta\psi_A$ and $\delta\omega_A$ to the IAU 1976 precession have to be added.

The expressions of Lieske *et al.* (1977) are

$$
\begin{aligned}
\psi_A &= 5038.7784''t - 1.07259''t^2 - 0.001147''t^3, \\
\omega_A &= \epsilon_0 + 0.05127''t^2 - 0.007726''t^3, \\
\epsilon_A &= \epsilon_0 - 46.8150''t - 0.00059''t^2 + 0.001813''t^3, \\
\chi_A &= 10.5526''t - 2.38064''t^2 - 0.001125''t^3 \quad ,
\end{aligned}
\tag{30}
$$

and

$$
\begin{aligned}
\zeta_A &= 2306.2181''t + 0.30188''t^2 + 0.017998''t^3, \\
\theta_A &= 2004.3109''t - 0.42665''t^2 - 0.041833''t^3, \\
z_A &= 2306.2181''t + 1.09468''t^2 + 0.018203''t^3,
\end{aligned}
\tag{31}
$$

with $\epsilon_0 = 84381.448''$.

Due to their theoretical bases, the original development of the precession quantities as function of time can be considered as being expressed in TDB.

The expressions compatible with the IAU 2000A precession and nutation are:

$$
\begin{aligned}
\psi_A &= 5038.47875''t - 1.07259''t^2 - 0.001147''t^3, \\
\omega_A &= \epsilon_0 - 0.02524''t + 0.05127''t^2 - 0.007726''t^3, \\
\epsilon_A &= \epsilon_0 - 46.84024''t - 0.00059''t^2 + 0.001813''t^3, \\
\chi_A &= 10.5526''t - 2.38064''t^2 - 0.001125''t^3 \quad ,
\end{aligned}
\tag{32}
$$

and the following series has been developed (Capitaine *et al.*, 2003c) in order to match the 4-rotation series for precession $R_1(-\epsilon_0) \cdot R_3(\psi_A) \cdot R_1(\omega_A) \cdot R_3(-\chi_A)$, called the "canonical 4-rotation method," to sub-microarcsecond accuracy over 4 centuries:

$$
\begin{aligned}
\zeta_A &= 2.5976176'' + 2306.0809506''t + 0.3019015''t^2 + 0.0179663''t^3 \\
&\quad -0.0000327''t^4 - 0.0000002''t^5, \\
\theta_A &= 2004.1917476''t - 0.4269353''t^2 - 0.0418251''t^3 \\
&\quad -0.0000601''t^4 - 0.0000001''t^5, \\
z_A &= -2.5976176'' + 2306.0803226''t + 1.0947790''t^2 + 0.0182273''t^3 \\
&\quad +0.0000470''t^4 - 0.0000003''t^5.
\end{aligned}
\tag{33}
$$

Note that the new expression for the quantities ζ_A and z_A include a constant term (with opposite signs) which originates from the ratio between the precession rate in ω_A and in $\psi_A \sin\epsilon_0$.

TT is used in the above expressions in place of TDB. The largest term in the difference TDB−TT being 1.7 ms $\times \sin l'$, the resulting error in the precession quantity ψ_A is periodic, with an annual period and an amplitude of $2.7'' \times 10^{-9}$, which is significantly under the required microarcsecond accuracy.

5.6   Procedure to be used for the Transformation consistent with IAU 2000 Resolutions

There are several ways to implement the IAU 2000 Precession-Nutation Model, and the precession developments to be used should be consistent with the procedure being used. The subroutines available for the different procedures are described below.

Using the new paradigm, the complete procedure to transform from the GCRS to the ITRS compatible with the IAU 2000A precession-nutation is based on the expressions provided by (15) and (16) and Tables 5.2 for the positions of the CIP and the CEO in the GCRS. These already contain the proper expressions for the new precession-nutation model and the frame biases. Another procedure can also be used for the computation of the coordinates X and Y of the CIP in the GCRS using expressions (18) to (22). This must be based on the MHB 2000 nutation series, on offsets at J2000.0 as well as on precession quantities $\psi_A, \omega_A, \epsilon_A, \chi_A$, taking into account the corrections to the IAU 1976 precession rates. (See expressions (32).)

In support of the classical paradigm, the IAU2000A subroutine provides the components of the precession-nutation model including the contributions of the correction to the IAU 1976 precession rates for ζ_A, θ_Z, z_A (see expressions (31)). Expressions (33) give the same angles but taking into account the IAU 2000 corrections.

The recommended option for implementing the IAU 2000A/B model using the classical transformation between the TRS and the GCRS is to follow a rigorous procedure described by Wallace (in Capitaine *et al.*, 2002). This procedure is composed of the classical nutation matrix using the MHB 2000 series, the precession matrix including four rotations $(R_1(-\epsilon_0) \cdot R_3(\psi_A) \cdot R_1(\omega_A) \cdot R_3(-\chi_A))$ using the updated developments (32) for these quantities and a separate rotation matrix for the frame bias.

In the case when one elects to continue using the classical expressions based on the IAU 1976 Precession Model and IAU 1980 Theory of Nutation, one should proceed as in the past as described in the IERS Conventions 1996 (McCarthy, 1996) and then apply the corrections to the model provided by the appropriate IAU 2000A/B software.

5.7 Expression of Greenwich Sidereal Time referred to the CEO

Greenwich Sidereal Time (GST) is related to the "Earth Rotation Angle" θ referred to the CEO by the following relationship (Aoki and Kinoshita, 1983; Capitaine and Gontier, 1993) at a microarcsecond level:

$$\text{GST} = dT_0 + \theta + \int_{t_0}^{t} (\dot{\widehat{\psi_A + \Delta\psi_1}}) \cos(\omega_A + \Delta\epsilon_1) dt - \chi_A + \Delta\psi \cos\epsilon_A - \Delta\psi_1 \cos\omega_A, \quad (34)$$

$\Delta\psi_1$, $\Delta\epsilon_1$, given by (22), being the nutation angles in longitude and obliquity referred to the ecliptic of epoch and χ_A, whose development is given in (32), the planetary precession along the equator.

The last four parts of (34) account for the accumulated precession and nutation in right ascension from J2000.0 to the epoch t. $\text{GST} - \theta$ provides the right ascension of the CEO measured from the equinox along the moving equator, and dT_0 is a constant term to be fitted in order to ensure continuity in UT1 at the date of change (1 January 2003). The numerical expression consistent with the IAU 2000 Precession-Nutation Model has been obtained, using computations similar to those performed for s and following a procedure, which is described below, to ensure consistency at a microarcsecond level with the new transformation as well as continuity in UT1 at the date of change (Capitaine *et al.*, 2003b). The series providing the expression for Greenwich Sidereal Time based on the IAU2000A Precession-Nutation Model is available on the IERS Convention Center website at `tab5.4.txt`.

Referring to the notations similar to those used in Table 5.2c, the numerical expression is

$$
\begin{aligned}
\text{GST} \quad = \quad & 0.014506'' + \theta + 4612.15739966''t + 1.39667721''t^2 \\
& -0.00009344''t^3 + 0.00001882''t^4 + \Delta\psi\cos\epsilon_A \\
& -\textstyle\sum_k C_k'\sin\alpha_k - 0.00000087''t\ \sin\Omega.
\end{aligned}
\tag{35}
$$

The last two terms of GST, $-\sum_k C_k'\sin\alpha_k - 0.87\ \mu\text{as}\ t\ \sin\Omega$, are the complementary terms to be added to the current "equation of the equinoxes," $\Delta\psi\cos\epsilon_A$, to provide the relationship between GST and θ with microarcsecond accuracy. This replaces the two complementary terms provided in the IERS Conventions 1996. A secular term similar to that appearing in the quantity s is included in expression (35). This expression for GST used in the classical transformation based on the IAU 2000A precession-nutation ensures consistency at the microarcsecond level after one century with the new transformation using expressions (14) for θ, (15) and (16) for the celestial coordinates of the CIP and Table 5.2c for s. The numerical values for the constant term dT_0 in GST which ensures continuity in UT1 at the date of change (1 January 2003) and for the corresponding constant term in s have been found to be

$$
\begin{aligned}
dT_0 \quad &= \quad +14506\mu\text{as}, \\
s_0 \quad &= \quad +94\mu\text{as}.
\end{aligned}
\tag{36}
$$

The change in the polynomial part of GST due to the correction in the precession rates (27) corresponds to a change $d\text{GMST}$ (see also Williams, 1994) in the current relationship between GMST and UT1 (Aoki $et\ al.$, 1982). Its numerical expression derived from expressions (35) for GST and (13) for $\theta(\text{UT1})$, minus the expression for $\text{GMST}_{1982}(\text{UT1})$, can be written in microarcseconds as

$$
d\text{GMST} = 14506 - 274950.12t + 117.21t^2 - 0.44t^3 + 18.82t^4.
\tag{37}
$$

The new expression for GST clearly distinguishes between θ, which is expressed as a function of UT1, and the accumulated precession-nutation in right ascension, which is expressed in TDB (or, in practice, TT), whereas the $\text{GMST}_{1982}(\text{UT1})$ expression used only UT1. This gives rise to an additional difference in $d\text{GMST}$ of $(\text{TT} - \text{UT1})$ multiplied by the speed of precession in right ascension. Using TT−TAI=32.184 s, this can be expressed as: $47\,\mu\text{as} +1.5\mu\text{as}$ (TAI−UT1), where TAI−UT1 is in seconds. On 1 January 2003, this difference will be about $94\,\mu\text{as}$ (see Gontier in Capitaine $et\ al.$, 2002), using an estimated value of 32.3 s for TAI−UT1. This contribution for the effect of time scales is included in the value for dT_0 and s_0.

5.8 The Fundamental Arguments of Nutation Theory

5.8.1 The Multipliers of the Fundamental Arguments of Nutation Theory

Each of the lunisolar terms in the nutation series is characterized by a set of five integers N_j which determines the ARGUMENT for the term as a linear combination of the five Fundamental Arguments F_j, namely the Delaunay variables $(\ell, \ell', F, D, \Omega)$: $\text{ARGUMENT} = \sum_{j=1}^{5} N_j F_j$, where the values $(N_1, \cdots, N_5)$ of the multipliers characterize the term. The F_j are functions of time, and the angular frequency of the nutation described by the term is given by

$$
\omega \equiv d(\text{ARGUMENT})/dt.
\tag{38}
$$

The frequency thus defined is positive for most terms, and negative for some. Planetary nutation terms differ from the above only in that $\text{ARGUMENT} = \sum_{j=1}^{14} N_j' F_j'$, F_6 to F_{13}, as noted in Table 5.3, are the mean longitudes of the planets Mercury to Neptune including the Earth

$(l_{Me}, l_{Ve}, l_E, l_{Ma}, l_{Ju}, l_{Sa}, l_{Ur}, l_{Ne})$ and F_{14} is the general precession in longitude p_a.

Over time scales involved in nutation studies, the frequency ω is effectively time-independent, and one may write, for the kth term in the nutation series,

$$\text{ARGUMENT} = \omega_k t + \alpha_k. \tag{39}$$

Different tables of nutations in longitude and obliquity do not necessarily assign the same set of multipliers N_j to a particular term in the nutation series. The differences in the assignments arises from the fact that the replacement $(N_{j=1,14}) \rightarrow -(N_{j=1,14})$ accompanied by reversal of the sign of the coefficient of $\sin(\text{ARGUMENT})$ in the series for $\Delta\psi$ and $\Delta\epsilon$ leaves these series unchanged.

5.8.2 Development of the Arguments of Lunisolar Nutation

The expressions for the fundamental arguments of nutation are given by the following developments where t is measured in Julian centuries of TDB (Simon *et al.*, 1994: Tables 3.4 (b.3) and 3.5 (b)) based on IERS 1992 constants and Williams *et al.* (1991) for precession.

$$
\begin{aligned}
F_1 \equiv l \;\; &= Mean\ Anomaly\ of\ the\ Moon \\
&= 134.96340251° + 1717915923.2178''t + 31.8792''t^2 \\
&\quad +0.051635''t^3 - 0.00024470''t^4, \\[6pt]
F_2 \equiv l' \;\; &= Mean\ Anomaly\ of\ the\ Sun \\
&= 357.52910918° + 129596581.0481''t - 0.5532''t^2 \\
&\quad +0.000136''t^3 - 0.00001149''t^4, \\[6pt]
F_3 \equiv F &= L - \Omega \\
&= 93.27209062° + 1739527262.8478''t - 12.7512''t^2 \\
&\quad -0.001037''t^3 + 0.00000417''t^4, \\[6pt]
F_4 \equiv D &= Mean\ Elongation\ of\ the\ Moon\ from\ the\ Sun \\
&= 297.85019547° + 1602961601.2090''t - 6.3706''t^2 \\
&\quad +0.006593''t^3 - 0.00003169''t^4, \\[6pt]
F_5 \equiv \Omega &= Mean\ Longitude\ of\ the\ Ascending\ Node\ of\ the\ Moon \\
&= 125.04455501° - 6962890.5431''t + 7.4722''t^2 \\
&\quad +0.007702''t^3 - 0.00005939''t^4
\end{aligned} \tag{40}
$$

where L is the Mean Longitude of the Moon.

5.8.3 Development of the Arguments for the Planetary Nutation

Note that in the MHB 2000 code, simplified expressions are used for the planetary nutation. The maximum difference in the nutation amplitudes is less than 0.1μas.

The mean longitudes of the planets used in the arguments for the planetary nutations are those provided by Souchay *et al.* (1999), based on theories and constants of VSOP82 (Bretagnon, 1982) and ELP 2000 (Chapront-Touzé and Chapront, 1983) and developments of Simon *et al.* (1994). Their developments are given below in radians with t in Julian centuries.

In the original expressions, t is measured in TDB. However, TT can be used in place of TDB as the difference due to TDB−TT is 0.9 mas $\times \sin l'$ for the largest effect in the nutation arguments, which produces a negligible difference (less than $10^{-2}\mu$as with a period of one year) in the corresponding amplitudes of nutation.

$$
\begin{aligned}
F_6 &\equiv l_{Me} &&= 4.402608842 + 2608.7903141574 \times t, \\
F_7 &\equiv l_{Ve} &&= 3.176146697 + 1021.3285546211 \times t, \\
F_8 &\equiv l_E &&= 1.753470314 + 628.3075849991 \times t, \\
F_9 &\equiv l_{Ma} &&= 6.203480913 + 334.0612426700 \times t, \\
F_{10} &\equiv l_{Ju} &&= 0.599546497 + 52.9690962641 \times t, \\
F_{11} &\equiv l_{Sa} &&= 0.874016757 + 21.3299104960 \times t, \\
F_{12} &\equiv l_{Ur} &&= 5.481293872 + 7.4781598567 \times t, \\
F_{13} &\equiv l_{Ne} &&= 5.311886287 + 3.8133035638 \times t, \\
F_{14} &\equiv p_a &&= 0.024381750 \times t + 0.00000538691 \times t^2.
\end{aligned}
\tag{41}
$$

5.9 Prograde and Retrograde Nutation Amplitudes

The quantities $\Delta\psi(t)\sin\epsilon_0$ and $\Delta\epsilon(t)$ may be viewed as the components of a moving two-dimensional vector in the mean equatorial frame, with the positive X and Y axes pointing along the directions of increasing $\Delta\psi$ and $\Delta\epsilon$, respectively. The purely periodic parts of $\Delta\psi(t)\sin\epsilon_0$ and $\Delta\epsilon(t)$ for a term of frequency ω_k are made up of in-phase and out-of-phase parts

$$
\begin{aligned}
(\Delta\psi^{ip}(t)\sin\epsilon_0, \ \Delta\epsilon^{ip}(t)) &= (\Delta\psi_k^{ip}\sin\epsilon_0\sin(\omega_k t + \alpha_k), \ \Delta\epsilon_k^{ip}\cos(\omega_k t + \alpha_k)), \\
(\Delta\psi^{op}(t)\sin\epsilon_0, \ \Delta\epsilon^{op}(t)) &= (\Delta\psi_k^{op}\sin\epsilon_0\cos(\omega_k t + \alpha_k), \ \Delta\epsilon_k^{op}\sin(\omega_k t + \alpha_k)),
\end{aligned}
\tag{42}
$$

respectively. Each of these vectors may be decomposed into two uniformly rotating vectors, one constituting a prograde circular nutation (rotating in the same sense as from the positive X axis towards the positive Y axis) and the other a retrograde one rotating in the opposite sense. The decomposition is facilitated by factoring out the sign q_k of ω_k from the argument, q_k being such that

$$
q_k\omega_k \equiv |\omega_k|.
\tag{43}
$$

and writing

$$
\omega_k t + \alpha_k = q_k(|\omega_k|t + q_k\alpha_k) \equiv q_k\chi_k,
\tag{44}
$$

with χ_k increasing linearly with time. The pair of vectors above then becomes

$$
\begin{aligned}
(\Delta\psi^{ip}(t)\sin\epsilon_0, \ \Delta\epsilon^{ip}(t)) &= (q_k\Delta\psi_k^{ip}\sin\epsilon_0\sin\chi_k, \ \Delta\epsilon_k^{ip}\cos\chi_k), \\
(\Delta\psi^{op}(t)\sin\epsilon_0, \ \Delta\epsilon^{op}(t)) &= (\Delta\psi_k^{op}\sin\epsilon_0\cos\chi_k, \ q_k\Delta\epsilon_k^{op}\sin\chi_k).
\end{aligned}
\tag{45}
$$

Because χ_k increases linearly with time, the mutually orthogonal unit vectors $(\sin\chi_k, -\cos\chi_k)$ and $(\cos\chi_k, \sin\chi_k)$ rotate in a prograde sense and the vectors obtained from these by the replacement $\chi_k \rightarrow -\chi_k$, namely $(-\sin\chi_k, -\cos\chi_k)$ and $(\cos\chi_k, -\sin\chi_k)$ are in retrograde rotation. On resolving the in-phase and out-of-phase vectors in terms of these, one obtains

$$
\begin{aligned}
(\Delta\psi^{ip}(t)\sin\epsilon_0, \ \Delta\epsilon^{ip}(t)) &= A_k^{pro\ ip}(\sin\chi_k, \ -\cos\chi_k) + A_k^{ret\ ip}(-\sin\chi_k, \ -\cos\chi_k), \\
(\Delta\psi^{op}(t)\sin\epsilon_0, \ \Delta\epsilon^{op}(t)) &= A_k^{pro\ op}(\cos\chi_k, \ \sin\chi_k) + A_k^{ret\ op}(\cos\chi_k, \ -\sin\chi_k),
\end{aligned}
\tag{46}
$$

where

$$
\begin{aligned}
A_k^{pro\ ip} &= \tfrac{1}{2}\,(q_k\Delta\psi_k^{ip}\sin\epsilon_0 - \Delta\epsilon_k^{ip}), \\
A_k^{ret\ ip} &= -\tfrac{1}{2}\,(q_k\Delta\psi_k^{ip}\sin\epsilon_0 + \Delta\epsilon_k^{ip}), \\
A_k^{pro\ op} &= \tfrac{1}{2}\,(\Delta\psi_k^{op}\sin\epsilon_0 + q_k\Delta\epsilon_k^{op}), \\
A_k^{ret\ op} &= \tfrac{1}{2}\,(\Delta\psi_k^{op}\sin\epsilon_0 - q_k\Delta\epsilon_k^{op}).
\end{aligned}
\tag{47}
$$

The expressions providing the corresponding nutation in longitude and in obliquity from circular terms are

$$
\begin{aligned}
\Delta\psi_k^{ip} &= \frac{q_k}{\sin\epsilon_0}\left(A_k^{pro\ ip} - A_k^{ret\ ip}\right), \\
\Delta\psi_k^{op} &= \frac{1}{\sin\epsilon_0}\left(A_k^{pro\ op} + A_k^{ret\ op}\right), \\
\Delta\epsilon_k^{ip} &= -\left(A_k^{pro\ ip} + A_k^{ret\ ip}\right), \\
\Delta\epsilon_k^{op} &= q_k\left(A_k^{pro\ op} - A_k^{ret\ op}\right).
\end{aligned}
\tag{48}
$$

The contribution of the k-term of the nutation to the position of the Celestial Intermediate Pole (CIP) in the mean equatorial frame is thus given by the complex coordinate

$$
\Delta\psi(t)\sin\epsilon_0 + i\Delta\epsilon(t) = -i\left(A_k^{pro}e^{i\chi_k} + A_k^{ret}e^{-i\chi_k}\right),
\tag{49}
$$

where A_k^{pro} and A_k^{ret} are the amplitudes of the prograde and retrograde components, respectively, and are given by

$$
A_k^{pro} = A_k^{pro\ ip} + iA_k^{pro\ op}, \qquad A_k^{ret} = A_k^{ret\ ip} + iA_k^{ret\ op}.
\tag{50}
$$

The decomposition into prograde and retrograde components is important for studying the role of resonance in nutation because any resonance (especially in the case of the nonrigid Earth) affects A_k^{pro} and A_k^{ret} unequally.

In the literature (Wahr, 1981) one finds an alternative notation, frequently followed in analytic formulations of nutation theory, that is:

$$
\Delta\epsilon(t) + i\Delta\psi(t)\sin\epsilon_0 = -i\left(A_k^{pro\ -}e^{-i\chi_k} + A_k^{ret\ -}e^{i\chi_k}\right),
\tag{51}
$$

with

$$
A_k^{pro\ -} = A_k^{pro\ ip} - iA_k^{pro\ op}, \qquad A_k^{ret\ -} = A_k^{ret\ ip} - iA_k^{ret\ op}.
\tag{52}
$$

Further detail concerning this topic can be found in Defraigne *et al.*, (1995) and Bizouard *et al.* (1998).

5.10   Procedures and IERS Routines for Transformations from ITRS to GCRS

Fortran routines that implement the IAU 2000 transformations are provided on the IERS Conventions web page, which is at <[7]>.

The following routines are provided:

BPN2000	CEO-based intermediate-to-celestial matrix
CBPN2000	equinox-based true-to-celestial matrix
EE2000	equation of the equinoxes (EE)
EECT2000	EE complementary terms
ERA2000	Earth Rotation Angle
GMST2000	Greenwich Mean Sidereal Time
GST2000	Greenwich (apparent) Sidereal Time
NU2000A	nutation, IAU 2000A
NU2000B	nutation, IAU 2000B
POM2000	form polar-motion matrix
SP2000	the quantity s'
T2C2000	form terrestrial to celestial matrix
XYS2000A	X, Y, s

---

[7] ftp://maia.usno.navy.mil/conv2000/chapter5

The above routines are to a large extent self-contained, but in some cases use simple utility routines from the IAU *Standards of Fundamental Astronomy* software collection. This may be found at $<^8>$.

The SOFA collection includes its own implementations of the IAU 2000 models, together with tools to facilitate their rigorous use.

Two equivalent ways to implement the IAU Resolutions in the transformation from ITRS to GCRS provided by expression (1) can be used, namely (a) the new transformation based on the Celestial Ephemeris Origin and the Earth Rotation Angle and (b) the classical transformation based on the equinox and Greenwich Sidereal Time. They are called respectively "CEO-based" and "equinox-based" transformations in the following.

For both transformations, the procedure is to form the various components of expression (1), or their classical counterparts, and then to combine these components into the complete terrestrial-to-celestial matrix.

Common to all cases is generating the polar-motion matrix, $W(t)$ in expression (1), by calling POM2000. This requires the polar coordinates x_p, y_p and the quantity s'; the latter can be estimated using SP2000.

The matrix for the combined effects of nutation, precession and frame bias is $Q(t)$ in expression (1). For the CEO-based transformation, this is the intermediate-to-celestial matrix and can be obtained using the routine BPN2000, given the CIP position X, Y and the quantity s that defines the position of the CEO. The IAU 2000A X, Y, s are available by calling the routine XYS2000A. In the case of the equinox-based transformation, the counterpart to matrix $Q(t)$ is the true-to-celestial matrix. To obtain this matrix requires the nutation components $\Delta\psi$ and $\Delta\epsilon$; these can be predicted using the IAU 2000A model by means of the routine NU2000A. Faster but lower-accuracy predictions are available from the NU2000B routine, which implements the IAU 2000B truncated model. Once $\Delta\psi$ and $\Delta\epsilon$ are known, the true-to-celestial matrix can be obtained by calling the routine CBPN2000.

The intermediate component is the angle for Earth rotation that defines matrix $R(t)$ in expression (1). For the CEO-based transformation, the angle in question is the Earth Rotation Angle, θ, which can be obtained by calling the routine ERA2000. The counterpart in the case of the equinox-based transformation is the Greenwich (apparent) Sidereal Time. This can be obtained by calling the routine GST2000, given the nutation in longitude, $\Delta\psi$, that was obtained earlier.

The three components are then assembled into the final terrestrial-to-celestial matrix by means of the routine T2C2000.

Three methods of applying the above scheme are set out below.

Method (1): CEO-based transformation consistent with
IAU 2000A precession-nutation

This uses the new (X, Y, s, θ) transformation, which is consistent with IAU 2000A Precession-Nutation.

Having called SP2000 to obtain the quantity s', and knowing the polar motion x_p, y_p, the matrix $W(t)$ can be obtained by calling POM2000. The Earth Rotation Angle provided by expression (13) can be predicted with ERA2000, as a function of UT1. The X, Y, s series, based on expressions (15) and (16) for X and Y, the coordinates of the CIP, and on Table 5.2c for the quantity s, that defines the position of the CEO, can be generated using the XYS2000A routine. (Note that this routine computes the full series for s rather than the summary model in Table 5.2c.) The

---

[8]http://www.iau-sofa.rl.ac.uk

matrix $Q(t)$ that transforms from the intermediate system to the GCRS coordinates can then be generated by means of `BPN2000`. The finished terrestrial-to-celestial matrix is obtained by calling the `T2C2000` routine, specifying the polar-motion matrix, the Earth Rotation Angle and the intermediate-to-celestial matrix.

Method (2A): the equinox-based transformation, using
IAU 2000A precession-nutation

An alternative is the classical, equinox-based, transformation, using the IAU 2000A Precession-Nutation Model and the new IAU-2000-compatible expression for GST.

As for Method 1, the first step is to use `SP2000` and `POM2000` to obtain the matrix $W(t)$, given x_p, y_p. Next, compute the nutation components (lunisolar + planetary) by calling `NU2000A`. The Greenwich (apparent) Sidereal Time is predicted by calling `GST2000`. This requires $\Delta\psi$ and TT as well as UT1. The matrix that transforms from the true equator and equinox of date to GCRS coordinates can then be generated by means of `CBPN2000`. Finally, the finished terrestrial-to-celestial matrix is obtained by calling the `T2C2000` routine, specifying the polar-motion matrix, the Greenwich Sidereal Time and the intermediate-to-celestial matrix.

Method (2B): the classical transformation, using
IAU 2000B precession-nutation

The third possibility is to carry out the classical transformation as for Method 2A, but based on the truncated IAU 2000B Precession-Nutation Model. Using IAU 2000B limits the accuracy to about 1 mas, but the computations are significantly less onerous than when using the full IAU 2000A model.

The same procedure as in Method (2A) is used, but substituting `NU2000B` for `NU2000A`. Depending on the accuracy requirements, further efficiency optimizations are possible, including setting s' to zero, omitting the equation of the equinoxes complementary terms and even neglecting the polar motion.

5.11   Notes on the new Procedure to Transform from ICRS to ITRS

The transformation from the GCRS to ITRS, which is provided in detail in this chapter for use in the IERS Conventions, is also part of the more general transformation for computing directions of celestial objects in intermediate systems.

The procedure to be followed in transforming from the celestial (ICRS) to the terrestrial (ITRS) systems has been clarified to be consistent with the improving observational accuracy. See Figure 5.1 (McCarthy and Capitaine (in Capitaine *et al.*, 2002)) for a diagram of the new and old procedures to be followed. As before, we make use of an intermediate reference system in transforming to a terrestrial system. In this case we call that system the Intermediate Celestial Reference System. (See also Seidelmann and Kovalevsky (2002).) The Celestial Intermediate Pole (CIP) that is realized by the IAU2000A/B Precession-Nutation model defines its equator and the Conventional Ephemeris Origin replaces the equinox.

The position in this reference system is called the intermediate right ascension and declination and is analogous to the previous designation of "apparent right ascension and declination."
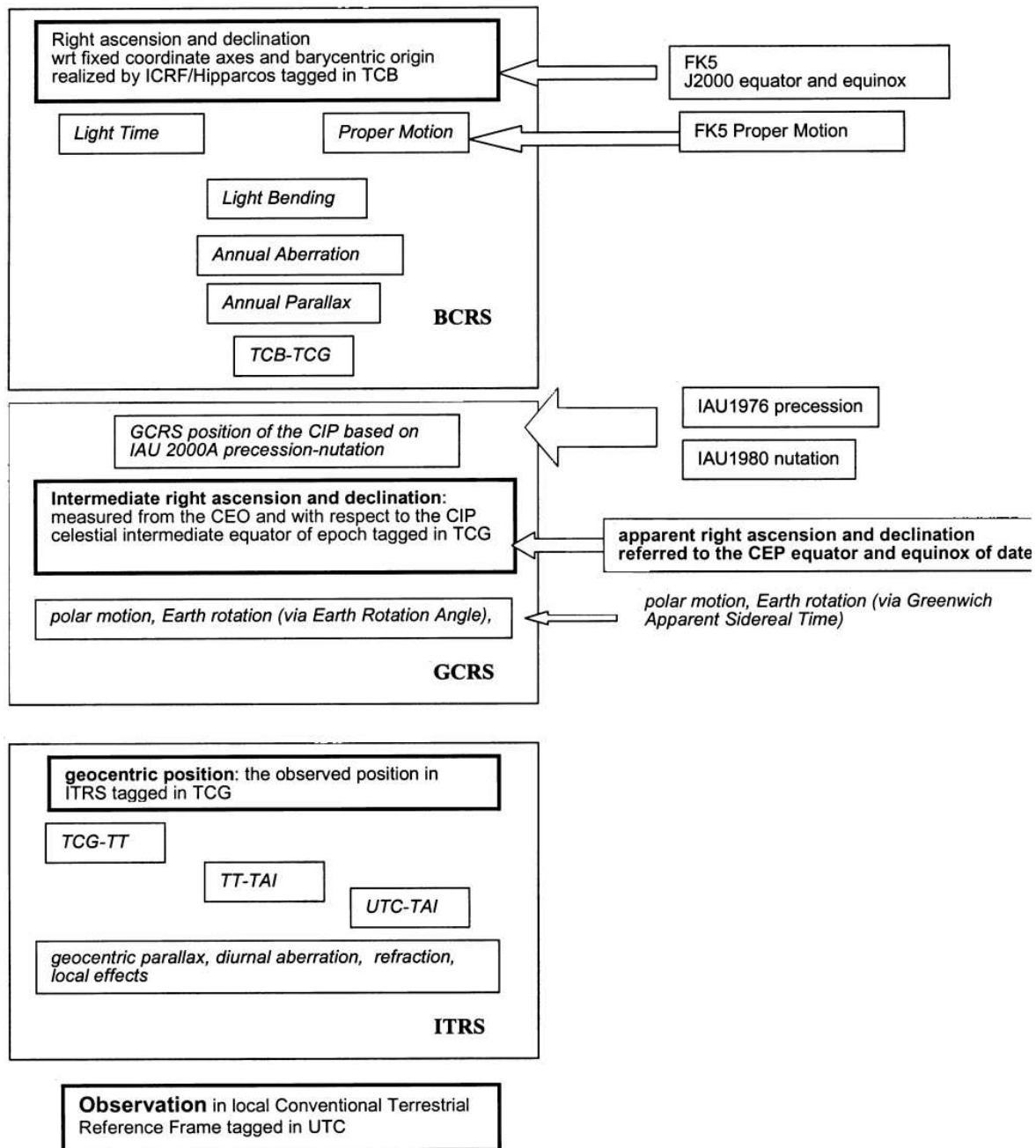
Fig. 5.1   Process to transform from celestial to terrestrial systems. Differences with the past process are shown on the right of the diagram.

References

Cartwright, D. E. and Tayler, R. J., 1971, "New Computations of the Tide-Generating Potential," *Geophys. J. Roy. astr. Soc.*, **23**, pp. 45–74.

Aoki, S., Guinot, B., Kaplan, G. H., Kinoshita, H., McCarthy, D. D., and Seidelmann, P. K., 1982, "The New Definition of Universal Time," *Astron. Astrophys.*, **105**, pp. 359–361.

Aoki, S. and Kinoshita, H., 1983, "Note on the relation between the equinox and Guinot's non-rotating origin," *Celest. Mech.*, **29**, pp. 335–360.

Bizouard, Ch., Brzeziński, A., and Petrov, S., 1998, "Diurnal atmospheric forcing and temporal variability of the nutation amplitudes," *J. Geod.*, **72**, pp. 561–577.

Bizouard, Ch., Folgueira, M., and Souchay, J., 2000, "Comparison of the short period rigid Earth nutation series," in Proc. IAU Colloquium 178, Publications of the Astron. Soc. Pac. Conf. Ser., Dick, S., McCarthy, D., and Luzum, B. (eds.), pp. 613–617.

Bizouard, Ch., Folgueira, M., and Souchay, J., 2001, "Short periodic nutations: comparison between series and influence on polar motion," in Proc. of the *Journées 2000 Systèmes de Référence Spatio-Temporels*, Capitaine, N. (ed.), Observatoire de Paris, pp. 260–265.

Bretagnon, P., 1982, " Théorie du mouvement de l'ensemble des planètes. solution VSOP82," *Astron. Astrophys.*, **114**, pp. 278–288.

Bretagnon, P., Rocher, P., and Simon, J.-L., 1997. "Theory of the rotation of the rigid Earth," *Astron. Astrophys.*, **319**, pp. 305–317.

Brzeziński, A., 2001, "Diurnal and subdiurnal terms of nutation: a simple theoretical model for a nonrigid Earth," in the Proc. of the *Journées Systèmes de Référence Spatio-temporels* 2000, N. Capitaine (ed.), Observatoire de Paris, pp. 243–251.

Brzeziński, A., July 2002, Circular 2, IAU Commission 19 WG "Precession-nutation," being prepared for publication.

Brzeziński, A., and Capitaine N., 2002, "Lunisolar perturbations in Earth rotation due to the triaxial figure of the Earth: geophysical aspects," in the Proc. of the *Journées Systèmes de Référence Spatio-temporels* 2001, N. Capitaine (ed.), Observatoire de Paris, pp. 51–58.

Buffett, B. A., Mathews, P. M., and Herring, T., 2002, "Modeling of nutation-precession: Effects of electromagnetic coupling," *J. Geophys. Res.*, **107, B4**, 10.1029/2001JB000056.

Capitaine, N., 1990, "The Celestial Pole Coordinates," *Celest. Mech. Dyn. Astr.*, **48**, pp. 127–143.

Capitaine, N., 2000, "Definition of the Celestial Ephemeris Pole and the Celestial Ephemeris Origin," in *Towards Models and Constants for Sub-Microarcsecond Astrometry*, Johnston, K. J., McCarthy, D. D., Luzum, B. J., and Kaplan, G. H. (eds.), U.S. Naval Observatory, pp. 153–163.

Capitaine, N., Guinot, B., and Souchay, J., 1986, "A Non-rotating Origin on the Instantaneous Equator: Definition, Properties and Use," *Celest. Mech.*, **39**, pp. 283–307.

Capitaine, N. and Gontier A.-M., 1993, "Accurate procedure for deriving UT1 at a submilliarcsecond accuracy from Greenwich Sidereal Time or from stellar angle," *Astron. Astrophys.*, **275**, pp. 645–650.

Capitaine, N., Guinot, B., and McCarthy, D. D., 2000, "Definition of the Celestial Ephemeris origin and of UT1 in the International Reference Frame," *Astron. Astrophys.*, **355**, pp. 398–405.

Capitaine, N., Gambis, D., McCarthy, D. D., Petit, G., Ray, J., Richter, B., Rothacher, M., Standish, M., and Vondrák, J., (eds.), 2002, *IERS Technical Note*, **29** Proceedings of the IERS Workshop on the Implementation of the New IAU Resolutions, 2002, `http://www.iers.org/iers/publications/tn/tn29/`, Verlag des Bundesamts für Kartographie und Geodäsie, Frankfurt am Main.

Capitaine, N., Chapront, J., Lambert, S., and Wallace, P., 2003**a**, "Expressions for the Celestial Intermediate Pole and Celestial Ephemeris Origin consistent with the IAU 2000A precession-nutation model," *Astron. Astrophys.*, **400**, pp. 1145–1154.

Capitaine, N., Wallace, P. T., and McCarthy, D. D., 2003**b**, "Expressions to Implement the IAU 2000 Definition of UT1," *Astron. Astrophys.*, **406**, pp. 1135-1149.

Capitaine, N., Wallace, P. T., and Chapront, J., and 2003c, "Expressions for IAU 2000 precession quantities," accepted to *Astron. Astrophys.*.

Chapront-Touzé, M. and Chapront, J., 1983, "The lunar ephemeris ELP 2000," *Astron. Astrophys.*, **124**, pp. 50–62.

Chapront, J., Chapront-Touzé, M. and Francou, G., 2002, "A new determination of lunar orbital parameters, precession constant and tidal acceleration from LLR measurements," *Astron. Astrophys.*, **387**, pp. 700–709.

Defraigne, P., Dehant, V., and Pâquet, P., 1995, "Link between the retrograde-prograde nutations and nutations in obliquity and longitude," *Celest. Mech. Dyn. Astr.*, **62**, pp. 363–376.

Dehant, V., Arias, F., Bizouard, Ch., Bretagnon, P., Brzeziński, A., Buffett, B., Capitaine, N., Defraigne, P., de Viron, O., Feissel, M., Fliegel, H., Forte, A., Gambis, D., Getino, J., Gross., R., Herring, T., Kinoshita, H., Klioner, S., Mathews, P. M., McCarthy, D., Moisson, X., Petrov, S., Ponte, R. M., Roosbeek, F., Salstein, D., Schuh, H., Seidelmann, K., Soffel, M., Souchay, J., Vondrák, J., Wahr, J. M., Weber, R., Williams, J., Yatskiv, Y., Zharov, V., and Zhu, S. Y., 1999, "Considerations concerning the non-rigid Earth nutation theory," *Celest. Mech. Dyn. Astr.*, **72**, pp. 245–310.

Escapa, A., Getino, J., and Ferrándiz, J. M., 2002a, "Indirect effect of the triaxiality in the Hamiltonian theory for the rigid Earth nutations," *Astron. Astrophys.*, **389**, pp. 1047–1054.

Escapa, A., Getino, J., and Ferrándiz, J. M., 2002b, "Influence of the triaxiality of the non-rigid Earth on the J2 forced nutations," in the Proc. of the *Journées Systèmes de Référence Spatio-temporels* 2001, N. Capitaine (ed.), Observatoire de Paris, pp. 275–281.

Folgueira, M., Souchay, J., and Kinoshita, S., 1998a, "Effects on the nutation of the non-zonal harmonics of third degree," *Celest. Mech. Dyn. Astr.*, **69**, pp. 373–402.

Folgueira, M., Souchay, J., and Kinoshita, S., 1998b, "Effects on the nutation of C4m and S4m harmonics," *Celest. Mech. Dyn. Astr.*, **70**, pp. 147–157.

Folgueira, M., Bizouard, C., and Souchay, J., 2001, "Diurnal and subdiurnal luni-solar nutations: comparisons and effects," *Celest. Mech. Dyn. Astr.*, **81**, pp. 191–217.

Fukushima, T., 1991, "Geodesic Nutation," *Astron. Astrophys.*, **244**, pp. L11–L12.

Getino, J., Ferrándiz, J. M. and Escapa, A., 2001, "Hamiltonian theory for the non-rigid Earth: semi-diurnal terms," *Astron. Astrophys.*, **370**, pp. 330–341.

Guinot, B., 1979, "Basic Problems in the Kinematics of the Rotation of the Earth," in *Time and the Earth's Rotation*, McCarthy, D. D. and Pilkington, J. D. (eds.), D. Reidel Publishing Company, pp. 7–18.

Herring, T., Mathews P. M., and Buffett, B. A., 2002, "Modeling of nutation-precession: Very long baseline interferometry results," *J. Geophys. Res.*, **107, B4,** 10.1029/2001JB000165.

Lambert, S. and Bizouard, C., 2002, "Positioning the Terrestrial Ephemeris Origin in the International Terrestrial Frame," *Astron. Astrophys.*, **394**, pp. 317–321.

Lieske, J. H., Lederle, T., Fricke, W., and Morando, B., 1977, "Expressions for the Precession Quantities Based upon the IAU (1976) System of Astronomical Constants," *Astron. Astrophys.*, **58**, pp. 1–16.

Ma, C., Arias, E. F., Eubanks, T. M., Fey, A., Gontier, A.-M., Jacobs, C. S., Sovers, O. J., Archinal, B. A., and Charlot, P., 1998, "The International Celestial Reference Frame as realized By Very Long Baseline Interferometry," *Astron. Astrophys.*, **116**, pp. 516–546.

Mathews, P. M., Herring, T. A., and Buffett B. A., 2002, "Modeling of nutation-precession: New nutation series for nonrigid Earth, and insights into the Earth's Interior," *J. Geophys. Res.*, **107, B4,** 10.1029/2001JB000390.

Mathews, P. M. and Bretagnon, P., 2002, "High frequency nutation," in the Proc. of the *Journées Systèmes de Référence Spatio-temporels* 2001, N. Capitaine (ed.), Observatoire de Paris, pp. 28–33.

McCarthy, D. D. (ed.), 1996, IERS Conventions, *IERS Technical Note*, **21**, Observatoire de Paris, Paris.

McCarthy, D. D. and Luzum, B. J., 2003, "An Abridged Model of the Precession-Nutation of the Celestial Pole," *Celest. Mech. Dyn. Astr.*, **85**, pp. 37–49.

Roosbeek, F., 1999,"Diurnal and subdiurnal terms in RDAN97 series," *Celest. Mech. Dyn. Astr.*, **74**, pp. 243–252.

Seidelmann, P. K., 1982, "1980 IAU Nutation: The Final Report of the IAU Working Group on Nutation," *Celest. Mech.*, **27**, pp. 79–106.

Seidelmann, P. K. and Kovalevksy, J., 2002, "Application of the new concepts and definitions (ICRS, CIP and CEO) in fundamental astronomy," *Astron. Astrophys.*, **392**, pp. 341–351.

Simon, J.-L., Bretagnon, P., Chapront, J., Chapront-Touzé, M., Francou, G., and Laskar, J., 1994, "Numerical Expressions for Precession Formulae and Mean Elements for the Moon and Planets," *Astron. Astrophys.*, **282**, pp. 663–683.

Souchay, J. and Kinoshita, H., 1997, "Corrections and new developments in rigid-Earth nutation theory. II. Influence of second-order geopotential and direct planetary effect," *Astron. Astrophys.*, **318**, pp. 639–652.

Souchay, J., Loysel, B., Kinoshita, H., and Folgueira, M., 1999, "Corrections and new developments in rigid Earth nutation theory: III. Final tables REN-2000 including crossed-nutation and spin-orbit coupling effects," *Astron. Astrophys. Supp. Ser.*, **135**, pp. 111–131.

Standish, E. M., 1981, "Two differing definitions of the dynamical equinox and the mean obliquity," *Astron. Astrophys.*, **101**, p. L17.

Wahr, J. M., 1981, "The forced nutation of an elliptical, rotating, elastic and oceanless Earth," *Geophys. J. R. astr. Soc.*, **64**, pp. 705–727.

Williams, J. G., Newhall, X. X., and Dickey, J. O., 1991, "Luni-solar precession — Determination from lunar laser ranges," *Astron. J.*, **241**, pp. L9–L12.

Williams, J. G., 1994, "Contributions to the Earth's obliquity rate, precession, and nutation," *Astron. J.*, **108**, pp. 711–724.

6 Geopotential

Gravitational models commonly used in current (2003) precision orbital analysis by contributors to the International Laser Ranging Service (ILRS) include EGM96 (Lemoine *et al.*, 1998), JGM-3 (Tapley *et al.*, 1996), and GRIM5-C1 (Gruber *et al.*, 2000). For products of interest to IERS, similar accuracy is achievable with any of these models. IERS, recognizing the continuous development of new gravitational models, and anticipating the results of upcoming geopotential mapping missions, recommends at this time the EGM96 model as the conventional model. The $GM_\oplus$ and a_e values reported with EGM96 (398600.4415 km^3/s^2 and 6378136.3 m) should be used as scale parameters with the geopotential coefficients. The recommended $GM_\oplus = 398600.4418$ should be used with the two-body term when working with Geocentric Coordinate Time (TCG) (398600.4415 or 398600.4356 should be used by those still working with Terrestrial Time (TT) or Barycentric Dynamical Time (TDB) units, respectively). EGM96 is available at $<^9>$.

Values for the C_{21} and S_{21} coefficients are included in the EGM96 model. The C_{21} and S_{21} coefficients describe the position of the Earth's figure axis. When averaged over many years, the figure axis should closely coincide with the observed position of the rotation pole averaged over the same time period. Any differences between the mean figure and mean rotation pole averaged would be due to long-period fluid motions in the atmosphere, oceans, or Earth's fluid core (Wahr, 1987; 1990). At present, there is no independent evidence that such motions are important. The EGM96 values for C_{21} and S_{21} give a mean figure axis that corresponds to the mean pole position recommended in Chapter 4 Terrestrial Reference Frame.

This choice for C_{21} and S_{21} is realized as follows. First, to use the geopotential coefficients to solve for a satellite orbit, it is necessary to rotate from the Earth-fixed frame, where the coefficients are pertinent, to an inertial frame, where the satellite motion is computed. This transformation between frames should include polar motion. We assume the polar motion parameters used are relative to the IERS Reference Pole. If $\bar{x}$ and $\bar{y}$ are the angular displacements of the pole of the Terrestrial Reference Frame described in Chapter 4 relative to the IERS Reference Pole, then the values

$$
\begin{aligned}
\bar{C}_{21} &= \sqrt{3}\bar{x}\bar{C}_{20} &-& \bar{x}\bar{C}_{22} &+& \bar{y}\bar{S}_{22}, \\
\bar{S}_{21} &= -\sqrt{3}\bar{y}\bar{C}_{20} &-& \bar{y}\bar{C}_{22} &-& \bar{x}\bar{S}_{22},
\end{aligned}
$$

where $\bar{x} = 0.262 \times 10^{-6}$ radians (equivalent to 0.054 arcsec) and $\bar{y} = 1.730 \times 10^{-6}$ radians (equivalent to 0.357 arcsec) are those determined from observations available from the IERS at $<^{10}>$, so that the mean figure axis coincides with the pole described in Chapter 4. The EGM96 values at 1 January 2000 are $\bar{C}_{20} = -4.84165209 \times 10^{-4}$ (tide free), $\bar{C}_{20} = -4.84169382 \times 10^{-4}$ (zero tide), and $d\bar{C}_{20}/dt = +1.162755 \times 10^{-11}$/year.

This gives normalized coefficients of

$$
\begin{aligned}
\bar{C}_{21}(\text{IERS}) &= -2.23 &\times& 10^{-10}, \quad \text{and} \\
\bar{S}_{21}(\text{IERS}) &= 14.48 &\times& 10^{-10}.
\end{aligned}
$$

$\bar{C}_{21}$ and $\bar{S}_{21}$ are time variable. The values above are associated with the epoch of 1 January 2000. The complete definition of the instantaneous values of the two coefficients to use when computing orbits is given by:

$$
\begin{aligned}
\bar{C}_{21} &= \bar{C}_{21}(t_0) &+& d\bar{C}_{21}/dt[t-t_0], \quad \text{and} \\
\bar{S}_{21} &= \bar{S}_{21}(t_0) &+& d\bar{S}_{21}/dt[t-t_0],
\end{aligned}
$$

---

[9]http://www.nima.mil/GandG/wgsegm/egm96.html
[10]http://maia.usno.navy.mil/conv2000/chapter7/annual.pole

where $d\bar{C}_{21}/dt$ and $d\bar{S}_{21}/dt$ are the time derivatives determined at epoch t_0 to be -0.337×10^{-11}/y and $+1.606 \times 10^{-11}$/y respectively. It is also necessary to account for the solid Earth pole tide described later in this chapter.

6.1   Effect of Solid Earth Tides

The changes induced by the solid Earth tides in the free space potential are most conveniently modeled as variations in the standard geopotential coefficients C_{nm} and S_{nm} (Eanes *et al.*, 1983). The contributions ΔC_{nm} and ΔS_{nm} from the tides are expressible in terms of the k Love number. The effects of ellipticity and of the Coriolis force due to Earth rotation on tidal deformations necessitates the use of three k parameters, $k_{nm}^{(0)}$ and $k_{nm}^{(\pm)}$ (except for $n = 2$) to characterize the changes produced in the free space potential by tides of spherical harmonic degree and order (nm) (Wahr, 1981); only two parameters are needed for $n = 2$ because $k_{2m}^{(-)} = 0$ is zero due to mass conservation.

Anelasticity of the mantle causes $k_{nm}^{(0)}$ and $k_{nm}^{(\pm)}$ to acquire small imaginary parts (reflecting a phase lag in the deformational response of the Earth to tidal forces), and also gives rise to a variation with frequency which is particularly pronounced within the long period band. Though modeling of anelasticity at the periods relevant to tidal phenomena (8 hours to 18.6 years) is not yet definitive, it is clear that the magnitudes of the contributions from anelasticity cannot be ignored (see below). Recent evidence relating to the role of anelasticity in the accurate modeling of nutation data (Mathews *et al.*, 2002) lends support to the model employed herein, at least up to diurnal tidal periods; and there is no compelling reason at present to adopt a different model for the long period tides.

Solid Earth tides within the diurnal tidal band (for which $(nm) = (21)$) are not wholly due to the direct action of the tide generating potential (TGP) on the solid Earth; they include the deformations (and associated geopotential changes) arising from other effects of the TGP, namely, ocean tides and wobbles of the mantle and the core regions. Deformation due to wobbles arises from the incremental centrifugal potentials caused by the wobbles; and ocean tides load the crust and thus cause deformations. Anelasticity affects the Earth's deformational response to all these types of forcing.

The wobbles, in turn, are affected by changes in the Earth's moment of inertia due to deformations from all sources, and in particular, from the deformation due to loading by the $(nm) = (21)$ part of the ocean tide; wobbles are also affected by the anelasticity contributions to all deformations, and by the coupling of the fluid core to the mantle and the inner core through the action of magnetic fields at its boundaries (Mathews *et al.*, 2002). Resonances in the wobbles—principally, the Nearly Diurnal Free Wobble resonance associated with the Free Core Nutation (FCN)— and the consequent resonances in the contribution to tidal deformation from the centrifugal perturbations associated with the wobbles, cause the body tide and load Love/Shida number parameters of the diurnal tides to become strongly frequency dependent. For the derivation of resonance formulae of the form (6) below to represent this frequency dependence, see Mathews *et al.*, (1995). The resonance expansions assume that the Earth parameters entering the wobble equations are all frequency independent. However the ocean tide induced deformation makes a frequency dependent contribution to deformability parameters which are among the Earth parameters just referred to. It becomes necessary therefore to add small corrections to the Love number parameters computed using the resonance formulae. These corrections are included

in the tables of Love number parameters given in this chapter and the next.

The deformation due to ocean loading is itself computed in the first place using frequency independent load Love numbers (see the penultimate section of this chapter and the first section of Chapter 7). Corrections to take account of the resonances in the load Love numbers are incorporated through equivalent corrections to the *body tide* Love numbers, following Wahr and Sasao (1981), as explained further below. These corrections are also included in the tables of Love numbers.

The degree 2 tides produce time dependent changes in C_{2m} and S_{2m}, through $k_{2m}^{(0)}$, which can exceed 10^{-8} in magnitude. They also produce changes exceeding 3×10^{-12} in C_{4m} and S_{4m} through $k_{2m}^{(+)}$. (The direct contributions of the degree 4 tidal potential to these coefficients are negligible.) The only other changes exceeding this cutoff are in C_{3m} and S_{3m}, produced by the degree 3 part of the tide generating potential.

The computation of the tidal contributions to the geopotential coefficients is most efficiently done by a three-step procedure. In Step 1, the $(2m)$ part of the tidal potential is evaluated in the time domain for each m using lunar and solar ephemerides, and the corresponding changes ΔC_{2m} and ΔS_{2m} are computed using frequency independent nominal values k_{2m} for the respective $k_{2m}^{(0)}$. The contributions of the degree 3 tides to C_{3m} and S_{3m} through $k_{3m}^{(0)}$ and also those of the degree 2 tides to C_{4m} and S_{4m} through $k_{2m}^{(+)}$ may be computed by a similar procedure; they are at the level of 10^{-11}.

Step 2 corrects for the deviations of the $k_{21}^{(0)}$ of several of the constituent tides of the diurnal band from the constant nominal value k_{21} assumed for this band in the first step. Similar corrections need to be applied to a few of the constituents of the other two bands also.

Steps 1 and 2 can be used to compute the total tidal contribution, including the time independent (permanent) contribution to the geopotential coefficient $\bar{C}_{20}$, which is adequate for a "conventional tide free" model such as EGM96. When using a "zero tide" model, this permanent part should not be counted twice, this is the goal of Step 3 of the computation. See section 6.3.

With frequency-independent values k_{nm} (Step 1), changes induced by the (nm) part of the tide generating potential in the normalized geopotential coefficients having the same (nm) are given in the time domain by

$$\Delta \bar{C}_{nm} - i \Delta \bar{S}_{nm} = \frac{k_{nm}}{2n+1} \sum_{j=2}^{3} \frac{GM_j}{GM_\oplus} \left(\frac{R_e}{r_j}\right)^{n+1} \bar{P}_{nm}(\sin \Phi_j) e^{-im\lambda_j} \quad (1)$$

(with $\bar{S}_{n0} = 0$), where

$$
\begin{aligned}
k_{nm} &= \text{nominal Love number for degree } n \text{ and order } m, \\
R_e &= \text{equatorial radius of the Earth,} \\
GM_\oplus &= \text{gravitational parameter for the Earth,} \\
GM_j &= \text{gravitational parameter for the Moon } (j = 2) \\
&\quad \text{and Sun } (j = 3), \\
r_j &= \text{distance from geocenter to Moon or Sun,} \\
\Phi_j &= \text{body fixed geocentric latitude of Moon or Sun,} \\
\lambda_j &= \text{body fixed east longitude (from Greenwich) of} \\
&\quad \text{Moon or Sun,}
\end{aligned}
$$

and $\bar{P}_{nm}$ is the normalized associated Legendre function related to the classical (unnormalized) one by

$$\bar{P}_{nm} = N_{nm}P_{nm}, \qquad (2a)$$

where

$$N_{nm} = \sqrt{\frac{(n-m)!(2n+1)(2-\delta_{om})}{(n+m)!}}. \qquad (2b)$$

Correspondingly, the normalized geopotential coefficients $(\bar{C}_{nm}, \bar{S}_{nm})$ are related to the unnormalized coefficients (C_{nm}, S_{nm}) by

$$C_{nm} = N_{nm}\bar{C}_{nm}, \quad S_{nm} = N_{nm}\bar{S}_{nm}. \qquad (3)$$

Equation (1) yields $\Delta\bar{C}_{nm}$ and $\Delta\bar{S}_{nm}$ for both $n = 2$ and $n = 3$ for all m, apart from the corrections for frequency dependence to be evaluated in Step 2. (The particular case $(nm) = (20)$ needs special consideration, however, as already indicated.)

One further computation to be done in Step 1 is that of the changes in the degree 4 coefficients produced by the degree 2 tides. They are given by

$$\Delta\bar{C}_{4m} - i\Delta\bar{S}_{4m} = \frac{k_{2m}^{(+)}}{5}\sum_{j=2}^{3}\frac{GM_j}{GM_\oplus}\left(\frac{R_e}{r_j}\right)^3 \bar{P}_{2m}(\sin\Phi_j)e^{-im\lambda_j}, \quad (m = 0, 1, 2), \quad (4)$$

which has the same form as Equation (1) for $n = 2$ except for the replacement of k_{2m} by $k_{2m}^{(+)}$.

The parameter values for the computations of Step 1 are given in Table 6.1. The choice of these nominal values has been made so as to minimize the number of terms for which corrections will have to be applied in Step 2. The nominal value for $m = 0$ has to be chosen real because there is no closed expression for the contribution to $\bar{C}_{20}$ from the imaginary part of $k_{20}^{(0)}$.

Table 6.1   Nominal values of solid Earth tide external potential Love numbers.

		Elastic Earth		Anelastic Earth		
n	m	k_{nm}	k_{nm}^+	Re k_{nm}	Im k_{nm}	k_{nm}^+
2	0	0.29525	−0.00087	0.30190	−0.00000	−0.00089
2	1	0.29470	−0.00079	0.29830	−0.00144	−0.00080
2	2	0.29801	−0.00057	0.30102	−0.00130	−0.00057
3	0	0.093	$\cdots$			
3	1	0.093	$\cdots$			
3	2	0.093	$\cdots$			
3	3	0.094	$\cdots$			

The frequency dependence corrections to the $\Delta\bar{C}_{nm}$ and $\Delta\bar{S}_{nm}$ values obtained from Step 1 are computed in Step 2 as the sum of contributions from a number of tidal constituents belonging to the respective bands. The contribution to $\Delta\bar{C}_{20}$ from the long period tidal constituents of various frequencies f is

$$\text{Re}\sum_{f(2,0)}(A_0\delta k_f H_f)\,e^{i\theta_f} = \sum_{f(2,0)}[(A_0 H_f\delta k_f^R)\cos\theta_f - (A_0 H_f\delta k_f^I)\sin\theta_f], \qquad (5a)$$

while the contribution to $(\Delta\bar{C}_{21} - i\Delta\bar{S}_{21})$ from the diurnal tidal constituents and to $\Delta\bar{C}_{22} - i\Delta\bar{S}_{22}$ from the semidiurnals are given by

$$\Delta\bar{C}_{2m} - i\Delta\bar{S}_{2m} = \eta_m\sum_{f(2,m)}(A_m\delta k_f H_f)\,e^{i\theta_f}, \quad (m = 1, 2), \qquad (5b)$$

where

$$A_0 = \frac{1}{R_e\sqrt{4\pi}} = 4.4228 \times 10^{-8} \text{ m}^{-1}, \qquad (5c)$$

$$A_m = \frac{(-1)^m}{R_e\sqrt{8\pi}} = (-1)^m(3.1274 \times 10^{-8}) \text{ m}^{-1}, \qquad (m \neq 0), \qquad (5d)$$

$$\eta_1 = -i, \ \eta_2 = 1, \qquad (5e)$$

δk_f = difference between k_f defined as $k_{2m}^{(0)}$ at frequency f and the nominal value k_{2m}, in the sense $k_f - k_{2m}$, plus a contribution from ocean loading,

δk_f^R = real part of δk_f, and

δk_f^I = imaginary part of δk_f, i.e., $\delta k_f = \delta k_f^R + i\delta k_f^I$,

H_f = amplitude (in meters) of the term at frequency f from the harmonic expansion of the tide generating potential, defined according to the convention of Cartwright and Tayler (1971), and

θ_f = $\bar{n} \cdot \bar{\beta} = \sum_{i=1}^{6} n_i\beta_i$,   or

θ_f = $m(\theta_g + \pi) - \bar{N} \cdot \bar{F} = m(\theta_g + \pi) - \sum_{j=1}^{5} N_j F_j$,

where

$\bar{\beta}$ = six-vector of Doodson's fundamental arguments β_i, (τ, s, h, p, N', p_s),

$\bar{n}$ = six-vector of multipliers n_i (for the term at frequency f) of the fundamental arguments,

$\bar{F}$ = five-vector of fundamental arguments F_j (the Delaunay variables l, l', F, D, Ω) of nutation theory,

$\bar{N}$ = five-vector of multipliers N_i of the Delaunay variables for the nutation of frequency $-f + d\theta_g/dt$,

and θ_g is the Greenwich Mean Sidereal Time expressed in angle units (*i.e.* $24^h = 360°$; see Chapter 5).

(π in $(\theta_g + \pi)$ is now to be replaced by 180.)

For the fundamental arguments (l, l', F, D, Ω) of nutation theory and the convention followed here in choosing their multipliers N_j, see Chapter 5. For conversion of tidal amplitudes defined according to different conventions to the amplitude H_f corresponding to the Cartwright-Tayler convention, use Table 6.5 given at the end of this chapter.

For diurnal tides, the frequency dependent values of any load or body tide Love number parameter L (such as $k_{21}^{(0)}$ or $k_{21}^{(+)}$ in the present context) may be represented as a function of the tidal excitation frequency σ by a resonance formula

$$L(\sigma) = L_0 + \sum_{\alpha=1}^{3} \frac{L_\alpha}{(\sigma - \sigma_\alpha)}, \qquad (6)$$

except for the small corrections referred to earlier. (They are to take account of frequency dependent contributions to a few of the Earth's deformability parameters, which make (6) inexact.) The σ_α, ($\alpha = 1, 2, 3$), are the respective resonance frequencies associated with the Chandler wobble (CW), the retrograde free core nutation (FCN), and the prograde free core nutation (PFCN, also known as the free inner core nutation, FICN), and the L_α are the corresponding resonance coefficients. All the parameters are complex. The σ_α and σ are expressed in cycles per sidereal day, with the convention that positive (negative) frequencies represent retrograde (prograde) waves. (This sign convention, followed in tidal theory, is the opposite of that employed in analytical theories of

nutation.) In particular, given the tidal frequency f in degrees per hour, one has
$$\sigma = f/(15 \times 1.002737909),$$
the factor 1.002737909 being the number of sidereal days per solar day. The values used herein for the σ_α are from Mathews $et\ al.$ (2002), adapted to the sign convention used here:

$$
\begin{aligned}
\sigma_1 &= & -0.0026010 &- & 0.0001361 \ i \\
\sigma_2 &= & 1.0023181 &+ & 0.000025 \ \ i \\
\sigma_3 &= & 0.999026 &+ & 0.000780 \ \ i.
\end{aligned}
\tag{7}
$$

They were estimated from a fit of nutation theory to precession rate and nutation amplitude estimates found from an analyis of very long baseline interferometry (VLBI) data.

Table 6.2 lists the values of L_0 and L_α in resonance formulae of the form (6) for $k_{21}^{(0)}$ and $k_{21}^{(+)}$. They were obtained by evaluating the relevant expressions from Mathews $et\ al.$ (1995), using values taken from computations of Buffett and Mathews (unpublished) for the needed deformability parameters together with values obtained for the wobble resonance parameters in the course of computations of the nutation results of Mathews $et\ al.$ (2002). The deformability parameters for an elliptical, rotating, elastic, and oceanless Earth model based on the 1 sec PREM with the ocean layer replaced by solid, and corrections to these for the effects of mantle anelasticity, were found by integration of the tidal deformation equations. Anelasticity computations were based on the Widmer $et\ al.$ (1991) model of mantle Q. As in Wahr and Bergen (1986), a power law was assumed for the frequency dependence of Q, with $200\ s$ as the reference period; the value $\alpha = 0.15$ was used for the power law index. The anelasticity contribution (out-of-phase and in-phase) to the tidal changes in the geopotential coefficients is at the level of one to two percent in-phase, and half to one percent out-of-phase, $i.e.$, of the order of 10^{-10}. The effects of anelasticity, ocean loading and currents, and electromagnetic couplings on the wobbles result in indirect contributions to $k_{21}^{(0)}$ and $k_{21}^{(+)}$ which are almost fully accounted for through the values of the wobble resonance parameters. Also shown in Table 6.2 are the resonance parameters for the load Love numbers h'_{21}, k'_{21}, and l'_{21}, which are relevant to the solid Earth deformation caused by ocean tidal loading and to the consequential changes in the geopotential. (Only the real parts are shown: the small imaginary parts make no difference to the effect to be now considered which is itself small.)

Table 6.2   Parameters in the resonance formulae for $k_{21}^{(0)}$, $k_{21}^{(+)}$ and the load Love numbers.

	$k^{(0)}$		$k^{(+)}$	
α	Re L_α	Im L_α	Re L_α	Im L_α
0	0.29954	-0.1412×10^{-2}	-0.804×10^{-3}	0.237×10^{-5}
1	-0.77896×10^{-3}	-0.3711×10^{-4}	0.209×10^{-5}	0.103×10^{-6}
2	0.90963×10^{-4}	-0.2963×10^{-5}	-0.182×10^{-6}	0.650×10^{-8}
3	-0.11416×10^{-5}	0.5325×10^{-7}	-0.713×10^{-9}	-0.330×10^{-9}

Load Love Numbers (Real parts only)

	h'_{21}	l'_{21}	k'_{21}
0	-0.99500	0.02315	-0.30808
1	1.6583×10^{-3}	2.3232×10^{-4}	8.1874×10^{-4}
2	2.8018×10^{-4}	-8.4659×10^{-6}	1.4116×10^{-4}
3	5.5852×10^{-7}	1.0724×10^{-8}	3.4618×10^{-7}

The expressions given in the penultimate section of this chapter for the contributions from ocean tidal loading assume the constant nominal value $k_2'^{(nom)} = -0.3075$ for k' of the degree 2 tides. Further contributions arise from the frequency dependence of k_{21}'. These may be expressed, following Wahr and Sasao (1981), in terms of an effective ocean tide contribution $\delta k^{(OT)}(\sigma)$ to the body tide Love number $k_{21}^{(0)}$:

$$\delta k^{(OT)}(\sigma) = [k_{21}'(\sigma) - k_2'^{(nom)}] \left(\frac{4\pi G \rho_w R}{5\bar{g}} \right) A_{21}(\sigma), \qquad (8)$$

where G is the constant of universal gravitation, ρ_w is the density of sea water (1025 kg m^{-3}), R is the Earth's mean radius (6.371 $\times$ 10^6 m), $\bar{g}$ is the mean acceleration due to gravity at the Earth's surface (9.820 m s^{-2}), and $A_{21}(\sigma)$ is the admittance for the degree 2 tesseral component of the ocean tide of frequency σ cpsd:

$$A_{21}(\sigma) = \zeta_{21}(\sigma)/\bar{H}(\sigma).$$

ζ_{21} is the complex amplitude of the height of the $(nm) = (21)$ component of the ocean tide, and $\bar{H}$ is the height equivalent of the amplitude of the tide generating potential, the bar being a reminder that the spherical harmonics used in defining the two amplitudes should be identically normalized. Wahr and Sasao (1981) employed the factorized form

$$A_{21}(\sigma) = f_{FCN}(\sigma)\, f_{OD}(\sigma),$$

wherein the first factor represents the effect of the FCN resonance, and the second, that of other ocean dynamic factors. The following empirical formulae (Mathews et $al.$, 2002) which provide good fits to the FCN factors of a set of 11 diurnal tides (Desai and Wahr, 1995) and to the admittances obtainable from the ocean load angular momenta of four principal tides (Chao et $al.$, 1996) are used herein:

$$f_{OD}(\sigma) = (1.3101 - 0.8098\,i) - (1.1212 - 0.6030\,i)\sigma,$$

$$f_{FCN}(\sigma) = 0.1732 + 0.9687\, f_{eqm}(\sigma),$$

$$f_{eqm}(\sigma) = \frac{\gamma(\sigma)}{1 - (3\rho_w/5\bar{\rho})\gamma'(\sigma)},$$

where $\gamma = 1 + k - h$ and $\gamma' = 1 + k' - h'$, $\bar{\rho}$ is the Earth's mean density. (Here k stands for $k_{21}^{(0)}$, and similarly for the other symbols. Only the real parts need be used.) f_{eqm} is the FCN factor for a global equilibrium ocean.

Table 6.3a shows the values of

$$\delta k_f \equiv (k_{21}^{(0)}(\sigma) - k_{21}) + \delta k_{21}^{OT}(\sigma),$$

along with the real and imaginary parts of the amplitude $(A_1 \delta k_f H_f)$. The tides listed are those for which either of the parts is at least 10^{-13} after round-off. (A cutoff at this level is used for the individual terms in order that accuracy at the level of 3×10^{-12} be not affected by the accumulated contributions from the numerous smaller terms that are disregarded.) Roughly half the value of the imaginary part comes from the ocean tide term, and the real part contribution from this term is of about the same magnitude.

Table 6.3a   The in-phase (ip) amplitudes $(A_1\delta k_f^R H_f)$ and the out-of-phase (op) amplitudes $(A_1\delta k_f^I H_f)$ of the corrections for frequency dependence of $k_{21}^{(0)}$, taking the nominal value k_{21} for the diurnal tides as $(0.29830 - i\,0.00144)$. Units: 10^{-12}. The entries for δk_f^R and δk_f^I are in units of 10^{-5}. Multipliers of the Doodson arguments identifying the tidal terms are given, as also those of the Delaunay variables characterizing the nutations produced by these terms.

Name	deg/hr	Doodson No.	τ	s	h	p	N'	p_s	ℓ	ℓ'	F	D	Ω	δk_f^R 10^{-5}	δk_f^I 10^{-5}	Amp. (ip)	Amp. (op)
$2Q_1$	12.85429	125,755	1	-3	0	2	0	0	2	0	2	0	2	-29	3	-0.1	0.0
σ_1	12.92714	127,555	1	-3	2	0	0	0	0	0	2	2	2	-30	3	-0.1	0.0
	13.39645	135,645	1	-2	0	1	-1	0	1	0	2	0	1	-45	5	-0.1	0.0
Q_1	13.39866	135,655	1	-2	0	1	0	0	1	0	2	0	2	-46	5	-0.7	0.1
ρ_1	13.47151	137,455	1	-2	2	-1	0	0	-1	0	2	2	2	-49	5	-0.1	0.0
	13.94083	145,545	1	-1	0	0	-1	0	0	0	2	0	1	-82	7	-1.3	0.1
O_1	13.94303	145,555	1	-1	0	0	0	0	0	0	2	0	2	-83	7	-6.8	0.6
τ_1	14.02517	147,555	1	-1	2	0	0	0	0	0	0	2	0	-91	9	0.1	0.0
$N\tau_1$	14.41456	153,655	1	0	-2	1	0	0	1	0	2	-2	2	-168	14	0.1	0.0
	14.48520	155,445	1	0	0	-1	-1	0	-1	0	2	0	1	-193	16	0.1	0.0
LK_1	14.48741	155,455	1	0	0	-1	0	0	-1	0	2	0	2	-194	16	0.4	0.0
NO_1	14.49669	155,655	1	0	0	1	0	0	1	0	0	0	0	-197	16	1.3	-0.1
	14.49890	155,665	1	0	0	1	1	0	1	0	0	0	1	-198	16	0.3	0.0
χ_1	14.56955	157,455	1	0	2	-1	0	0	-1	0	0	2	0	-231	18	0.3	0.0
	14.57176	157,465	1	0	2	-1	1	0	-1	0	0	2	1	-233	18	0.1	0.0
π_1	14.91787	162,556	1	1	-3	0	0	1	0	1	2	-2	2	-834	58	-1.9	0.1
	14.95673	163,545	1	1	-2	0	-1	0	0	0	2	-2	1	-1117	76	0.5	0.0
P_1	14.95893	163,555	1	1	-2	0	0	0	0	0	2	-2	2	-1138	77	-43.4	2.9
	15.00000	164,554	1	1	-1	0	0	-1	0	-1	2	-2	2	-1764	104	0.6	0.0
S_1	15.00000	164,556	1	1	-1	0	0	1	0	1	0	0	0	-1764	104	1.6	-0.1
	15.02958	165,345	1	1	0	-2	-1	0	-2	0	2	0	1	-3048	92	0.1	0.0
	15.03665	165,535	1	1	0	0	-2	0	0	0	0	0	-2	-3630	195	0.1	0.0
	15.03886	165,545	1	1	0	0	-1	0	0	0	0	0	-1	-3845	229	-8.8	0.5
K_1	15.04107	165,555	1	1	0	0	0	0	0	0	0	0	0	-4084	262	470.9	-30.2
	15.04328	165,565	1	1	0	0	1	0	0	0	0	0	1	-4355	297	68.1	-4.6
	15.04548	165,575	1	1	0	0	2	0	0	0	0	0	2	-4665	334	-1.6	0.1
	15.07749	166,455	1	1	1	-1	0	0	-1	0	0	1	0	85693	21013	0.1	0.0
	15.07993	166,544	1	1	1	0	-1	-1	0	-1	0	0	-1	35203	2084	-0.1	0.0
ψ_1	15.08214	166,554	1	1	1	0	0	-1	0	-1	0	0	0	22794	358	-20.6	-0.3
	15.08214	166,556	1	1	1	0	0	1	0	1	-2	2	-2	22780	358	0.3	0.0
	15.08434	166,564	1	1	1	0	1	-1	0	-1	0	0	1	16842	-85	-0.3	0.0
	15.11392	167,355	1	1	2	-2	0	0	-2	0	0	2	0	3755	-189	-0.2	0.0
	15.11613	167,365	1	1	2	-2	1	0	-2	0	0	2	1	3552	-182	-0.1	0.0
ϕ_1	15.12321	167,555	1	1	2	0	0	0	0	0	-2	2	-2	3025	-160	-5.0	0.3
	15.12542	167,565	1	1	2	0	1	0	0	0	-2	2	-1	2892	-154	0.2	0.0
	15.16427	168,554	1	1	3	0	0	-1	0	-1	-2	2	-2	1638	-93	-0.2	0.0
θ_1	15.51259	173,655	1	2	-2	1	0	0	1	0	0	-2	0	370	-20	-0.5	0.0
	15.51480	173,665	1	2	-2	1	1	0	1	0	0	-2	1	369	-20	-0.1	0.0
	15.58323	175,445	1	2	0	-1	-1	0	-1	0	0	0	-1	325	-17	0.1	0.0
J_1	15.58545	175,455	1	2	0	-1	0	0	-1	0	0	0	0	324	-17	-2.1	0.1
	15.58765	175,465	1	2	0	-1	1	0	-1	0	0	0	1	323	-16	-0.4	0.0
SO_1	16.05697	183,555	1	3	-2	0	0	0	0	0	0	-2	0	194	-8	-0.2	0.0
	16.12989	185,355	1	3	0	-2	0	0	-2	0	0	0	0	185	-7	-0.1	0.0
OO_1	16.13911	185,555	1	3	0	0	0	0	0	0	-2	0	-2	184	-7	-0.6	0.0
	16.14131	185,565	1	3	0	0	1	0	0	0	-2	0	-1	184	-7	-0.4	0.0
	16.14352	185,575	1	3	0	0	2	0	0	0	-2	0	0	184	-7	-0.1	0.0
ν_1	16.68348	195,455	1	4	0	-1	0	0	-1	0	-2	0	-2	141	-4	-0.1	0.0
	16.68569	195,465	1	4	0	-1	1	0	-1	0	-2	0	-1	141	-4	-0.1	0.0

The values used for $k_{21}^{(0)}(\sigma)$ in evaluating δk_f are from an exact computation necessarily involving use of the framework of nutation-wobble theory which is outside the scope of this chapter. If the (approximate) resonance formula were used instead for the computation, the resulting numbers for δk_f^R and δk_f^I would require small corrections to match the exact values. In units of 10^{-5}, they are (in-phase, out-of-phase) (1, 1) for Q_1, (1, 1) for O_1 and its companion having Doodson numbers 145,545, (1, 0) for NO_1, (0, −1) for P_1, (244, 299) for ψ_1, (12, 12) for ϕ_1, (3, 2) for J_1, and (2, 1) for OO_1 and its companion with Doodson numbers 185,565. These are the only tides for which the corrections would contribute nonneglibily to the numbers listed in the last two columns of the table.

Calculation of the correction due to any tidal constituent is illustrated by the following example for K_1. Given that $A_m = A_1 = -3.1274 \times 10^{-8}$, and that $H_f = 0.36870$, $\theta_f = (\theta_g + \pi)$, and $k_{21}^{(0)} = (0.25746 + 0.00118\,i)$ for this tide, one finds on subtracting the nominal value $(0.29830 - 0.00144\,i)$ that $\delta k_f = (-0.04084 + 0.00262\,i)$. Equation (5b) then yields:

$$
\begin{aligned}
(\Delta \bar{C}_{21})_{K_1} &= 470.9 \times 10^{-12} \sin(\theta_g + \pi) - 30.2 \times 10^{-12} \cos(\theta_g + \pi), \\
(\Delta \bar{S}_{21})_{K_1} &= 470.9 \times 10^{-12} \cos(\theta_g + \pi) + 30.2 \times 10^{-12} \sin(\theta_g + \pi).
\end{aligned}
$$

The variation of $k_{20}^{(0)}$ across the zonal tidal band, $(nm) = (20)$, is due to mantle anelasticity; it is described by the formula

$$
k_{20}^{(0)} = 0.29525 - 5.796 \times 10^{-4} \left\{ \cot \frac{\alpha \pi}{2} \left[1 - \left(\frac{f_m}{f} \right)^\alpha \right] + i \left(\frac{f_m}{f} \right)^\alpha \right\} \quad (9)
$$

on the basis of the anelasticity model referred to earlier. Here f is the frequency of the zonal tidal constituent, f_m is the reference frequency equivalent to a period of 200 s, and $\alpha = 0.15$. The δk_f in Table 6.3b are the differences between $k_{20}^{(0)}$ computed from the above formula and the nominal value $k_{20} = 0.30190$ given in Table 6.1.

The total variation in geopotential coefficient $\bar{C}_{20}$ is obtained by adding to the result of Step 1 the sum of the contributions from the tidal constituents listed in Table 6.3b computed using equation (5a). The tidal variations in $\bar{C}_{2m}$ and $\bar{S}_{2m}$ for the other m are computed similarly, except that equation (5b) is to be used together with Table 6.3a for $m = 1$ and Table 6.3c for $m = 2$.

6.2 Solid Earth Pole Tide

The pole tide is generated by the centrifugal effect of polar motion, characterized by the potential

$$
\begin{aligned}
\Delta V(r, \theta, \lambda) &= -\frac{\Omega^2 r^2}{2} \sin 2\theta \, (m_1 \cos \lambda + m_2 \sin \lambda) \\
&= -\frac{\Omega^2 r^2}{2} \sin 2\theta \, \mathbf{Re} \left[(m_1 - im_2) e^{i\lambda} \right].
\end{aligned} \quad (10)
$$

(See sub-section 7.1.4 for further details, including the relation of the wobble variables (m_1, m_2) to the polar motion variables (x_p, y_p).) The deformation which constitutes this tide produces a perturbation

$$
-\frac{\Omega^2 r^2}{2} \sin 2\theta \, \mathbf{Re} \left[k_2 \, (m_1 - im_2) e^{i\lambda} \right]
$$

in the external potential, which is equivalent to changes in the geopotential coefficients C_{21} and S_{21}. Using for k_2 the value $0.3077 + 0.0036\,i$ appropriate to the polar tide yields

$$
\begin{aligned}
\Delta \bar{C}_{21} &= -1.333 \times 10^{-9} (m_1 - 0.0115 m_2), \\
\Delta \bar{S}_{21} &= -1.333 \times 10^{-9} (m_2 + 0.0115 m_1),
\end{aligned}
$$

where m_1 and m_2 are in seconds of arc.

Table 6.3b   Corrections for frequency dependence of $k_{20}^{(0)}$ of the zonal tides due to anelasticity. Units: 10^{-12}. The nominal value k_{20} for the zonal tides is taken as 0.30190. The real and imaginary parts δk_f^R and δk_f^I of δk_f are listed, along with the corresponding in-phase (ip) amplitude $(A_0 H_f \delta k_f^R)$ and out-of-phase (op) amplitude $(-A_0 H_f \delta k_f^I)$ to be used in equation (5a).

Name	Doodson No.	deg/hr	τ	s	h	p	N'	p_s	ℓ	ℓ'	F	D	Ω	δk_f^R	Amp. (ip)	δk_f^I	Amp. (op)
	55,565	0.00221	0	0	0	0	1	0	0	0	0	0	1	0.01347	16.6	-0.00541	-6.7
	55,575	0.00441	0	0	0	0	2	0	0	0	0	0	2	0.01124	-0.1	-0.00488	0.1
S_a	56,554	0.04107	0	0	1	0	0	-1	0	-1	0	0	0	0.00547	-1.2	-0.00349	0.8
S_{sa}	57,555	0.08214	0	0	2	0	0	0	0	0	-2	2	-2	0.00403	-5.5	-0.00315	4.3
	57,565	0.08434	0	0	2	0	1	0	0	0	-2	2	-1	0.00398	0.1	-0.00313	-0.1
	58,554	0.12320	0	0	3	0	0	-1	0	-1	-2	2	-2	0.00326	-0.3	-0.00296	0.2
M_{sm}	63,655	0.47152	0	1	-2	1	0	0	1	0	0	-2	0	0.00101	-0.3	-0.00242	0.7
	65,445	0.54217	0	1	0	-1	-1	0	-1	0	0	0	-1	0.00080	0.1	-0.00237	-0.2
M_m	65,455	0.54438	0	1	0	-1	0	0	-1	0	0	0	0	0.00080	-1.2	-0.00237	3.7
	65,465	0.54658	0	1	0	-1	1	0	-1	0	0	0	1	0.00079	0.1	-0.00237	-0.2
	65,655	0.55366	0	1	0	1	0	0	1	0	-2	0	-2	0.00077	0.1	-0.00236	-0.2
M_{sf}	73,555	1.01590	0	2	-2	0	0	0	0	0	0	-2	0	-0.00009	0.0	-0.00216	0.6
	75,355	1.08875	0	2	0	-2	0	0	-2	0	0	0	0	-0.00018	0.0	-0.00213	0.3
M_f	75,555	1.09804	0	2	0	0	0	0	0	0	-2	0	-2	-0.00019	0.6	-0.00213	6.3
	75,565	1.10024	0	2	0	0	1	0	0	0	-2	0	-1	-0.00019	0.2	-0.00213	2.6
	75,575	1.10245	0	2	0	0	2	0	0	0	-2	0	0	-0.00019	0.0	-0.00213	0.2
M_{stm}	83,655	1.56956	0	3	-2	1	0	0	1	0	-2	-2	-2	-0.00065	0.1	-0.00202	0.2
M_{tm}	85,455	1.64241	0	3	0	-1	0	0	-1	0	-2	0	-2	-0.00071	0.4	-0.00201	1.1
	85,465	1.64462	0	3	0	-1	1	0	-1	0	-2	0	-1	-0.00071	0.2	-0.00201	0.5
M_{sqm}	93,555	2.11394	0	4	-2	0	0	0	0	0	-2	-2	-2	-0.00102	0.1	-0.00193	0.2
M_{qm}	95,355	2.18679	0	4	0	-2	0	0	-2	0	-2	0	-2	-0.00106	0.1	-0.00192	0.1

Table 6.3c   Amplitudes $(A_2 \delta k_f H_f)$ of the corrections for frequency dependence of $k_{22}^{(0)}$, taking the nominal value k_{22} for the sectorial tides as $(0.30102 - i\, 0.00130)$. Units: 10^{-12}. The corrections are only to the real part.

Name	Doodson No.	deg/hr	τ	s	h	p	N'	p_s	ℓ	ℓ'	F	D	Ω	δk_f^R	Amp.
N_2	245,655	28.43973	2	-1	0	1	0	0	1	0	2	0	2	0.00006	-0.3
M_2	255,555	28.98410	2	0	0	0	0	0	0	0	2	0	2	0.00004	-1.2

6.3   Treatment of the Permanent Tide

The degree 2 zonal tide generating potential has a mean (time average) value that is nonzero. This time independent $(nm) = (20)$ potential produces a permanent deformation and a consequent time independent contribution to the geopotential coefficient $\bar{C}_{20}$. In formulating a geopotential model, two approaches may be taken (see Chapter 1). When the time independent contribution is included in the adopted value of $\bar{C}_{20}$, then the value is termed "zero tide" and will be noted here $\bar{C}_{20}^{zt}$. This is the case for the JGM-3 model. If the time independent contribution is not included in the adopted value of $\bar{C}_{20}$, then the value is termed "conventional tide free" and will be noted here $\bar{C}_{20}^{tf}$. This is the case of the EGM96 model.

When using the EGM96 geopotential model as originally disseminated, *i.e.* as a "conventional tide free" model with $\bar{C}_{20}^{tf} = -0.4841653717 \times 10^{-3}$ at epoch 2000, the full tidal model given by (1), computed according to the preceding sections, should be used.

In the case of a "zero tide" geopotential model, the model of tidal effects to be added should not once again contain a time independent part. One must not then use the expression (1) as it stands for modeling $\Delta\bar{C}_{20}$; its permanent part must first be restored. This is Step 3 of the computation, which provides us with $\Delta\bar{C}_{20}$.

The symbol $\Delta\bar{C}_{20}$ will hereafter be reserved for the temporally varying part of (1) while the full expression will be redesignated as $\Delta\bar{C}_{20}^*$ and the time independent part $\Delta\bar{C}_{20}^{perm}$. Thus

$$\Delta\bar{C}_{20} = \Delta\bar{C}_{20}^* - \langle\Delta\bar{C}_{20}^*\rangle, \tag{11}$$

where

$$\Delta\bar{C}_{20}^* = \frac{k_{20}}{5} \sum_{j=2}^{3} \frac{GM_j}{GM_\oplus} \left(\frac{R_e}{r_j}\right)^3 \bar{P}_{20}(\sin\Phi_j),$$

$$\langle\Delta\bar{C}_{20}^*\rangle = A_0 H_0 k_{20} = (4.4228 \times 10^{-8})(-0.31460)k_{20}. \tag{12}$$

In evaluating it, the same value must be used for k_{20} in both $\Delta\bar{C}_{20}^*$ and $\langle\Delta\bar{C}_{20}\rangle$. With $k_{20} = 0.30190$, $\langle\Delta\bar{C}_{20}\rangle = -4.201 \times 10^{-9}$. EGM96 has been computed using $k_{20} = 0.3$, therefore $\langle\Delta\bar{C}_{20}\rangle = -4.173 \times 10^{-9}$ and $\bar{C}_{20}^{zt} = -0.484169382 \times 10^{-3}$ at epoch 2000.

The use of "zero tide" values and the subsequent removal of the effect of the permanent tide from the tide model is presented for consistency with the 18th IAG General Assembly Resolution 16.

6.4 Effect of the Ocean Tides

The dynamical effects of ocean tides are most easily incorporated by periodic variations in the normalized Stokes' coefficients. These variations can be written as

$$\Delta\bar{C}_{nm} - i\Delta\bar{S}_{nm} = F_{nm} \sum_{s(n,m)} \sum_{+}^{-} (C_{snm}^\pm \mp iS_{snm}^\pm)e^{\pm i\theta_f}, \tag{13}$$

where

$$F_{nm} = \frac{4\pi G\rho_w}{g_e} \sqrt{\frac{(n+m)!}{(n-m)!(2n+1)(2-\delta_{om})}} \left(\frac{1+k_n'}{2n+1}\right),$$

g_e and G are given in Chapter 1,
ρ_w = density of seawater = 1025 kg m^{-3},
k_n' = load deformation coefficients (k_2' =−0.3075,
        k_3' =−0.195, k_4' =−0.132, k_5' =−0.1032, k_6' =−0.0892),
$C_{snm}^\pm, S_{snm}^\pm$ = ocean tide coefficients (m) for the tide constituent s
θ_s = argument of the tide constituent s as defined in the
        solid tide model (Chapter 7).

The summation over $+$ and $-$ denotes the respective addition of the retrograde waves using the top sign and the prograde waves using the bottom sign. The $C_{snm}^\pm$ and $S_{snm}^\pm$ are the coefficients of a spherical harmonic decomposition of the ocean tide height for the ocean tide due to the constituent s of the tide generating potential.

For each constituent s in the diurnal and semidiurnal tidal bands, these coefficients were obtained from the CSR 3.0 ocean tide height model (Eanes and Bettadpur, 1995), which was estimated from the TOPEX/ Poseidon satellite altimeter data. For each constituent s in the long period band, the self-consistent equilibrium tide model of Ray and Cartwright (1994) was used. The list of constituents for which the coefficients were determined was obtained from the Cartwright and Tayler (1971) expansion of the tide generating potential.

These ocean tide height harmonics are related to the Schwiderski convention (Schwiderski, 1983) according to

$$C_{snm}^{\pm} - iS_{snm}^{\pm} = -i\hat{C}_{snm}^{\pm}e^{i(\epsilon_{snm}^{\pm}+\chi_s)}, \tag{14}$$

where

$\hat{C}_{snm}^{\pm}$	=	ocean tide amplitude for constituent s using the Schwiderski notation,
$\epsilon_{snm}^{\pm}$	=	ocean tide phase for constituent s, and
χ_s		is obtained from Table 6.4, with H_s being the Cartwright and Tayler (1971) amplitude at frequency s.

Table 6.4   Values of χ_s for long-period, diurnal and semidiurnal tides.

Tidal Band	$H_s > 0$	$H_s < 0$
Long Period	π	0
Diurnal	$\frac{\pi}{2}$	$-\frac{\pi}{2}$
Semidiurnal	0	π

For clarity, the terms in equation 1 are repeated in both conventions:

$$\Delta\bar{C}_{nm} = F_{nm} \sum_{s(n,m)} [(C_{snm}^{+}+C_{snm}^{-})\cos\theta_s + (S_{snm}^{+}+S_{snm}^{-})\sin\theta_s] \tag{15a}$$

or

$$\Delta\bar{C}_{nm} = F_{nm} \sum_{s(n,m)} [\hat{C}_{snm}^{+}\sin(\theta_s+\epsilon_{snm}^{+}+\chi_s) + \hat{C}_{snm}^{-}\sin(\theta_s+\epsilon_{snm}^{-}+\chi_s)], \tag{15b}$$

$$\Delta\bar{S}_{nm} = F_{nm} \sum_{s(n,m)} [(S_{snm}^{+}-S_{snm}^{-})\cos\theta_s - (C_{snm}^{+}-C_{snm}^{-})\sin\theta_s] \tag{15c}$$

or

$$\Delta\bar{S}_{nm} = F_{nm} \sum_{s(n,m)} [\hat{C}_{snm}^{+}\cos(\theta_s+\epsilon_{snm}^{+}+\chi_s) - \hat{C}_{snm}^{-}\cos(\theta_s+\epsilon_{snm}^{-}+\chi_s)]. \tag{15d}$$

The orbit element perturbations due to ocean tides can be loosely grouped into two classes. The resonant perturbations arise from coefficients for which the order (m) is equal to the first Doodson's argument multiplier n_1 of the tidal constituent s (See Note), and have periodicities from a few days to a few years. The non-resonant perturbations arise when the order m is not equal to index n_1. The most important of these are due to ocean tide coefficients for which $m = n_1 + 1$ and have periods of about 1 day.

Certain selected constituents (e.g. S_a and S_2) are strongly affected by atmospheric mass distribution (Chapman and Lindzen, 1970). The resonant harmonics (for $m = n_1$) for some of these constituents were determined by their combined effects on the orbits of several satellites. These multi-satellite values then replaced the corresponding values from the CSR 3.0 altimetric ocean tide height model.

Based on the predictions of the linear perturbation theory outlined in Casotto (1989), the relevant tidal constituents and spherical harmonics were selected for several geodetic and altimetric satellites. For geodetic satellites, both resonant and non-resonant perturbations were analyzed,whereas for altimetric satellites, only the non-resonant perturbations were analyzed. For the latter, the adjustment of empirical parameters during orbit determination removes the errors in modeling resonant accelerations. The resulting selection of ocean tidal harmonics was then

merged into a single recommended ocean tide force model. With this selection the error of omission on TOPEX is approximately 5 mm along-track, and for Lageos it is 2 mm along-track. The recommended ocean tide harmonic selection is available via anonymous ftp from $<^{11}>$.

For high altitude geodetic satellites like Lageos, in order to reduce the required computing time, it is recommended that out of the complete selection, only the constituents whose Cartwright and Tayler amplitudes H_s is greater than 0.5 mm be used, with their spherical harmonic expansion terminated at maximum degree and order 8. The omission errors from this reduced selection on Lageos is estimated at approximately 1 cm in the transverse direction for short arcs.

NOTE: The Doodson variable multipliers ($\bar{n}$) are coded into the argument number (A) after Doodson (1921) as:

$$A = n_1(n_2 + 5)(n_3 + 5).(n_4 + 5)(n_5 + 5)(n_6 + 5).$$

6.5 Conversion of Tidal Amplitudes defined according to Different Conventions

The definition used for the amplitudes of tidal terms in the recent high-accuracy tables differ from each other and from Cartwright and Tayler (1971). Hartmann and Wenzel (1995) tabulate amplitudes in units of the potential (m²s⁻²), while the amplitudes of Roosbeek (1996), which follow the Doodson (1921) convention, are dimensionless. To convert them to the equivalent tide heights H_f of the Cartwright-Tayler convention, multiply by the appropriate factors from Table 6.5. The following values are used for the constants appearing in the conversion factors: Doodson constant $D_1 = 2.63358352855$ m² s⁻²; $g_e \equiv g$ at the equatorial radius $= 9.79828685$ (from $GM = 3.986004415 \times 10^{14}$ m³ s⁻², $R_e = 6378136.55$ m).

Table 6.5   Factors for conversion to Cartwright-Tayler amplitudes from those defined according to Doodson's and Hartmann and Wenzel's conventions.

From Doodson	From Hartmann & Wenzel
$f_{20} = -\frac{\sqrt{4\pi}}{\sqrt{5}}\frac{D_1}{g_e} = -0.426105$	$f'_{20} = \frac{2\sqrt{\pi}}{g_e} = 0.361788$
$f_{21} = -\frac{2\sqrt{24\pi}}{3\sqrt{5}}\frac{D_1}{g_e} = -0.695827$	$f'_{21} = -\frac{\sqrt{8\pi}}{g_e} = -0.511646$
$f_{22} = \frac{\sqrt{96\pi}}{3\sqrt{5}}\frac{D_1}{g_e} = 0.695827$	$f'_{22} = \frac{\sqrt{8\pi}}{g_e} = 0.511646$
$f_{30} = -\frac{\sqrt{20\pi}}{\sqrt{7}}\frac{D_1}{g_e} = -0.805263$	$f'_{30} = \frac{2\sqrt{\pi}}{g_e} = 0.361788$
$f_{31} = \frac{\sqrt{720\pi}}{8\sqrt{7}}\frac{D_1}{g_e} = 0.603947$	$f'_{31} = \frac{\sqrt{8\pi}}{g_e} = 0.511646$
$f_{32} = \frac{\sqrt{1440\pi}}{10\sqrt{7}}\frac{D_1}{g_e} = 0.683288$	$f'_{32} = \frac{\sqrt{8\pi}}{g_e} = 0.511646$
$f_{33} = -\frac{\sqrt{2880\pi}}{15\sqrt{7}}\frac{D_1}{g_e} = -0.644210$	$f'_{33} = -\frac{\sqrt{8\pi}}{g_e} = -0.511646$

---

[11]ftp.csr.utexas.edu/pub/tide

References

Cartwright, D. E. and Tayler, R. J., 1971, "New Computations of the Tide-Generating Potential," *Geophys. J. Roy. astr. Soc.*, **23**, pp. 45–74.

Casotto, S., 1989, "Ocean Tide Models for TOPEX Precise Orbit Determination," Ph.D. Dissertation, The Univ. of Texas at Austin.

Chapman, S. and Lindzen, R., 1970, *Atmospheric Tides*, D. Reidel, Dordrecht, 200 pp.

Chao, B. F., Ray, R. D., Gipson, J. M., Egbert, G. D. and Ma, C., 1996, "Diurnal/semidiurnal polar motion excited by oceanic tidal angular momentum," *J. Geophys. Res.*, **101**, pp. 20151–20163.

Desai, S. and Wahr, J. M., 1995, "Empirical ocean tide models estimated from Topex/Poseidon altimetry," *J. Geophys. Res.*, **100**, pp. 25205–25228.

Doodson, A. T., 1921, "The Harmonic Development of the Tide-Generating Potential," *Proc. R. Soc. A.*, **100**, pp. 305–329.

Eanes, R. J., Schutz, B., and Tapley, B., 1983, "Earth and Ocean Tide Effects on Lageos and Starlette," in *Proc. of the Ninth International Symposium on Earth Tides*, Kuo, J. T. (ed.), E. Sckweizerbart'sche Verlagabuchhandlung, Stuttgart.

Eanes R. J. and Bettadpur, S., 1995, "The CSR 3.0 global ocean tide model," *Technical Memorandum CSR-TM-95-06*, Center for Space Research, University of Texas, Austin, TX.

Gruber, Th., Bode, A., Reigber, Ch., Schwintzer, P., Balmino, G., Biancale, R., and Lemoine, J.-M., 2000, *Geophys. Res. Lett.*, **27**, pp. 4005–4008.

Hartmann, T. and Wenzel, H.-G., 1995, "The HW95 Tidal Potential Catalogue," *Geophys. Res. Lett.*, **22**, pp. 3553–3556.

Lemoine, F. G., Kenyon, S. C., Factor, J. K., Trimmer, R. G., Pavlis, N. K., Chinn, D. S., Cox, C. M., Klosko, S. M., Luthke, S. B., Torrance, M. H., Wang, Y. M., Williamson, R. G., Pavlis, E. C., Rapp, R. H., and Olson, T. R., 1998, "The Development of the Joint NASA GSFC and National Imagery and Mapping Agency (NIMA) Geopotential Model EGM96," *NASA/TP-1998-206861*, Goddard Space Flight Center, Greenbelt, Maryland.

Mathews, P. M., Buffett, B. A., and Shapiro,. I. I., 1995, "Love numbers for diurnal tides: Relation to wobble admittances and resonance expansions," *J. Geophys. Res.*, **100**, pp. 9935–9948.

Mathews, P. M., Herring, T. A., and Buffett, B. A., 2002, "Modeling of nutation-precession: New nutation series for nonrigid Earth, and insights into the Earth's interior," *J. Geophys. Res.*, **107, B4**, 10.1029/2001JB000390.

Ray, R. D. and Cartwright, D. E., 1994, "Satellite altimeter observations of the M_f and M_m ocean tides, with simultaneous orbit corrections," *Gravimetry and Space Techniques Applied to Geodynamics and Ocean Dynamics*, Geophysical Monograph 82, IUGG Volume 17, pp. 69–78.

Roosbeek, F., 1996, "RATGP95: a harmonic development of the tide-generating potential using an analytical method," *Geophys. J. Int.*, **126**, pp. 197–204.

Schwiderski, E., 1983, "Atlas of Ocean Tidal Charts and Maps, Part I: The Semidiurnal Principal Lunar Tide M2," *Marine Geodesy*, **6**, pp. 219–256.

Souchay, J. and Folgueira, M., 2000, "The effect of zonal tides on the dynamical ellipticity of the Earth and its influence on the mutation," *Earth, Moon and Planets*, **81**, pp. 201–216.

Tapley, B. D., Watkins, M. M., Ries, J. C., Davis, G. W., Eanes, R. J., Poole, S. R., Rim, H. J., Schutz, B. E., Shum, C. K., Nerem, R. S., Lerch, F. J., Marshall, J. A., Klosko, S. M., Pavlis, N. K., and Williamson, R. G., 1996, "The Joint Gravity Model 3," *J. Geophys. Res*, **101**, pp. 28029–28049.

Wahr, J. M., 1981, "The Forced Nutations of an Elliptical, Rotating, Elastic, and Oceanless Earth," *Geophys. J. Roy. Astron. Soc.*, **64**, pp. 705–727.

Wahr, J., 1987, "The Earth's C_{21} and S_{21} gravity coefficients and the rotation of the core," *Geophys. J. Roy. astr. Soc.*, **88**, pp. 265–276.

Wahr, J. M. and Sasao, T., 1981, "A diurnal resonance in the ocean tide and the Earth's load response due to the resonant free "core nutation"," *Geophys. J. R. astr. Soc.*, **64**, pp. 747–765.

Wahr, J., 1990, "Corrections and Update to 'The Earth's C_{21} and S_{21} gravity coefficients and the rotation of the core'," *Geophys. J. Int.*, **101**, pp. 709–711.

Wahr, J. and Bergen, Z., 1986, "The effects of mantle elasticity on nutations, Earth tides, and tidal variations in the rotation rate," *Geophys. J. R. astr. Soc.*, **87**, 633–668.

Widmer, R., Masters, G., and Gilbert, F., 1991, "Spherically symmetric attenuation within the Earth from normal mode data," *Geophys. J. Int.*, **104**, pp. 541–553.

7   Displacement of Reference Points

Models describing the displacements of reference points due to various effects are provided. These models relate the regularized position $X_R(t)$ of the reference points (see Chapter 4) to their instantaneous positions. Two kinds of displacements are distinguished: those that affect the reference markers on the crust and those that affect the reference points of the instruments, which are technique-dependent. The first category includes (a) deformations of the solid Earth due to ocean tidal loading as well as those due to the body tides arising from the direct effect of the external tide generating potential and centrifugal perturbations caused by Earth rotation variations, including the pole tide, (b) atmospheric loading. The second category presently only includes the thermal deformation of a VLBI antenna.

7.1   Displacement of Reference Markers on the Crust

7.1.1   Local Site Displacement due to Ocean Loading

Ocean tides cause a temporal variation of the ocean mass distribution and the associated load on the crust and produce time-varying deformations of the Earth. The modeling of the associated site displacement is dealt with in this section. The displacement model does not include the translation of the solid Earth that counterbalances the motion of the oceans' center of mass. This convention follows Farrell (1972).

Ocean Loading

Three-dimensional site displacements due to ocean tide loading are computed using the following scheme. Let Δc denote a displacement component (radial, west, south) at a particular site and time t. Let W denote the tide generating potential (*e.g.* Hartmann and Wenzel, 1995; Tamura, 1987; Cartwright and Tayler, 1971; Cartwright and Edden, 1973),

$$W = g \sum_j K_j P_2^{m_j}(\cos\psi)\cos(\omega_j t + \chi_j + m_j\lambda), \qquad (1)$$

where only degree two harmonics are retained. The symbols designate colatitude ψ, longitude λ, tidal angular velocity ω_j, amplitude K_j and the astronomical argument χ_j at $t = 0^h$. Spherical harmonic order m_j distinguishes the fundamental bands, *i.e.* long-period ($m = 0$), diurnal ($m = 1$) and semidiurnal ($m = 2$). The parameters H_j and ω_j are used to obtain the most completely interpolated form

$$\Delta c = \sum_j a_{cj}\cos(\omega_j t + \chi_j - \phi_{cj}), \qquad (2)$$

with

$$
\begin{aligned}
a_{cj}\cos\phi_{cj} &= H_j\left[\frac{A_{ck}\cos\Phi_{ck}}{\bar{H}_k}(1-p) + \frac{A_{c,k+1}\cos\Phi_{c,k+1}}{\bar{H}_{k+1}}p\right], \\
a_{cj}\sin\phi_{cj} &= H_j\left[\frac{A_{ck}\sin\Phi_{ck}}{\bar{H}_k}(1-p) + \frac{A_{c,k+1}\sin\Phi_{c,k+1}}{\bar{H}_{k+1}}p\right].
\end{aligned}
$$

For each site, the amplitudes A_{ck} and phases $\Phi_{ck}, 1 \le k \le 11$, are taken from models such as those listed in Table 7.2. For clarity, symbols written with bars overhead designate tidal potential quantities associated with the small set of partial tides represented in the table. These are the semidiurnal waves M_2, S_2, N_2, K_2, the diurnal waves K_1, O_1, P_1, Q_1, and the long-period waves M_f, M_m, and S_{sa}.

Interpolation is possible only within a fundamental band, *i.e.* we demand

$$\bar{m}_k = m_j = \bar{m}_{k+1}. \tag{3}$$

Then

$$p = \frac{\omega_j - \bar{\omega}_k}{\bar{\omega}_{k+1} - \bar{\omega}_k}, \qquad \bar{\omega}_k \le \omega_j \le \bar{\omega}_{k+1}.$$

If no $\bar{\omega}_k$ or $\bar{\omega}_{k+1}$ can be found meeting (3), p is set to zero or one, respectively.

A shorter form of (2) is obtained if the summation considers only the tidal species shown in Table 7.1 and corrections for the modulating effect of the lunar node. Then,

$$\Delta c = \sum_j f_j A_{cj} \cos(\omega_j t + \chi_j + u_j - \Phi_{cj}), \tag{4}$$

where f_j and u_j depend on the longitude of the lunar node. The astronomical arguments needed in (4) can be computed with subroutine ARG. The code for this subroutine can be obtained by anonymous ftp to <[12]>. The Tamura tide potential is available from the International Centre for Earth Tides, Observatoire Royal de Belgique, Bruxelles.

Information similar to that provided in Table 7.1 is available electronically from the ocean loading service site at <[13]>. Some precomputed tables are available at <[14]>.

Coefficients for stations that are farther away than 10 km from precomputed ones should always be recomputed.

The coefficients shown in Table 7.1 have been computed according to Scherneck (1991). Tangential displacements are to be taken positive in west and south directions. Tables are available derived from different ocean tide maps, GOT99.2 (Ray, 1999), CSR4.0 and CSR 3.0 (Eanes and Bettadpur, 1995), and models due to LeProvost *et al.* (1994). The automatic service computes coefficients selectably from a range of eleven ocean tide models, see Table 7.2.

The use of the most recent of these models is recommended (GOT00.2 for a TOPEX/POSEIDON derived solution, FES99 for a hydrodynamic solution). However, older models might be preferred for internal consistency. Since many space geodesy stations are inland or near coasts, the accuracy of the tide models in the shelf areas is more crucial than in the open sea. Refined coastlines have been derived from the topographic data sets ETOPO5 and Terrain Base (Row *et al.*, 1995) of the National Geophysical Data Center, Boulder, CO. Ocean tide mass budgets have been constrained using a uniform co-oscillating oceanic layer. Load convolution employed a disk-generating Green's function method (Farrell, 1972; Zschau, 1983; Scherneck, 1990). An assessment of the accuracy of the loading model is given in Scherneck (1993).

Additional contributions to ocean-induced displacement arise from the frequency dependence of the load Love numbers due to the Nearly Diurnal Free Wobble in the diurnal tidal band. The effect of this dependence may be taken into account, following Wahr and Sasao (1981), by incrementing the *body tide* Love numbers as explained further below.

---

[12]maia.usno.navy.mil/conv2000/chapter7
[13]http://www.oso.chalmers.se/∼loading
[14]http://www.oso.chalmers.se/∼hgs/README.html

Table 7.1   Sample of ocean loading table file. Each site record shows a header with the site name, the CDP monument number, geographic coordinates and comments. First three rows of numbers designate amplitudes (meter), radial, west, south, followed by three lines with the corresponding phase values (degrees).

Columns designate partial tides $M_2, S_2, N_2, K_2, K_1, O_1, P_1, Q_1, M_f, M_m$, and S_{sa}.

```
$$
   ONSALA60 7213
$$
$$ Computed by H.G. Scherneck, Uppsala University, 1989
$$ ONSALA 7213    lon/lat: 11.9263 57.3947
  .00384   .00091   .00084   .00019   .00224   .00120   .00071   .00003   .00084   .00063   .00057
  .00124   .00034   .00031   .00009   .00042   .00041   .00015   .00006   .00018   .00010   .00010
  .00058   .00027   .00021   .00008   .00032   .00017   .00009   .00004   .00007   .00001   .00020
    -56.0    -46.1    -90.7    -34.4    -44.5   -123.2    -49.6    178.4     14.9     37.3     24.6
     75.4     97.6     40.8     94.8    119.0     25.4     98.7    -14.1   -177.0   -126.7   -175.8
     84.2    131.3     77.7    103.9     17.2    -55.0     25.2   -165.0    173.3    121.8     91.3
```

Table 7.2   Ocean tide models available at the automatic loading service.

Model code	Reference	Input	Resolution
SCHW	Schwiderski and Szeto (1981)	Tide gauge	$1° \times 1°$
CSR3.0, CSR4.0	Eanes (1994)	Topex/Poseidon Altim.	$1° \times 1°$
	Eanes and Bettadpur (1995)	T/P + LEPR loading	$0.5° \times 0.5°$
TPX0.5	Egbert *et al.* (1994)	inverse hydrodyn, solution	
		from T/P Altim.	256×512
FES94 (LEPR)	Le Provost *et al.* (1994)	numerical model	$0.5° \times 0.5°$
FES95			
FES98	Le Provost *et al.* (1998)	num. mdl. + assim. Altim.	$0.5° \times 0.5°$
FES99	Lefèvre *et al.* (2000)	numerical model	$0.25° \times 0.25°$
GOT99.2, GOT00.2	Ray (1999)	T/P	$0.5° \times 0.5°$
NAO99.b	Matsumoto *et al.* (2000)	num. + T/P assim.	$0.5° \times 0.5°$

7.1.2   Effects of the Solid Earth Tides

Site displacements caused by tides of spherical harmonic degree and order (nm) are characterized by the Love number h_{nm} and the Shida number l_{nm}. The effective values of these numbers depend on station latitude and tidal frequency (Wahr, 1981). The latitude dependence and a small interband variation are caused by the Earth's ellipticity and the Coriolis force due to Earth rotation. A strong frequency dependence within the diurnal band is produced by the Nearly Diurnal Free Wobble resonance associated with the free core nutation (FCN) in the wobbles of the Earth and its core regions which contribute to the tidal deformations via their centrifugal effects. Additionally, the resonance in the deformation due to ocean tidal loading, which is not included in the computations of the last section which use constant load Love numbers, may be represented in terms of effective contributions to h_{21} and l_{21}. A further frequency dependence, which is most pronounced in the long-period tidal band, arises from mantle anelasticity leading to corrections to the elastic Earth Love numbers. The contributions to the Love number parameters from anelasticity and ocean tidal loading as well as those from the centrifugal perturbations due to the wobbles have imaginary parts which cause the tidal displacements to lag slightly behind the tide generating potential. All these effects need to be taken into account when an accuracy of 1 mm is desired in determining station positions.

In order to account for the latitude dependence of the effective Love and Shida numbers, the representation in terms of multiple h and l parameters employed by Mathews *et al.* (1995) is used. In this representation, parameters $h^{(0)}$ and $l^{(0)}$ play the roles of h_{2m} and l_{2m}, while the latitude dependence is expressed in terms of additional parameters $h^{(2)}, h'$ and $l^{(1)}, l^{(2)}, l'$. These parameters are defined through their contributions to the site displacement as given by equations (5) below. Their numerical values as listed in the Conventions 1996 have since been revised, and the new values presented in Table 7.4 are used here. These values pertain to the elastic Earth and anelasticity models referred to in Chapter 6.

The vector displacement due to a tidal term of frequency f is given in terms of the several parameters by the following expressions that result from evaluation of the defining equation (6) of Mathews *et al.* (1995):

For a long-period tide of frequency f:

$$
\Delta \vec{r}_f = \sqrt{\tfrac{5}{4\pi}} H_f \left\{ \begin{array}{l} \left[h(\phi) \left(\tfrac{3}{2} \sin^2 \phi - \tfrac{1}{2} \right) + \sqrt{\tfrac{4\pi}{5}} h' \right] \cos \theta_f \; \hat{r} \\[2mm] + 3 l(\phi) \sin \phi \cos \phi \cos \theta_f \; \hat{n} \\[2mm] + \cos \phi \left[3 l^{(1)} \sin^2 \phi - \sqrt{\tfrac{4\pi}{5}} l' \right] \sin \theta_f \; \hat{e} \end{array} \right\}. \tag{5a}
$$

For a diurnal tide of frequency f:

$$
\begin{aligned}
\Delta \vec{r}_f = & -\sqrt{\tfrac{5}{24\pi}} H_f \left\{ h(\phi) 3 \sin \phi \cos \phi \sin(\theta_f + \lambda) \; \hat{r} \right. \\[2mm]
& + \left[3 l(\phi) \cos 2\phi - 3 l^{(1)} \sin^2 \phi + \sqrt{\tfrac{24\pi}{5}} l' \right] \sin(\theta_f + \lambda) \; \hat{n} \\[2mm]
& + \left. \left[\left(3 l(\phi) - \sqrt{\tfrac{24\pi}{5}} l' \right) \sin \phi - 3 l^{(1)} \sin \phi \cos 2\phi \right] \cos(\theta_f + \lambda) \; \hat{e} \right\}.
\end{aligned} \tag{5b}
$$

For a semidiurnal tide of frequency f:

$$
\begin{aligned}
\Delta \vec{r}_f = & \sqrt{\tfrac{5}{96\pi}} H_f \left\{ \; [h(\phi) 3 \cos^2 \phi \cos(\theta_f + 2\lambda) \; \hat{r} \right. \\
& - 6 \sin \phi \cos \phi [l(\phi) + l^{(1)}] \cos(\theta_f + 2\lambda) \; \hat{n} \\
& - \left. 6 \cos \phi [l(\phi) + l^{(1)} \sin^2 \phi] \sin(\theta_f + 2\lambda) \; \hat{e} \}. \right.
\end{aligned} \tag{5c}
$$

In the above expressions,

$$
\begin{aligned}
h(\phi) &= h^{(0)} + h^{(2)} [(3/2) \sin^2 \phi - 1/2], \\
l(\phi) &= l^{(0)} + l^{(2)} [(3/2) \sin^2 \phi - 1/2],
\end{aligned} \tag{6}
$$

H_f = amplitude (m) of the tidal term of frequency f,

ϕ = geocentric latitude of station,

λ = east longitude of station,

θ_f = tide argument for tidal constituent with frequency f,

$\hat{r}$ = unit vector in the radial direction,

$\hat{e}$ = unit vector in the east direction,

$\hat{n}$ = unit vector at right angles to $\hat{r}$ in the northward direction.

The convention used in defining the tidal amplitude H_f is as in Cartwright and Tayler (1971). To convert amplitudes defined according to other conventions that have been employed in recent more accurate tables, use the conversion factors given in Chapter 6, Table 6.5.

Equations (5) assume that the Love and Shida number parameters are all real. Generalization to the case of complex parameters is done simply by making the following replacements for the combinations $L\cos(\theta_f + m\lambda)$ and $L\sin(\theta_f + m\lambda)$, wherever they occur in those equations:

$$L\cos(\theta_f + m\lambda) \to L^R \cos(\theta_f + m\lambda) - L^I \sin(\theta_f + m\lambda), \qquad (7a)$$

$$L\sin(\theta_f + m\lambda) \to L^R \sin(\theta_f + m\lambda) + L^I \cos(\theta_f + m\lambda), \qquad (7b)$$

where L is a generic symbol for $h^{(0)}, h^{(2)}, h', l^{(0)}, l^{(1)}, l^{(2)}$, and l', and L^R and L^I stand for their respective real and imaginary parts.

The complex values of these 7 parameters are computed for the diurnal body tides from resonance formulae of the form given in equation (6) of Chapter 6 using the values listed in equation (7) of that chapter for the resonance frequencies σ_α and those listed in Table 7.3 for the coefficients L_0 and L_α relating to each of the multiple h and l Love/Shida numbers. The manner in which σ_α and the L_α were computed is explained in Chapter 6, where mention is also made of the models used for the elastic Earth and for mantle anelasticity. As was noted in that chapter, the frequency dependence of the ocean tide contributions to certain Earth parameters in the equations of motion for the wobbles has the effect of making the resonance formulae inexact. The difference between the exact and resonance formula values is included in the tabulated values of $h_{21}^{(0)}$ and $l_{21}^{(0)}$ in Table 7.4. (The only case where this difference makes a contribution above the cut-off in Table 7.5a is in the radial displacement due to the ψ_1 tide.) Also included in the values listed in Table 7.4 are the resonant ocean tidal loading corrections outlined in the next paragraph.

Table 7.3   Parameters in the Resonance Formulae for the Displacement Love Numbers.

	$h^{(0)}$		$h^{(2)}$	
α	Re L_α	Im L_α	Re L_α	Im L_α
0	$0.60671 \times 10^{+0}$	-0.2420×10^{-2}	-0.615×10^{-3}	-0.122×10^{-4}
1	-0.15777×10^{-2}	-0.7630×10^{-4}	0.160×10^{-5}	0.116×10^{-6}
2	0.18053×10^{-3}	-0.6292×10^{-5}	0.201×10^{-6}	0.279×10^{-8}
3	-0.18616×10^{-5}	0.1379×10^{-6}	-0.329×10^{-7}	-0.217×10^{-8}

	$l^{(0)}$		$l^{(1)}$	
α	Re L_α	Im L_α	Re L_α	Im L_α
0	$.84963 \times 10^{-1}$	$-.7395 \times 10^{-3}$	$.121 \times 10^{-2}$	$.136 \times 10^{-6}$
1	$-.22107 \times 10^{-3}$	$-.9646 \times 10^{-5}$	$-.316 \times 10^{-5}$	$-.166 \times 10^{-6}$
2	$-.54710 \times 10^{-5}$	$-.2990 \times 10^{-6}$	$.272 \times 10^{-6}$	$-.858 \times 10^{-8}$
3	$-.29904 \times 10^{-7}$	$-.7717 \times 10^{-8}$	$-.545 \times 10^{-8}$	$.827 \times 10^{-11}$

	$l^{(2)}$		l'	
α	Re L_α	Im L_α	Re L_α	Im L_α
0	$.19334 \times 10^{-3}$	$-.3819 \times 10^{-5}$	$-.221 \times 10^{-3}$	$-.474 \times 10^{-7}$
1	$-.50331 \times 10^{-6}$	$-.1639 \times 10^{-7}$	$.576 \times 10^{-6}$	$.303 \times 10^{-7}$
2	$-.66460 \times 10^{-8}$	$.5076 \times 10^{-9}$	$.128 \times 10^{-6}$	$-.378 \times 10^{-8}$
3	$.10372 \times 10^{-7}$	$.7511 \times 10^{-9}$	$-.655 \times 10^{-8}$	$-.291 \times 10^{-9}$

Site displacements caused by solid Earth deformations due to ocean tidal loading have been dealt with in the first section of this chapter. Constant nominal values were assumed for the load Love numbers in computing these. The values used for tides of degree 2 were

$$h_2'^{(nom)} = -1.001, \quad l_2'^{(nom)} = 0.0295, \quad k_2'^{(nom)} = -0.3075.$$

Since resonances in the diurnal band cause the values of the load Love numbers too to vary, corrections need to be applied to the results of the first section. These corrections can be expressed in terms of effective ocean tide contributions $\delta h^{(OT)}$ and $\delta l^{(OT)}$ to the respective body tide Love numbers $h_{21}^{(0)}$ and $l_{21}^{(0)}$. $\delta h^{(OT)}$ and $\delta l^{(OT)}$ are given by expressions of the form (8) of Chapter 6, with appropriate replacements. They were computed using the same ocean tide admittances as in that chapter, and using the resonance parameters listed in Table 6.2 for the load Love numbers; they are included in the values listed in Table 7.4 under $h^{(0)R}$ and $h^{(0)I}$ for the diurnal tides.

The variation of $h_{20}^{(0)}$ and $l_{20}^{(0)}$ across the zonal tidal band, $(nm) = (20)$, due to mantle anelasticity, is described by the formulae

$$h_{20}^{(0)} = 0.5998 - 9.96 \times 10^{-4} \left\{ \cot \frac{\alpha\pi}{2} \left[1 - \left(\frac{f_m}{f} \right)^\alpha \right] + i \left(\frac{f_m}{f} \right)^\alpha \right\}, \quad (8a)$$

$$l_{20}^{(0)} = 0.0831 - 3.01 \times 10^{-4} \left\{ \cot \frac{\alpha\pi}{2} \left[1 - \left(\frac{f_m}{f} \right)^\alpha \right] + i \left(\frac{f_m}{f} \right)^\alpha \right\} \quad (8b)$$

on the basis of the anelasticity model already referred to. Here f is the frequency of the zonal tidal constituent, f_m is the reference frequency equivalent to a period of 200 s, and $\alpha = 0.15$.

Table 7.4 lists the values of $h^{(0)}, h^{(2)}, h', l^{(0)}, l^{(1)}, l^{(2)}$, and l' for those tidal frequencies for which they are needed for use in the computational procedure described below. The tidal frequencies shown in the table are in cycles per sidereal day (*cpsd*). Periods, in solar days, of the nutations associated with the diurnal tides are also shown.

Computation of the variations of station coordinates due to solid Earth tides, like that of geopotential variations, is done most efficiently by the use of a two-step procedure. The evaluations in the first step use the expression in the time domain for the full degree 2 tidal potential or for the parts that pertain to particular bands ($m = 0, 1$, or 2). Nominal values common to all the tidal constituents involved in the potential and to all stations are used for the Love and Shida numbers h_{2m} and l_{2m} in this step. They are chosen with reference to the values in Table 7.4 so as to minimize the computational effort needed in Step 2. Along with expressions for the dominant contributions from $h^{(0)}$ and $l^{(0)}$ to the tidal displacements, relatively small contributions from some of the other parameters are included in Step 1 for reasons of computational efficiency. The displacements caused by the degree 3 tides are also computed in the first step, using constant values for h_3 and l_3.

Corrections to the results of the first step are needed to take account of the frequency dependent deviations of the Love and Shida numbers from their respective nominal values, and also to compute the out-of-phase contributions from the zonal tides. Computations of these corrections constitute Step 2. The total displacement due to the tidal potential is the sum of the displacements computed in Steps 1 and 2.

The full scheme of computation is outlined in the chart on page 79.

Table 7.4   Displacement Love number parameters for degree 2 tides. Super-
scripts R and I identify the real and imaginary parts, respectively.

Name	Period	Frequency	$h^{(0)R}$	$h^{(0)I}$	$h^{(2)}$	h'
Semidiurnal		-2 *cpsd*	.6078	-.0022	-.0006	
Diurnal						
$2Q_1$	6.86	0.85461	.6039	-.0027	-.0006	
σ_1	7.10	0.85946	.6039	-.0026	-.0006	
135,645	9.12	0.89066	.6036	-.0026	-.0006	
Q_1	9.13	0.89080	.6036	-.0026	-.0006	
ρ_1	9.56	0.89565	.6035	-.0026	-.0006	
145,545	13.63	0.92685	.6028	-.0025	-.0006	
O_1	13.66	0.92700	.6028	-.0025	-.0006	
τ_1	14.77	0.93246	.6026	-.0025	-.0006	
$N\tau_1$	23.94	0.95835	.6011	-.0024	-.0006	
NO_1	27.55	0.96381	.6005	-.0023	-.0006	
χ_1	31.81	0.96865	.5998	-.0023	-.0006	
π_1	121.75	0.99181	.5878	-.0015	-.0006	
P_1	182.62	0.99454	.5817	-.0011	-.0006	
S_1	365.26	0.99727	.5692	-.0004	-.0006	
165,545	6798.38	0.99985	.5283	.0023	-.0007	
K_1	infinity	1.00000	.5236	.0030	-.0007	
165,565	-6798.38	1.00015	.5182	.0036	-.0007	
165,575	-3399.19	1.00029	.5120	.0043	-.0007	
ψ_1	-365.26	1.00273	1.0569	.0036	-.0001	
166,564	-346.64	1.00288	.9387	-.0050	-.0003	
ϕ_1	-182.62	1.00546	.6645	-.0059	-.0006	
θ_1	-31.81	1.03135	.6117	-.0030	-.0006	
J_1	-27.55	1.03619	.6108	-.0030	-.0006	
OO_1	-13.66	1.07300	.6080	-.0028	-.0006	
Long period						
55,565	6798.38	.000147	.6344	-.0093	-.0006	.0001
S_{sa}	182.62	.005461	.6182	-.0054	-.0006	.0001
M_m	27.55	.036193	.6126	-.0041	-.0006	.0001
M_f	13.66	.073002	.6109	-.0037	-.0006	.0001
75,565	13.63	.073149	.6109	-.0037	-.0006	.0001

Name	Period	Frequency	$l^{(0)R}$	$l^{(0)I}$	$l^{(1)}$	$l^{(2)}$	l'
Semidiurnal		-2 *cpsd*	.0847	-.0007	.0024	.0002	
Diurnal							
Q_1	9.13	0.89080	.0846	-.0006	.0012	.0002	-.0002
145,545	13.63	0.92685	.0846	-.0006	.0012	.0002	-.0002
O_1	13.66	0.92700	.0846	-.0006	.0012	.0002	-.0002
NO_1	27.55	0.96381	.0847	-.0006	.0012	.0002	-.0002
P_1	182.62	0.99454	.0853	-.0006	.0012	.0002	-.0002
165,545	6798.38	0.99985	.0869	-.0006	.0011	.0002	-.0003
K_1	infinity	1.00000	.0870	-.0006	.0011	.0002	-.0003
165,565	-6798.38	1.00015	.0872	-.0006	.0011	.0002	-.0003
ψ_1	-365.26	1.00273	.0710	-.0020	.0019	.0002	.0001
ϕ_1	-182.62	1.00546	.0828	-.0007	.0013	.0002	-.0002
J_1	-27.55	1.03619	.0845	-.0006	.0012	.0002	-.0002
OO_1	-13.66	1.07300	.0846	-.0006	.0012	.0002	-.0002
Long period							
55,565	6798.38	.000147	.0936	-.0028	.0000	.0002	
S_{sa}	182.62	.005461	.0886	-.0016	.0000	.0002	
M_m	27.55	.036193	.0870	-.0012	.0000	.0002	
M_f	13.66	.073002	.0864	-.0011	.0000	.0002	
75,565	13.63	.073149	.0864	-.0011	.0000	.0002	

CORRECTIONS FOR THE STATION TIDAL DISPLACEMENTS

Step 1: Corrections to be computed in the time domain

in-phase	for degree 2 and 3	Nominal values
	. for degree 2 → eq (9)	$h_2 \rightarrow h(\phi) = h^{(0)} + h^{(2)}[(3\sin^2\phi - 1)/2]$
		$l_2 \rightarrow l(\phi) = l^{(0)} + l^{(2)}[(3\sin^2\phi - 1)/2]$
		$h^{(0)} = 0.6078,\ h^{(2)} = -0.0006;\ l^{(0)} = 0.0847,\ l^{(2)} = 0.0002$
	. for degree 3 → eq (10)	$h_3 = 0.292$ and $l_3 = 0.015$

out-of-phase	for degree 2 only	Nominal values
	. diurnal tides → eq (14)	$h^I = -0.0025$ and $l^I = -0.0007$
	. semidiurnal tides → eq (15)	$h^I = -0.0022$ and $l^I = -0.0007$

contribution	from latitude dependence	Nominal values
	. diurnal tides → eq (12)	$l^{(1)} = 0.0012$
	. semidiurnal tides → eq (13)	$l^{(1)} = 0.0024$

Step 2: Corrections to be computed in the frequency domain and to be added to results of Step 1

in-phase	for degree 2	
	. diurnal tides → eqs (16)	→ Sum over all the components of Table 7.5a
	. semidiurnal tides	negligible
in-phase	and out-of-phase for degree 2	
	. long-period tides → eqs (17)	→ Sum over all the components of Table 7.5b

Displacement due to degree 2 tides, with nominal values for $h_{2m}^{(0)}$ and $l_{2m}^{(0)}$

The first stage of the Step 1 calculations employs real nominal values h_2 and l_2 common to all the degree 2 tides for the Love and Shida numbers. It is found to be computationally most economical to choose these to be the values for the semidiurnal tides (which have very little intra-band variation). On using the nominal values, the vector displacement of the station due to the degree 2 tides is given by

$$\Delta \vec{r} = \sum_{j=2}^{3} \frac{GM_j R_e^4}{GM_\oplus R_j^3} \left\{ h_2\ \hat{r} \left(\frac{3}{2}(\hat{R}_j \cdot \hat{r})^2 - \frac{1}{2} \right) + 3l_2(\hat{R}_j \cdot \hat{r})[\hat{R}_j - (\hat{R}_j \cdot \hat{r})\ \hat{r}] \right\}, \quad (9)$$

where $h_{22}^{(0)}$ and $l_{22}^{(0)}$ of the semidiurnal tides are chosen as the nominal values h_2 and l_2. The out-of-phase displacements due to the imaginary parts of the Love numbers are dealt with separately below. In equation (9),

GM_j	=	gravitational parameter for the Moon ($j = 2$) or the Sun ($j = 3$),
$GM_\oplus$	=	gravitational parameter for the Earth,
$\hat{R}_j, R_j$	=	unit vector from the geocenter to Moon or Sun and the magnitude of that vector,
R_e	=	Earth's equatorial radius,
$\hat{r}, r$	=	unit vector from the geocenter to the station and the magnitude of that vector,
h_2	=	nominal degree 2 Love number,
l_2	=	nominal degree 2 Shida number.

Note that the part proportional to h_2 gives the radial (not vertical) component of the tide-induced station displacement, and the terms in l_2 represent the vector displacement transverse to the radial direction (and not in the horizontal plane).

The computation just described may be generalized to include the latitude dependence arising through $h^{(2)}$ by simply adding $h^{(2)}[(3/2)\sin^2\phi - (1/2)]$ to the constant nominal value given above, with $h^{(2)} = -0.0006$. The addition of a similar term (with $l^{(2)} = 0.0002$) to the nominal value of l_2 takes care of the corresponding contribution to the transverse displacement. The resulting incremental displacements are small, not exceeding 0.4 mm radially and 0.2 mm in the transverse direction.

Displacements due to degree 3 tides

The Love numbers of the degree 3 tides may be taken as real and constant in computations to the degree of accuracy aimed at here. The vector displacement due to these tides is then given by

$$\Delta\vec{r} = \sum_{j=2}^{3} \frac{GM_j R_e^5}{GM_\oplus R_j^4}\left\{ h_3\ \hat{r}\left(\frac{5}{2}(\hat{R}_j\cdot\hat{r})^3 - \frac{3}{2}(\hat{R}_j\cdot\hat{r})\right) + l_3\left(\frac{15}{2}(\hat{R}_j\cdot\hat{r})^2 - \frac{3}{2}\right)[\hat{R}_j - (\hat{R}_j\cdot\hat{r})\hat{r}]\right\}. \quad (10)$$

Only the Moon's contribution ($j = 2$) need be computed, the term due to the Sun being quite ignorable. The transverse part of the displacement (10) does not exceed 0.2 mm, but the radial displacement can reach 1.7 mm.

Contributions to the transverse displacement due to the $l^{(1)}$ term

The imaginary part of $l^{(1)}$ is completely ignorable, as is the intra-band variation of Re $l^{(1)}$; and $l^{(1)}$ is effectively zero in the zonal band.

In the expressions given below, and elsewhere in this chapter,

Φ_j = body fixed geocentric latitude of Moon or Sun, and
λ_j = body fixed east longitude (from Greenwich) of Moon or Sun.

The following formulae may be employed when the use of Cartesian coordinates X_j, Y_j, Z_j of the body relative to the terrestrial reference frame is preferred:

$$P_2^0(\sin\Phi_j) = \tfrac{1}{R_j^2}\left(\tfrac{3}{2}Z_j^2 - \tfrac{1}{2}R_j^2\right), \quad (11a)$$

$$P_2^1(\sin\Phi_j)\cos\lambda_j = \tfrac{3X_j Z_j}{R_j^2},$$
$$P_2^1(\sin\Phi_j)\sin\lambda_j = \tfrac{3Y_j Z_j}{R_j^2}, \quad (11b)$$

$$P_2^2(\sin\Phi_j)\cos 2\lambda_j = \tfrac{3}{R_j^2}(X_j^2 - Y_j^2),$$
$$P_2^2(\sin\Phi_j)\sin 2\lambda_j = \tfrac{6}{R_j^2}X_j Y_j. \quad (11c)$$

Contribution from the diurnal band (with $l^{(1)} = 0.0012$):

$$\delta\vec{t} = -l^{(1)}\sin\phi\sum_{j=2}^{3}\frac{GM_j R_e^4}{GM_\oplus R_j^3}P_2^1(\sin\Phi_j)[\sin\phi\cos(\lambda - \lambda_j)\ \hat{n} - \cos 2\phi\sin(\lambda - \lambda_j)\ \hat{e}]. \quad (12)$$

Contribution from the semidiurnal band (with $l^{(1)} = 0.0024$):

$$\delta\vec{t} = -\frac{1}{2}l^{(1)}\sin\phi\cos\phi\sum_{j=2}^{3}\frac{GM_j R_e^4}{GM_\oplus R_j^3}P_2^2(\sin\Phi_j)[\cos 2(\lambda - \lambda_j)\ \hat{n} + \sin\phi\sin 2(\lambda - \lambda_j)\ \hat{e}]. \quad (13)$$

The contributions of the $l^{(1)}$ term to the transverse displacements caused by the diurnal and semidiurnal tides could be up to 0.8 mm and 1.0 mm respectively.

Out of phase contributions from the imaginary parts of $h_{2m}^{(0)}$ and $l_{2m}^{(0)}$

In the following, h^I and l^I stand for the imaginary parts of $h_{2m}^{(0)}$ and $l_{2m}^{(0)}$.

Contributions δr to radial and $\vec{\delta t}$ to transverse displacements from diurnal tides (with $h^I = -0.0025$, $l^I = -0.0007$):

$$\delta r = -\frac{3}{4}h^I \sum_{j=2}^{3} \frac{GM_j R_e^4}{GM_\oplus R_j^3} \sin 2\Phi_j \sin 2\phi \sin(\lambda - \lambda_j), \qquad (14a)$$

$$\vec{\delta t} = -\frac{3}{2}l^I \sum_{j=2}^{3} \frac{GM_j R_e^4}{GM_\oplus R_j^3} \sin 2\Phi_j [\cos 2\phi \sin(\lambda - \lambda_j)\ \hat{n} + \sin\phi \cos(\lambda - \lambda_j)\ \hat{e}]. \qquad (14b)$$

Contributions from semidiurnal tides (with $h^I = -0.0022$, $l^I = -0.0007$):

$$\delta r = -\frac{3}{4}h^I \sum_{j=2}^{3} \frac{GM_j R_e^4}{GM_\oplus R_j^3} \cos^2 \Phi_j \cos^2 \phi \sin 2(\lambda - \lambda_j), \qquad (15a)$$

$$\vec{\delta t} = \frac{3}{4}l^I \sum_{j=2}^{3} \frac{GM_j R_e^4}{GM_\oplus R_j^3} \cos^2 \Phi_j [\sin 2\phi \sin 2(\lambda - \lambda_j)\ \hat{n} - 2\cos\phi \cos 2(\lambda - \lambda_j)\ \hat{e}]. \quad (15b)$$

The out-of-phase contributions from the zonal tides has no closed expression in the time domain.

Computations of Step 2 are to take account of the intra-band variation of $h_{2m}^{(0)}$ and $l_{2m}^{(0)}$. Variations of the imaginary parts are negligible except as stated below. For the zonal tides, however, the contributions from the imaginary part have to be computed in Step 2.

Correction for frequency dependence of the Love and Shida numbers

(a) Contributions from the diurnal band

Corrections to the radial and transverse station displacements δr and $\vec{\delta t}$ due to a diurnal tidal term of frequency f are obtainable from equation (5b):

$$\delta r = [\delta R_f^{(ip)} \sin(\theta_f + \lambda) + \delta R_f^{(op)} \cos(\theta_f + \lambda)] \sin 2\phi, \qquad (16a)$$

$$\begin{aligned}\vec{\delta t} = \ & [\delta T_f^{(ip)} \cos(\theta_f + \lambda) - \delta T_f^{(op)} \sin(\theta_f + \lambda)] \sin\phi\ \hat{e} \\ + \ & [\delta T_f^{(ip)} \sin(\theta_f + \lambda) + \delta T_f^{(op)} \cos(\theta_f + \lambda)] \cos 2\phi\ \hat{n},\end{aligned} \qquad (16b)$$

where

$$\begin{aligned}\begin{pmatrix} \delta R_f^{(ip)} \\ \delta R_f^{(op)} \end{pmatrix} &= -\frac{3}{2}\sqrt{\frac{5}{24\pi}} H_f \begin{pmatrix} \delta h_f^R \\ \delta h_f^I \end{pmatrix}, \\ \begin{pmatrix} \delta T_f^{(ip)} \\ \delta T_f^{(op)} \end{pmatrix} &= -3\sqrt{\frac{5}{24\pi}} H_f \begin{pmatrix} \delta l_f^R \\ \delta l_f^I \end{pmatrix},\end{aligned} \qquad (16c)$$

and

δh_f^R and δh_f^I are the differences of $h^{(0)R}$ and $h^{(0)I}$ at frequency f from the nominal values h_2 and h^I used in equations (9) and (14a), respectively,

δl_f^R and δl_f^I are the differences of $l^{(0)R}$ and $l^{(0)I}$ at frequency f from the nominal values l_2 and l^I used in equations (9) and (14b), respectively.

Table 7.5a   Corrections due to the frequency variation of Love and Shida numbers for diurnal tides. Units: mm. All terms with radial correction ≥ 0.05 mm are shown. Nominal values are $h_2 = 0.6078$ and $l_2 = 0.0847$ for the real parts, and $h^I = -0.0025$ and $l^I = -0.0007$ for the imaginary parts. Frequencies shown are in degrees per hour.

Name	Frequency	Doodson	τ	s	h	p	N'	p_s	ℓ	ℓ'	F	D	Ω	$\Delta R_f^{(ip)}$	$\Delta R_f^{(op)}$	$\Delta T_f^{(ip)}$	$\Delta T_f^{(op)}$
Q_1	13.39866	135,655	1	-2	0	1	0	0	1	0	2	0	2	-0.08	0.00	-0.01	0.01
	13.94083	145,545	1	-1	0	0	-1	0	0	0	2	0	1	-0.10	0.00	0.00	0.00
O_1	13.94303	145,555	1	-1	0	0	0	0	0	0	2	0	2	-0.51	0.00	-0.02	0.03
NO_1	14.49669	155,655	1	0	0	1	0	0	1	0	0	0	0	0.06	0.00	0.00	0.00
π_1	14.91787	162,556	1	1	-3	0	0	1	0	1	2	-2	2	-0.06	0.00	0.00	0.00
P_1	14.95893	163,555	1	1	-2	0	0	0	0	0	2	-2	2	-1.23	-0.07	0.06	0.01
	15.03886	165,545	1	1	0	0	-1	0	0	0	0	0	-1	-0.22	0.01	0.01	0.00
K_1	15.04107	165,555	1	1	0	0	0	0	0	0	0	0	0	12.00	-0.78	-0.67	-0.03
	15.04328	165,565	1	1	0	0	1	0	0	0	0	0	1	1.73	-0.12	-0.10	0.00
ψ_1	15.08214	166,554	1	1	1	0	0	-1	0	-1	0	0	0	-0.50	-0.01	0.03	0.00
ϕ_1	15.12321	167,555	1	1	2	0	0	0	0	0	-2	2	-2	-0.11	0.01	0.01	0.00

(b) Contributions from the long-period band

Corrections δr and $\delta \vec{t}$ due to a zonal tidal term of frequency f include both in-phase (ip) and out-of-phase (op) parts. From equations (5a) and (7) one finds that

$$\delta r = \left(\frac{3}{2} \sin^2 \phi - \frac{1}{2} \right) \left(\delta R_f^{(ip)} \cos \theta_f + \delta R_f^{(op)} \sin \theta_f \right), \qquad (17a)$$

and

$$\delta \vec{t} = \left(\delta T_f^{(ip)} \cos \theta_f + \delta T_f^{(op)} \sin \theta_f \right) \sin 2\phi \; \hat{n}, \qquad (17b)$$

where

$$\begin{pmatrix} \delta R_f^{(ip)} \\ \delta R_f^{(op)} \end{pmatrix} = \sqrt{\frac{5}{4\pi}} H_f \begin{pmatrix} \delta h_f^R \\ -\delta h_f^I \end{pmatrix},$$

and   (17c)

$$\begin{pmatrix} \delta T_f^{(ip)} \\ \delta T_f^{(op)} \end{pmatrix} = \frac{3}{2} \sqrt{\frac{5}{4\pi}} H_f \begin{pmatrix} \delta l_f^R \\ -\delta l_f^I \end{pmatrix}.$$

Table 7.5b   Corrections due to frequency variation of Love and Shida numbers for zonal tides. Units: mm. All terms with radial correction ≥ 0.05 mm are shown. Nominal values are $h = 0.6078$ and $l = 0.0847$.

Name	Frequency	Doodson	τ	s	h	p	N'	p_s	ℓ	ℓ'	F	D	Ω	$\Delta R_f^{(ip)}$	$\Delta R_f^{(op)}$	$\Delta T_f^{(ip)}$	$\Delta T_f^{(op)}$
	0.00221	55,565	0	0	0	0	1	0	0	0	0	0	1	0.47	0.16	0.23	0.07
S_{sa}	0.08214	57,555	0	0	2	0	0	0	0	0	-2	2	-2	-0.20	-0.11	-0.12	-0.05
M_m	0.54438	65,455	0	1	0	-1	0	0	-1	0	0	0	0	-0.11	-0.09	-0.08	-0.04
M_f	1.09804	75,555	0	2	0	0	0	0	0	0	-2	0	-2	-0.13	-0.15	-0.11	-0.07
	1.10024	75,565	0	2	0	0	1	0	0	0	-2	0	-1	-0.05	-0.06	-0.05	-0.03

Values of ΔR_f and ΔT_f listed in Tables 7.5a and 7.5b are for the constituents that must be taken into account to ensure an accuracy of 1 mm.

A FORTRAN program for computing the various corrections is available at $<$[15]$>$.

---

[15] ftp://omaftp.oma.be/dist/astro/dehant/IERS/

7.1.3 Permanent deformation

The tidal model described above does contain in principle a time independent part so that the coordinates obtained by taking into account this model in the analysis will be "conventional tide free" values. (Note that they do *not* correspond to what would be observed in the absence of tidal perturbation. See the discussion in Chapter 1.) This section allows a user to compute "mean tide" coordinates from "conventional tide free" coordinates.

Specifically, the degree 2 zonal tide generating potential includes a spectral component of zero frequency and amplitude $H_0 = -0.31460$ m, and its effect enters the tidal displacement model through the time independent component of the expression (9). Evaluation of this component may be done using equations (5a) and (6) with $H_f = H_0, \theta_f = 0$, and with the same nominal values for the Love number parameters as were used in Step 1: $h_2 = 0.6078, l_2 = 0.0847$ along with $h^{(2)} = -0.0006$ and $l^{(2)} = 0.0002$. One finds the radial component of the permanent displacement according to (9) to be

$$[-0.1206 + 0.0001 P_2(\sin\phi)] P_2(\sin\phi) \text{ m}, \tag{18a}$$

and the transverse component to be

$$[-0.0252 - 0.0001 P_2(\sin\phi)] \sin 2\phi \text{ m} \tag{18b}$$

northwards, where $P_2(\sin\phi) = (3\sin^2\phi - 1)/2$.

These are the components of the vector to be added to the "conventional tide free" computed tide-corrected position to obtain the "mean tide" position. The radial component of this restitution to obtain the "mean tide" values amounts to about -12 cm at the poles and about $+6$ cm at the equator.

7.1.4 Rotational Deformation due to Polar Motion

The variation of station coordinates caused by the pole tide can amount to a couple of centimeters and needs to be taken into account.

Let us choose $\hat{x}, \hat{y}$ and $\hat{z}$ as a terrestrial system of reference. The $\hat{z}$ axis is oriented along the Earth's mean rotation axis, the $\hat{x}$ axis is in the direction of the adopted origin of longitude and the $\hat{y}$ axis is orthogonal to the $\hat{x}$ and $\hat{z}$ axes and in the plane of the 90° E meridian.

The centrifugal potential caused by the Earth's rotation is

$$V = \frac{1}{2}[r^2|\vec{\Omega}|^2 - (\vec{r}\cdot\vec{\Omega})^2], \tag{19}$$

where $\vec{\Omega} = \Omega(m_1\ \hat{x} + m_2\ \hat{y} + (1 + m_3)\ \hat{z})$. Ω is the mean angular velocity of rotation of the Earth; m_1, m_2 describe the time dependent offset of the instantaneous rotation pole from the mean, and m_3, the fractional variation in the rotation rate; r is the geocentric distance to the station.

Neglecting the variations in m_3 which induce displacements that are below the mm level, the m_1 and m_2 terms give a first order perturbation in the potential V (Wahr, 1985)

$$\Delta V(r, \theta, \lambda) = -\frac{\Omega^2 r^2}{2}\sin 2\theta\,(m_1\cos\lambda + m_2\sin\lambda). \tag{20}$$

The radial displacement S_r and the horizontal displacements S_θ and S_λ (positive upwards, south and east respectively in a horizon system at the station) due to ΔV are obtained using the formulation of tidal Love numbers (Munk and MacDonald, 1960):

$$S_r = h_2\frac{\Delta V}{g}, \qquad S_\theta = \frac{\ell_2}{g}\partial_\theta\Delta V, \qquad S_\lambda = \frac{\ell_2}{g}\frac{1}{\sin\theta}\partial_\lambda\Delta V. \tag{21}$$

The position of the Earth's mean rotation pole has a secular variation, and its coordinates in the Terrestrial Reference Frame discussed in Chapter 4 are given, in terms of the polar motion variables (x_p, y_p) defined in Chapter 5, by appropriate running averages $\bar{x}_p$ and $-\bar{y}_p$. Then

$$m_1 = x_p - \bar{x}_p, \qquad m_2 = -(y_p - \bar{y}_p). \tag{22}$$

For the most accurate results, estimates of the mean pole should be used. These are provided by the IERS Earth Orientation Centre and are made available at $<^{16}>$. It is also possible to approximate the pole path by a linear trend. The estimates below are derived from the same IERS Earth Orientation Centre data.

$$\bar{x}_p(t) = \bar{x}_p(t_0) + (t - t_0)\dot{\bar{x}}_p(t_0), \quad \bar{y}_p = \bar{y}_p(t_0) + (t - t_0)\dot{\bar{y}}_p(t_0), \tag{23a}$$

$$\bar{x}_p(t_0) = 0.054, \quad \dot{\bar{x}}_p(t_0) = 0.00083, \quad \bar{y}_p(t_0) = 0.357, \quad \dot{\bar{y}}_p(t_0) = 0.00395, \tag{23b}$$

where $\bar{x}_p, \bar{y}_p$ are in arcseconds, their rates are in arcseconds per year, and t_0 is 2000.

Using Love number values appropriate to the frequency of the pole tide ($h = 0.6027$, $l = 0.0836$) and $r = a = 6.378 \times 10^6$m, one finds

$$
\begin{aligned}
S_r &= -32 \sin 2\theta \, (m_1 \cos \lambda + m_2 \sin \lambda) \text{ mm}, \\
S_\theta &= -9 \cos 2\theta \, (m_1 \cos \lambda + m_2 \sin \lambda) \text{ (mm)}, \\
S_\lambda &= 9 \cos \theta \, (m_1 \sin \lambda - m_2 \cos \lambda) \text{ mm},
\end{aligned}
\tag{24}
$$

with m_1 and m_2 given in seconds of arc.

Taking into account that m_1 and m_2 vary, at most, 0.8 arcsec, the maximum radial displacement is approximately 25 mm, and the maximum horizontal displacement is about 7 mm.

If X, Y, and Z are Cartesian coordinates of a station in a right-handed equatorial coordinate system, the changes in them due to polar motion are

$$[dX, dY, dZ]^T = R^T [S_\theta, S_\lambda, S_r]^T, \tag{25}$$

where

$$
R = \begin{pmatrix}
\cos\theta\cos\lambda & \cos\theta\sin\lambda & -\sin\theta \\
-\sin\lambda & \cos\lambda & 0 \\
\sin\theta\cos\lambda & \sin\theta\sin\lambda & \cos\theta
\end{pmatrix}. \tag{26}
$$

7.1.5 Atmospheric Loading

Temporal variations in the geographic distribution of atmospheric mass load the Earth and deform its surface. For example, pressure variations on the order of 20 HPa (and even larger) at mid-latitudes, are observed in synoptic pressure systems with length scales for 1000-2000 km and periods of approximately two weeks. Seasonal pressure changes due to air mass movements between the continents and oceans can have amplitudes of up to 10 HPa in particular over the large land masses of the Northern Hemisphere. At the interannual periods, basin-wide air pressure signals with amplitudes of several HPa also contribute to the spectrum of the loading signal.

Other surface loads due to changes in snow and ice cover, soil moisture and groundwater, as well as ocean-bottom pressure also contribute to surface displacements. For example, at seasonal time scales, it is expected that the contribution of hydrological loads to surface displacements exceeds the one from air pressure (Blewitt *et al.*, 2001). However, while the atmospheric load is fairly well known from global air pressure data sets, no suffcient models for ocean bottom pressure, snow and soil moisture exists at this time. Therefore, in the following, focus is on atmospheric loading. However, the discussion applies also to any other surface load.

---

[16]ftp://maia.usno.navy.mil/conv2000/chapter7/annual.pole

Theoretical studies by Rabbel and Zschau (1985), Rabbel and Schuh (1986), vanDam and Wahr (1987), and Manabe *et al.* (1991) demonstrate that vertical crustal displacements of up to 25 mm are possible at mid-latitude stations due to synoptic pressure systems. Annual signals in the vertical are on the order of 1-2 mm but maximum signals of more than 3 mm are possible over large parts of Asia, Antarctica, Australia and Greenland (Mangarotti *et al.*, 2001; Dong *et al.*, 2002). Pressure loading effects are larger at higher latitude sites due to the more intensive weather systems (larger in amplitude and more spatially coherent) found there. Effects are smaller at mid-latitude sites and at locations within 500 km of the sea or ocean due to the inverted barometer response of the ocean. In all cases, horizontal crustal deformations are about one-third the amplitude of the vertical effects.

Two basic methods for computing atmospheric loading corrections to geodetic data have been applied so far: 1) using geophysical models or simple approximations derived from these models and 2) using empirical models based on site-dependent data.

The standard geophysical model approach is based on the estimation of atmospheric loading effects (vertical and horizontal deformations, gravity, tilt and strain) via the convolution of Green's functions with a global surface pressure field. The geophysical approach is analogous to methods used to calculate ocean tidal loading effects. However, due to the continuous spectrum of the atmospheric pressure variations, the compution of the atmospheric loading signal must be carried out in the time domain. The major advantage of the geophysical model approach is that loading effects can be computed in a standardized way for any point on the Earth's surface more or less instantaneously. The geophysical approach currently suffers from a number of problems including: the requirement of a global pressure data set, a minimum of 24 hours in time delay in the availability of the global pressure data set, limitations of the pressure data itself (low temporal and spatial resolution), uncertainties in the Green's functions and uncertainties in the ocean response model.

In the empirical approach, site-dependent pressure loading effects are computed by determining the fit of local pressure variations to the geodetic observations of the vertical crustal motion. This approach is likely to produce better results (than the geophysical approach) for a given site but has a number of drawbacks as well. 1.) Geodetic observations have to be available for a certain period of time before a reliable regression coeffcient can be determined; this period of time may be as large as serveral years. 2.) The regression coefficients cannot be extraploated to a new site (for which no data exist); 4.) The regression coefficient has been observed to change with time and with observing technique; 4.) Regression coefficients at coastal sites are time dependent due to interannual changes in the regional weather pattern (H.-P. Plag, personal communication, 2002); 5.) The regession coefficient can only be used for vertical crustal motions; and 6.) It is uncertain that other pressure correlated geodetic signals are not being 'absorbed' into the regression coefficient determination. So while this approach would lower the scatter on a given geodetic time series the most, one would always be uncertain whether only atmospheric loading effects were being removed with the correlation coefficient.

In a hybrid method, regression coefficients determined from a geophysical model instead of geodetic observations could be used to operationally correct observed vertical position determinations from local air pressure alone. The vertical deformation caused by the change in pressure, in this case, can then be given in terms of a local pressure anomaly. The regression coefficients can be determined by fitting local pressure to the vertical deformation predicted by the geophysical model. Regression coefficients determined in this manner would still suffer from both the

uncertainty in the Green's function and the quality of the air pressure data.

In February 2002, the Special Bureau on Loading (SBL) was established within the IERS. The charge of the SBL is to promote, stimulate and coordinate work and progress towards a service providing information on Earth surface deformation due to surface mass loading, including the atmosphere, ocean and continental hydrosphere. In establishing the SBL the IERS is recommending that the convention for computing atmospheric loading corrections will be based on the geophysical model approach.

At the 2002 IERS Meeting in Munich, the IERS adopted the convention that corrections for surface load variations including the atmosphere should be determined using the geophysical model approach. Further, these corrections should be obtained from the IERS SBL. The point of this recommendation is to ensure that comparisons of geodetic time series between different observing techniques or within the same technique but at different times and locations have a consistent atmospheric pressure loading (and later also non-tidal ocean and continental hydrological loading) correction applied.

The ultimate goal of the SBL is to provide in near real-time a consistent global solution data set, describing at the surface, deformation due to all surface loads (including atmospheric pressure variations) in reference frames relevant for direct comparison with geodetic observing techniques. The SBL will provide global gridded solutions of 3-D displacements and time series of displacements for all IERS sites. Time series will be determined from 1985 to the present. Displacements will be determined for both the European Center for Medium Range Weather Forecasts and the National Center for Environmental Prediction operational pressure data sets for the inverted barometer and the non-inverted barometer ocean models. For more information see: $<^{17}>$.

Regression coefficients based on a geophysical model are already available for a number of VLBI sites through the SBL web page and the IERS Convention's web page $<^{18}>$. The regression coefficients were computed using 18 years of the NCEP Reanalysis Data (1 Jan. 1980 to 31 Dec. 1997). The data are 6 hourly values of surface pressure given on a $2.5° \times 2.5°$ global grid. Vertical crustal motions at a particular site are modeled by convolving Farrell's (1972) Greens functions for a Gutenberg-Bullen A Earth model. The ocean was assumed to be inverse barometric for the calculations. The regression results (mm/mbar) are determined via a linear regression between the modeled crustal displacements and the local surface pressure determined from the NCEP data set. An inverted barometer model was used in determining the ocean's response to pressure.

For more information on atmospheric pressure loading and geodetic time series, see the references listed in the extended bibliography.

7.2   Displacement of Reference Points of Instruments

7.2.1   VLBI Antenna Thermal Deformation

The following has been excerpted from the Explanatory Supplement to the IERS Conventions (1996) Chapters 6 and 7 (Schuh, 1999).

Most VLBI telescopes are of Cassegrain type with alt-azimuth or polar mount and secondary focus. Figures 7.1 and 7.2, based on Nothnagel *et al.* (1995), show the principles of these antenna mounts. The height of the concrete foundation is denoted by h_f, the height of the antenna

---

[17]http://www.gdiv.statkart.no/sbl
[18]ftp://maia.usno.navy.mil/conv2000/chapter7/atmospheric.regr
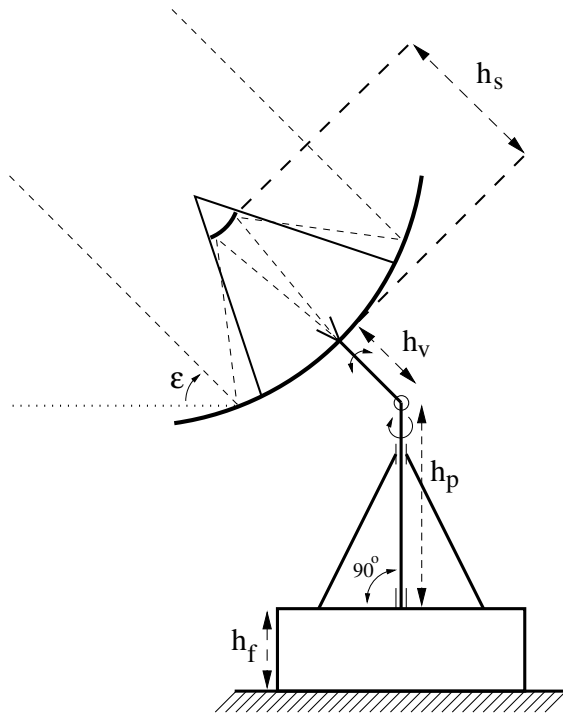
Fig. 7.1   Alt-azimuthal telescope mount.
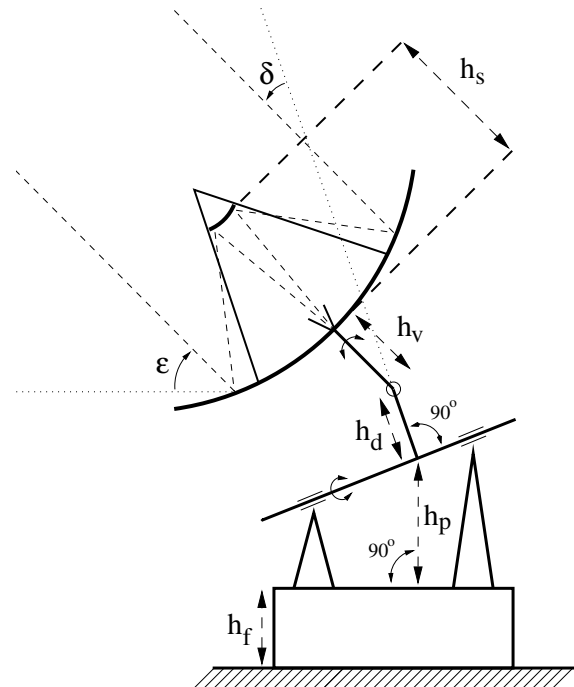
Fig. 7.2   Polar telescope mount.

pillar by h_p, the height of the vertex by h_v, the height of the subreflector by h_s and the declination shaft by h_d.

Then, the thermal deformation effect $\Delta\tau$ in s on the VLBI delay measurement τ can be modeled. For alt-azimuth mounts

$$
\begin{aligned}
\Delta\tau &= \tfrac{1}{c} \cdot \Big[\gamma_f \cdot (T(t-\Delta t_f) - T_0) \cdot (h_f \cdot \sin(\varepsilon)) \\
&\quad + \gamma_a \cdot (T(t-\Delta t_a) - T_0) \cdot (h_p \cdot \sin(\varepsilon) + h_v - 1.8 \cdot h_s) \Big].
\end{aligned}
\tag{28}
$$

For polar mounts

$$
\begin{aligned}
\Delta\tau &= \tfrac{1}{c} \cdot \Big[\gamma_f \cdot (T(t-\Delta t_f) - T_0) \cdot (h_f \cdot \sin(\varepsilon)) \\
&\quad + \gamma_a \cdot (T(t-\Delta t_a) - T_0) \cdot (h_p \cdot \sin(\varepsilon) \\
&\quad + h_v - 1.8 \cdot h_s + h_d \cdot \cos(\delta)) \Big].
\end{aligned}
\tag{29}
$$

In the above equations (28) and (29) c in m/s is the speed of light, γ_f and γ_a in $1/°C$ are the expansion coefficents for the foundation and for the antenna, respectively, and h_f, h_p, h_v, h_s and h_d are the dimensions of the telescopes in m. For prime focus antennas, the factor for h_s is 0.9 instead of 1.8. The temperature of the telescope structure is denoted by T, and T_0 is a reference temperature, *e.g.* 20°C which is the usual reference temperature used when designing and constructing buildings. If the actual temperature of the telescope structure is not available, which might be the case at most VLBI sites, the surrounding air temperature can be taken instead. The time delay between the change in the surrounding air temperature and the expansion of the telescope structure is denoted by Δt_f for the foundation part and by Δt_a for the antenna part and depend strongly on the material of the telescope. Measurements yielded values of Δt_a=2 hours for a steel telescope structure (Nothnagel *et al.*, 1995) and of Δt_f=6 hours for a concrete telescope structure (Elgered and Carlsson, 1995). The elevation and declination of the observed

radio source are denoted by ε and δ. Table 7.6 contains the dimensions of some frequently used geodetic VLBI antennas and mean expansion coefficients.

Table 7.7 gives the thermal variation $\Delta\tau$ of the VLBI delay observable, based on the telescope dimensions and expansion coefficients given in Table 7.6 and equations (28) and (29). Temperature variation $(T - T_0)$ of 10°C and radio source elevations between 5° and 90° were entered, time lags Δt_f and Δt_a were assumed to be zero.

For big VLBI telescopes, variations in the VLBI delay observations of several picoseconds can occur. Regarding a baseline of two telescopes with the signal from the radio source arriving first at site 1, the total effect on the measured delay on the baseline is:

$$\Delta\tau_{baseline} = \Delta\tau_1 - \Delta\tau_2.$$

Table 7.6   Dimensions and expansion coefficients of frequently used geodetic VLBI telescopes.

Telescope	Foundation part (concrete)		Antenna part (steel)				
	h_f m	γ_f 1/°C	h_p m	h_v m	h_s m	h_d m	γ_a 1/°C
Effelsberg	0.0	1.0×10^{-5}	50.0	8.5	28.0	−	1.2×10^{-5}
Hartebeesthoek	0.0	1.0×10^{-5}	12.7	2.3	9.4	6.7	1.2×10^{-5}
Madrid	3.0	1.0×10^{-5}	16.8	2.7	10.8	−	1.2×10^{-5}
Matera	3.0	1.0×10^{-5}	10.5	3.8	5.7	−	1.2×10^{-5}
Medicina	2.3	1.0×10^{-5}	15.5	4.3	4.3	−	1.2×10^{-5}
Noto	2.2	1.0×10^{-5}	15.7	4.2	5.0	−	1.2×10^{-5}
O'Higgins	1.0	1.0×10^{-5}	6.2	−	−	−	1.2×10^{-5}
Onsala	11.3	1.0×10^{-5}	2.9	3.4	5.5	−	1.2×10^{-5}
Westford	16.9	1.0×10^{-5}	2.0	3.0	3.6	−	1.2×10^{-5}
Wettzell	8.0	1.0×10^{-5}	4.0	3.7	7.9	−	1.2×10^{-5}

Table 7.7   Thermal variations $\Delta\tau$ in ps of the VLBI delay observable for frequently used geodetic VLBI telescopes for a temperature variation of 10°C and different radio source elevations.

Telescope	$(T-T_0)$=10°C Elevation ε			
	5° $\Delta\tau$ ps	30° $\Delta\tau$ ps	60° $\Delta\tau$ ps	90° $\Delta\tau$ ps
Effelsberg	−15.0	−6.8	+0.6	+3.2
Hartebeesthoek	−7.8	−5.0	−1.9	+0.1
Madrid	−6.0	−2.8	0.0	+1.0
Matera	−2.1	0.0	+1.9	+2.6
Medicina	−0.8	+2.1	+4.6	+5.6
Noto	−1.3	+1.6	+4.2	+5.1
O'Higgins	0.2	+1.4	+2.4	+2.8
Onsala	−2.2	−0.1	+1.7	+2.3
Westford	−0.8	+1.8	+4.2	+5.0
Wettzell	−3.8	−2.0	−0.5	0.0

References

Blewitt, G., Lavallée, D., Clarke, P., and Nurutdinov, K., 2001, "A new global mode of the Earth deformation: Seasonal cycle detected," *Science*, **294**, pp. 2342–2345.

Cartwright, D. E. and Tayler, R. J., 1971, "New Computations of the Tide-Generating Potential," *Geophys. J. Roy. astr. Soc.*, **23**, pp. 45–74.

Cartwright, D. E. and Edden, A. C., 1973, "Corrected Tables of Tidal Harmonics," *Geophys. J. Roy. astr. Soc.*, **33**, pp. 253–264.

Chelton, D. B. and Enfield, D. B., 1986, "Ocean Signals in Tide Gauge Records," *J. Geophys. Res.*, **91**, pp. 9081–9098.

Dong, D., Fang, P., Bock, Y., Cheng, M. K., and Miyazaki, S., 2002, "Anatomy of apparent seasonal variations from GPS-derived site position time series," *J. Geophys. Res.*, **107(B4)**, ETG 9-1–9-8.

Doodson, A. T., 1928, "The Analysis of Tidal Observations," *Phil. Trans. Roy. Soc. Lond.*, **227**, pp. 223–279.

Eanes, R. J., 1994, "Diurnal and semidiurnal tides from TOPEX/ POSEIDON altimetry," paper G32B-6, presented at the Spring Meeting of the AGU, Baltimore, MD, *EOS Trans AGU*, **75**, p. 108.

Eanes R. J. and Bettadpur, S., 1995, "The CSR 3.0 global ocean tide model," *Technical Memorandum CSR-TM-95-06*, Center for Space Research, University of Texas, Austin, TX.

Egbert, G. D., Bennett, A. F., and Foreman, M. G. G. , 1994, "TOPEX/ POSEIDON tides estimated using a global inverse model," *J. Geophys. Res.*, **99**, pp. 24,821–24,852.

Elgered, G. and Carlsson, T. R., 1995, "Temperature Stability of the Onsala 20-m Antenna and its Impact on Geodetic VLBI," *Proc. of the 10th Working Meeting on European VLBI for Geodesy and Astrometry*, Lanotte, R. and Bianco, G. (eds.), Matera, pp. 69–78.

Farrell, W. E., 1972, "Deformation of the Earth by Surface Loads," *Rev. Geophys. Space Phys.*, **10**, pp. 761–797.

Haas, R., 1996, "Untersuchungen zu Erddeformationsmodellen fur die Auswertung von geodatischen VLBI-Messungen", PhD Thesis, Deutsche Geodatische Kommission, Reihe C, Heft Nr. 466, 103 pp.

Haas, R., H.-G. Scherneck, and H. Schuh, 1997, "Atmospheric loading corrections in Geodetic VLBI and determination of atmospheric loading coefficients," in *Proc. of the 12 Working Meeting on European VLBI for Geodesy and Astronomy*, Pettersen, B.R. (ed.), Honefoss, Norway, 1997, pp. 122–132.

Hartmann, T. and Wenzel, H.-G., 1995, "The HW95 Tidal Potential Catalogue," *Geophys. Res. Lett.*, **22**, pp. 3553–3556.

Le Provost, C., Genco, M. L., Lyard, F., Incent, P., and Canceil, P., 1994, "Spectroscopy of the world ocean tides from a finite element hydrological model," *J. Geophys. Res.*, **99**, pp. 24777–24798.

Le Provost, C., Lyard, F., Molines, J. M., Genco, M. L., and Rabilloud, F., 1998, "A hydrodynamic ocean tide model improved by assimilating a satellite altimeter-derived data set," *J. Geophys. Res.*, **103**, pp. 5513–5529.

Lefèvre, F., Lyard, F. H., and Le Provost, C. , 2000, "FES98: A new global tide finite element solution independent of altimetry," *Geophys. Res. Lett.*, **27**, pp. 2717–2720.

MacMillan, D. S. and Gipson, J. M., 1994, "Atmospheric Pressure Loading Parameters from Very Long Baseline Interferometry Observations," *J. Geophys. Res.*, **99**, pp. 18081–18087.

Manabe, S. T., Sato, T., Sakai, S., and Yokoyama, K., 1991, "Atmospheric Loading Effects on VLBI Observations," in Proc. of the AGU Chapman Conference on Geodetic VLBI: Monitoring Global Change, *NOAA Tech. Rep. NOS 137 NGS 49*, pp. 111–122.

Mangiarotti, S., Cazenave A., Soudarin L., and Cretaux J. F., 2001, "Annual vertical crustal motions predicted from surface mass redistribution and observed by space geodesy," *J. Geophys. Res.*, **106**, pp. 4277–4291.

Mathers, E. L. and Woodworth, P. L., 2001, "Departures from the local inverse barometer model observed in altimeter and tide gauge data and in a global barotropic numerical model," *J. Geophys. Res.*, **106**, pp. 6957–6972.

Mathews, P. M., Buffett, B. A., and Shapiro, I. I., 1995, "Love numbers for a rotating spheroidal Earth: New definitions and numerical values," *Geophys. Res. Lett.*, **22**, pp. 579–582.

Matsumoto, K., Takanezawa, T. and Ooe, M., 2000, "Ocean Tide Models Developed by Assimilating TOPEX/ POSEIDON Altimeter Data into Hydrodynamical Model: A Global Model and a Regional Model Around Japan," *J. Oceanog.*, **56**, pp. 567–581.

Munk, W. H. and MacDonald, G. J. F., 1960, *The Rotation of the Earth*, Cambridge Univ. Press, New York, pp. 24–25.

Nothnagel, A., Pilhatsch, M., and Haas, R., 1995, "Investigations of Thermal Height Changes of Geodetic VLBI Radio Telescopes," in *Proceedings of the 10th Working Meeting on European VLBI for Geodesy and Astrometry*, Lanotte, R. and Bianco, G. (eds.), Matera, pp. 121–133.

Ponte, R. M., Salstein, D. A., and Rosen, R. D., 1991, "Sea Level Response to Pressure Forcing in a Barotropic Numerical Model," *J. Phys. Oceanogr.*, **21**, pp. 1043–1057.

Rabbel, W. and Schuh, H., 1986, "The Influence of Atmospheric Loading on VLBI Experiments," *J. Geophys.*, **59**, pp. 164–170.

Rabbel, W. and Zschau, J., 1985, "Static Deformations and Gravity Changes at the Earth's Surface due to Atmospheric Loading," *J. Geophys.*, **56**, pp. 81–99.

Ray, R., 1999, "A Global Ocean Tide Model From TOPEX/POSEIDON Altimetry: GOT99.2," *NASA Technical Memorandum, NASA/ TM-1999-209478*, National Aeronautics and Space Administration, Goddard Space Flight Center, Greenbelt, MD.

Row, L. W., Hastings, D. A., and Dunbar, P. K., 1995, "TerrainBase Worldwide Digital Terrain Data," NOAA, National Geophysical Data Center, Boulder CO.

Scherneck, H.-G., 1990, "Loading Green's functions for a continental shield with a Q-structure for the mantle and density constraints from the geoid," *Bull. d'Inform. Marées Terr.*, **108**, pp. 7757–7792.

Scherneck, H. G., 1991, "A Parameterized Solid Earth Tide Model and Ocean Tide Loading Effects for Global Geodetic Baseline Measurements," *Geophys. J. Int.*, **106**, pp. 677–694.

Scherneck, H. G., 1993, "Ocean Tide Loading: Propagation of Errors from the Ocean Tide into Loading Coefficients," *Man. Geod.*, **18**, pp. 59–71.

Schuh, H. (ed.), 1999, *Explanatory Supplement to the IERS Conventions (1996) Chapters 6 and 7*, DGFI Report 71.

Schwiderski, E. W. and Szeto, L. T., 1981, "The NSWC global ocean tide data tape (GOTD), its features and application, random-point timde program," *NSWC-TR 81–254*, Naval Surface Weapons Center, Dahlgren, VA, 19 pp.

Sun, H. P., Ducarme, B., and Dehant, V., 1995, "Effect of the Atmospheric Pressure on Surface Displacements," *J. Geod.*, **70**, pp. 131–139.

Tamura, Y., 1987, "A harmonic development of the tide-generating potential," *Bull. d'Inform. Marées Terr.*, **99**, pp. 6813–6855.

vanDam, T. M. and Wahr, J. M., 1987, "Displacements of the Earth's Surface due to Atmospheric Loading: Effects on Gravity and Baseline Measurements," *J. Geophys. Res.*, **92**, pp. 1281–1286.

vanDam, T. M. and Herring, T. A., 1994, "Detection of Atmospheric Pressure Loading Using Very Long Baseline Interferometry Measurements," *J. Geophys. Res.*, **99**, pp. 4505–4517.

vanDam, T. M., Blewitt, G., and Heflin, M. B., 1994, "Atmospheric Pressure Loading Effects on Global Positioning System Coordinate Determinations," *J. Geophys. Res.*, **99**, pp. 23,939–23,950.

Wahr, J. M., 1981, "The Forced Nutations of an Elliptical, Rotating, Elastic, and Oceanless Earth," *Geophys. J. Roy. astr. Soc.*, **64**, pp. 705–727.

Wahr, J. M., 1985, "Deformation Induced by Polar Motion," *J. Geophys. Res.*, **90**, pp. 9363–9368.

Wahr, J. M. and Sasao, T., 1981, "A diurnal resonance in the ocean tide and the Earth's load response due to the resonant free "core nutation"," *Geophys. J. R. astr. Soc.*, **64**, pp. 747–765.

Zschau, J., 1983, "Rheology of the Earth's mantle at tidal and Chandler Wobble periods," *Proc. Ninth Int. Symp. Earth Tides*, New York, 1981, Kuo, J. T. (ed.), Schweizerbart'sche Verlagsbuchhandlung, Stuttgart, pp. 605–630.

8   Tidal Variations in the Earth's Rotation

Periodic variations in UT1 due to tidal deformation of the polar moment of inertia were first derived by Yoder *et al.* (1981) and included the tidal deformation of the Earth with a decoupled core, an elastic mantle and an equilibrium ocean tide. This model used effective Love numbers that differ from the bulk value of 0.301 because of the oceans and the fluid core, producing different theoretical values of the ratio k/C for the fortnightly and monthly terms. However, Yoder *et al.* recommend the value of 0.94 for k/C for both cases. Tables in previous IERS Technical Notes defined UT1R−UTC, $\Delta - \Delta$R, and $\omega - \omega$R where Δ refers to the length of day and ω the Earth's rotational speed.

Periodic variations in UT1 due to tidal deformations for an Earth model with a decoupled core and an inelastic mantle have been computed by Defraigne and Smits (1999). The mantle inelasticity model is the same as for the displacement and potential Love numbers (Chapters 6 and 7), *i.e.* a frequency dependence of $(f_m/f)^\alpha$ where $\alpha = 0.15$, f_m is the seismic frequency corresponding to a period of 200 s, and f is the tidal frequency. The ocean effects are included in the model using a transfer function that is constant with frequency (k_{ocean}=0.044) computed by Mathews *et al.* (2002) for an equilibrium ocean tide model. Note that Dickman (2003) finds a value k_{ocean}=0.04323 for dynamic oceans. The decision to use a constant admittance is due to the absence of agreement between the existing models of non-equilibrium ocean tide effects for the long-period tides (Dickman, 1993; Seiler and Wünsch, 1995).

Table 8.1 provides corrections for the tidal variations in the Earth's rotation with periods from five days to 18.6 years. These corrections (δUT1, $\delta\Delta$, $\delta\omega$) represent the effect of tidal deformation on the physical variations in the rotation of the Earth. To obtain variations free from tidal effects, these corrections should be subtracted from the observed UT1−UTC, length of day (Δ) and rotation velocity (ω).

$$\delta\text{UT1} = \sum_{i=1}^{62} B_i \sin \xi_i + C_i \cos \xi_i,$$

$$\delta\Delta = \sum_{i=1}^{62} B_i' \cos \xi_i + C_i' \sin \xi_i,$$

$$\delta\omega = \sum_{i=1}^{62} B_i'' \cos \xi_i + C_i'' \sin \xi_i,$$

$$\xi_i = \sum_{j=1}^{5} a_{ij} \alpha_j,$$

B_i, C_i, B_i', C_i', B_i'', and C_i'' are given in columns 7–12 respectively in Table 8.1. a_{ij} = integer multipliers of the α_j (l, l', F, D or Ω) for the ith tide given in the first five columns of Table 8.1.

To avoid confusion among possible tidal models, it is recommended that the terms δUT1, $\delta\Delta$, $\delta\omega$ be followed by the model name in parenthesis, *e.g.* δUT1(Defraigne and Smits, 1999).

Software to provide corrections modeling the diurnal and sub-diurnal variations in polar motion and UT1 are available from the IERS Conventions web page. These are provided by Eanes (2000) and are based on Ray *et al.* (1994). The software includes 71 tidal constituents with amplitudes on the order of tenths of milliarcseconds in polar motion and tens of microseconds in UT1.

Table 8.1   Zonal tide terms. δUT1, $\delta\Delta$, and $\delta\omega$ represent the regularized forms of UT1, the duration of the day Δ, and the angular velocity of the Earth, ω. The units are 10^{-4} s for UT1, 10^{-5} s for Δ, and 10^{-14} rad/s for ω.

	ARGUMENT				PERIOD	δUT1		$\delta\Delta$		$\delta\omega$	
								Coefficient of			
l	l'	F	D	Ω	Days	Sin	Cos	Cos	Sin	Cos	Sin
1	0	2	2	2	5.64	-0.02	0.00	0.26	0.00	-0.22	0.00
2	0	2	0	1	6.85	-0.04	0.00	0.38	0.00	-0.32	0.00
2	0	2	0	2	6.86	-0.10	0.00	0.91	0.00	-0.76	0.00
0	0	2	2	1	7.09	-0.05	0.00	0.45	0.00	-0.38	0.00
0	0	2	2	2	7.10	-0.12	0.00	1.09	0.01	-0.92	-0.01
1	0	2	0	0	9.11	-0.04	0.00	0.27	0.00	-0.22	0.00
1	0	2	0	1	9.12	-0.41	0.00	2.84	0.02	-2.40	-0.01
1	0	2	0	2	9.13	-1.00	0.01	6.85	0.04	-5.78	-0.03
3	0	0	0	0	9.18	-0.02	0.00	0.12	0.00	-0.11	0.00
-1	0	2	2	1	9.54	-0.08	0.00	0.54	0.00	-0.46	0.00
-1	0	2	2	2	9.56	-0.20	0.00	1.30	0.01	-1.10	-0.01
1	0	0	2	0	9.61	-0.08	0.00	0.50	0.00	-0.42	0.00
2	0	2	-2	2	12.81	0.02	0.00	-0.11	0.00	0.09	0.00
0	1	2	0	2	13.17	0.03	0.00	-0.12	0.00	0.10	0.00
0	0	2	0	0	13.61	-0.30	0.00	1.39	0.01	-1.17	-0.01
0	0	2	0	1	13.63	-3.22	0.02	14.86	0.09	-12.54	-0.08
0	0	2	0	2	13.66	-7.79	0.05	35.84	0.22	-30.25	-0.18
2	0	0	0	-1	13.75	0.02	0.00	-0.10	0.00	0.08	0.00
2	0	0	0	0	13.78	-0.34	0.00	1.55	0.01	-1.31	-0.01
2	0	0	0	1	13.81	0.02	0.00	-0.08	0.00	0.07	0.00
0	-1	2	0	2	14.19	-0.02	0.00	0.11	0.00	-0.09	0.00
0	0	0	2	-1	14.73	0.05	0.00	-0.20	0.00	0.17	0.00
0	0	0	2	0	14.77	-0.74	0.00	3.14	0.02	-2.65	-0.02
0	0	0	2	1	14.80	-0.05	0.00	0.22	0.00	-0.19	0.00
0	-1	0	2	0	15.39	-0.05	0.00	0.21	0.00	-0.17	0.00
1	0	2	-2	1	23.86	0.05	0.00	-0.13	0.00	0.11	0.00
1	0	2	-2	2	23.94	0.10	0.00	-0.26	0.00	0.22	0.00
1	1	0	0	0	25.62	0.04	0.00	-0.10	0.00	0.08	0.00
-1	0	2	0	0	26.88	0.05	0.00	-0.11	0.00	0.09	0.00
-1	0	2	0	1	26.98	0.18	0.00	-0.41	0.00	0.35	0.00
-1	0	2	0	2	27.09	0.44	0.00	-1.02	-0.01	0.86	0.01
1	0	0	0	-1	27.44	0.54	0.00	-1.23	-0.01	1.04	0.01
1	0	0	0	0	27.56	-8.33	0.06	18.99	0.13	-16.03	-0.11
1	0	0	0	1	27.67	0.55	0.00	-1.25	-0.01	1.05	0.01
0	0	0	1	0	29.53	0.05	0.00	-0.11	0.00	0.09	0.00
1	-1	0	0	0	29.80	-0.06	0.00	0.12	0.00	-0.10	0.00
-1	0	0	2	-1	31.66	0.12	0.00	-0.24	0.00	0.20	0.00
-1	0	0	2	0	31.81	-1.84	0.01	3.63	0.02	-3.07	-0.02
-1	0	0	2	1	31.96	0.13	0.00	-0.26	0.00	0.22	0.00
1	0	-2	2	-1	32.61	0.02	0.00	-0.04	0.00	0.03	0.00
-1	-1	0	2	0	34.85	-0.09	0.00	0.16	0.00	-0.13	0.00
0	2	2	-2	2	91.31	-0.06	0.00	0.04	0.00	-0.03	0.00
0	1	2	-2	1	119.61	0.03	0.00	-0.02	0.00	0.01	0.00
0	1	2	-2	2	121.75	-1.91	0.02	0.98	0.01	-0.83	-0.01
0	0	2	-2	0	173.31	0.26	0.00	-0.09	0.00	0.08	0.00
0	0	2	-2	1	177.84	1.18	-0.01	-0.42	0.00	0.35	0.00
0	0	2	-2	2	182.62	-49.06	0.43	16.88	0.15	-14.25	-0.13
0	2	0	0	0	182.63	-0.20	0.00	0.07	0.00	-0.06	0.00
2	0	0	-2	-1	199.84	0.05	0.00	-0.02	0.00	0.01	0.00
2	0	0	-2	0	205.89	-0.56	0.01	0.17	0.00	-0.14	0.00
2	0	0	-2	1	212.32	0.04	0.00	-0.01	0.00	0.01	0.00
0	-1	2	-2	1	346.60	-0.05	0.00	0.01	0.00	-0.01	0.00
0	1	0	0	-1	346.64	0.09	0.00	-0.02	0.00	0.01	0.00
0	-1	2	-2	2	365.22	0.82	-0.01	-0.14	0.00	0.12	0.00

(continued on next page)

(Table 8.1: continued)

0	1	0	0	0	365.26	-15.65	0.15	2.69	0.03	-2.27	-0.02
0	1	0	0	1	386.00	-0.14	0.00	0.02	0.00	-0.02	0.00
1	0	0	-1	0	411.78	0.03	0.00	0.00	0.00	0.00	0.00
2	0	-2	0	0	1095.17	-0.14	0.00	-0.01	0.00	0.01	0.00
-2	0	2	0	1	1305.47	0.43	-0.01	-0.02	0.00	0.02	0.00
-1	1	0	1	0	3232.85	-0.04	0.00	0.00	0.00	0.00	0.00
0	0	0	0	2	3399.18	8.20	0.11	0.15	0.00	-0.13	0.00
0	0	0	0	1	6798.38	-1689.54	-25.04	-15.62	0.23	13.18	-0.20

Table 8.2a   Coefficients of sin(argument) and cos(argument) of diurnal variations in pole coordinates x_p and y_p caused by ocean tides. The units are μas; χ denotes GMST+π.

Tide	\multicolumn{6}{c}{argument}	Doodson	Period	\multicolumn{2}{c}{x_p}	\multicolumn{2}{c}{y_p}
	χ	l	l'	F	D	Ω	number	(days)	sin	cos	sin	cos
	1	-1	0	-2	-2	-2	117.655	1.2113611	0.0	0.9	-0.9	-0.1
	1	-2	0	-2	0	-1	125.745	1.1671262	0.1	0.6	-0.6	0.1
2Q1	1	-2	0	-2	0	-2	125.755	1.1669259	0.3	3.4	-3.4	0.3
	1	0	0	-2	-2	-1	127.545	1.1605476	0.1	0.8	-0.8	0.1
σ1	1	0	0	-2	-2	-2	127.555	1.1603495	0.5	4.2	-4.1	0.5
	1	-1	0	-2	0	-1	135.645	1.1196993	1.2	5.0	-5.0	1.2
Q1	1	-1	0	-2	0	-2	135.655	1.1195148	6.2	26.3	-26.3	6.2
	1	1	0	-2	-2	-1	137.445	1.1136429	0.2	0.9	-0.9	0.2
RO1	1	1	0	-2	-2	-2	137.455	1.1134606	1.3	5.0	-5.0	1.3
	1	0	0	-2	0	0	145.535	1.0761465	-0.3	-0.8	0.8	-0.3
	1	0	0	-2	0	-1	145.545	1.0759762	9.2	25.1	-25.1	9.2
O1	1	0	0	-2	0	-2	145.555	1.0758059	48.8	132.9	-132.9	48.8
	1	-2	0	0	0	0	145.755	1.0750901	-0.3	-0.9	0.9	-0.3
T01	1	0	0	0	-2	0	147.555	1.0695055	-0.7	-1.7	1.7	-0.7
	1	-1	0	-2	2	-2	153.655	1.0406147	-0.4	-0.9	0.9	-0.4
	1	1	0	-2	0	-1	155.445	1.0355395	-0.3	-0.6	0.6	-0.3
	1	1	0	-2	0	-2	155.455	1.0353817	-1.6	-3.5	3.5	-1.6
M1	1	-1	0	0	0	0	155.655	1.0347187	-4.5	-9.6	9.6	-4.5
	1	-1	0	0	0	-1	155.665	1.0345612	-0.9	-1.9	1.9	-0.9
χ1	1	1	0	0	-2	0	157.455	1.0295447	-0.9	-1.8	1.8	-0.9
π1	1	0	-1	-2	2	-2	162.556	1.0055058	1.5	3.0	-3.0	1.5
	1	0	0	-2	2	-1	163.545	1.0028933	-0.3	-0.6	0.6	-0.3
P1	1	0	0	-2	2	-2	163.555	1.0027454	26.1	51.2	-51.2	26.1
	1	0	1	-2	2	-2	164.554	1.0000001	-0.2	-0.4	0.4	-0.2
S1	1	0	-1	0	0	0	164.556	0.9999999	-0.6	-1.2	1.2	-0.6
	1	0	0	0	0	1	165.545	0.9974159	1.5	3.0	-3.0	1.5
K1	1	0	0	0	0	0	165.555	0.9972695	-77.5	-151.7	151.7	-77.5
	1	0	0	0	0	-1	165.565	0.9971233	-10.5	-20.6	20.6	-10.5
	1	0	0	0	0	-2	165.575	0.9969771	0.2	0.4	-0.4	0.2
ψ1	1	0	1	0	0	0	166.554	0.9945541	-0.6	-1.2	1.2	-0.6
ϕ1	1	0	0	2	-2	2	167.555	0.9918532	-1.1	-2.1	2.1	-1.1
TT1	1	-1	0	0	2	0	173.655	0.9669565	-0.7	-1.4	1.4	-0.7
J1	1	1	0	0	0	0	175.455	0.9624365	-3.5	-7.3	7.3	-3.5
	1	1	0	0	0	-1	175.465	0.9623003	-0.7	-1.4	1.4	-0.7
SO1	1	0	0	0	2	0	183.555	0.9341741	-0.4	-1.1	1.1	-0.4
	1	2	0	0	0	0	185.355	0.9299547	-0.2	-0.5	0.5	-0.2
OO1	1	0	0	2	0	2	185.555	0.9294198	-1.1	-3.4	3.4	-1.1
	1	0	0	2	0	1	185.565	0.9292927	-0.7	-2.2	2.2	-0.7
	1	0	0	2	0	0	185.575	0.9291657	-0.1	-0.5	0.5	-0.1
ν1	1	1	0	2	0	2	195.455	0.8990932	0.0	-0.6	0.6	0.0
	1	1	0	2	0	1	195.465	0.8989743	0.0	-0.4	0.4	0.0

Table 8.2b   Coefficients of sin(argument) and cos(argument) of semidiurnal variations in pole coordinates x_p and y_p caused by ocean tides. The units are μas; χ denotes GMST+ π.

			argument				Doodson	Period	x_p		y_p	
$Tide$	χ	l	l'	F	D	Ω	number	(days)	sin	cos	sin	cos
	2	-3	0	-2	0	-2	225.855	0.5484264	-0.5	0.0	0.6	0.2
	2	-1	0	-2	-2	-2	227.655	0.5469695	-1.3	-0.2	1.5	0.7
2N2	2	-2	0	-2	0	-2	235.755	0.5377239	-6.1	-1.6	3.1	3.4
μ2	2	0	0	-2	-2	-2	237.555	0.5363232	-7.6	-2.0	3.4	4.2
	2	0	1	-2	-2	-2	238.554	0.5355369	-0.5	-0.1	0.2	0.3
	2	-1	-1	-2	0	-2	244.656	0.5281939	0.5	0.1	-0.1	-0.3
	2	-1	0	-2	0	-1	245.645	0.5274721	2.1	0.5	-0.4	-1.2
N2	2	-1	0	-2	0	-2	245.655	0.5274312	-56.9	-12.9	11.1	32.9
	2	-1	1	-2	0	-2	246.654	0.5266707	-0.5	-0.1	0.1	0.3
ν2	2	1	0	-2	-2	-2	247.455	0.5260835	-11.0	-2.4	1.9	6.4
	2	1	1	-2	-2	-2	248.454	0.5253269	-0.5	-0.1	0.1	0.3
	2	-2	0	-2	2	-2	253.755	0.5188292	1.0	0.1	-0.1	-0.6
	2	0	-1	-2	0	-2	254.556	0.5182593	1.1	0.1	-0.1	-0.7
	2	0	0	-2	0	-1	255.545	0.5175645	12.3	1.0	-1.4	-7.3
M2	2	0	0	-2	0	-2	255.555	0.5175251	-330.2	-27.0	37.6	195.9
	2	0	1	-2	0	-2	256.554	0.5167928	-1.0	-0.1	0.1	0.6
λ2	2	-1	0	-2	2	-2	263.655	0.5092406	2.5	-0.3	-0.4	-1.5
L2	2	1	0	-2	0	-2	265.455	0.5079842	9.4	-1.4	-1.9	-5.6
	2	-1	0	0	0	0	265.655	0.5078245	-2.4	0.4	0.5	1.4
	2	-1	0	0	0	-1	265.665	0.5077866	-1.0	0.2	0.2	0.6
T2	2	0	-1	-2	2	-2	272.556	0.5006854	-8.5	3.5	3.3	5.1
S2	2	0	0	-2	2	-2	273.555	0.5000000	-144.1	63.6	59.2	86.6
R2	2	0	1	-2	2	-2	274.554	0.4993165	1.2	-0.6	-0.5	-0.7
	2	0	0	0	0	1	275.545	0.4986714	0.5	-0.2	-0.2	-0.3
K2	2	0	0	0	0	0	275.555	0.4986348	-38.5	19.1	17.7	23.1
	2	0	0	0	0	-1	275.565	0.4985982	-11.4	5.8	5.3	6.9
	2	0	0	0	0	-2	275.575	0.4985616	-1.2	0.6	0.6	0.7
	2	1	0	0	0	0	285.455	0.4897717	-1.8	1.8	1.7	1.0
	2	1	0	0	0	-1	285.465	0.4897365	-0.8	0.8	0.8	0.5
	2	0	0	2	0	2	295.555	0.4810750	-0.3	0.6	0.7	0.2

Table 8.3a   Coefficients of sin(argument) and cos(argument) of diurnal variations in UT1 and
LOD caused by ocean tides. The units are μs; χ denotes GMST$+ \pi$.

| Tide | | | | argument | | | Doodson | Period | UT1 | | LOD | |
	χ	l	l'	F	D	Ω	number	(days)	sin	cos	sin	cos
	1	-1	0	-2	-2	-2	117.655	1.2113611	0.40	-0.08	-0.41	-2.06
	1	-2	0	-2	0	-1	125.745	1.1671262	0.19	-0.06	-0.32	-1.05
2Q1	1	-2	0	-2	0	-2	125.755	1.1669259	1.03	-0.31	-1.69	-5.57
	1	0	0	-2	-2	-1	127.545	1.1605476	0.22	-0.07	-0.39	-1.21
σ1	1	0	0	-2	-2	-2	127.555	1.1603495	1.19	-0.39	-2.09	-6.43
	1	-1	0	-2	0	-1	135.645	1.1196993	0.97	-0.47	-2.66	-5.42
Q1	1	-1	0	-2	0	-2	135.655	1.1195148	5.12	-2.50	-14.02	-28.72
	1	1	0	-2	-2	-1	137.445	1.1136429	0.17	-0.09	-0.51	-0.97
RO1	1	1	0	-2	-2	-2	137.455	1.1134606	0.91	-0.47	-2.68	-5.14
	1	0	0	-2	0	0	145.535	1.0761465	-0.09	0.07	0.41	0.54
	1	0	0	-2	0	-1	145.545	1.0759762	3.03	-2.28	-13.31	-17.67
O1	1	0	0	-2	0	-2	145.555	1.0758059	16.02	-12.07	-70.47	-93.58
	1	-2	0	0	0	0	145.755	1.0750901	-0.10	0.08	0.46	0.60
T01	1	0	0	0	-2	0	147.555	1.0695055	-0.19	0.15	0.91	1.14
	1	-1	0	-2	2	-2	153.655	1.0406147	-0.08	0.07	0.45	0.50
	1	1	0	-2	0	-1	155.445	1.0355395	-0.06	0.05	0.31	0.35
	1	1	0	-2	0	-2	155.455	1.0353817	-0.31	0.27	1.65	1.87
M1	1	-1	0	0	0	0	155.655	1.0347187	-0.86	0.75	4.56	5.20
	1	-1	0	0	0	-1	155.665	1.0345612	-0.17	0.15	0.91	1.04
χ1	1	1	0	0	-2	0	157.455	1.0295447	-0.16	0.14	0.84	0.98
π1	1	0	-1	-2	2	-2	162.556	1.0055058	0.31	-0.19	-1.18	-1.97
	1	0	0	-2	2	-1	163.545	1.0028933	-0.06	0.03	0.22	0.39
P1	1	0	0	-2	2	-2	163.555	1.0027454	5.51	-3.10	-19.40	-34.54
	1	0	1	-2	2	-2	164.554	1.0000001	-0.05	0.02	0.16	0.30
S1	1	0	-1	0	0	0	164.556	0.9999999	-0.13	0.07	0.44	0.84
	1	0	0	0	0	1	165.545	0.9974159	0.35	-0.17	-1.07	-2.19
K1	1	0	0	0	0	0	165.555	0.9972695	-17.62	8.55	53.86	111.01
	1	0	0	0	0	-1	165.565	0.9971233	-2.39	1.16	7.30	15.07
	1	0	0	0	0	-2	165.575	0.9969771	0.05	-0.03	-0.16	-0.33
ψ1	1	0	1	0	0	0	166.554	0.9945541	-0.14	0.06	0.41	0.91
ϕ1	1	0	0	2	-2	2	167.555	0.9918532	-0.27	0.11	0.70	1.69
TT1	1	-1	0	0	2	0	173.655	0.9669565	-0.29	0.04	0.28	1.87
J1	1	1	0	0	0	0	175.455	0.9624365	-1.61	0.19	1.22	10.51
	1	1	0	0	0	-1	175.465	0.9623003	-0.32	0.04	0.24	2.09
SO1	1	0	0	0	2	0	183.555	0.9341741	-0.41	-0.01	-0.04	2.74
	1	2	0	0	0	0	185.355	0.9299547	-0.21	-0.01	-0.03	1.44
OO1	1	0	0	2	0	2	185.555	0.9294198	-1.44	-0.04	-0.25	9.70
	1	0	0	2	0	1	185.565	0.9292927	-0.92	-0.02	-0.16	6.23
	1	0	0	2	0	0	185.575	0.9291657	-0.19	0.00	-0.03	1.30
ν1	1	1	0	2	0	2	195.455	0.8990932	-0.40	-0.02	-0.17	2.77
	1	1	0	2	0	1	195.465	0.8989743	-0.25	-0.02	-0.11	1.77

Table 8.3b   Coefficients of sin(argument) and cos(argument) of semidiurnal variations in UT1 and LOD caused by ocean tides. The units are μs; χ denotes GMST$+ \pi$.

Tide			argument				Doodson	Period	UT1		LOD	
	χ	l	l'	F	D	Ω	number	(days)	sin	cos	sin	cos
	2	-3	0	-2	0	-2	225.855	0.5484264	-0.09	-0.01	-0.12	1.02
	2	-1	0	-2	-2	-2	227.655	0.5469695	-0.22	-0.03	-0.37	2.57
2N2	2	-2	0	-2	0	-2	235.755	0.5377239	-0.64	-0.18	-2.06	7.44
μ2	2	0	0	-2	-2	-2	237.555	0.5363232	-0.74	-0.22	-2.61	8.72
	2	0	1	-2	-2	-2	238.554	0.5355369	-0.05	-0.02	-0.18	0.58
	2	-1	-1	-2	0	-2	244.656	0.5281939	0.03	0.01	0.16	-0.39
	2	-1	0	-2	0	-1	245.645	0.5274721	0.14	0.06	0.70	-1.68
N2	2	-1	0	-2	0	-2	245.655	0.5274312	-3.79	-1.56	-18.57	45.20
	2	-1	1	-2	0	-2	246.654	0.5266707	-0.03	-0.01	-0.18	0.41
ν2	2	1	0	-2	-2	-2	247.455	0.5260835	-0.70	-0.30	-3.57	8.33
	2	1	1	-2	-2	-2	248.454	0.5253269	-0.03	-0.01	-0.16	0.38
	2	-2	0	-2	2	-2	253.755	0.5188292	0.05	0.02	0.27	-0.60
	2	0	-1	-2	0	-2	254.556	0.5182593	0.06	0.03	0.31	-0.68
	2	0	0	-2	0	-1	255.545	0.5175645	0.60	0.27	3.23	-7.34
M2	2	0	0	-2	0	-2	255.555	0.5175251	-16.19	-7.15	-86.79	196.58
	2	0	1	-2	0	-2	256.554	0.5167928	-0.05	-0.02	-0.26	0.59
λ2	2	-1	0	-2	2	-2	263.655	0.5092406	0.11	0.03	0.43	-1.37
L2	2	1	0	-2	0	-2	265.455	0.5079842	0.42	0.12	1.44	-5.25
	2	-1	0	0	0	0	265.655	0.5078245	-0.11	-0.03	-0.36	1.32
	2	-1	0	0	0	-1	265.665	0.5077866	-0.05	-0.01	-0.16	0.58
T2	2	0	-1	-2	2	-2	272.556	0.5006854	-0.44	-0.02	-0.24	5.48
S2	2	0	0	-2	2	-2	273.555	0.5000000	-7.55	-0.16	-2.00	94.83
R2	2	0	1	-2	2	-2	274.554	0.4993165	0.06	0.00	0.00	-0.80
	2	0	0	0	0	1	275.545	0.4986714	0.03	0.00	-0.01	-0.34
K2	2	0	0	0	0	0	275.555	0.4986348	-2.10	0.04	0.52	26.51
	2	0	0	0	0	-1	275.565	0.4985982	-0.63	0.01	0.19	7.91
	2	0	0	0	0	-2	275.575	0.4985616	-0.07	0.00	0.02	0.86
	2	1	0	0	0	0	285.455	0.4897717	-0.15	0.04	0.48	1.87
	2	1	0	0	0	-1	285.465	0.4897365	-0.06	0.02	0.21	0.82
	2	0	0	2	0	2	295.555	0.4810750	-0.05	0.02	0.24	0.63

References

Defraigne, P. and Smits, I., 1999, "Length of day variations due to zonal tides for an elastic earth in non-hydrostatic equilibrium," *Geophys. J. Int.*, **139**, pp. 563–572.

Dickman, S.R., 1993, "Dynamic ocean tide effects on Earth's rotation," *Geophys. J. Int.*, **112**, pp. 448–470.

Dickman, S.R., 2003, "Evaluation of "Effective Angular Momentum Function" Formulations with respect to Core-Mantle Coupling," *Geophys. J. Int.*, March 2003.

Eanes, R., 2000, personal communication.

Mathews, P. M., Herring, T. A., and Buffet, B. A., 2002, "Modeling of nutation-precession: New nutation series for non-rigid Earth, and insights into Earth's interior," *J. Geophys. Res.*, **107**, B4, 10.1029/2001JB000390.

Ray, R. D., Steinberg, D. J., Chao, B. F., and Cartwright, D. E., 1994, "Diurnal and Semidiurnal Variations in the Earth's Rotation Rate Induced by Oceanic Tides," *Science*, **264**, pp. 830–832.

Seiler, U. and Wünsch, J., 1995, "A refined model for the influence of ocean tides on UT1 and polar motion," *Astron. Nachr.*, **316**, p. 419.

Yoder, C. F., Williams, J. G., and Parke, M. E., 1981, "Tidal Variations of Earth Rotation," *J. Geophys. Res.*, **86**, pp. 881–891.

9 Tropospheric Model

9.1 Optical Techniques

The formulation of Marini and Murray (1973) is commonly used in laser ranging. The formula has been tested by comparison with ray tracing radiosonde profiles.

The correction to a one-way range is

$$\Delta R = \frac{f(\lambda)}{f(\phi, H)} \cdot \frac{A + B}{\sin E + \dfrac{B/(A + B)}{\sin E + 0.01}}, \tag{1}$$

where

$$A = 0.002357 P_0 + 0.000141 e_0, \tag{2}$$

$$B = (1.084 \times 10^{-8}) P_0 T_0 K + (4.734 \times 10^{-8}) \frac{P_0^2}{T_0} \frac{2}{(3 - 1/K)}, \tag{3}$$

$$K = 1.163 - 0.00968 \cos 2\phi - 0.00104 T_0 + 0.00001435 P_0, \tag{4}$$

where

$$
\begin{aligned}
\Delta R &= \text{range correction (meters),} \\
E &= \text{true elevation of satellite,} \\
P_0 &= \text{atmospheric pressure at the laser site} \\
&\quad \text{(in } 10^{-1} \text{ kPa, equivalent to millibars),} \\
T_0 &= \text{atmospheric temperature at the laser site} \\
&\quad \text{(degrees Kelvin),} \\
e_0 &= \text{water vapor pressure at the laser site} \\
&\quad (10^{-1} \text{ kPa, equivalent to millibars),} \\
f(\lambda) &= \text{laser frequency parameter} \\
&\quad (\lambda = \text{wavelength in micrometers),} \\
f(\phi, H) &= \text{laser site function, and} \\
\phi &= \text{geodetic latitude.}
\end{aligned}
$$

Additional definitions of these parameters are available. The water vapor pressure, e_0, should be calculated from a relative humidity measurement, $R_h(\%)$ by

$$e_0 = \frac{R_h}{100} \times e_s f_w,$$

where the saturation vapor pressure, e_s, is computed using the following formula (Giacomo, 1982; Davis, 1992):

$$e_s = 0.01 exp(1.2378847 \times 10^{-5} T_0^2 - 1.9121316 \times 10^{-2} T_0 + 33.93711047 - 6.3431645 \times 10^3 T_0^{-1})$$

The enhancement factor, f_w, is computed by (Giacomo, 1982):

$$f_w = 1.00062 + 3.14 \times 10^{-6} P_0 + 5.6 \times 10^{-7} (T_0 - 273.15)^2.$$

The laser frequency parameter, $f(\lambda)$, is

$$f(\lambda) = 0.9650 + \frac{0.0164}{\lambda^2} + \frac{0.000228}{\lambda^4}.$$

$f(\lambda) = 1$ for a ruby laser, [i.e. $f(0.6943) = 1$], while $f(\lambda_G) = 1.02579$ and $f(\lambda_{IR}) = 0.97966$ for green and infrared YAG lasers.

The laser site function is

$$f(\phi, H) = 1 - 0.0026 \cos 2\phi - 0.00031 H,$$

where ϕ is the geodetic latitude of the site and H is the height above the geoid (km).

Traditionally the correction of the atmospheric delay at optical wavelengths has been performed using the formulation of Marini and Murray (1973), a model developed for the 0.6943 μm wavelength. The model includes the zenith delay determination and the mapping function, to project the zenith delay to a given elevation angle, in a non-explicit form. In the last few years, the computation of the refractive index at optical wavelengths has received special attention and, as a consequence, the International Association of Geodesy (IUGG, 1999) recommended a new procedure to compute the group refractivity, following Ciddor (1996) and Ciddor and Hill (1999). Based on this formulation, Mendes *et al.* (2002) have derived new mapping functions for optical wavelengths, using a large database of ray tracing radiosonde profiles. These mapping functions are tailored for the 0.532 μm wavelength and are valid for elevation angles greater than 3 degrees, if we neglect the contribution of horizontal refractivity gradients. The new mapping functions represent a significant improvement over other mapping functions available and have the advantage of being easily combined with different zenith delay models. The analysis of two years of SLR data from LAGEOS and LAGEOS 2 indicate a clear improvement both in the estimated station heights and adjusted tropospheric zenith delay biases (Mendes *et al.*, 2002).

For the computation of the zenith delay, the available models seem to have identical precision, but variable biases. Preliminary results indicate that the Saastamoinen (1973) zenith delay model, updated with the dispersion factor given in Ciddor (1996) gives satisfactory results, but further studies are needed to validate it over the entire spectrum of wavelengths encountered in satellite laser ranging today (355 to 1064 nm).

9.2 Radio Techniques

The non-dispersive delay imparted by the atmosphere on a radio signal up to 30 GHz in frequency, is divided into "hydrostatic" and "wet" components. The hydrostatic delay is caused by the refractivity of the dry gases in the troposphere and by the nondipole component of water vapor refractivity. The dipole component of the water vapor refractivity is responsible for the wet delay. The hydrostatic delay component typically accounts for about 90% of the total delay at any given site but is highly predictable based on surface pressure. For the most accurate *a priori* hydrostatic delay, desirable when the accuracy of the estimate of the zenith wet delay is important, the formula of Saastamoinen (1972) as given by Davis *et al.* (1985) should be used.

$$D_{hz} = \frac{[(0.0022768 \pm 0.0000005)]P_0}{f_s(\phi, H)}$$

where

$$
\begin{aligned}
D_{hz} &= \text{zenith hydrostatic delay in meters,} \\
P_0 &= \text{total atmospheric pressure in millibars at the antenna} \\
&\quad \text{reference point (}e.g.\text{ intersection of the axes of rotation} \\
&\quad \text{for a radio antenna),} \\
f_s(\phi, H) &= (1 - 0.00266\cos 2\phi - 0.00028H), \text{ where } \phi \text{ is the geodetic} \\
&\quad \text{latitude of the site and } H \text{ is the height above the} \\
&\quad \text{geoid (km).}
\end{aligned}
$$

In precise applications where millimeter accuracy is desired, the delay must be estimated with the other geodetic quantities of interest. The estimation is facilitated by a simple parameterization of the tropospheric delay, where the line of sight delay, D_L, is expressed as a function of four parameters as follows:

$$D_L = m_h(e)D_{hz} + m_w(e)D_{wz} + m_g(e)[G_N \cos(a) + G_E \sin(a)].$$

The four parameters in this expression are the zenith hydrostatic delay, D_{hz}, the zenith wet delay, D_{wz}, and a horizontal delay gradient with components G_N and G_E. m_h, m_w and m_g are the hydrostatic, wet, and gradient mapping functions, respectively, and e is the elevation angle at which the signal is received. a is the azimuth angle in which the signal is received, measured east of north. The estimation of tropospheric gradients was shown by Chen and Herring (1997) and MacMillan (1995) to be beneficial in VLBI, and by Bar-sever *et al.* (1998) to be beneficial in GPS. Davis *et al.* (1993) and MacMillan (1995) recommend using either $m_g(e) = m_h(e)\cot(e)$ or $m_g(e) = m_w(e)\cot(e)$. Chen and Herring (1997) propose using $m_g(e) = 1/(\sin e \tan e + 0.0032)$. The various forms agree to within 10% for elevation angles higher then 10°, but the differences reach 50% for 5° elevation due to the singularity of the $\cot(e)$ function. The estimate of gradients is only worthwhile when using data lower than 15° in elevation. In the case of GPS analyses, such low-elevation data should be deweighted because of multipath effects.

Comparisons of many mapping functions with the ray tracing of a global distribution of radiosonde data have been made by Mendes and Langley (1998b). For observations below 10° elevation, which may be included in geodetic programs in order to increase the precision of the vertical component of the site position, the mapping functions of Lanyi (1984) as modified by Sovers and Jacobs (1996), Ifadis (1986), Herring (1992, designated MTT) and Niell (1996, designated NMF) are the most accurate. Only the last three were developed for observations below an elevation of 6°, with MTT and NMF being valid to 3° and Ifadis to 2°. Each of these mapping functions consists of a component for the water vapor and a component for either the total atmosphere (Lanyi) or the hydrostatic contribution to the total delay (Ifadis, MTT, and NMF). In all cases the wet mapping should be used as the function partial derivative for estimating the residual atmosphere zenith delay.

The most commonly used hydrostatic and wet mapping functions in precise geodetic applications are those derived by Lanyi (1984) as modified by Sovers and Jacobs (1996), Herring (1992), and Niell (1996). The first two allow for input of meteorological data although Lanyi's function requires information on the vertical temperature profile for best results, whereas Herring's requires only surface data. Niell's mapping function is based on global climatology of the delay and requires only input of time and location. Only the wet zenith delay is typically estimated, and an *a priori* value is used for the hydrostatic zenith delay.

The parameters of the atmosphere that are readily accessible at the time of the observation are the surface temperature, pressure, and relative humidity. The mapping functions of Lanyi, Ifadis, and Herring were developed to make use of this information. Lanyi additionally requires parameterization in terms of the height of a surface isothermal layer, the lapse rate from the top of this layer to the tropopause, and the height of the tropopause. If only the surface meteorology is used without also modeling these parameters (as described, for example, in Sovers and Jacobs (1996)), the agreement with radiosonde-derived delays is significantly worse than any of the other mapping functions. Mendes and Langley (1998a) found that the use of nominal values to parametrize the Lanyi mapping function degrades its performance significantly. They concluded that the best results are obtained using either an interpolation scheme developed by Sovers and Jacobs (1996) or having the temperature-profile parameters predicted from surface mean temperature using models (Mendes and Langley, 1998a).

The mapping functions of Niell differ from the other three in being independent of surface meteorology. The hydrostatic mapping function relies instead on the greater contribution by the conditions in the atmosphere above approximately 1 km, which are strongly season dependent, while the wet mapping function depends only on latitude.

Based on comparison with total delays calculated by ray tracing temperature and relative humidity profiles from a globally distributed set of radiosonde data, Mendes and Langley (1998b) conclude that Ifadis, Lanyi (which must be used with temperature profile modeling), and NMF provide the best accuracy down to 10°, while Ifadis and NMF are the most accurate at 6°. Niell (1996) compared the hydrostatic and wet mapping functions directly with ray tracing of radiosonde profiles and found that Ifadis, MTT, and NMF are comparable in accuracy at 5° elevation. (Lanyi was tested without temperature profile modeling.)

A recent assessment study using more than 32,000 traces corresponding to a one-year data set of radiosonde profiles from 50 stations distributed worldwide (Mendes and Langley, 1998b) concluded that none of these mapping functions has a clear supremacy over the others, for all elevation angles and at all latitudes. Nevertheless, the Ifadis mapping function yields the best overall performance, both in bias and rms scatter, especially for lower elevation angles. In the absence of reliable meteorological data, NMF is preferred.

References

Bar-Sever, Y. E., Koger, P. M., and Borjesson, J. A., 1998, "Estimating horizontal gradients of tropospheric delay with a single GPS receiver," *J. Geophys. Res.*, **103**, pp. 5019–5035.

Chen, G. and Herring, T. A., 1997, "Effects of atmospheric azimuthal asymmetry on the analysis of space geodetic data," *J. Geophys. Res.*, **102**, pp. 20,489–20,502.

Ciddor, P. E., 1996, "Refractive index of air: New equations for the visible and near infrared," *Applied Optics*, **35**, pp. 1566–1573.

Ciddor, P. E. and Hill, R. J., 1999, "Refractive index of air. 2. Group index," *Applied Optics*, **38**, pp. 1663–1667.

Davis, J. L., Herring, T. A., Shapiro, I. I., Rogers, A. E. E., and Elgered, G., 1985, "Geodesy by Radio Interferometry: Effects of Atmospheric Modelling Errors on Estimates of Baseline Length," *Radio Science*, **20, No. 6**, pp. 1593–1607.

Davis, J. L., Elgered, G., Niell, A. E., and Kuehn, C. E., 1993, "Ground-based measurements of the gradients in the "Wet" radio refractivity of air," *Radio Sci.*, **28**, pp. 1003–1018.

Davis, R. S., 1992, "Equation for the determination of the density of moist air (1981/91)," *Metrologia*, **29**, pp. 67–70.

Giacomo, P., 1982, "Equation for the determination of the density of moist air (1981)," *Metrologia*, **18**, pp. 33–40.

Herring, T. A., 1992, "Modeling Atmospheric Delays in the Analysis of Space Geodetic Data," *Proceedings of Refraction of Transatmospheric Signals in Geodesy*, Netherlands Geodetic Commission Series, **36**, The Hague, Netherlands, pp. 157–164.

Ifadis, I. I., 1986, "The Atmospheric Delay of Radio Waves: Modeling the Elevation Dependence on a Global Scale," *Technical Report No. 38L*, Chalmers U. of Technology, Göteburg, Sweden.

International Union of Geodesy and Geophysics (IUGG), 1999, "Resolution 3 of the International Association of Geodesy," *Comptes Rendus of the XXII General Assembly*, 19–30 July 1999, Birmingham, 110–111.

Lanyi, G., 1984, "Tropospheric Delay Affecting Radio Interferometry," *TDA Progress Report*, pp. 152–159; see also *Observation Model and Parameter Partials for the JPL VLBI Parameter Estimation Software 'MASTERFIT'-1987*, 1987, JPL Publication 83-39, Rev. 3.

MacMillan, D. S., 1995, "Atmospheric gradients from very long baseline interferometry observations," *Geophys. Res. Lett.*, **22**, pp. 1041–1044.

Marini, J. W. and Murray, C. W., 1973, "Correction of laser range tracking data for atmospheric refraction at elevations above 10 degrees," NASA-TM-X-70555, Goddard Space Flight Center, Greenbelt, MD.

Mendes, V. B. and Langley, R. B., 1998a, "Optimization of tropospheric delay mapping function performance for high-precision geodetic applications," Proceedings of DORIS Days, 27–29 April 1998, Toulouse, France.

Mendes, V. B. and Langley, R. B., 1998b, "An analysis of high-accuracy tropospheric delay mapping functions," *Phys. and Chem. of the Earth, Part A*, **25, Issue 12**, pp. 809–812).

Mendes, V. B., Prates, G., Pavlis, E. C., Pavlis, D. E., and Langley, R. B., 2002, "Improved mapping functions for atmospheric refraction correction in SLR," *Geophys. Res. Lett.*, **29**, 10, p. 1414, doi:10.1029/2001GL014394.

Niell, A. E., 1996, "Global Mapping Functions for the Atmosphere Delay of Radio Wavelengths," *J. Geophys. Res.*, **101**, pp. 3227–3246.

Saastamoinen, J., 1972, "Atmospheric Correction for the Troposphere and Stratosphere in Radio Ranging of Satellites," *Geophysical Monograph 15*, Henriksen (ed), pp. 247–251.

Saastamoinen, J., 1973, "Contributions to the theory of atmospheric refraction," In three parts, *Bull. Gèod.*, **105**, pp. 279–298, **106**, pp. 383–397, **107**, pp. 13–34.

Sovers, O. J. and Jacobs, C. S., 1996, "Observation Model and Parameter Partials for the JPL VLBI Parameter Estimation Software MODEST – 1996," JPL Publication 83-39, Rev. 6, Jet Propulsion Laboratory, California Institute of Technology, Pasadena, CA.

10 General Relativistic Models for Space-time Coordinates and Equations of Motion

10.1 Time Coordinates

IAU resolution A4 (1991) set the framework presently used to define the barycentric reference system (BRS) and the geocentric reference system (GRS). Its third recommendation defined Barycentric Coordinate Time (TCB) and Geocentric Coordinate Time (TCG) as time coordinates of the BRS and GRS, respectively. In the fourth recommendation another time coordinate is defined for the GRS, Terrestrial Time (TT). This framework was further refined by the IAU Resolutions B1.3 and B1.4 (2000) to provide consistent definitions for the coordinates and metric tensor of the reference systems at the full post-Newtonian level (Soffel, 2000). At the same time IAU Resolution B1.5 (2000) applied this framework to time coordinates and time transformations between reference systems, and IAU Resolution B1.9 (2000) re-defined Terrestrial Time (Petit, 2000). TT differs from TCG by a constant rate, $dTT/dTCG = 1 - L_G$, where L_G is a defining constant. The value of L_G (see Table 1.1) has been chosen to provide continuity with the former definition of TT, *i.e.* that the unit of measurement of TT agrees with the SI second on the geoid. The difference between TCG and TT may be expressed as

$$\text{TCG} - \text{TT} = \text{L}_\text{G} \times (\text{MJD} - 43144.0) \times 86400 \text{ s},$$

where MJD refers to the modified Julian date of International Atomic Time (TAI). TAI is a realization of TT, apart from a constant offset:

TT = TAI + 32.184 s.

Before 1991, previous IAU definitions of the time coordinates in the barycentric and geocentric frames required that only periodic differences exist between Barycentric Dynamical Time (TDB) and Terrestrial Dynamical Time (TDT) (Kaplan, 1981). As a consequence, the spatial coordinates in the barycentric frame had to be rescaled to keep the speed of light unchanged between the barycentric and the geocentric frames (Misner, 1982; Hellings, 1986). Thus, when barycentric (or TDB) units of length were compared to geocentric (or TDT) units of length, a scale difference, L, appeared (see also Chapter 1). This is no longer required with the use of the TCG/TCB time scales.

The relation between TCB and TDB is linear. It may be given in seconds by

$$\text{TCB} - \text{TDB} = \text{L}_\text{B} \times (\text{MJD} - 43144.0) \times 86400 + P_0, \quad P_0 \approx 6.55 \times 10^{-5} s.$$

However, since no precise definition of TDB exists, there is no definitive value of L_B and such an expression should be used with caution.

Figure 10.1 shows graphically the relationships between the time scales. See *IERS Technical Note 13*, pages 137–142 for copies of the IAU Resolution A4 (1991) and Appendix 1 of this volume for copies of the resolutions of the 24th IAU General Assembly (2000) relating to reference systems and time coordinates.

The difference between Barycentric Coordinate Time (TCB) and Geocentric Coordinate Time (TCG) involves a four-dimensional transformation,

$$\text{TCB} - \text{TCG} = c^{-2}\left\{\int_{t_0}^{t}[\frac{v_e^2}{2} + U_{ext}(\vec{x}_e)]dt + \vec{v}_e \cdot (\vec{x} - \vec{x}_e)\right\} + O(c^{-4}),$$

where $\vec{x}_e$ and $\vec{v}_e$ denote the barycentric position and velocity of the Earth's center of mass, $\vec{x}$ is the barycentric position of the observer and

U_{ext} is the Newtonian potential of all of the solar system bodies apart from the Earth evaluated at the geocenter. In this formula, t is TCB and t_0 is chosen to be consistent with 1977 January 1, $0^h0^m0^s$ TAI. This formula is only valid to within the neglected terms, of order 10^{-16} in rate, and IAU Resolution B1.5 (2000) provides formulas to compute the $O(c^{-4})$ terms within given uncertainty limits.
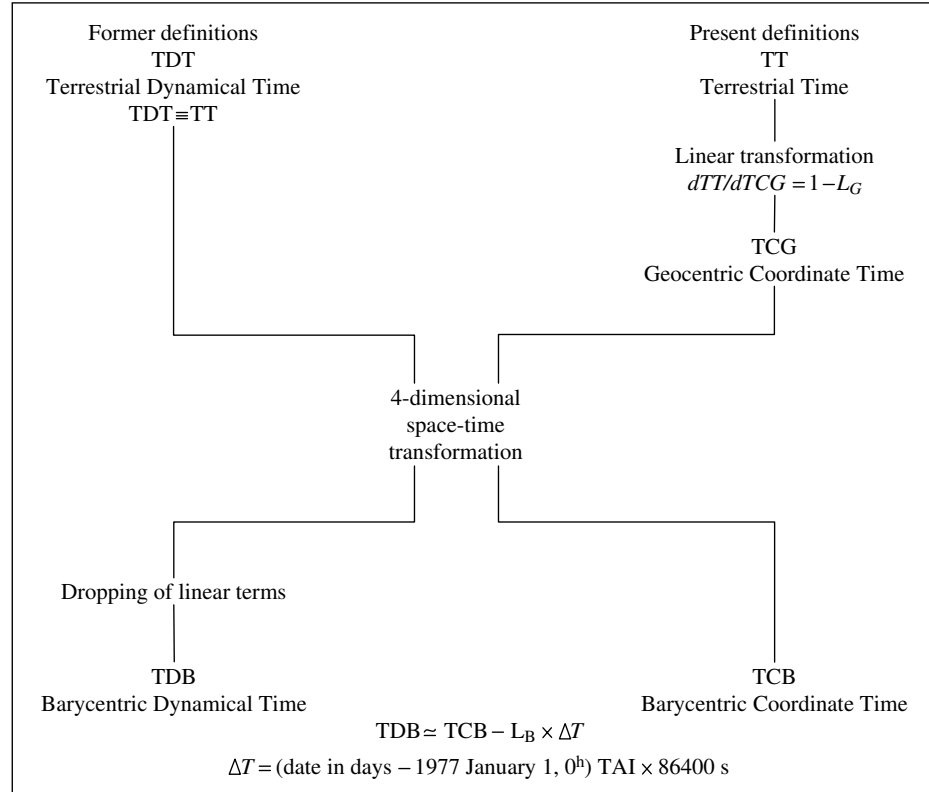
Former definitions
TDT
Terrestrial Dynamical Time
TDT≡TT

Present definitions
TT
Terrestrial Time

Linear transformation
$dTT/dTCG = 1 - L_G$

TCG
Geocentric Coordinate Time

4-dimensional
space-time
transformation

Dropping of linear terms

TDB
Barycentric Dynamical Time

TCB
Barycentric Coordinate Time

$TDB \simeq TCB - L_B \times \Delta T$

$\Delta T = (\text{date in days} - 1977 \text{ January 1, } 0^h) \text{ TAI} \times 86400 \text{ s}$

Fig. 10.1   Relations between time scales.

An approximation of the TCB−TCG formula is given by

$$(\text{TCB} - \text{TCG}) = \frac{L_C \times (TT - TT_0) + P(TT) - P(TT_0)}{(1 - L_B)} + c^{-2}\vec{v_e} \cdot (\vec{x} - \vec{x_e})$$

where TT_0 corresponds to JD 2443144.5 TAI (1977 January 1, 0 ^{h}) and where the values of L_C and L_B may be found in Table 1.1. Periodic terms denoted by $P(TT)$ have a maximum amplitude of around 1.6 ms and can be evaluated by the "FB" analytical model (Fairhead and Bretagnon, 1990; Bretagnon 2001). Alternately, $P(TT) - P(TT_0)$ may be provided by a numerical time ephemeris such as TE405 (Irwin and Fukushima, 1999), which provides values with an accuracy of 0.1 ns from 1600 to 2200. Irwin (2003) has shown that TE405 and the 2001 version of the FB model differ by less than 15 ns over the years 1600 to 2200 and by only a few ns over several decades around the present time. Finally a series, HF2002, providing the value of $L_C \times (TT - TT_0) + P(TT) - P(TT_0)$ as a function of TT over the years 1600–2200 has been fit (Harada and Fukushima, 2002) to TE405. This fit differs from TE405 by less than 3 ns over the years 1600–2200 with an RMS error of 0.5 ns. Note that in this section on the computation of TCB−TCG, TT is used as a time argument while the actual argument of the different realizations is T_{eph} (see Chapter 3). The resulting error in TCB−TCG is at most approximately 20 ps.

The time ephemeris TE405 is available in a Chebyshev form at $<^{19}>$. The 2001 version of the FB model is available at $<^{20}>$, where the files of interest are fb2001.f, fb2001.dat, fb2001.in, fb2001.out, and README.fb2001.f. The HF2002 model is available in the same directory, where the files of interest are Xhf2002.f, HF2002.DAT and hf2002.out.

10.2   Equations of Motion for an Artificial Earth Satellite [21]

The relativistic treatment of the near-Earth satellite orbit determination problem includes corrections to the equations of motion, the time transformations, and the measurement model. The two coordinate systems generally used when including relativity in near-Earth orbit determination solutions are the solar system barycentric frame of reference and the geocentric or Earth-centered frame of reference.

Ashby and Bertotti (1986) constructed a locally inertial E-frame in the neighborhood of the gravitating Earth and demonstrated that the gravitational effects of the Sun, Moon, and other planets are basically reduced to their tidal forces, with very small relativistic corrections. Thus the main relativistic effects on a near-Earth satellite are those described by the Schwarzschild field of the Earth itself. This result makes the geocentric frame more suitable for describing the motion of a near-Earth satellite (Ries *et al.*, 1989). Later on, two advanced relativistic formalisms have been elaborated to treat the problem of astronomical reference systems in the first post-Newtonian approximation of general relativity. One formalism is due to Brumberg and Kopeikin (Kopeikin, 1988; Brumberg and Kopeikin, 1989; Brumberg, 1991) and another one is due to Damour, Soffel and Xu (Damour, Soffel, Xu, 1991, 1992, 1993, 1994). These allow a full post-Newtonian treatment (Soffel, 2000) and form the basis of IAU Resolutions B1.3 and B1.4 (2000).

The relativistic correction to the acceleration of an artificial Earth satellite is

$$
\begin{aligned}
\Delta \ddot{\vec{r}} = \ & \frac{GM_E}{c^2 r^3} \left\{ \left[2(\beta + \gamma) \frac{GM_E}{r} - \gamma \dot{\vec{r}} \cdot \dot{\vec{r}} \right] \vec{r} + 2(1+\gamma)(\vec{r} \cdot \dot{\vec{r}}) \dot{\vec{r}} \right\} + \\
& (1+\gamma) \frac{GM_E}{c^2 r^3} \left[\frac{3}{r^2} (\vec{r} \times \dot{\vec{r}})(\vec{r} \cdot \vec{J}) + (\dot{\vec{r}} \times \vec{J}) \right] + \\
& \left\{ (1+2\gamma) \left[\dot{\vec{R}} \times \left(\frac{-GM_S \vec{R}}{c^2 R^3} \right) \times \dot{\vec{r}} \right] \right\},
\end{aligned} \tag{1}
$$

where

$$c = \text{speed of light},$$

$$\beta, \gamma = \text{PPN parameters equal to 1 in General Relativity},$$

$\vec{r}$ is the position of the satellite with respect to the Earth,

$\vec{R}$ is the position of the Earth with respect to the Sun,

$\vec{J}$ is the Earth's angular momentum per unit mass ($|\vec{J}| \cong 9.8 \times 10^8 \text{m}^2/\text{s}$), and

GM_E and GM_S are the gravitational coefficients of the Earth and Sun, respectively.

---

[19]ftp://astroftp.phys.uvic.ca in the directory /pub/irwin/tephemeris
[20]ftp://maia.usno.navy.mil in the directory /conv2000/chapter10/software
[21]The IAU Resolutions B1.3 and B1.4 (2000) and references therein now provide a consistent framework for the definition of the geocentric and barycentric reference systems at the full post-Newtonian level using harmonic coordinates. The equations of motion for spherically-symmetric and uniformly rotating bodies in these systems are the same as those previously derived in a Parametrized Post-Newtonian system.

The effects of Lense-Thirring precession (frame-dragging), geodesic (de Sitter) precession have been included. The relativistic effects of the Earth's oblateness have been neglected here but, if necessary, they could be included using the full post-Newtonian framework of IAU Resolutions B1.3 and B1.4 (2000). The independent variable of the satellite equations of motion may be, depending on the time transformation being used, either TT or TCG. Although the distinction is not essential to compute this relativistic correction, it is important to account for it properly in the Newtonian part of the acceleration.

10.3 Equations of Motion in the Barycentric Frame

(see footnote 21 preceeding page)

The n-body equations of motion for the solar system frame of reference (the isotropic Parameterized Post-Newtonian system with Barycentric Coordinate Time (TCB) as the time coordinate) are required to describe the dynamics of the solar system and artificial probes moving about the solar system (for example, see Moyer, 1971). These are the equations applied to the Moon's motion for Lunar Laser Ranging (Newhall *et al.*, 1987). In addition, relativistic corrections to the laser range measurement, the data timing, and the station coordinates are required (see Chapter 11).

References

Bar-Sever, Y. E., Koger, P. M., and Borjesson, J. A., 1998, "Estimating horizontal gradients of tropospheric delay with a single GPS receiver," *J. Geophys. Res.*, **103**, pp. 5019–5035.

Ashby, N. and Bertotti, B., 1986, "Relativistic Effects in Local Inertial Frames," *Phys. Rev. D*, **34 (8)**, p. 2246.

Bretagnon, P., 2001, Personal Communication.

Brumberg, V. A., 1991, *Essential Relativistic Celestial Mechanics*, Adam Hilger, Bristol, 280 pp.

Brumberg, V. A. and Kopeikin, S. M., 1989, *Nuovo Cimento*, **B103**, pp. 63–98.

Damour, T., Soffel, M., and Xu, C., 1991, "General-relativistic celestial mechanics I. Method and definition of reference systems," *Phys. Rev. D*, **43**, pp. 3273–3307.

Damour, T., Soffel, M., and Xu, C., 1992, "General-relativistic celestial mechanics II. Translational equations of motion," *Phys. Rev. D*, **45**, pp. 1017–1044.

Damour, T., Soffel, M., and Xu, C., 1993, "General-relativistic celestial mechanics III. Rotational equations of motion," *Phys. Rev. D*, **47**, pp. 3124–3135.

Damour, T., Soffel, M., and Xu, C., 1994, "General-relativistic celestial mechanics IV. Theory of satellite motion," *Phys. Rev. D*, **49**, pp. 618–635.

Fairhead, L. and Bretagnon, P., 1990, "An Analytic Formula for the Time Transformation TB−TT," *Astron. Astrophys.*, **229**, pp. 240–247.

Harada, W. and Fukushima, T., 2003, "Harmonic Decomposition of Time Ephemeris TE405," *Astron. J.*, **126**, pp. 2557–2561.

Hellings, R. W., 1986, "Relativistic Effects in Astronomical Timing Measurement," *Astron. J.*, **91 (3)**, pp. 650–659. Erratum, *ibid.*, p. 1446.

Irwin A. W. and Fukushima, T., 1999, "A Numerical Time Ephemeris of the Earth," *Astron. Astrophys.*, **348**, pp. 642–652.

Irwin A., 2003, Personal Communication.

Kaplan, G. H., 1981, *The IAU Resolutions on Astronomical Constants, Time Scale and the Fundamental Reference Frame*, U. S. Naval Observatory Circular No. 163.

Kopeikin, S. M., 1988, "Celestial coordinate reference systems in curved space-time," *Celest. Mech.*, **44**, pp. 87–115.

Misner, C. W., 1982, *Scale Factors for Relativistic Ephemeris Coordinates*, NASA Contract NAS5-25885, Report, EG&G, Washington Analytical Services Center, Inc.

Moyer, T. D., 1971, *Mathematical Formulation of the Double-precision Orbit Determination Program*, JPL Technical Report 32–1527.

Newhall, X.X., Williams, J. G., and Dickey, J. O., 1987, "Relativity Modeling in Lunar Laser Ranging Data Analysis," in *Proc. of the International Association of Geodesy (IAG) Symposia*, Vancouver, pp. 78–82.

Petit, G., 2000, "Report of the BIPM/IAU Joint Committee on relativity for space-time reference systems and metrology", in *Proc. of IAU Colloquium 180*, Johnston, K. J., McCarthy, D. D., Luzum, B. J. and Kaplan, G. H. (eds.), U. S. Naval Observatory, Washington, D. C., pp. 275–282.

Ries, J. C., Huang, C., Watkins, M. M., and Tapley, B. D., 1989, "The Effects of General Relativity on Near-Earth Satellites," *Astrodynamics 1989*, **71**, *Advances in the Astronautical Sciences*, Thornton, C. L., Proulx, J. E., Prussing, J. E., and Hoots, F. R. (ed.), pp. 85–93.

Soffel, M., 2000, "Report of the Working Group Relativity for Celestial Mechanics and Astrometry", in *Proc. of IAU Colloquium 180*, Johnston, K. J., McCarthy, D. D., Luzum B. J., and Kaplan, G. H. (eds.), U. S. Naval Observatory, Washington, D. C., pp. 283–292.

11 General Relativistic Models for Propagation

11.1 VLBI Time Delay

11.1.1 Historical Background

To resolve differences between numerous procedures used in the 1980s to model the VLBI delay, and to arrive at a standard model, a workshop was held at the U. S. Naval Observatory on 12 October 1990. The proceedings of this workshop have been published (Eubanks, 1991) and the model given there was called the 'consensus model.' It was derived from a combination of five different relativistic models for the geodetic delay. These are the Masterfit/Modest model, due to Fanselow and Thomas (see Treuhaft and Thomas, in Eubanks (1991), and Sovers and Fanselow (1987)), the I. I. Shapiro model (see Ryan, in Eubanks, (1991)), the Hellings-Shahid-Saless model (Shahid-Saless *et al.*, 1991) and in Eubanks (1991), the Soffel, Muller, Wu and Xu model (Soffel *et al.*, 1991) and in Eubanks (1991), and the Zhu-Groten model (Zhu and Groten, 1988) and in Eubanks (1991). At the same epoch, a relativistic model of VLBI observations was also presented in Kopeikin (1990) and in Klioner (1991).

The 'consensus model' formed the basis of that proposed in the IERS Standards (McCarthy, 1992). Over the years, there was considerable discussion and misunderstanding on the interpretation of the stations' coordinates obtained from the VLBI analyses. Particularly the IERS Conventions (McCarthy, 1996) proposed a modification of the delay, erroneously intending to comply with the XXIIst General Assembly of the International Astronomical Union in 1991 and the XXIst General Assembly of the International Union of Geodesy and Geophysics in 1991 Resolutions defining the Geocentric reference system. It seems, however, that this modification was not implemented by IERS analysis centers.

In the presentation below, the model is developed in the frame of the IAU Resolutions *i.e.* general relativity ($\gamma = 1$) using the Barycentric Celestial Reference System (BCRS) and Geocentric Celestial Reference System (GCRS) (as defined in the Appendix). However two approaches are presented for its usage, depending on the choice of coordinate time in the geocentric system. It is discussed how the Terrestrial Reference System (TRS) VLBI station coordinates submitted to the IERS, and the resulting ITRF2000 coordinates (Chapter 4), should be interpreted in relation to the IAU and IUGG Resolutions.

The 'step-by-step' procedure presented here to compute the VLBI time delay is taken from (Eubanks, 1991) and the reader is urged to consult that publication for further details.

11.1.2 Specifications and Domain of Application

The model is designed primarily for the analysis of VLBI observations of extra-galactic objects acquired from the surface of the Earth.[22] All terms of order 10^{-13} seconds or larger are included to ensure that the final result is accurate at the picosecond level. It is assumed that a linear combination of dual frequency measurements is used to remove the dispersive effect of the ionosphere, so that atmospheric effects are only due to the troposphere.

The model is not intended for use with observations of sources in the solar system, nor is it intended for use with observations made from space-based VLBI, from either low or high Earth orbit, or from the surface of the Moon (although it would be suitable with obvious changes for observations made entirely from the Moon).

---

[22]The case of radio sources inside our galaxy has been considered in *e.g.* Sovers and Fanselow (1987); Klioner (1991)

The geocentric celestial reference system (GCRS) is kinematically non-rotating (not dynamically non-rotating) and, included in the precession constant and nutation series, are the effects of the geodesic precession ($\sim$ 19 milli arc seconds / y). If needed, Soffel *et al.* (1991) and Shahid-Saless *et al.* (1991) give details of a dynamically inertial VLBI delay equation. At the picosecond level, there is no practical difference for VLBI geodesy and astrometry except for the adjustment in the precession constant.

11.1.3   The Analysis of VLBI Measurements: Definitions and Interpretation of Results

In principle, the observable quantities in the VLBI technique are recorded signals measured in the proper time of the station clocks. On the other hand, the VLBI model is expressed in terms of coordinate quantities in a given reference system (see Chapter 10 for a presentation of the different coordinate times used). For practical considerations, particularly because the station clocks do not produce ideal proper time (they even are, in general, synchronized and syntonized to UTC to some level, *i.e.* they have the same rate as the coordinate time Terrestrial Time (TT)), the VLBI delay produced by a correlator center may be considered to be, within the uncertainty aimed at in this chapter, equal to the TT coordinate time interval d_{TT} between two events: the arrival of a radio signal from the source at the reference point of the first station and the arrival of the same signal at the reference point of the second station. Note that we model here only the propagation delay and do not account for the desynchronization or desyntonization of the station clocks. From a TT coordinate interval, d_{TT}, one may derive a Geocentric Coordinate Time (TCG) coordinate interval, d_{TCG}, by simple scaling: $d_{TCG} = d_{TT}/(1 - L_G)$, where L_G is given in Table 1.1. In the following, two different approaches are presented using two different geocentric coordinate system with either TCG or TT as coordinate time.

The VLBI model presented below (formula (9)) relates the TCG coordinate interval $d_{TCG} = t_{v_2} - t_{v_1}$ to a baseline $\vec{b}$ expressed in GCRS coordinates (see the definition of notations in the next section). In the first approach, therefore, if the VLBI delay was scaled to a TCG coordinate interval, as described above, the results of the VLBI analysis would be directly obtained in terms of the spatial coordinates of the GCRS, as is recommended by the IUGG Resolution 2 (1991) and IAU Resolution B6 (1997), *i.e.* one would obtain TRS coordinates that are termed "consistent with TCG," here denoted x_{TCG}.

In the second approach, if the VLBI model (formula (9)) is used with VLBI delays as directly provided by correlators (*i.e.* equivalent to a TT coordinate interval d_{TT} without transformation to TCG), the baseline $\vec{b}$ is not expressed in GCRS but in some other coordinate system. The transformation of these coordinates to GCRS reduces, at the level of uncertainty considered here, to a simple scaling. The TRS space coordinates resulting from the VLBI analysis (here denoted x_{VLBI}) are then termed "consistent with TT" and the TRS coordinates recommended by the IAU and IUGG resolutions, x_{TCG}, may be obtained *a posteriori* by $x_{TCG} = x_{VLBI}/(1 - L_G)$ (see Petit, 2000).

All VLBI analysis centers submitting to the IERS have used this second approach and, therefore, the VLBI space coordinates are of the type x_{VLBI}. For continuity, an ITRF workshop (November 2000) decided to continue to use this approach, making it the present conventional choice for submission to the IERS. Note that the use of space coordinates "consistent with TT" is also the present conventional choice of SLR analysis results submitted to the IERS. At the ITRF workshop, it was also decided that the coordinates should not be re-scaled to x_{TCG} for the computation of ITRF2000 (see Chapter 4) so that the scale of ITRF2000 **does not comply with IAU and IUGG resolutions**.

11.1.4   The VLBI Delay Model

Table 11.1   Notation used in the model.

t_i	the TCG time of arrival of a radio signal at the ith VLBI receiver
T_i	the TCB time of arrival of a radio signal at the ith VLBI receiver
t_{g_i}	the "geometric" TCG time of arrival of a radio signal at the ith VLBI receiver including the gravitational "bending" delay and the change in the geometric delay caused by the existence of the atmospheric propagation delay but neglecting the atmospheric propagation delay itself
t_{v_i}	the "vacuum" TCG time of arrival of a radio signal at the ith VLBI receiver including the gravitational delay but neglecting the atmospheric propagation delay and the change in the geometric delay caused by the existence of the atmospheric propagation delay
δt_{atm_i}	the atmospheric propagation TCG delay for the ith receiver $= t_i - t_{g_i}$
T_{i_J}	the approximation to the TCB time that the ray path to station i passed closest to gravitating body J
ΔT_{grav}	the differential TCB gravitational time delay
$\vec{x}_i(t_i)$	the GCRS radius vector of the ith receiver at t_i
$\vec{b}$	$\vec{x}_2(t_1) - \vec{x}_1(t_1)$ and is thus the GCRS baseline vector at the time of arrival t_1
$\delta\vec{b}$	a variation (e.g. true value minus a priori value) in the GCRS baseline vector
$\vec{w}_i$	the geocentric velocity of the ith receiver
$\hat{K}$	the unit vector from the barycenter to the source in the absence of gravitational or aberrational bending
$\hat{k}_i$	the unit vector from the ith station to the source after aberration
$\vec{X}_i$	the barycentric radius vector of the ith receiver
$\vec{X}_\oplus$	the barycentric radius vector of the geocenter
$\vec{X}_J$	the barycentric radius vector of the Jth gravitating body
$\vec{R}_{i_J}$	the vector from the Jth gravitating body to the ith receiver
$\vec{R}_{\oplus_J}$	the vector from the Jth gravitating body to the geocenter
$\vec{R}_{\oplus\odot}$	the vector from the Sun to the geocenter
$\hat{N}_{i_J}$	the unit vector from the Jth gravitating body to the ith receiver
$\vec{V}_\oplus$	the barycentric velocity of the geocenter
U	the gravitational potential at the geocenter, neglecting the effects of the Earth's mass. At the picosecond level, only the solar potential need be included in U so that $U = GM_\odot/\|\vec{R}_{\oplus\odot}\|$
M_i	the rest mass of the ith gravitating body
$M_\oplus$	the rest mass of the Earth
c	the speed of light
G	the Gravitational Constant

Vector magnitudes are expressed by the absolute value sign $[|x| = (\Sigma x_i^2)^{\frac{1}{2}}]$. Vectors and scalars expressed in geocentric coordinates are denoted by lower case (e.g. $\vec{x}$ and t), while quantities in barycentric coordinates are in upper case (e.g. $\vec{X}$ and T). A lower case subscript (e.g. $\vec{x}_i$) denotes a particular VLBI receiver, while an upper case subscript (e.g. $\vec{x}_J$) denotes a particular gravitating body. The SI system of units is used throughout.

Although the delay to be calculated is the time of arrival at station 2 minus the time of arrival at station 1, it is the time of arrival at station 1 that serves as the time reference for the measurement. Unless explicitly stated otherwise, all vector and scalar quantities are assumed to be calculated at t_1, the time of arrival at station 1 including the effects of the troposphere. The VLBI hardware provides the UTC time tag for this event. For quantities such as $\vec{X}_J$, $V_\oplus$, $\vec{w}_i$, or U it is assumed that a table (or numerical formula) is available as a function of a given time argument. The UTC time tag should be transformed to the appropriate timescale corresponding to the time argument to be used to compute each element of the geometric model.

The baseline vector $\vec{b}$ is given in the kinematically non-rotating GCRS. It must be transformed to the rotating terrestrial reference frame defined in Chapter 4 of the present VLBI Conventions in accordance to the transformations introduced in Chapter 5.

(a) Gravitational Delay[23]

The general relativistic delay, ΔT_{grav}, is given for the Jth gravitating body by

$$\Delta T_{grav_J} = 2\frac{GM_J}{c^3} \ln \frac{|\vec{R}_{1_J}| + \vec{K} \cdot \vec{R}_{1_J}}{|\vec{R}_{2_J}| + \vec{K} \cdot \vec{R}_{2_J}}. \tag{1}$$

At the picosecond level it is possible to simplify the delay due to the Earth, $\Delta T_{grav_\oplus}$, which becomes

$$\Delta T_{grav_\oplus} = 2\frac{GM_\oplus}{c^3} \ln \frac{|\vec{x}_1| + \vec{K} \cdot \vec{x}_1}{|\vec{x}_2| + \vec{K} \cdot \vec{x}_2}. \tag{2}$$

The Sun, the Earth and Jupiter must be included, as well as the other planets in the solar system along with the Earth's Moon, for which the maximum delay change is several picoseconds. The major satellites of Jupiter, Saturn and Neptune should also be included if the ray path passes close to them. This is very unlikely in normal geodetic observing but may occur during planetary occultations. Note that in case of observations very close to some massive bodies, extra terms (*e.g.* due to the multipole moments and spin of the bodies) should be taken into account to obtain an uncertainty of 1 ps (see Klioner, 1991).

The effect on the bending delay of the motion of the gravitating body during the time of propagation along the ray path is small for the Sun but can be several hundred picoseconds for Jupiter (see Sovers and Fanselow (1987) page 9). Since this simple correction, suggested by Sovers and Fanselow (1987) and Hellings (1986) among others, is sufficient at the picosecond level, it was adapted for the consensus model. It is also necessary to account for the motion of station 2 during the propagation time between station 1 and station 2. In this model $\vec{R}_{i_J}$, the vector from the Jth gravitating body to the ith receiver, is iterated once, giving

$$t_{1_J} = \min \left[t_1, t_1 - \frac{\hat{K} \cdot (\vec{X}_J(t_1) - \vec{X}_1(t_1))}{c} \right], \tag{3}$$

so that

$$\vec{R}_{1_J}(t_1) = \vec{X}_1(t_1) - \vec{X}_J(t_{1_J}), \tag{4}$$

and

$$\vec{R}_{2_J} = \vec{X}_2(t_1) - \frac{\vec{V}_\oplus}{c}(\hat{K} \cdot \vec{b}) - \vec{X}_J(t_{1_J}). \tag{5}$$

Only this one iteration is needed to obtain picosecond level accuracy for solar system objects.

$\vec{X}_1(t_1)$ is not tabulated, but can be inferred from $\vec{X}_\oplus(t_1)$ using

$$\vec{X}_i(t_1) = \vec{X}_\oplus(t_1) + \vec{x}_i(t_1), \tag{6}$$

which is of sufficient accuracy for use in equations 3, 4, and 5, when substituted into equation 1 but not for use in computing the geometric

---

[23]The formulas in this section are unchanged from the previous edition of the Conventions. The more advanced theory in Kopeikin and Schäfer (1999) provides a rigorous physical solution for the light propagation in the field of moving bodies. For Earth-based VLBI, the formulas in this section and those proposed in Kopeikin and Schäfer (1999) are numerically equivalent with an uncertainty of 0.1 ps (Klioner and Soffel, 2001).

delay. The total gravitational delay is the sum over all gravitating bodies including the Earth,

$$\Delta T_{grav} = \sum_J \Delta T_{grav_J}. \tag{7}$$

(b) Geometric Delay

In the barycentric frame the vacuum delay equation is, to a sufficient level of approximation:

$$T_2 - T_1 = -\frac{1}{c}\hat{K} \cdot (\vec{X}_2(T_2) - \vec{X}_1(T_1)) + \Delta T_{grav}. \tag{8}$$

This equation is converted into a geocentric delay equation using known quantities by performing the relativistic transformations relating the barycentric vectors $\vec{X}_i$ to the corresponding geocentric vectors $\vec{x}_i$, thus converting equation 8 into an equation in terms of $\vec{x}_i$. The related transformation between barycentric and geocentric time can be used to derive another equation relating $T_2 - T_1$ and $t_2 - t_1$, and these two equations can then be solved for the geocentric delay in terms of the geocentric baseline vector $\vec{b}$. In the rational polynomial form the total geocentric vacuum delay is given by

$$t_{v_2} - t_{v_1} = \frac{\Delta T_{grav} - \frac{\hat{K}\cdot\vec{b}}{c}\left[1 - \frac{(1+\gamma)U}{c^2} - \frac{|\vec{V}_\oplus|^2}{2c^2} - \frac{\vec{V}_\oplus\cdot\vec{w}_2}{c^2}\right] - \frac{\vec{V}_\oplus\cdot\vec{b}}{c^2}(1 + \hat{K}\cdot\vec{V}_\oplus/2c)}{1 + \frac{\hat{K}\cdot(\vec{V}_\oplus+\vec{w}_2)}{c}}. \tag{9}$$

Given this expression for the vacuum delay, the total delay is found to be

$$t_2 - t_1 = t_{v_2} - t_{v_1} + (\delta t_{atm_2} - \delta t_{atm_1}) + \delta t_{atm_1}\frac{\hat{K}\cdot(\vec{w}_2 - \vec{w}_1)}{c}. \tag{10}$$

For convenience the total delay can be divided into separate geometric and propagation delays. The geometric delay is given by

$$t_{g_2} - t_{g_1} = t_{v_2} - t_{v_1} + \delta t_{atm_1}\frac{\hat{K}\cdot(\vec{w}_2 - \vec{w}_1)}{c}, \tag{11}$$

and the total delay can be found at some later time by adding the propagation delay:

$$t_2 - t_1 = t_{g_2} - t_{g_1} + (\delta t_{atm_2} - \delta t_{atm_1}). \tag{12}$$

The tropospheric propagation delay in equations 11 and 12 need not be from the same model. The estimate in equation 12 should be as accurate as possible, while the δt_{atm} model in equation 11 need only be accurate to about an air mass (~ 10 nanoseconds). If equation 10 is used instead, the model should be as accurate as is possible. Note that the tropospheric delay is computed in the rest frame of each station and can be directly added to the geocentric delay (equation 11), at the uncertainty level considered here (see Eubanks, 1991; Treuhaft and Thomas, 1991).

If $\delta\vec{b}$ is the difference between the *a priori* baseline vector and the true baseline, the true delay may be computed from the *a priori* delay as follows. If $\delta\vec{b}$ is less than roughly three meters, then it suffices to add $-(\hat{K}\cdot\delta\vec{b})/c$ to the *a priori* delay. If this is not the case, however, the *a priori* delay must be modified by adding

$$\Delta(t_{g_2} - t_{g_1}) = -\frac{\frac{\hat{K}\cdot\delta\vec{b}}{c}}{1 + \frac{\hat{K}\cdot(\vec{V}_\oplus+\vec{w}_2)}{c}} - \frac{\vec{V}_\oplus \cdot \delta\vec{b}}{c^2}. \tag{13}$$

(c) Observations Close to the Sun

For observations made very close to the Sun, higher order relativistic time delay effects become increasingly important. The largest correction is due to the change in delay caused by the bending of the ray path by the gravitating body described in Richter and Matzner (1983) and Hellings (1986). The change to ΔT_{grav} is

$$\delta T_{grav_i} = \frac{4G^2 M_i^2}{c^5} \frac{\vec{b} \cdot (\hat{N}_{1_i} + \hat{K})}{(|\vec{R}|_{1_i} + \vec{R}_{1_i} \cdot \hat{K})^2}, \tag{14}$$

which should be added to the ΔT_{grav} in equation 1.

(d) Summary

Assuming that the reference time is the UTC time arrival of the VLBI signal at receiver 1, and that it is transformed to the appropriate time-scale to be used to compute each element of the geometric model, the following steps are recommended to compute the VLBI time delay.

1. Use equation 6 to estimate the barycentric station vector for receiver 1.

2. Use equations 3, 4, and 5 to estimate the vectors from the Sun, the Moon, and each planet except the Earth to receiver 1.

3. Use equation 1 to estimate the differential gravitational delay for each of those bodies.

4. Use equation 2 to find the differential gravitational delay due to the Earth.

5. Sum to find the total differential gravitational delay.

6. Compute the vacuum delay from equation 9.

7. Calculate the aberrated source vector for use in the calculation of the tropospheric propagation delay:

$$\vec{k}_i = \hat{K} + \frac{\vec{V}_\oplus + \vec{w}_i}{c} - \hat{K}\frac{\hat{K} \cdot (\vec{V}_\oplus + \vec{w}_i)}{c}. \tag{15}$$

8. Add the geometric part of the tropospheric propagation delay to the vacuum delay, equation 11.

9. The total delay can be found by adding the best estimate of the tropospheric propagation delay

$$t_2 - t_1 = t_{g_2} - t_{g_1} + [\delta t_{atm_2}(t_1 - \frac{\hat{K} \cdot \vec{b}}{c}, \vec{k}_2) - \delta t_{atm_1}(\vec{k}_1)]. \tag{16}$$

10. If necessary, apply equation 13 to correct for "post-model" changes in the baseline by adding equation 13 to the total time delay from equation step 9.

11.2   Laser Ranging

In a reference system centered on an ensemble of masses, if a light signal is emitted from x_1 at coordinate time t_1 and is received at x_2 at coordinate time t_2, the coordinate time of propagation is given by

$$t_2 - t_1 = \frac{|\vec{x}_2(t_2) - \vec{x}_1(t_1)|}{c} + \sum_J \frac{2GM_J}{c^3} \ln\left(\frac{r_{J1} + r_{J2} + \rho}{r_{J1} + r_{J2} - \rho}\right), \tag{17}$$

where the sum is carried out over all bodies J with mass M_J centered at x_J and where $r_{J1} = |\vec{x}_1 - \vec{x}_J|$, $r_{J2} = |\vec{x}_2 - \vec{x}_J|$ and $\rho = |\vec{x}_2 - \vec{x}_1|$.

For near-Earth satellites (SLR), practical analysis is done in the geocentric frame of reference, and the only body to be considered is the Earth (Ries *et al.*, 1988). For lunar laser ranging (LLR), which is formulated in the solar system barycentric reference frame, the Sun and the Earth must be taken into account, with the contribution of the Moon being of order 1 ps (*i.e.* about 1 mm for a return trip). Moreover, in the analysis of LLR data, the body-centered coordinates of an Earth station and a lunar reflector should be transformed into barycentric coordinates. The transformation of $\vec{r}$, a geocentric position vector expressed in the GCRS, to $\vec{r}_b$, the vector expressed in the BCRS, is provided with an uncertainty lower than 1 mm by the equation

$$\vec{r}_b = \vec{r}\left(1 - \frac{U}{c^2}\right) - \frac{1}{2}\left(\frac{\vec{V}\cdot\vec{r}}{c^2}\right)\vec{V}, \tag{18}$$

where U is the gravitational potential at the geocenter (excluding the Earth's mass) and $\vec{V}$ is the barycentric velocity of the Earth. A similar equation applies to the selenocentric reflector coordinates.

In general, however, the geocentric and barycentric systems are chosen so that the geocentric space coordinates are "consistent with TT" (position vector $\vec{r}_{TT}$) and that the barycentric space coordinates are "consistent with TDB" (position vector $\vec{r}_{TDB}$). The transformation of $\vec{r}_{TT}$ to $\vec{r}_{TDB}$, is then given by

$$\vec{r}_{TDB} = \vec{r}_{TT}\left(1 - \frac{U}{c^2} - L_C\right) - \frac{1}{2}\left(\frac{\vec{V}\cdot\vec{r}_{TT}}{c^2}\right)\vec{V}, \tag{19}$$

where L_C is given in Table 1.1.

References

Eubanks, T. M. (ed.), 1991, *Proceedings of the U. S. Naval Observatory Workshop on Relativistic Models for Use in Space Geodesy*, U. S. Naval Observatory, Washington, D. C.

Hellings, R. W., 1986, "Relativistic effects in Astronomical Timing Measurements," *Astron. J.*, **91**, pp. 650–659. Erratum, *ibid.*, p. 1446.

Klioner, S. A., 1991, "General relativistic model of VLBI observables," in *Proc. AGU Chapman Conf. on Geodetic VLBI: Monitoring Global Change*, Carter, W. E. (ed.), NOAA Technical Report NOS 137 NGS 49, American Geophysical Union, Washington D.C, pp. 188–202.

Klioner, S. A. and Soffel, M. H., 2001, personnal communication.

Kopeikin, S., 1990, "Theory of relativity in observational radio astronomy," *Sov. Astron.*, **34(1)**, pp. 5–10.

Kopeikin, S. and Schäfer, G., 1999, "Lorentz-covariant Theory of Light Propagation in Time Dependent Gravitational Fields of Arbitrary Moving Bodies," *Phys. Rev. D*, **60**, pp. 124002/1–44.

McCarthy, D. D. (ed.), 1992, IERS Standards, IERS Technical Note, **13**, Observatoire de Paris, Paris.

McCarthy, D. D. (ed.), 1996, IERS Conventions, IERS Technical Note **21**, Observatoire de Paris, Paris.

Petit, G., 2000, "Importance of a common framework for the realization of space-time reference systems," *Proc. IAG Symposium IGGOS*, Springer-Verlag, pp. 3–7.

Richter, G. W. and Matzner, R. A., 1983, "Second-order Contributions to Relativistic Time Delay in the Parameterized Post-Newtonian Formalism," *Phys. Rev. D*, **28**, pp. 3007–3012.

Ries, J. C., Huang, C., and Watkins, M. M., 1988, "The Effect of General Relativity on Near-Earth Satellites in the Solar System Barycentric and Geocentric Reference Frames," *Phys. Rev. Lett.*, **61**, pp. 903–906.

Shahid-Saless, B., Hellings, R. W., and Ashby, N., 1991, "A Picosecond Accuracy Relativistic VLBI Model via Fermi Normal Coordinates," *Geophys. Res. Lett.*, **18**, pp. 1139–1142.

Soffel, M. H., Muller, J., Wu, X., and Xu, C., 1991, "Consistent Relativistic VLBI Theory with Picosecond Accuracy," *Astron. J.*, **101**, pp. 2306–2310.

Sovers, O. J. and Fanselow, J. L., 1987, *Observation Model and Parameter Partials for the JPL VLBI Parameter Estimation Software 'Masterfit'-1987*, JPL Pub. 83–89, Rev. 3.

Treuhaft R. N. and Thomas J. B., 1991, "Incorporating atmospheric delay into the relativistic VLBI time delay," *JPL Technical Memorandum* IOM 335.6–91–016.

Zhu, S. Y. and Groten, E., 1988, "Relativistic Effects in the VLBI Time Delay Measurement," *Man. Geod.*, **13**, pp. 33–39.

A IAU Resolutions Adopted at the XXIVth General Assembly

A.1 Resolution B1.1: Maintenance and Establishment of Reference Frames and Systems

The XXIVth International Astronomical Union

Noting

1. that Resolution B2 of the XXIIIrd General Assembly (1997) specifies that "the fundamental reference frame shall be the International Celestial Reference Frame (ICRF) constructed by the IAU Working Group on Reference Frames,"

2. that Resolution B2 of the XXIIIrd General Assembly(1997) specifies "That the Hipparcos Catalogue shall be the primary realization of the ICRS at optical wavelengths", and

3. the need for accurate definition of reference systems brought about by unprecedented precision, and

Recognizing

1. the importance of continuing operational observations made with Very Long Baseline Interferometry (VLBI) to maintain the ICRF,

2. the importance of VLBI observations to the operational determination of the parameters needed to specify the time-variable transformation between the International Celestial and Terrestrial Reference Frames,

3. the progressive shift between the Hipparcos frame and the ICRF, and

4. the need to maintain the optical realization as close as possible to the ICRF

Recommends

1. that IAU Division I maintain the Working Group on Celestial Reference Systems formed from Division I members to consult with the International Earth Rotation Service (IERS) regarding the maintenance of the ICRS,

2. that the IAU recognize the International VLBI service (IVS) for Geodesy and Astrometry as an IAU Service Organization,

3. that an official representative of the IVS be invited to participate in the IAU Working Group on Celestial Reference Systems,

4. that the IAU continue to provide an official representative to the IVS Directing Board,

5. that the astrometric and geodetic VLBI observing programs consider the requirements for maintenance of the ICRF and linking to the Hipparcos optical frame in the selection of sources to be observed (with emphasis on the Southern Hemisphere), design of observing networks, and the distribution of data, and

6. that the scientific community continue with high priority ground- and space-based observations (a) for the maintenance of the optical Hipparcos frame and frames at other wavelengths and (b) for the links of the frames to the ICRF.

A.2   Resolution B1.2: Hipparcos Celestial Reference Frame

The XXIVth International Astronomical Union

Noting

1. that Resolution B2 of the XXIIIrd General Assembly (1997) specifies, "That the Hipparcos Catalogue shall be the primary realization of the International Celestial Reference System (ICRS) at optical wavelengths,"

2. the need for this realization to be of the highest precision,

3. that the proper motions of many of the Hipparcos stars known, or suspected, to be multiple are adversely affected by uncorrected orbital motion,

4. the extensive use of the Hipparcos Catalogue as reference for the ICRS in extension to fainter stars,

5. the need to avoid confusion between the International Celestial Reference Frame (ICRF) and the Hipparcos frame, and

6. the progressive shift between the Hipparcos frame and the ICRF,

Recommends

1. that Resolution B2 of the XXIIIrd IAU General Assembly (1997) be amended by excluding from the optical realization of the ICRS all stars flagged C, G, O, V and X in the Hipparcos Catalogue, and

2. that this modified Hipparcos frame be labeled the Hipparcos Celestial Reference Frame (HCRF).

A.3   Resolution B1.3: Definition of Barycentric Celestial Reference System and Geocentric Celestial Reference System

The XXIVth International Astronomical Union

Considering

1. that the Resolution A4 of the XXIst General Assembly (1991) has defined a system of space-time coordinates for (a) the solar system (now called the Barycentric Celestial Reference System, (BCRS)) and (b) the Earth (now called the Geocentric Celestial Reference System (GCRS)), within the framework of General Relativity,

2. the desire to write the metric tensors both in the BCRS and in the GCRS in a compact and self-consistent form, and

3. the fact that considerable work in General Relativity has been done using the harmonic gauge that was found to be a useful and simplifying gauge for many kinds of applications,

Recommends

1. the choice of harmonic coordinates both for the barycentric and for the geocentric reference systems.

2. writing the time-time component and the space-space component of the barycentric metric $g_{\mu\nu}$ with barycentric coordinates (t, $\mathbf{x}$) (t = Barycentric Coordinate Time (TCB)) with a single scalar potential w(t,$\mathbf{x}$) that generalizes the Newtonian potential, and the space-time component with a vector potential w^i(t, $\mathbf{x}$); as a boundary condition it is assumed that these two potentials vanish far from the solar system,

   explicitly,

$$g_{00} = -1 + \frac{2w}{c^2} - \frac{2w^2}{c^4},$$
$$g_{0i} = -\frac{4}{c^3} w^i,$$
$$g_{ij} = \delta_{ij} \left(1 + \frac{2}{c^2} w\right),$$

with

$$w(t, \mathbf{x}) = G \int d^3 x' \frac{\sigma(t, \mathbf{x}')}{|\mathbf{x} - \mathbf{x}'|} + \frac{1}{2c^2} G \frac{\partial^2}{\partial t^2} \int d^3 x' \sigma(t, \mathbf{x}') |\mathbf{x} - \mathbf{x}'|$$
$$w^i(t, \mathbf{x}) = G \int d^3 x' \frac{\sigma^i(t, \mathbf{x}')}{|\mathbf{x} - \mathbf{x}'|}.$$

Here, σ and σ^i are the gravitational mass and current densities, respectively.

3. writing the geocentric metric tensor $G_{\alpha\beta}$ with geocentric coordinates $(T, \mathbf{X})$ ($T=$ Geocentric Coordinate Time (TCG)) in the same form as the barycentric one but with potentials $W(T, \mathbf{X})$ and $W^a(T, \mathbf{X})$; these geocentric potentials should be split into two parts — potentials W and W^a arising from the gravitational action of the Earth and external parts W_{ext} and W^a_{ext} due to tidal and inertial effects; the external parts of the metric potentials are assumed to vanish at the geocenter and admit an expansion into positive powers of $\mathbf{X}$, explicitly,

$$G_{00} = -1 + \frac{2W}{c^2} - \frac{2W^2}{c^4},$$
$$G_{0a} = -\frac{4}{c^3} W^a,$$
$$G_{ab} = \delta_{ab} \left(1 + \frac{2}{c^2} W\right).$$

The potentials W and W^a should be split according to

$$W(T, \mathbf{X}) = W_E(T, \mathbf{X}) + W_{ext}(T, \mathbf{X}),$$
$$W^a(T, \mathbf{X}) = W^a_E(T, \mathbf{X}) + W^a_{ext}(T, \mathbf{X}).$$

The Earth's potentials W_E and W^a_E are defined in the same way as w and w^i but with quantities calculated in the GCRS with integrals taken over the whole Earth.

4. using, if accuracy requires, the full post-Newtonian coordinate transformation between the BCRS and the GCRS as induced by the form of the corresponding metric tensors, explicitly, for the kinematically non-rotating GCRS ($T=$TCG, $t=$TCB, $r^i_E \equiv x^i - x^i_E(t)$ and a summation from 1 to 3 over equal indices is implied),

$$T = t - \frac{1}{c^2} \left[A(t) + v^i_E r^i_E\right] +$$
$$\frac{1}{c^4} \left[B(t) + B^i(t) r^i_E + B^{ij}(t) r^i_E r^j_E + C(t, \mathbf{x})\right] + O(c^{-5}),$$
$$X^a = \delta_{ai} \left[r^i_E + \frac{1}{c^2} \left(\frac{1}{2} v^i_E v^j_E r^j_E + w_{ext}(\mathbf{x_E}) r^i_E + r^i_E a^j_E r^j_E - \frac{1}{2} a^i_E r^2_E\right)\right] + O(c^{-4}),$$

where

$$\frac{d}{dt} A(t) = \frac{1}{2} v^2_E + w_{ext}(\mathbf{x_E}),$$
$$\frac{d}{dt} B(t) = -\frac{1}{8} v^4_E - \frac{3}{2} v^2_E w_{ext}(\mathbf{x_E}) + 4 v^i_E w^i_{ext}(\mathbf{x_E}) + \frac{1}{2} w^2_{ext}(\mathbf{x_E}),$$
$$B^i(t) = -\frac{1}{2} v^2_E v^i_E + 4 w^i_{ext}(\mathbf{x_E}) - 3 v^i_E w_{ext}(\mathbf{x_E}),$$
$$B^{ij}(t) = -v^i_E \delta_{aj} Q^a + 2 \frac{\partial}{\partial x^j} w^i_{ext}(\mathbf{x_E}) - v^i_E \frac{\partial}{\partial x^j} w_{ext}(\mathbf{x_E})$$
$$+ \frac{1}{2} \delta^{ij} \dot{w}_{ext}(\mathbf{x_E}),$$
$$C(t, \mathbf{x}) = -\frac{1}{10} r^2_E (\dot{a}^i_E r^i_E).$$

Here x^i_E, v^i_E, and a^i_E are the barycentric position, velocity and acceleration vectors of the Earth, the dot stands for the total derivative with respect to t, and

$$Q^a = \delta_{ai} \left[\frac{\partial}{\partial x_i} w_{ext}(\mathbf{x_E}) - a^i_E\right].$$

The external potentials, w_{ext} and w^i_{ext}, are given by

$$w_{ext} = \sum_{A \neq E} w_A, \quad w^i_{ext} = \sum_{A \neq E} w^i_A,$$

where E stands for the Earth and w_A and w^i_A are determined by the expressions for w and w^i with integrals taken over body A only.

Notes

It is to be understood that these expressions for w and w^i give g_{00} correct up to $O(c^{-5})$, g_{0i} up to $O(c^{-5})$, and g_{ij} up to $O(c^{-4})$. The densities σ and σ^i are determined by the components of the energy momentum tensor of the matter composing the solar system bodies as given in the references. Accuracies for $G_{\alpha\beta}$ in terms of c^{-n} correspond to those of $g_{\mu\nu}$.

The external potentials W_{ext} and W_{ext}^a can be written in the form

$$W_{ext} = W_{tidal} + W_{iner},$$
$$W_{ext}^a = W_{tidal}^a + W_{iner}^a.$$

W_{tidal} generalizes the Newtonian expression for the tidal potential. Post-Newtonian expressions for W_{tidal} and W_{tidal}^a can be found in the references. The potentials W_{iner}, W_{iner}^a are inertial contributions that are linear in X^a. The former is determined mainly by the coupling of the Earth's nonsphericity to the external potential. In the kinematically non-rotating Geocentric Celestial Reference System, W_{iner}^a describes the Coriolis force induced mainly by geodetic precession.

Finally, the local gravitational potentials W_E and W_E^a of the Earth are related to the barycentric gravitational potentials w_E and w_E^i by

$$W_E(T, \mathbf{X}) = w_e(t, \mathbf{x}) \left(1 + \tfrac{2}{c^2} v_E^2\right) - \tfrac{4}{c^2} v_E^i w_E^i(t, \mathbf{x}) + O(c^{-4}),$$
$$W_E^a(T, \mathbf{X}) = \delta_{ai}(w_E^i(t, \mathbf{x}) - v_E^i w_E(t, \mathbf{x})) + O(c^{-2}).$$

References

Brumberg, V. A., Kopeikin, S. M., 1988, *Nuovo Cimento*, **B103**, 63.

Brumberg, V. A., 1991, *Essential Relativistic Celestial Mechanics*, Hilger, Bristol.

Damour, T., Soffel, M., Xu, C., *Phys. Rev. D*, **43**, 3273 (1991); **45**, 1017 (1992); **47**, 3124 (1993); **49**, 618 (1994).

Klioner, S. A., Voinov, A. V., 1993, *Phys Rev. D*, **48**, 1451.

Kopeikin, S. M., 1989, *Celest. Mech.*, **44**, 87.

A.4   Resolution B1.4: Post-Newtonian Potential Coefficients

The XXIVth International Astronomical Union

Considering

1. that for many applications in the fields of celestial mechanics and astrometry a suitable parametri-zation of the metric potentials (or multipole moments) outside the massive solar-system bodies in the form of expansions in terms of potential coefficients are extremely useful, and

2. that physically meaningful post-Newtonian potential coefficients can be derived from the literature,

Recommends

1. expansion of the post-Newtonian potential of the Earth in the Geocentric Celestial Reference System (GCRS) outside the Earth in the form

$$W_E(T, \mathbf{X}) = \frac{GM_E}{R} \left[1 + \sum_{l=2}^{\infty} \sum_{m=0}^{+l} \left(\frac{R_E}{R}\right)^l P_{lm}(\cos\theta) \left(C_{lm}^E(T) \cos m\phi + S_{lm}^E(T) \sin m\phi\right)\right],$$

where C_{lm}^E and S_{lm}^E are, to sufficient accuracy, equivalent to the post-Newtonian multipole moments introduced in (Damour *et al.*, *Phys. Rev. D*, **43**, 3273, 1991), θ and ϕ are the polar angles corresponding to the spatial coordinates X^a of the GCRS and $R = |X|$, and

A.5 Resolution B1.5: Extended Relativistic Framework for Time Transformations ...

IERS
Technical
Note

No. 32

2. expression of the vector potential outside the Earth, leading to the well-known Lense-Thirring effect, in terms of the Earth's total angular momentum vector $\mathbf{S_E}$ in the form

$$W_E^a(T, \mathbf{X}) = -\frac{G}{2} \frac{(\mathbf{X} \times \mathbf{S_E})^a}{R^3}.$$

A.5 Resolution B1.5: Extended Relativistic Framework for Time Transformations and Realization of Coordinate Times in the Solar System

The XXIVth International Astronomical Union

Considering

1. that the Resolution A4 of the XXIst General Assembly(1991) has defined systems of space-time coordinates for the solar system (Barycentric Reference System) and for the Earth (Geocentric Reference System), within the framework of General Relativity,

2. that Resolution B1.3 entitled "Definition of Barycentric Celestial Reference System and Geocentric Celestial Reference System" has renamed these systems the Barycentric Celestial Reference System (BCRS) and the Geocentric Celestial Reference System (GCRS), respectively, and has specified a general framework for expressing their metric tensor and defining coordinate transformations at the first post-Newtonian level,

3. that, based on the anticipated performance of atomic clocks, future time and frequency measurements will require practical application of this framework in the BCRS, and

4. that theoretical work requiring such expansions has already been performed,

Recommends

that for applications that concern time transformations and realization of coordinate times within the solar system, Resolution B1.3 be applied as follows:

1. the metric tensor be expressed as

$$g_{00} = -\left(1 - \frac{2}{c^2}(w_0(t, \mathbf{x}) + w_L(t, \mathbf{x})) + \frac{2}{c^4}(w_0^2(t, \mathbf{x}) + \Delta(t, \mathbf{x}))\right),$$

$$g_{0i} = -\frac{4}{c^3} w^i(t, \mathbf{x}),$$

$$g_{ij} = \left(1 + \frac{2w_0(t, \mathbf{x})}{c^2}\right) \delta_{ij},$$

where (t $\equiv$ Barycentric Coordinate Time (TCB),$\mathbf{x}$) are the barycentric coordinates, $w_0 = G \sum_A M_A / r_A$ with the summation carried out over all solar system bodies A, $\mathbf{r}_A = \mathbf{x} - \mathbf{x}_A, \mathbf{x}_A$ are the coordinates of the center of mass of body A, $r_A = |\mathbf{r_A}|$, and where w_L contains the expansion in terms of multipole moments [see their definition in the Resolution B1.4 entitled "Post-Newtonian Potential Coefficients"] required for each body. The vector potential $w^i(t, \mathbf{x} = \sum_A w_A^i(t, \mathbf{x})$ and the function $\Delta(t, \mathbf{x}) = \sum_A \Delta_A(t, \mathbf{x})$ are given in note 2.

2. the relation between TCB and Geocentric Coordinate Time (TCG) can be expressed to sufficient accuracy by

$$\begin{aligned} TCB - TCG = \ & c^{-2}[\int_{t_0}^t (\tfrac{v_E^2}{2} + w_{0ext}(\mathbf{x}_E))dt + v_E^i r_E^i] \\ & -c^{-4}[\int_{t_0}^t (-\tfrac{1}{8}v_E^4 - \tfrac{3}{2}v_E^2 w_{0ext}(\mathbf{x}_E) + 4v_E^i w_{ext}^i(\mathbf{x}_E) + \tfrac{1}{2}w_{0ext}^2(\mathbf{x}_E))dt \\ & -(3w_{0ext}(\mathbf{x}_E) + \tfrac{v_E^2}{2})v_E^i r_E^i], \end{aligned}$$

where v_E is the barycentric velocity of the Earth and where the index ext refers to summation over all bodies except the Earth.

Notes

1. *This formulation will provide an uncertainty not larger than 5×10^{-18} in rate and, for quasi-periodic terms, not larger than 5×10^{-18} in rate amplitude and 0.2 ps in phase amplitude, for locations farther than a few solar radii from the Sun. The same uncertainty also applies to the transformation between TCB and TCG for locations within 50000 km of the Earth. Uncertainties in the values of astronomical quantities may induce larger errors in the formulas.*

2. *Within the above mentioned uncertainties, it is sufficient to express the vector potential $w_A^i(t, \mathbf{x})$ of body A as*

$$w_A^i(t, \mathbf{x}) = G \left[\frac{-(\mathbf{r}_A \times \mathbf{S}_A)^i}{2r_A^3} + \frac{M_A v_A^i}{r_A} \right],$$

where $\mathbf{S}_A$ is the total angular momentum of body A and v_A^i is the barycentric coordinate velocity of body A. As for the function $\Delta_A(t, \mathbf{x})$ it is sufficient to express it as

$$\Delta_A(t, \mathbf{x}) = \frac{GM_A}{r_A} \left[-2v_a^2 + \sum_{B \neq A} \frac{GM_B}{r_{BA}} + \frac{1}{2} \left(\frac{(r_A^k v_A^k)^2}{r_A^2} + r_A^k a_A^k \right) \right]$$
$$+ \frac{2G v_A^k (\mathbf{r}_A \times \mathbf{S}_A)^k}{r_A^3},$$

where $r_{BA} = |\mathbf{x}_B - \mathbf{x}_A|$ and a_A^k is the barycentric coordinate acceleration of body A. In these formulas, the terms in $\mathbf{S}_A$ are needed only for Jupiter ($S \approx 6.9 \times 10^{38} m^2 s^{-1} kg$) and Saturn ($S \approx 1.4 \times 10^{38} m^2 s^{-1} kg$), in the immediate vicinity of these planets.

3. *Because the present recommendation provides an extension of the IAU 1991 recommendations valid at the full first post-Newtonian level, the constants L_C and L_B that were introduced in the IAU 1991 recommendations should be defined as $< TCG/TCB > = 1 - L_C$ and $< TT/TCB > = 1 - L_B$, where TT refers to Terrestrial Time and $<>$ refers to a sufficiently long average taken at the geocenter. The most recent estimate of L_C is (Irwin, A. and Fukushima, T., Astron. Astroph., **348**, 642–652, 1999)*

$$L_C = 1.48082686741 \times 10^{-8} \pm 2 \times 10^{-17}.$$

From Resolution B1.9 on "Redefinition of Terrestrial Time TT", one infers $L_B = 1.55051976772 \times 10^{-8} \pm 2 \times 10^{-17}$ by using the relation $1 - L_B = (1 - L_C)(1 - L_G)$. L_G is defined in Resolution B1.9.

Because no unambiguous definition may be provided for L_B and L_C, these constants should not be used in formulating time transformations when it would require knowing their value with an uncertainty of order 1×10^{-16} or less.

4. *If $TCB - TCG$ is computed using planetary ephemerides which are expressed in terms of a time argument (noted T_{eph}) which is close to Barycentric Dynamical Time (TDB), rather than in terms of TCB, the first integral in Recommendation 2 above may be computed as*

$$\int_{t_0}^t \left(\frac{v_E^2}{2} + w_{0ext}(\mathbf{x}_E) \right) dt = \left[\int_{T_{eph_0}}^{T_{eph}} \left(\frac{v_E^2}{2} + w_{0ext}(\mathbf{x}_E) \right) dt \right] / (1 - L_B).$$

A.6   Resolution B1.6: IAU 2000 Precession-Nutation Model

The XXIVth International Astronomical Union

Recognizing

1. that the International Astronomical Union and the International Union of Geodesy and Geophysics Working Group (IAU-IUGG WG) on 'Non-rigid Earth Nutation Theory' has met its goals by

   (a) establishing new high precision rigid Earth nutation series, such as (1) SMART97 of Bretagnon *et al.*, 1998, *Astron. Astroph.*, **329**, 329–338; (2) REN2000 of Souchay *et al.*, 1999, *Astron. Astroph. Supl. Ser.*, **135**, 111–131; (3) RDAN97 of Roosbeek and Dehant 1999, *Celest. Mech.*, **70**, 215–253;

   (b) completing the comparison of new non-rigid Earth transfer functions for an Earth initially in non-hydrostatic equilibrium, incorporating mantle anelasticity and a Free Core Nutation period in agreement with observations,

   (c) noting that numerical integration models are not yet ready to incorporate dissipation in the core, and

   (d) noting the effects of other geophysical and astronomical phenomena that must be modelled, such as ocean and atmospheric tides, that need further development;

2. that, as instructed by IAU Recommendation C1 in 1994, the International Earth Rotation Service (IERS) will publish in the IERS Conventions (2000) a precession-nutation model that matches the observations with a weighted rms of 0.2 milliarcsecond (mas);

3. that semi-analytical geophysical theories of forced nutation are available which incorporate some or all of the following — anelasticity and electromagnetic couplings at the core-mantle and inner core-outer core boundaries, annual atmospheric tide, geodesic nutation, and ocean tide effects;

4. that ocean tide corrections are necessary at all nutation frequencies; and

5. that empirical models based on a resonance formula without further corrections do also exist;

Accepts

the conclusions of the IAU-IUGG WG on Non-rigid Earth Nutation Theory published by Dehant *et al.*, 1999, *Celest. Mech.* **72(4)**, 245–310 and the recent comparisons between the various possibilities, and

Recommends

that, beginning on 1 January 2003, the IAU 1976 Precession Model and IAU 1980 Theory of Nutation, be replaced by the precession-nutation model IAU 2000A (MHB2000, based on the transfer functions of Mathews, Herring and Buffett, 2000 - submitted to the *Journal of Geophysical Research*) for those who need a model at the 0.2 mas level, or its shorter version IAU 2000B for those who need a model only at the 1 mas level, together with their associated precession and obliquity rates, and their associated celestial pole offsets, as published in the IERS Conventions 2000, and

Encourages

1. the continuation of theoretical developments of non-rigid Earth nutation series,

2. the continuation of VLBI observations to increase the accuracy of the nutation series and the nutation model, and to monitor the unpredictable free core nutation, and

3. the development of new expressions for precession consistent with the IAU 2000A model.

A.7   Resolution B1.7: Definition of Celestial Intermediate Pole

The XXIVth International Astronomical Union

Noting

the need for accurate definition of reference systems brought about by unprecedented observational precision, and

Recognizing

1. the need to specify an axis with respect to which the Earth's angle of rotation is defined,

2. that the Celestial Ephemeris Pole (CEP) does not take account of diurnal and higher frequency variations in the Earth's orientation,

Recommends

1. that the Celestial Intermediate Pole (CIP) be the pole, the motion of which is specified in the Geocentric Celestial Reference System (GCRS, see Resolution B1.3) by motion of the Tisserand mean axis of the Earth with periods greater than two days,

2. that the direction of the CIP at J2000.0 be offset from the direction of the pole of the GCRS in a manner consistent with the IAU 2000A (see Resolution B1.6) precession-nutation model,

3. that the motion of the CIP in the GCRS be realized by the IAU 2000A model for precession and forced nutation for periods greater than two days plus additional time-dependent corrections provided by the International Earth Rotation Service (IERS) through appropriate astro-geodetic observations,

4. that the motion of the CIP in the International Terrestrial Reference System (ITRS) be provided by the IERS through appropriate astro-geodetic observations and models including high-frequency variations,

5. that for highest precision, corrections to the models for the motion of the CIP in the ITRS may be estimated using procedures specified by the IERS, and

6. that implementation of the CIP be on 1 January 2003.

Notes

1. *The forced nutations with periods less than two days are included in the model for the motion of the CIP in the ITRS.*

2. *The Tisserand mean axis of the Earth corresponds to the mean surface geographic axis, quoted B axis, in Seidelmann, 1982, Celest. Mech.,* **27***, 79–106.*

3. *As a consequence of this resolution, the Celestial Ephemeris Pole is no longer necessary.*

A.8   Resolution B1.8: Definition and use of Celestial and Terrestrial Ephemeris Origin

The XXIVth International Astronomical Union

Recognizing

1. the need for reference system definitions suitable for modern realizations of the conventional reference systems and consistent with observational precision,

2. the need for a rigorous definition of sidereal rotation of the Earth,

3. the desirability of describing the rotation of the Earth independently from its orbital motion, and

Noting

that the use of the "non-rotating origin" (Guinot, 1979) on the moving equator fulfills the above conditions and allows for a definition of UT1 which is insensitive to changes in models for precession and nutation at the microarcsecond level,

Recommends

1. the use of the "non-rotating origin" in the Geocentric Celestial Reference System (GCRS) and that this point be designated as the Celestial Ephemeris Origin (CEO) on the equator of the Celestial Intermediate Pole (CIP),

2. the use of the "non-rotating origin" in the International Terrestrial Reference System (ITRS) and that this point be designated as the Terrestrial Ephemeris Origin (TEO) on the equator of the CIP,

3. that UT1 be linearly proportional to the Earth Rotation Angle defined as the angle measured along the equator of the CIP between the unit vectors directed toward the CEO and the TEO,

4. that the transformation between the ITRS and GCRS be specified by the position of the CIP in the GCRS, the position of the CIP in the ITRS, and the Earth Rotation Angle,

5. that the International Earth Rotation Service (IERS) take steps to implement this by 1 January 2003, and

6. that the IERS will continue to provide users with data and algorithms for the conventional transformations.

Note

1. *The position of the CEO can be computed from the IAU 2000A model for precession and nutation of the CIP and from the current values of the offset of the CIP from the pole of the ICRF at J2000.0 using the development provided by Capitaine et al. (2000).*

2. *The position of the TEO is only slightly dependent on polar motion and can be extrapolated as done by Capitaine et al. (2000) using the IERS data.*

3. *The linear relationship between the Earth's rotation angle θ and UT1 should ensure the continuity in phase and rate of UT1 with the value obtained by the conventional relationship between Greenwich Mean Sidereal Time (GMST) and UT1. This is accomplished by the following relationship:*

$$\theta(UT1) = 2\pi(0.7790572732640 + 1.00273781191135448 \times (Julian\ UT1\ date - 2451545.0))$$

References

Guinot, B., 1979, in D.D. McCarthy and J.D. Pilkington (eds.), *Time and the Earth's Rotation*, D. Reidel Publ., 7–18.

Capitaine, N., Guinot, B, McCarthy, D.D., 2000, "Definition of the Celestial Ephemeris Origin and of UT1 in the International Celestial Reference Frame", *Astron. Astrophys.*, **355**, 398–405.

A.9   Resolution B1.9: Re-definition of Terrestrial Time TT

The XXIVth International Astronomical Union

Considering

1. that IAU Resolution A4 (1991) has defined Terrestrial Time (TT) in its Recommendation 4, and

2. that the intricacy and temporal changes inherent to the definition and realization of the geoid are a source of uncertainty in the definition and realization of TT, which may become, in the near future, the dominant source of uncertainty in realizing TT from atomic clocks,

Recommends

that TT be a time scale differing from TCG by a constant rate:
$dTT/dTCG = 1-L_G$, where $L_G = 6.969290134 \times 10^{-10}$ is a defining constant,

Note

L_G was defined by the IAU Resolution A4 (1991) in its Recommendation 4 as equal to U_G/c^2 where U_G is the geopotential at the geoid. L_G is now used as a defining constant.

A.10   Resolution B2: Coordinated Universal Time

The XXIVth International Astronomical Union

Recognizing

1. that the definition of Coordinated Universal Time (UTC) relies on the astronomical observation of the UT1 time scale in order to introduce leap seconds,

2. that the unpredictable leap seconds affects modern communication and navigation systems,

3. that astronomical observations provide an accurate estimate of the secular deceleration of the Earth's rate of rotation

Recommends

1. that the IAU establish a working group reporting to Division I at the General Assembly in 2003 to consider the redefinition of UTC,

2. that this study discuss whether there is a requirement for leap seconds, the possibility of inserting leap seconds at pre-determined intervals, and the tolerance limits for UT1−UTC, and

3. that this study be undertaken in cooperation with the appropriate groups of the International Union of Radio Science (URSI), the International Telecommunications Union (ITU-R), the International Bureau for Weights and Measures (BIPM), the International Earth Rotation Service (IERS) and relevant navigational agencies.

B   Glossary

AGN	Active Galactic Nuclei
BCRS	Barycentric Celestial Reference System
BIH	Bureau International de l'Heure
BIPM	Bureau International des Poids et Mesures
BTS	BIH Terrestrial System
CEO	Celestial Ephemeris Origin
CEP	Celestial Ephemeris Pole
CIP	Celestial Intermediate Pole
CRS	Celestial Reference System
CSR	Center for Space Research, University of Texas
CSTG	Commission on International Coordination of Space Techniques for Geodesy and Geodynamics
CTRF	Conventional Terrestrial Reference Frame
CTRS	Conventional Terrestrial Reference System
CW	Chandler Wobble
DOMES	Directory Of MERIT Sites
DORIS	Doppler Orbit determination and Radiopositioning Integrated on Satellite
EE	Equation of the Equinoxes
EOP	Earth Orientation Parameters
FCN	Free Core Nutation
FICN	Free Inner Core Nutation
GCRS	Geocentric Celestial Reference System
GLOSS	Global Sea Level Observing System
GMST	Greenwich Mean Sidereal Time
GPS	Global Positioning System
GST	Greenwich Sidereal Time
IAG	International Association of Geodesy
IAU	International Astronomical Union
IERS	International Earth Rotation and Reference Systems Service
ICRF	International Celestial Reference Frame
ICRS	International Celestial Reference System
IGS	International GPS Service
ILRS	International Laser Ranging Service
ITRF	International Terrestrial Reference Frame
IUGG	International Union for Geodesy and Geophysics
IVS	International VLBI Service for Geodesy and Astrometry
JPL	Jet Propulsion Laboratory
LLR	Lunar Laser Ranging
MERIT	Monitoring Earth Rotation and Intercomparison of Techniques
NNSS	Navy Navigation Satellite System
NOAA	National Oceanic and Atmospheric Administration
NRO	Non Rotating Origin
SI	Système International (International System of units)
SLR	Satellite Laser Ranging
TAI	Temps Atomique International (International Atomic Time)
TCB	Barycentric Coordinate Time
TCG	Geocentric Coordinate Time
TDB	Barycentric Dynamical Time
TEO	Terrestrial Ephemeris Origin
TGP	Tide Generating Potential
TRS	Terrestrial Reference System
TT	Terrestrial Time
USNO	United States Naval Observatory
UTC	Coordinated Universal Time
UT1	Universal Time 1
VLBI	Very Long Baseline Interferometry